

GAS TURBINE ENGINE PROGNOSTICS USING
TIME-SERIES BASED APPROACHES

MARYAM GHOLAMHOSSEIN

A THESIS
IN
THE DEPARTMENT
OF
ELECTRICAL AND COMPUTER ENGINEERING

PRESENTED IN PARTIAL FULFILLMENT OF THE REQUIREMENTS
FOR THE DEGREE OF MASTER OF APPLIED SCIENCE
CONCORDIA UNIVERSITY
MONTRÉAL, QUÉBEC, CANADA

JUNE 2014

© MARYAM GHOLAMHOSSEIN, 2014

CONCORDIA UNIVERSITY
School of Graduate Studies

This is to certify that the thesis prepared

By: Maryam Gholamhossein

Entitled: Gas Turbine Engine Prognostics Using Time-Series Based Approaches

and submitted in partial fulfillment of the requirements for the degree of

Master of Applied Science

complies with the regulations of this University and meets the accepted standards with respect to originality and quality.

Signed by the final examining committee:

_____	Chair
Dr. P. Valizadeh	
_____	External Examiner
Dr. R. Sedaghati (MIE)	
_____	Examiner
Dr. L. A. Lopes	
_____	Supervisor
Dr. K. Khorasani	

Approved _____

Dr. W. E. Lynch, Chair

Department of Electrical and Computer Engineering

20 _____

Dr. C. W. Trueman

Interim Dean, Faculty of Engineering
and Computer Science

Abstract

Gas Turbine Engine Prognostics Using Time-Series Based Approaches

Maryam Gholamhossein

In today's market, the increasing demand on utilizing gas turbine engines can be quite costly if users rely only on traditional time-based maintenance schedules. Meeting both the safety and the economical aspects of such systems could be realized by using an appropriate maintenance strategy in which the prediction of the engine health condition is employed to ensure that the system is maintained only if necessary. Towards this end, in this thesis the prognosis problem in the gas turbine engines is investigated.

As in every rotational mechanical equipment, gas turbine rotating components also degrade during the engine operation which may deteriorate their performance. The engine degradation may originate from different sources such as aging, erosion, fouling, corrosion, etc. Hard particles mixed with the air can remove the materials from the flow path components (erosion) and cause aerodynamic changes in the blades, which can consequently reduce the affected components performance. Accumulated particles on the flow path components and annulus surfaces of the gas turbine (fouling) can also reduce the flow rate of the gas and consequently decrease the power and efficiency of the affected components. Among different degradation sources in the engine, erosion and fouling are considered as two well-known degradation phenomena and their effects on the engine system prognostics are studied in this thesis.

Towards the above end, a controller is designed to control the thrust level of the engine and a Matlab/Simulink platform is employed to incorporate the effects of the above degradation factors and the engine dynamic model. The engine performance degradation trends are modeled by using three types of time-series based techniques namely, the autoregressive integrated moving average (ARIMA), the vector autoregressive (VAR) and the hybrid fuzzy autoregressive integrated moving average (hybrid fuzzy ARIMA) models. One of the challenges associated with time-series approaches is selecting a proper model which represents the structure of the time-series and is employed for prediction and prognosis purposes. Two widely used criteria namely, the Akaike's information criterion (AIC) and

the Bayesian information criterion (BIC) are used in order to select the best model. The challenges of coping with the uncertainties due to variety of sources such as measurement noise, insufficient data and changing operating conditions are inevitable factors. Taking the above facts into account, it may not be practical to obtain or be concerned with an exact prediction information. Therefore, we construct instead confidence bounds that provide a realistic boundary for the prediction and this is applied to all our proposed approaches in this thesis.

The first method in this thesis deals with modeling a measurable parameter using its historical data which is a fine-tuned version of the ARMA model for non-stationary time series analysis. The second method, VAR model, models the measurable parameters by fusing historical data with the current and past data of some other engine measurable data in a vector form so that one can get benefit of more measurement parameters of the engine. The third method deals with fusing two measurable parameters using a Takagi-Sugeno fuzzy inference engine.

In this thesis we are focused on modeling the engine performance degradations due to the fouling and the erosion which are the two main causes of gas turbine engine deterioration. In order to evaluate the performance of the proposed methods, they are applied to three different scenarios. These scenarios include the compressor fouling, turbine erosion phenomena and their combination with different severities. Our numerical simulation results show that the performance of the hybrid fuzzy ARIMA model is superior to that of the ARIMA and VAR methods.

To my parents for their love and support.

Acknowledgments

First, I wish to express my gratitude and admiration to my supervisor Professor Khashayar Khorasani, who firstly gave me the opportunity to undertake this work and then supported me through my Masters studies. Completion of my masters would not have been possible without his ideas and suggestions. I appreciate all his contributions of time and ideas.

I would also like to thank my committee members Dr. Lopes, Dr. Sedaghati and Dr. Valizadeh for their time and guidance through reviewing and evaluating my work.

I am thankful to all my friends and colleagues, with whom I spent a lot of time both at work and in spare time. Their friendships have provided a warm and friendly environment for me and have made my time full of memorable moments.

Finally, my deepest gratitude goes to my parents and my brother for their unconditional love and prayers. For their persistent support and belief in me throughout my life.

Contents

List of Figures	x
List of Tables	xxi
Nomenclature	xxv
1 Introduction	1
1.1 Motivation of the Work	9
1.2 Literature Review	10
1.2.1 Fault Diagnostics	12
1.2.2 Failure Prognostics	21
1.3 Statement of the Research Problem	33
1.4 Thesis Contributions	34
1.5 Thesis Outline	37
2 Background Information	38
2.1 Time-Series Modeling and Prediction	39
Deterministic and Statistical Time-Series	40
Stationarity of the Stochastic Processes	40
2.1.1 Autoregressive Integrated Moving Average (ARIMA) Model	40
Stationarity	42
Invertibility	44
Model Parameter Estimation Methods	45
2.1.2 Vector Autoregressive (VAR) Model	53
2.1.3 Time-Series Model Selection	55
2.1.4 Time-Series Model for Prediction	56

2.2	Fuzzy Logic	57
2.2.1	Fuzzy Set	59
2.2.2	Fuzzy System Structure	66
	Fuzzification	66
	Rule Base	67
	Inference	67
	Defuzzification	68
2.3	Aircraft Gas Turbine Engine	70
2.3.1	Gas Turbine Cycles	72
2.3.2	Aircraft Gas Turbine Engine Mathematical Model	73
	Rotor Dynamics	74
	Volume Dynamics	75
	Components - Intake	75
	Components - Compressor	75
	Components - Combustion Chamber	76
	Components - Turbine	76
	Set of Governing Nonlinear Equations	77
2.3.3	Degradations in the Engine	78
2.3.4	Flight Phases	83
2.4	Integrating Engine Degradation into the Engine Model	84
2.5	Summary	90
3	VAR a Time-series Approach	91
3.1	Gas Turbine Engine Controller	91
3.2	ARIMA and VAR Model Selection	99
3.3	Case Study Scenarios	104
3.4	Simulation Results	105
3.4.1	ARIMA Model	105
	Data Preprocessing	106
	Scenario 1	108
	Scenario 2	120
	Scenario 3	131
3.4.2	VAR Model	142
	Data Preprocessing	143

Scenario 1	143
Scenario 2	159
Scenario 3	174
3.5 Comparison of VAR and ARIMA Models	188
3.6 Summary	189
4 Hybrid Fuzzy ARIMA Approach	191
4.1 Hybrid Fuzzy ARIMA Modeling	191
4.2 Case Study Scenarios	206
4.3 Simulation Results	206
Scenario 1	206
Scenario 2	217
Scenario 3	228
4.4 Comparison of Hybrid Fuzzy ARIMA Approach with ARIMA and VAR Models	240
4.5 Summary	240
5 Conclusions and Future Work	242
5.1 Thesis Summary	242
5.2 Suggestions for Future Work	243
Bibliography	246

List of Figures

1.1	Maintenance strategies relationships [1].	2
1.2	Maintenance policies relationships [1].	2
1.3	Prognostics and diagnostics in terms of time [2].	12
1.4	Comparison between hardware and analytical redundancy concepts [3]. . .	13
1.5	Concept of an analytical fault diagnosis structure [4].	14
1.6	Prognostics technical methods [5].	23
1.7	Uncertainty associated with RUL [2].	25
2.1	Monthly rainfall data for Auckland [6].	39
2.2	Classical and fuzzy definitions of a tall person [7].	58
2.3	Triangular membership function.	60
2.4	Trapezoidal membership function.	61
2.5	Gaussian membership function.	61
2.6	Membership function μ_w for the WARM temperature fuzzy set.	64
2.7	Membership function μ_c for the COLD temperature fuzzy set.	64
2.8	Membership function μ_{cw} for the COLDandWARM temperature fuzzy set. .	65
2.9	Membership functions defining five singleton fuzzy sets [8].	65
2.10	Fuzzy system structure [9].	66
2.11	Block diagram of an aircraft gas turbine engine (a) and a stationary gas turbine engine (b) [10].	71
2.12	Schematic of a single spool jet engine [11].	72
2.13	Working cycle pressure-volume graph in the gas turbine engine [12].	73
2.14	Flow diagram and interdependencies of different modules of the jet engine dynamics [13].	74
2.15	Gas Turbine Engine Performance Analysis [14],[15].	81
2.16	The blade fouling in the compressor [16].	82
2.17	The blade erosion [17].	82

2.18	The outputs of the degraded model associated with the fouling degradation [18].	87
2.19	The outputs of the degraded model associated with the erosion degradation [18].	88
3.1	Schematic of the fuel flow controller for the gas turbine engine.	93
3.2	Tracking the desired engine pressure ratio using the feed-forward and negative feedback controllers in the healthy condition.	94
3.3	Tracking error in the healthy condition.	95
3.4	The control input of the engine in the healthy condition.	95
3.5	Tracking the desired engine pressure ratio using a feed-forward and negative feedback in the presence of the compressor fouling.	96
3.6	Tracking error in the presence of the compressor fouling.	96
3.7	Tracking the desired engine pressure ratio using a feed-forward and negative feedback in the presence of the turbine erosion.	97
3.8	Tracking error in the presence of the turbine erosion.	97
3.9	Tracking the desired engine pressure ratio using a feed-forward and negative feedback in the presence of both fouling and erosion.	98
3.10	Tracking error in the presence of both fouling and erosion.	98
3.11	Ten step ahead prediction results by using the ARIMA(4,5) model without compensator for the first scenario.	107
3.12	Five step ahead prediction results by using the univariate ARIMA(4,5) model for the first scenario in presence of the measurement noise with the standard deviation of 1.	109
3.13	Ten step ahead prediction results by using the ARIMA(4,5) model including compensator for the first scenario in presence of the measurement noise with the standard deviation of 1.	110
3.14	Fifteen step ahead prediction results by using the univariate ARIMA(4,5) model for the first scenario in presence of the measurement noise with the standard deviation of 1.	111
3.15	Thirty step ahead prediction results by using the univariate ARIMA(4,5) model for the first scenario in presence of the measurement noise with the standard deviation of 1.	112

3.16	Five step ahead prediction results by using the univariate ARIMA(4,5) model for the first scenario in presence of the measurement noise with the standard deviation of 2.	113
3.17	Fifteen step ahead prediction results by using the univariate ARIMA(4,5) model for the first scenario in presence of the measurement noise with the standard deviation of 2.	114
3.18	Thirty step ahead prediction results by using the univariate ARIMA(4,5) model for the first scenario in presence of the measurement noise with the standard deviation of 2.	115
3.19	Five step ahead prediction results by using the univariate ARIMA(4,5) model for the first scenario in presence of the measurement noise with the standard deviation of 5.	117
3.20	Fifteen step ahead prediction results by using the univariate ARIMA(4,5) model for the first scenario in presence of the measurement noise with the standard deviation of 5.	118
3.21	Thirty step ahead prediction results by using the univariate ARIMA(4,5) model for the first scenario in presence of the measurement noise with the standard deviation of 5.	119
3.22	Five step ahead prediction results by using the univariate ARIMA(4,5) model for the second scenario in presence of the measurement noise with the standard deviation of 1.	121
3.23	Fifteen step ahead prediction results by using the univariate ARIMA(4,5) model for the second scenario in presence of the measurement noise with the standard deviation of 1.	122
3.24	Thirty step ahead prediction results by using the univariate ARIMA(4,5) model for the second scenario in presence of the measurement noise with the standard deviation of 1.	123
3.25	Five step ahead prediction results by using the univariate ARIMA(4,5) model for the second scenario in presence of the measurement noise with the standard deviation of 2.	124
3.26	Fifteen step ahead prediction results by using the univariate ARIMA(4,5) model for the second scenario in presence of the measurement noise with the standard deviation of 2.	125

3.27	Thirty step ahead prediction results by using the univariate ARIMA(4,5) model for the second scenario in presence of the measurement noise with the standard deviation of 2.	126
3.28	Five step ahead prediction results by using the univariate ARIMA(4,5) model for the second scenario in presence of measurement noise with the standard deviation of 5.	127
3.29	Fifteen step ahead prediction results by using the univariate ARIMA(4,5) model for the second scenario in presence of the measurement noise with the standard deviation of 5.	128
3.30	Thirty step ahead prediction results by using the univariate ARIMA(4,5) model for the second scenario in presence of the measurement noise with the standard deviation of 5.	129
3.31	Five step ahead prediction results by using the univariate ARIMA(4,5) model for the third scenario in presence of the measurement noise with the standard deviation of 1.	132
3.32	Fifteen step ahead prediction results by using the univariate ARIMA(4,5) model for the third scenario in presence of the measurement noise with the standard deviation of 1.	133
3.33	Thirty step ahead prediction results by using the univariate ARIMA(4,5) model for the third scenario in presence of the measurement noise with the standard deviation of 1.	134
3.34	Five step ahead prediction results by using the univariate ARIMA(4,5) model for the third scenario in presence of the measurement noise with the standard deviation of 2.	136
3.35	Fifteen step ahead prediction results by using the univariate ARIMA(4,5) model for the third scenario in presence of the measurement noise with the standard deviation of 2.	137
3.36	Thirty step ahead prediction results by using the univariate ARIMA(4,5) model for the third scenario in presence of the measurement noise with the standard deviation of 2.	138
3.37	Five step ahead prediction results by using the univariate ARIMA(4,5) model for the third scenario in presence of the measurement noise with the standard deviation of 5.	139

3.38	Fifteen step ahead prediction results by using the univariate ARIMA(4,5) model for the third scenario in presence of the measurement noise with the standard deviation of 5.	140
3.39	Thirty step ahead prediction results by using the univariate ARIMA(4,5) model for the third scenario in presence of the measurement noise with the standard deviation of 5.	141
3.40	Ten step ahead prediction results by using the VAR(6) model without compensator for the first scenario in presence of measurement noise with the standard deviation of 1.	144
3.41	Five step ahead turbine temperature prediction results by using the bivariate VAR(6) model for the first scenario in presence of measurement noise with the standard deviation of 1.	145
3.42	Five step ahead compressor temperature prediction results by using the bivariate VAR(6) model for the first scenario in presence of measurement noise with the standard deviation of 1.	146
3.43	Ten step ahead prediction results by using the VAR(6) model including compensator for the first scenario in presence of measurement noise with the standard deviation of 1.	147
3.44	Fifteen step ahead turbine temperature prediction results by using the bivariate VAR(6) model for the first scenario in presence of measurement noise with the standard deviation of 1.	148
3.45	Thirty step ahead turbine temperature prediction results by using the bivariate VAR(6) model for the first scenario in presence of measurement noise with the standard deviation of 1.	149
3.46	Five step ahead turbine temperature prediction results by using the bivariate VAR(6) model for the first scenario in presence of measurement noise with the standard deviation of 2.	150
3.47	Five step ahead compressor temperature prediction results by using the bivariate VAR(6) model for the first scenario in presence of measurement noise with the standard deviation of 2.	151
3.48	Fifteen step ahead turbine temperature prediction results by using the bivariate VAR(6) model for the first scenario in presence of measurement noise with the standard deviation of 2.	152

3.49	Thirty step ahead turbine temperature prediction results by using the bivariate VAR(6) model for the first scenario in presence of measurement noise with the standard deviation of 2.	153
3.50	Five step ahead turbine temperature prediction results by using the bivariate VAR(6) model for the first scenario in presence of measurement noise with the standard deviation of 5.	155
3.51	Five step ahead compressor temperature prediction results by using the bivariate VAR(6) model for the first scenario in presence of measurement noise with the standard deviation of 5.	156
3.52	Fifteen step ahead turbine temperature prediction results by using the bivariate VAR(6) model for the first scenario in presence of measurement noise with the standard deviation of 5.	157
3.53	Thirty step ahead turbine temperature prediction results by using the bivariate VAR(6) model for the first scenario in presence of measurement noise with the standard deviation of 5.	158
3.54	Five step ahead turbine temperature prediction results by using the bivariate VAR(6) model for the second scenario in presence of measurement noise with the standard deviation of 1.	160
3.55	Five step ahead compressor temperature prediction results by using the bivariate VAR(6) model for the second scenario in presence of measurement noise with the standard deviation of 1.	161
3.56	Fifteen step ahead turbine temperature prediction results by using the bivariate VAR(6) model for the second scenario in presence of measurement noise with the standard deviation of 1.	162
3.57	Thirty step ahead turbine temperature prediction results by using the bivariate VAR(6) model for the second scenario in presence of measurement noise with the standard deviation of 1.	163
3.58	Five step ahead turbine temperature prediction results by using the bivariate VAR(6) model for the second scenario in presence of measurement noise with the standard deviation of 2.	164
3.59	Five step ahead compressor temperature prediction results by using the bivariate VAR(6) model for the second scenario in presence of measurement noise with the standard deviation of 2.	165

3.60	Fifteen step ahead turbine temperature prediction results by using the bivariate VAR(6) model for the second scenario in presence of measurement noise with the standard deviation of 2.	166
3.61	Thirty step ahead turbine temperature prediction results by using the bivariate VAR(6) model for the second scenario in presence of measurement noise with the standard deviation of 2.	167
3.62	Five step ahead turbine temperature prediction results by using the bivariate VAR(6) model for the second scenario in presence of measurement noise with the standard deviation of 5.	170
3.63	Five step ahead compressor temperature prediction results by using the bivariate VAR(6) model for the second scenario in presence of measurement noise with the standard deviation of 5.	171
3.64	Fifteen step ahead turbine temperature prediction results by using the bivariate VAR(6) model for the second scenario in presence of measurement noise with the standard deviation of 5.	172
3.65	Thirty step ahead turbine temperature prediction results by using the bivariate VAR(6) model for the second scenario in presence of measurement noise with the standard deviation of 5.	173
3.66	Five step ahead turbine temperature prediction results by using the bivariate VAR(6) model for the third scenario in presence of measurement noise with the standard deviation of 1.	175
3.67	Five step ahead compressor temperature prediction results by using the bivariate VAR(6) model for the third scenario in presence of measurement noise with the standard deviation of 1.	176
3.68	Fifteen step ahead turbine temperature prediction results by using the bivariate VAR(6) model for the third scenario in presence of measurement noise with the standard deviation of 1.	177
3.69	Thirty step ahead turbine temperature prediction results by using the bivariate VAR(6) model for the third scenario in presence of measurement noise with the standard deviation of 1.	178
3.70	Five step ahead turbine temperature prediction results by using the bivariate VAR(6) model for the third scenario in presence of measurement noise with the standard deviation of 2.	180

3.71	Five step ahead compressor temperature prediction results by using the bivariate VAR(6) model for the third scenario in presence of measurement noise with the standard deviation of 2.	181
3.72	Fifteen step ahead turbine temperature prediction results by using the bivariate VAR(6) model for the third scenario in presence of measurement noise with the standard deviation of 2.	182
3.73	Thirty step ahead turbine temperature prediction results by using the bivariate VAR(6) model for the third scenario in presence of measurement noise with the standard deviation of 2.	183
3.74	Five step ahead turbine temperature prediction results by using the bivariate VAR(6) model for the third scenario in presence of measurement noise with the standard deviation of 5.	184
3.75	Five step ahead compressor temperature prediction results by using the bivariate VAR(6) model for the third scenario in presence of measurement noise with the standard deviation of 5.	185
3.76	Fifteen step ahead turbine temperature prediction results by using the bivariate VAR(6) model for the third scenario in presence of measurement noise with the standard deviation of 5.	186
3.77	Thirty step ahead turbine temperature prediction results by using the bivariate VAR(6) model for the third scenario in presence of measurement noise with the standard deviation of 5.	187
4.1	Trapezoidal functions defining the degree of memberships for $\alpha(N)$	195
4.2	Trapezoidal functions defining the degree of memberships for $\beta(N)$	196
4.3	Five step ahead prediction results by using the hybrid fuzzy ARIMA(4,5) model for the first scenario in presence of measurement noise with the standard deviation of 1.	207
4.4	Fifteen step ahead prediction results by using the hybrid fuzzy ARIMA(4,5) model for the first scenario in presence of measurement noise with the standard deviation of 1.	208
4.5	Thirty step ahead prediction results by using the hybrid fuzzy ARIMA(4,5) model for the first scenario in presence of measurement noise with the standard deviation of 1.	209

4.6	Five step ahead prediction results by using the hybrid fuzzy ARIMA(4,5) model for the first scenario in presence of measurement noise with the standard deviation of 2.	210
4.7	Fifteen step ahead prediction results by using the hybrid fuzzy ARIMA(4,5) model for the first scenario in presence of measurement noise with the standard deviation of 2.	211
4.8	Thirty step ahead prediction results by using the hybrid fuzzy ARIMA(4,5) model for the first scenario in presence of measurement noise with the standard deviation of 2.	212
4.9	Five step ahead prediction results by using the hybrid fuzzy ARIMA(4,5) model for the first scenario in presence of measurement noise with the standard deviation of 5.	214
4.10	Fifteen step ahead prediction results by using the hybrid fuzzy ARIMA(4,5) model for the first scenario in presence of measurement noise with the standard deviation of 5.	215
4.11	Thirty step ahead prediction results by using the hybrid fuzzy ARIMA(4,5) model for the first scenario in presence of measurement noise with the standard deviation of 5.	216
4.12	Five step ahead prediction results by using the hybrid fuzzy ARIMA(4,5) model for the second scenario in presence of measurement noise with the standard deviation of 1.	218
4.13	Fifteen step ahead prediction results by using the hybrid fuzzy ARIMA(4,5) model for the second scenario in presence of measurement noise with the standard deviation of 1.	219
4.14	Thirty step ahead prediction results by using the hybrid fuzzy ARIMA(4,5) model for the second scenario in presence of measurement noise with the standard deviation of 1.	220
4.15	Five step ahead prediction results by using the hybrid fuzzy ARIMA(4,5) model for the second scenario in presence of measurement noise with the standard deviation of 2.	221
4.16	Fifteen step ahead prediction results by using the hybrid fuzzy ARIMA(4,5) model for the second scenario in presence of measurement noise with the standard deviation of 2.	222

4.17	Thirty step ahead prediction results by using the hybrid fuzzy ARIMA(4,5) model for the second scenario in presence of measurement noise with the standard deviation of 2.	223
4.18	Five step ahead prediction results by using the hybrid fuzzy ARIMA(4,5) model for the second scenario in presence of measurement noise with the standard deviation of 5.	225
4.19	Fifteen step ahead prediction results by using the hybrid fuzzy ARIMA(4,5) model for the second scenario in presence of measurement noise with the standard deviation of 5.	226
4.20	Thirty step ahead prediction results by using the hybrid fuzzy ARIMA(4,5) model for the second scenario in presence of measurement noise with the standard deviation of 5.	227
4.21	Five step ahead prediction results by using the hybrid fuzzy ARIMA(4,5) model for the third scenario in presence of measurement noise with the standard deviation of 1.	229
4.22	Fifteen step ahead prediction results by using the hybrid fuzzy ARIMA(4,5) model for the third scenario in presence of measurement noise with the standard deviation of 1.	230
4.23	Thirty step ahead prediction results by using the hybrid fuzzy ARIMA(4,5) model for the third scenario in presence of measurement noise with the standard deviation of 1.	231
4.24	Five step ahead prediction results by using the hybrid fuzzy ARIMA(4,5) model for the third scenario in presence of measurement noise with the standard deviation of 2.	232
4.25	Fifteen step ahead prediction results by using the hybrid fuzzy ARIMA(4,5) model for the third scenario in presence of measurement noise with the standard deviation of 2.	233
4.26	Thirty step ahead prediction results by using the hybrid fuzzy ARIMA(4,5) model for the third scenario in presence of measurement noise with the standard deviation of 2.	234
4.27	Five step ahead prediction results by using the hybrid fuzzy ARIMA(4,5) model for the third scenario in presence of measurement noise with the standard deviation of 5.	236

4.28	Fifteen step ahead prediction results by using the hybrid fuzzy ARIMA(4,5) model for the third scenario in presence of measurement noise with the standard deviation of 5.	237
4.29	Thirty step ahead prediction results by using the hybrid fuzzy ARIMA(4,5) model for the third scenario in presence of measurement noise with the standard deviation of 5.	238

List of Tables

2.1	Per unit changes in the engine parameters corresponding to the fouling scenarios.	89
2.2	Per unit changes in the engine parameters corresponding to the erosion scenarios.	89
3.1	Steady state error % and settling time of the controller response under different engine conditions	93
3.2	BIC and AIC values for different orders of the ARIMA model in the presence of compressor fouling (FI 1%), Erosion (EI 1%) and both of them (FI 1% and EI 1%).	100
3.3	BIC and AIC values for different orders of the VAR model in the presence of compressor fouling (FI 1%), Erosion (EI 1%) and both of them (FI 1% and EI 1%).	101
3.4	The description of the mean and the standard deviation of the prediction errors for different orders of the ARIMA model for ten steps ahead prediction in the presence of compressor fouling (FI 1%), Erosion (EI 1%) and both of them (FI 1% and EI 1%).	102
3.5	The description of the mean and the standard deviation of the prediction errors for different order of the VAR model for ten steps ahead prediction in the presence of compressor fouling (FI 1%), Erosion (EI 1%) and both of them (FI 1% and EI 1%).	103
3.6	The description of the scenarios that are considered for conducting simulations.	105
3.7	Mean and standard deviation of the prediction errors for the ARIMA model for the first scenario in presence of the measurement noise with the standard deviation of 1.	116

3.8	Mean and standard deviation of the prediction errors for the ARIMA model for the first scenario in presence of the measurement noise with the standard deviation of 2.	116
3.9	Mean and standard deviation of the prediction errors for the ARIMA model for the first scenario in presence of the measurement noise with the standard deviation of 5.	120
3.10	Mean and standard deviation of the prediction errors for the ARIMA model for the second scenario in presence of the measurement noise with the standard deviation of 1.	130
3.11	Mean and standard deviation of the prediction errors for the ARIMA model for the second scenario in presence of measurement noise with the standard deviation of 2.	130
3.12	Mean and standard deviation of the prediction errors for the ARIMA model for the second scenario in presence of the measurement noise with the standard deviation of 5.	131
3.13	Mean and standard deviation of the prediction errors for the ARIMA model for the third scenario in presence of measurement noise with the standard deviation of 1.	135
3.14	Mean and standard deviation of the prediction errors for the ARIMA model for the third scenario in presence of measurement noise with the standard deviation of 2.	135
3.15	Mean and standard deviation of the prediction errors for the ARIMA model for the third scenario in presence of measurement noise with the standard deviation of 5.	142
3.16	Mean and standard deviation of the prediction errors for the VAR model for the first scenario in presence of measurement noise with the standard deviation of 1.	154
3.17	Mean and standard deviation of the prediction errors for the VAR model for the first scenario in presence of measurement noise with the standard deviation of 2.	154
3.18	Mean and standard deviation of the prediction errors for the VAR model for the first scenario in presence of measurement noise with the standard deviation of 5.	159

3.19	Mean and standard deviation of the prediction errors for the VAR model for the second scenario in presence of measurement noise with the standard deviation of 1.	168
3.20	Mean and standard deviation of the prediction errors for the VAR model for the second scenario in presence of measurement noise with the standard deviation of 2.	169
3.21	Mean and standard deviation of the prediction errors for the VAR model for the second scenario in presence of measurement noise with the standard deviation of 5.	174
3.22	Mean and standard deviation of the prediction errors for the VAR model for the third scenario in presence of measurement noise with the standard deviation of 1.	179
3.23	Mean and standard deviation of the prediction errors for the VAR model for the third scenario in presence of measurement noise with the standard deviation of 2.	179
3.24	Mean and standard deviation of the prediction errors for the VAR model for the third scenario in presence of measurement noise with the standard deviation of 5.	188
4.1	Mean and standard deviation of the prediction errors for the hybrid fuzzy ARIMA model for 10 steps ahead for different number of fuzzy rules. . . .	194
4.2	Rule base of $\alpha(N)$	198
4.2	Rule base of $\alpha(N)$	199
4.2	Rule base of $\alpha(N)$	200
4.2	Rule base of $\alpha(N)$	201
4.3	Rule base of $\beta(N)$	201
4.3	Rule base of $\beta(N)$	202
4.3	Rule base of $\beta(N)$	203
4.3	Rule base of $\beta(N)$	204
4.3	Rule base of $\beta(N)$	205
4.4	Mean and standard deviation of the prediction errors for the hybrid fuzzy ARIMA model for the first scenario in presence of measurement noise with the standard deviation of 1.	213

4.5	Mean and standard deviation of the prediction errors for the hybrid fuzzy ARIMA model for the first scenario in presence of measurement noise with the standard deviation of 2.	213
4.6	Mean and standard deviation of the prediction errors for the hybrid fuzzy ARIMA model for the first scenario in presence of measurement noise with the standard deviation of 5.	217
4.7	Mean and standard deviation of the prediction errors for the hybrid fuzzy ARIMA model for the second scenario in presence of measurement noise with the standard deviation of 1.	224
4.8	Mean and standard deviation of the prediction errors for the hybrid fuzzy ARIMA model for the second scenario in presence of measurement noise with the standard deviation of 2.	224
4.9	Mean and standard deviation of the prediction errors for the hybrid fuzzy ARIMA model for the second scenario in presence of measurement noise with the standard deviation of 5.	228
4.10	Mean and standard deviation of the prediction errors for the hybrid fuzzy ARIMA model for the third scenario in presence of measurement noise with the standard deviation of 1.	235
4.11	Mean and standard deviation of the prediction errors for the hybrid fuzzy ARIMA model for the third scenario in presence of measurement noise with the standard deviation of 2.	235
4.12	Mean and standard deviation of the prediction errors for the hybrid fuzzy ARIMA model for the third scenario in presence of measurement noise with the standard deviation of 5.	239

Nomenclature

β	Bypass ratio
\dot{m}	Mass flow rate, $\frac{Kg}{s}$
η	Efficiency
γ	Heat capacity ratio
π	Pressure ratio
<i>amb</i>	Ambient
<i>C</i>	Compressor
c_p	Specific heat at constant pressure, $\frac{J}{Kg.K}$
c_v	Specific heat at constant volume, $\frac{J}{Kg.K}$
<i>CC</i>	Combustion chamber
<i>d</i>	Intake
<i>f</i>	Fuel
H_u	Fuel specific heat, $\frac{J}{Kg}$
<i>J</i>	Rotational moment of inertia, $Kg.m^2$
<i>M</i>	Mach number
<i>M</i>	Mixer
<i>mech</i>	Mechanical

N	Rotational speed, RPM
n	Nozzle
P	Pressure, Pascal
P_0	Pressure at sea level at standard day
R	Gas constant, $\frac{J}{Kg.K}$
T	Temperature, K
T	Turbine
T_0	Temperature at sea level at standard day
V	Volume, m^3

CBM Condition Based Maintenance

DPHM Diagnosis, Prognosis and Health Management system

ARIMA Autoregressive Integrated Moving Average

VAR Vector Autoregressive

AIC Akaike's Information Criterion

BIC Bayesian Information Criterion

RCM Reliability Centered Maintenance

TPM Total Productive Maintenance

Chapter 1

Introduction

Increasing the complexity of sensitive and expensive systems along with necessity of meeting the safety and economic aspects of such systems have necessitated different maintenance strategies in every industry. In general, there are three main types of maintenance strategies namely unscheduled maintenance, programmed maintenance and maintenance of improvement [1]. Unscheduled maintenance or corrective maintenance is the most basic type of the maintenance. Because of the nature of this maintenance which is unplanned, it is also called "crisis maintenance". When a failure happens to the system or its subsystems, the system goes through the required maintenance services including a replacement, or a repairment service in order to bring the system back to its minimum acceptable performance and condition [19, 20]. Programmed maintenance is based on a predefined logic or a schedule and it can be categorized in two sections namely, preventive maintenance and condition based maintenance [1]. Preventive maintenance is performed based on specific accumulation of predefined hours cycles of the system, kilometers run, or other factors that have been selected according to the rate of failure of the system or other reliability measures of the system. Condition based maintenance (CBM) is performed based on the continuously monitoring the system health parameters. Though CBM is considerably more advanced than preventive maintenance, but it can be still perceived as a branch of preventive

maintenance as it also leads to forecast the system failure. Figure 1.1 shows the relationships between different maintenance strategies. As it is seen in this figure, CBM subtends predictive maintenance and proactive maintenance [1, 21]. Employing appropriate feedbacks, one can move from reactive maintenance to proactive maintenance or maintenance for improvement. The latter deals with prognostics techniques which will be explained in details later.

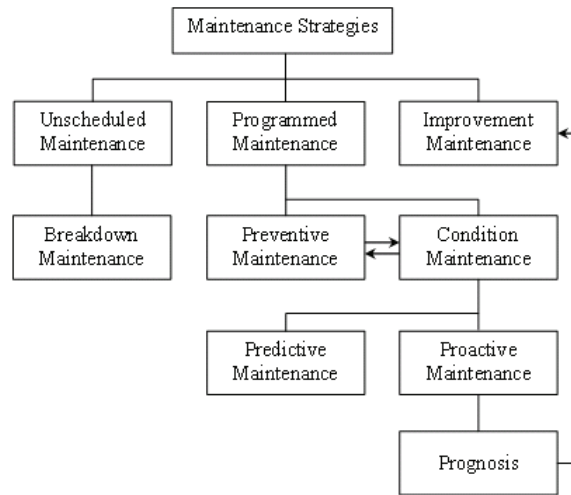


Figure 1.1: Maintenance strategies relationships [1].

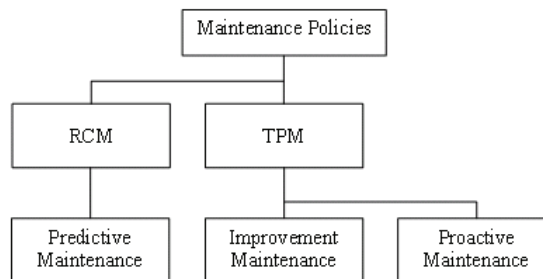


Figure 1.2: Maintenance policies relationships [1].

It is worth noting that there also exist maintenance policies describing the overall treatments that a company would take confronting the maintenance problems. Each policy deals with

some of the aforementioned maintenance strategies. The desired policy is chosen according to the type of the system, system sensitivity, economical limitations and other company strategies and measures [1]. Figure 1.2 shows the maintenance policies relationships.

Efficiency, maintainability, safety, cost, reliability, availability and their effects on each other are different factors that should be taken into consideration for choosing an efficient and proper maintenance strategy. It is clear that the more advanced maintenance strategies lead to have greater and more complex requirements such as equipments, trainings and their interrelationships [21].

Condition based maintenance by employing modern continuous monitoring systems can enable one to transform from reactive type to proactive type of maintenance policies. By utilizing continuous monitoring strategies and developing reliable prognosis techniques one can reach an efficient condition based maintenance [22]. Today it can be shown that following an old belief of fixing things before their breakdown may lead to facing more damages and unscheduled breakdowns [23].

However, among aforementioned maintenance strategies, CBM is the most preferable in terms of both total cost and reliability. CBM acts based on the actual condition of the system and not based on some predefined schedules and this difference makes CBM a predictive solution rather than a preventive solution. Most often there does not exist a direct connection between the aging of a system and its failure and this has been proven by researchers [23]. Moreover, the conventional maintenance which are time based can not be efficient for sensitive and complex systems and there is a need to extend and develop new maintenance methods which are operating based on the actual condition of the systems elements along with considering the propagation effects of faulty part on other parts of the system. This strategy decreases the total cost of the desired system and is recommended for the systems with costly maintenance. Because by using CBM the maximum use of each component based on the collected data over the monitoring procedure will be handled.

In other words, CBM of any equipment can be entailed by an association of different technologies, strategies, procedures for achieving a reliable evaluation of the system and efficient maintenance in terms of quantitative measures [23].

Non-destructive identification techniques are modern methods in area of systems and apparatus maintenance. These techniques can be assigned in the category of predictive maintenance which gets numerous benefits such as performing the maintenance based on the condition of the system, avoiding unforeseen downtimes, stopping chain reactions and causing the global reliability of the system to improve and at the same time reduce the maintenance cost [1]. The predictive maintenance is about predicting and identifying of incipient faults and informing the maintenance personnel to take necessary correcting measures before the breakdown point of the system happens and it is not about extending the mean time between failures (MTBF) value of the system or altering the cycle of failure. Here, the basic assumption is that rarely a component breaks down suddenly and for most of the systems such as mechanical, hydraulic and pneumatic systems it occurs after a progressive deterioration. Towards this end, in the first step we need to define the condition of the systems based on some parameters and in the second step, we attempt to detect and quantify them by using some measurement techniques such as visual inspection, non-destructive controls and finally operational or functional tests. These inspections and measurements should be performed on a regular schedule for each parameter of the system to allow the maintenance personnel detect the instant that system starts to deteriorate and predict the breakdown point of the system and repair or replace that component in advance. In more details this maintenance technique is performed based on the following steps [1]:

- Search for mechanical failure signs such as fatigue, welding defects and misalignments during the visual inspection
- Measure the measurable parameters of the system such as pressure, flow rate, temperature and speed and comparing it with their designed nominal values.

- Monitor the vibrations and noise of the system.
- Check the debris of the system resulting from the utilization of the system.

In predictive maintenance, one focuses on the trend of the monitored measurements. The possible failures are predicted based on the determined trends and the probability methodologies are not taking into consideration for accomplishing the failure prognosis. In some ways, one may perceive this type of the maintenance process as a diagnostic process due to its ability to deliver symptoms or indications, leading to perform maintenance procedure based on the latest condition of the system's components, regardless of their running time. Indeed this type of maintenance can be considered as an essential and important part of the complex mechanical systems which may minimize inactive time of the system owing to number of examinations and inspections. In order to monitor and determine the condition of any system, the necessary access to the system's components should be provided. Today, developing these necessary accesses are taken into consideration from the beginning of the designing phase of the systems. Identification of the components need to be checked, identification of the vital and informative parameters are the examples of these required tasks for determining the systems' components efficiency [1]. A list of benefits associated with employing CBM and how they deliver these benefits are listed below [1]:

1. **Increased safety** - CBM response time prevents the system reaching to the failure point.
2. **Increased availability of the system, lower maintenance cost** - CBM may provide greater intervals between two successive inspections and by procuring the required resources in advance, the down time will be decreased.
3. **Increased system efficiency** - CBM helps the system to work under its best operating condition and achieve better efficiency.

4. **Better opportunity to negotiate with the manufacturers** - Having the measured data of the system parameters from its new condition and later one can compare the data at the end of the period of the guarantee.
5. **Improved customer relations** - Ability of anticipating an incipient or possible failure provides a better organization of production.
6. **Opportunity to improve the design of the future systems** - Benefiting collected experiences of using a system may serve this goal.

Depending on the application and the environment in which the system is working, different condition based maintenance requirements should be considered. Today designers of complex systems take CBM requirements into consideration in the design stage so that changing the components, accessibility to the critical components can be accomplished easier and faster which eventually decrease down time of the system. If the CBM system is not designed from the design step of the system, compatibility requirements with the sensors and other components of the system should be met. Ultimately, a CBM system should improve system maintainability, safety, and decrease overall life cost of the system [5].

There are different types of engineering systems and they differ considerably in their nature and operation principles. Therefore, different techniques are needed to effectively monitor them. However, these techniques could be categorized as belonging to vibration monitoring, wear debris analysis, visual inspection, noise monitoring, and environment pollution monitoring [24]. For rotating machinery such as gas turbines and internal combustion engines the vibration monitoring and wear debris analysis methods are typically used [25].

The total number of different parts and components in a basic jet engine could be more than 20,000 and even more for heavy duty turbines which are worth millions of dollars.

Therefore, in the case of engine failure the direct expense is high and the indirect costs could be even greater. For this reason, all gas turbines and jet engines should be equipped with effective monitoring systems [25]. For gas turbine engine health monitoring and fault detection in addition to the aforementioned methods the gas path analysis (GPA) could be also used [26]. A more detailed description of gas turbine monitoring methods is given as follows [27, 28]:

- Oil and debris monitoring

The excessive wear and fatigue failure of engine moving components such as gearboxes and bearings result in abnormal size and number of debris in the lubricant oil. Therefore, monitoring the oil and debris inside it could be a good measure of health monitoring. In another technique which is somehow related to the debris in the gas paths in the inlet and exhaust section, the number of debris could be analysed in the same manner.

- Vibration monitoring

Loss of blades, fouling, erosion, or failure in rotating parts of the engine results in unbalance rotor and it can be detected by monitoring the engine vibration at all operating speeds.

- Life usage monitoring

In this approach the level of damage in critical components such as disks and blades are monitored and their remaining useful life are computed [29].

- Gas path performance monitoring

This method is also called gas path analysis and module performance analysis. It is performed based on the measurements of air/gas flow properties such as temperature, pressure, and density to detect failure in the engine components. In other words, the gas path analysis

is a performance analysis method that can also provide estimation of the fault severities. Since the first attempts in 1972 in this field, a vast body of works have appeared in this area and many research results are published [27, 26, 14, 30].

- Visual inspection

This is based on regular inspection of the engine and scheduled maintenance of the system.

- Borescope inspection, X-ray checks, eddy current checks, turbine exit spread monitoring, etc.

In order to examine possible mechanical damage, crack or other abnormalities in the airframe structure of the aircraft non-destructive testing methods which are cost effective inspection methods are conducted during the procedure of the gas turbine engine maintenance. Borescope inspection, X-ray checks and eddy current checks are the examples of non-destructive testing methods [31]. Borescope or endoprobes is a precise optical instrument which consists of a high precise optical system with high intensity light sources and is used to detect the above damages in the engine. More advanced borescopes are equipped with magnification options and other accessories that help the maintenance team to perform inspection procedure effectively. When a conductor of electricity is exposed to an alternating magnetic field, electrical currents are induced within the conductor which are well-known as Eddy currents. Eddy currents inspection are widely used to detect the surface and subsurface anomalies and corrosion in fastener holes of the engine [31].

However, in order to implement an effective and complete solution for fault diagnosis and health monitoring system of gas turbine engines usually a combination of above techniques is used. Fusion of vibration monitoring and gas path analysis is utilized in [32, 33]. In [34] Dempsey and Afjeh presented a hybrid fault detection method based on vibration and oil analysis of helicopter gearbox. In an ambitious program, which is initiated by NASA a while ago and presented in [35], the researchers attempted to fuse different data

sourced listed above. However, they faced several problems to fuse different available data streams and they fused two different gas path analysis (GPA) methods in their work [27].

Due to the nature of GPA, it results in a deep understanding of the engine components performance and therefore reveals gradual degradation mechanisms along with abrupt faults. Furthermore, it can be used to detect faults and malfunctions in sensors and engine control systems. It also provides estimation of the engine parameters such as shaft power, thrust, overall engine efficiency, specific fuel consumption and compressor surge margin which are not directly measurable. Another important engine health indicator that could be calculated based on GPA is the deviations in the measured variables that are caused by faults and deterioration of the engine [25].

In this section a number of advantages in employing an effective maintenance have been addressed. On the contrary, non-proper and poor maintenance of a system may cause severe and more frequent damages and failures in the system's components along with unexpected delays in production schedules [21].

1.1 Motivation of the Work

With emerging more complex systems, their maintenance procedures are becoming more and more expensive and more time consuming which eventually increase the down time of the system. This condition combined with necessity of meeting safety criteria and productivity need lead researchers to work on new possible methods and technologies in the maintenance field. One of the main drawbacks of conventional maintenance (corrective or preventive) methods is that a component may get changed before it is really necessary or it may go through the maintenance process when it undergoes the fault or a failure because of a broken component [2]. One of the common solutions to cope with these situations is employing condition based maintenance (CBM) techniques. Number of CBM techniques have been introduced in the literature so far but it predominantly consists of continuous

monitoring of the important parameters of the system or health parameters of the system to realize when they reach to their associated predefined thresholds and scheduling for appropriate actions based on the health state of the system [2].

Based on an analysis conducted by Trcka [36] main causes of aircraft accidents originated by factors such as flight crew, mechanical and maintenance, miscellaneous and unknown faults, 16% of the aircraft accidents are raised from mechanical and maintenance condition and in this category 70% of break down goes for engine and propulsion system.

One of the promising methods of maintenance to reduce the maintenance cost, system downtime, boost the safety of the system, plan successful missions, and finally the schedule maintenance is revealed to be prognostic. Furthermore, a growing interest has appeared in industries in this topic and it has become one of the most interested research areas [37].

1.2 Literature Review

As mentioned earlier, CBM is a combination of several procedures including data collection, signal processing, feature extraction of the collected data, fault detection and isolation, failure prognosis and finally decision making. In order to achieve an appropriate CBM for a process or a complex system, one needs to develop health monitoring and management strategies as well as employing a proper diagnostic, isolation and prognostic schemes so that the condition of all the critical components of the process are being monitored and analyzed. Next, the maintenance procedure will be scheduled based on the remaining useful lifetime (RUL) of the components which is the outcome of the health management analysis [38]. This complete framework is also known as a diagnosis, prognosis and health management system (DPHM). It is clear that the overall performance of a DPHM system is highly dependent on the performance of both the fault diagnosis and the failure prognosis schemes. These two schemes and their relationships will be presented in detail in the following sections.

Fault Diagnostics versus Prognostics

Any undesired or unexpected deviation in a system's behavior from its normal and desired function is called a fault. Fault diagnostics schemes comprise of three main tasks namely, fault detection, isolation and identification (FDI) [39]. In fault detection stage any unexpected abnormal behavior in the system of interest is detected. Then in the fault isolation step the faulty component in the system is determined and its location is spotted and finally the severity and type of the detected fault is estimated in the fault identification stage.

A number of definitions for prognostics has been rendered in the literature [40, 41]. "An estimation of time to failure and risk for one or more existing and future failure modes" is the definition introduced by International Standard Organization (ISO13381-1) [40]. Although there is no explicit and clear line of demarcation between fault diagnostics and prognostics, their relationship and dependence of prognostics on diagnostics is almost an acceptable fact in the literature [40]. Sikorska *et al.* in [40] rendered a demarcation between prognostics and diagnostics. According to their definition, in diagnostics one deals with identification and quantification of the damage or fault that has already happened to the system, whereas in prognostics one deals with predicting the damage which has not occurred yet. It is worth mentioning that despite the valuable outcomes of fault diagnostics methods such as fault signals, prognostics is dependent upon the diagnostics outcome.

Figure 1.3 depicts the demarcation line between fault diagnostics and prognostics. Automated fault detection following by identification and isolation of the detected faults is the modern notion of diagnostics and automated estimate of the time to a failure in the system is the modern definition of the prognostics [41]. Although research in the prognostic field is a relatively new area in the CBM, prognostics have shown promising results in reducing expensive downtime, disaster conditions, and increasing the safety and availability of the system of interest [41].

Prognostic is the ability to predict the time at which a component will no longer perform

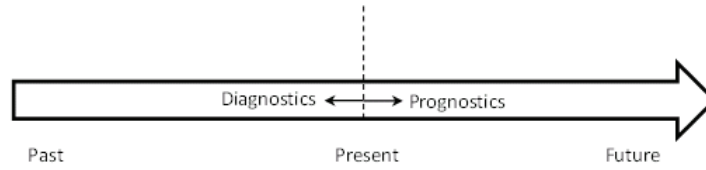


Figure 1.3: Prognostics and diagnostics in terms of time [2].

its desired task through continuous monitoring of the system and tracking the existing faults growth. Prognostic is willing to find the remaining useful lifetime of a component or a system [5].

1.2.1 Fault Diagnostics

Diagnostics methods can be categorized into two main categories namely, hardware redundancy and analytical redundancy [42]. Hardware redundancy is referring to the traditional diagnosis methods in which one uses multiple sensors, actuators and components to measure or control the variable of interest. Then, employing voting technique one can decide if any fault has occurred or not and based on the decision, one can identify the faulty component. The problems associated with this traditional diagnosis method are the required space for the redundant components which make the system of interest bulky and as well as high-cost of the extra components that are needed as hardware redundancy. On the contrary, in analytical redundancy or software redundancy one uses the analytical relationships between various variables measurements of the system and the difference between a measured variable and its estimation generates the residual signal which leads to determining whether a fault has occurred or not [39, 43]. As in analytical redundancy approach one employs the mathematical model of the system of interest instead of using the redundant components. This is also known as the model-based approach to fault diagnosis [3]. Figure 1.4 depicts the hardware and analytical redundancy concepts.

Generally, the analytical fault diagnosis approach is comprised of two main parts namely

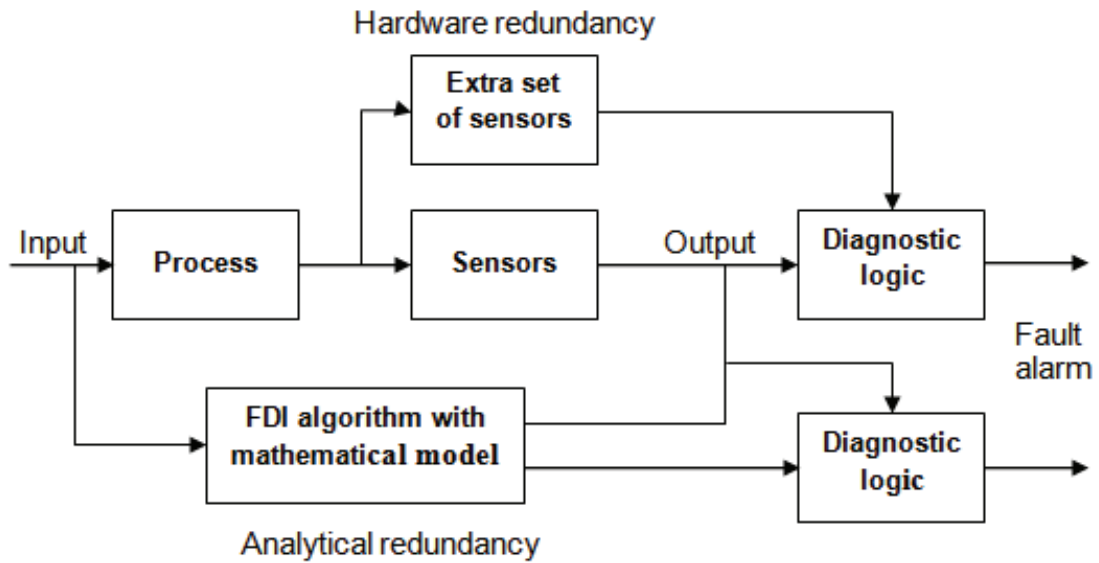


Figure 1.4: Comparison between hardware and analytical redundancy concepts [3].

residual generation and residual evaluation or decision-making [44]. In the residual generation step, one employs all the available measurements of the system under monitoring to generate the residual signals. As long as the residual signals are close to zero the system is fault-free. In the residual evaluation stage, one analyzes the generated residual signals in order to examine the likelihood of occurring faults. This procedure is accomplished based on a decision rule. There are number of approaches in the literature for selecting decision rules such as setting a predefined threshold on the moving average of the generated residuals or statistical approaches such as sequential probability ratio testing and likelihood ratio testing [45] or knowledge-based approaches such as fuzzy logic [46]. In [47], the authors have proposed an adaptive threshold for decision-making process. Figure 1.5 depicts the concept of the analytical fault diagnosis structure [4].

Analytical fault diagnosis approaches are based on the type of the required information

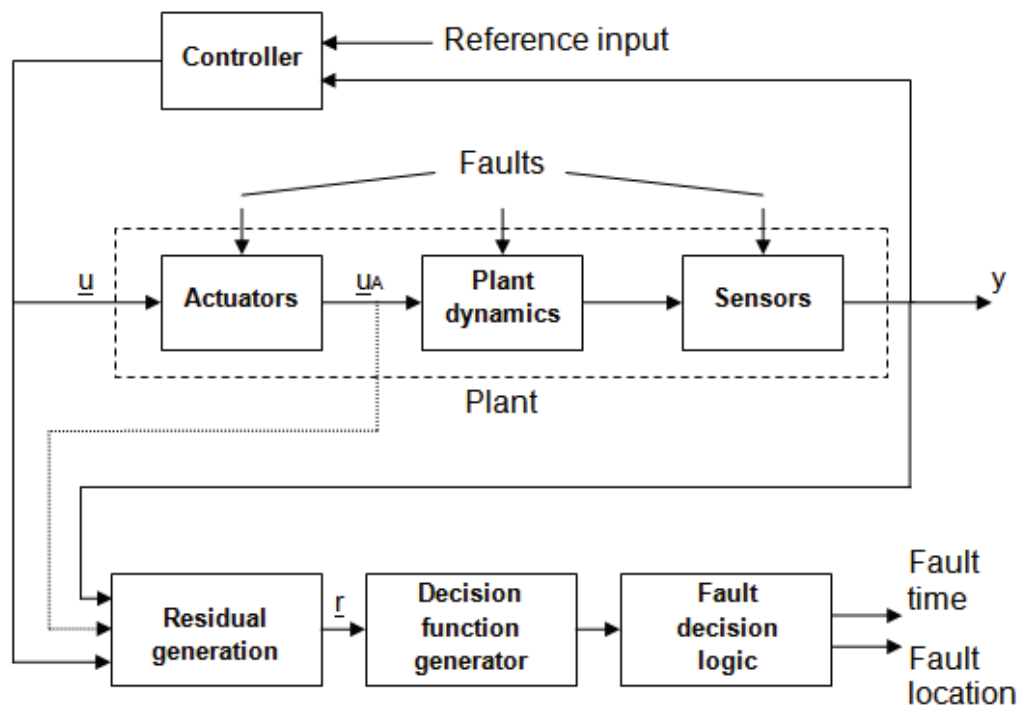


Figure 1.5: Concept of an analytical fault diagnosis structure [4].

about the system under study and can be categorized into two categories namely, model-based and computational intelligence (CI)-based fault diagnosis approaches [44]. In model-based fault diagnosis approach one uses system mathematical model derived based on the physical principles [48, 42] and one needs to have a good knowledge of the system in terms of the relationships among its variables that are not always feasible to obtain. Computational intelligence (CI)-based approach deals with historical data and data-driven models of the system under study and one does not require a precise mathematical model of the system [4, 43]. Model-based fault diagnosis methodology emerged in the early 1970s, affected by the observer theory which was proposed and established nearly at that time [42]. Beard and Jones [49, 50] introduced the first model-based fault detection approach which was called failure detection filters. Model-based fault detection has developed significantly since then and has become an important and inevitable part of any automatic control system [42]. Various techniques have been introduced in the literature for both the model-based and the CI-based fault diagnosis approaches including Isermann [48], Mrugalski [51], Frank [4] and Ding [42] which will be discussed further in this section.

In [4], Frank provided a complete survey on the major achievements in model-based fault diagnosis field and he classified the model-based techniques into the following three categories:

- Observer-based techniques
- Parity space techniques
- Parameter estimation techniques

In observer-based or filter-based techniques, one may employ Kalman filter (in stochastic framework), Luenberger observers (in deterministic framework) [52, 53] or sliding mode observers [54, 55] in order to obtain system states estimation from measurements [56]. The difference between the actual measurements and their associated estimates forms

the residual signal. According to [57, 42], it has been shown that there exist relationships between the above mentioned approaches. For example, the parity space methods can be considered as a special case of observer-based methods [58]. Moreover, the observer-based techniques and the parameter estimation techniques have similarities in residual generation stage of the fault diagnosis but they are different in the residual evaluation stage [42]. In addition, various choices of the observers along with increasing demands on using state-space models have made observer-based fault diagnosis techniques as one of the most popular approaches in this field [56].

In [59] a bank of Kalman filters were employed in order to detect and isolate sensor and actuator faults in conjunction with the components faults detection for an aircraft engine. In [13] the authors proposed a hierarchical multiple model approach by using both extended Kalman filter (EKF) and unscented Kalman filter (UKF) which could perform detection and isolation of concurrent faults in the jet engine.

In parity space techniques [60], in order to generate the residual signals one employs parity functions which are defined over a time window of the system input and output data. In other words, the residuals or parity vectors are generated through monitoring and verifying the existence of any inconsistency in the input and output data of the system under study over a predefined time window [56]. As mentioned earlier, the parity space approach is a special case of the observer-based method when the high-gain observer-method is employed [44]. Due to the higher sensitivity of the parity space approach to the measurement and process noise as compared to the observer-based approach which is more robust to the disturbance and measurement noise, observer-based methods are of more interest among the researchers. In [61] a parity space-based fault diagnosis framework is used in order to detect and isolate sensor faults in the vehicle lateral dynamics control system.

Faults may arise from sensors, actuators or physical system under study. Sensor faults occur due to incorrect readings from the installed sensors on the system. Actuator faults

indicate malfunction in control action of the system and component faults indicate changes in the physical parameters of the system under study [62]. The third group of the faults, i.e. component faults are usually handled by parameter estimation techniques [63]. In parameter estimation-based fault diagnosis techniques, the system parameters are estimated on-line and the estimated parameters are compared to the parameters of the reference model which was obtained initially when the system was fault-free. References [62, 64] have provided more details on parameter estimation-based approaches for fault diagnosis and its implementation for some applications.

Due to the computational simplicity of the parameter estimation-based techniques along with the recent development of the parallel computing techniques, the parameter estimation-based techniques are promising candidates for performing real-time fault diagnosis for the systems with low complexity. Parameter estimation-based techniques are also used for fault tolerant control (FTC) design as in the parameter estimation-based methods the faulty model parameters are estimated continuously which can be used for updating the controller parameters [65]. Main disadvantages of the parameter estimation-based techniques are weak robustness to the external disturbances and performing an accurate parameter estimation by these techniques are very time consuming and may not be applicable for many complex systems. For these reasons many researchers such as [66] and [57] are employing parameter estimation-based techniques with other techniques such as parity space methods or CI-based techniques in order to get better results in terms of accuracy and robustness. Computational intelligence-based fault diagnosis approaches can be categorized into the following three categories [67]:

- Artificial neural networks
- Fuzzy logic-based techniques
- Evolutionary algorithms

Artificial neural networks consists of a number elements known as neurons which are highly interconnected through weighted links. According to the selected neural network architecture and the weighted links, each neuron acts as a mathematical function which maps the inputs to the output space. The outputs of the neurons have an effect on one another and all the neurons together may represent the complex process or system under study [68]. Neural networks have been frequently used for fault diagnosis purposes in many applications [69, 70]. Dynamic neural networks [71, 72], autoassociative neural networks [43, 73, 74], recurrent neural networks [75, 76], multi-layer perceptron networks [77], wavelet neural networks [78], radial basis function neural networks [79] and their integration with other methods such as fuzzy logic and genetic algorithms [80, 81, 82] show the variety of utilization of artificial neural networks in the field of fault diagnosis.

Mohammadi *et al.* in [71] proposed a dynamic neural network-based fault diagnosis platform in jet engines which is similar to the feed-forward multi-layer perceptron neural network except that the neurons in the proposed neural network have dynamical properties. In their work each dynamic neuron entails three modules namely, adder, linear finite impulse filter and a nonlinear activation module. Autoassociative neural networks have been widely used for data validation and faulty sensor correction purposes. In [43] autoassociative neural network is utilized for noise reduction, filtering outliers and sensor correction in aircraft jet engine. Autoassociative neural networks have shown considerable robustness in presence of sensor faults and noise [43]. In [74] the authors have utilized a set of autoassociative neural networks in which each neural network has been set for particular fault mode in power transformers. A recurrent neural network-based fault diagnosis approach namely, recurrent adaptive time delay neural networks (ATDNN) has been developed in [75] for a satellite. The faults are originated from the actuators in the attitude control subsystem of the satellite. Their proposed recurrent neural network is capable of performing fault detection and isolation of concurrent faults satisfactory.

As mentioned earlier, neural network-based fault diagnosis approaches have been utilized in many applications and domains. In [77] a multi-layer perceptron neural network was employed in order to perform detection and isolation of the high impedance faults in distribution networks and to identify this type of fault from other similar faults such as adjacent feeders faults and insulator leakage current. The features which were used for training part of these neural networks were obtained by using a new pattern recognition-based algorithm. Yangwen in [78] has investigated two neural network-based fault diagnosis approaches namely, wavelet neural network and back propagation neural network for rotating machinery systems. Wavelet neural network is formed based on wavelet transform principles in which a wavelet function is used as excitation functions of the neurons. The results and comparisons in his work have shown that wavelet neural network could overcome the drawbacks of back propagation neural network. Chen *et al.* in [83] investigated neural network-based fault diagnosis schemes for the fuel system of an automobile engine and radial basis function neural network has shown better performance when the system is under multiple fault symptoms. In radial basis function neural networks the nonlinear mapping function associated with each node in hidden layer of the network is different from each other and this leads to have a faster learning speed [83].

In [80] the author proposed a hybrid neural network-based fault diagnosis scheme in which the optimal link weights are obtained by using genetic algorithms for a chemical reactor and it was compared with conventional back propagation neural networks. Li *et al.* in [81] have employed genetic algorithm in order to optimize the radial basis function neural network for fault diagnosis purposes in analog circuits. Genetic algorithms have enhanced the performance of the neural network in terms of getting trapped into the local minima. Zhang *et al.* [82] have proposed fuzzy neural network-based fault diagnosis approach for rotary machines of an oil plant water pump sets. In this approach based on defining a series of standard fault pattern pairs (fault symptoms and fault) and using fuzzy logic the fault

diagnosis system is capable of functioning when the unknown samples are inputs to the system.

Fuzzy systems are promising candidates for decision making purposes when the measurements are not precise and for systems in which the interpretation of the measurements depends on the context and the human judgment i.e. in the form of *if-then* rules [68, 70]. It is worth mentioning that in many applications, one may not be able to obtain a comprehensive expert knowledge nor qualitative physics of the system of interest in order to provide the fuzzy *if-then* rules and this can be considered as a disadvantage for fuzzy logic-based approaches. However, when providing the proper set of rules for a system is feasible one is able to get benefits from advantages offered by implementing expert systems or fuzzy logic-based fault diagnosis approaches such as transparent reasoning and ability to function under uncertainty in order to find the reason and its associated case [84].

There are many articles investigating different expert system-based fault diagnosis approaches for engineering applications such as [85] and [86]. A hierarchical fault diagnosis scheme based on fuzzy logic was proposed in [87] for satellites formation flight. The proposed method improved the autonomous fault diagnosis procedure at ground stations. It is prompting the operator to the potential faulty components that need to be closely observed. In order to improve the performance of the fault diagnosis schemes similar to neural network-based fault diagnosis approaches, integrating fuzzy logic-based with other non-model-based [84] or model-based techniques [88] is quite popular.

Salar *et al.* [88] have proposed a hybrid extended Kalman filter-fuzzy based fault detection and isolation for industrial gas turbines. Employing extended Kalman filter the health parameter changes of the system are estimated and then a fuzzy system obtained by empirical data and the Kalman filter outputs performs the fault locations in the compressor or turbine. In [84] the authors developed a fuzzy logic-based fault diagnosis scheme for performing gas turbine fault isolation. In order to maximize the fault isolation success rate

in their work a genetic algorithm is used to tune the fuzzy sets. Their results showed how the errors originated from human trial and error decreased in the design phase of the fuzzy system. Also in [84] the authors used a radial basis function neural network for preprocessing the measurements before the isolation stage which eventually led to a robust fault diagnosis approach.

Evolutionary algorithms are dealing with stochastic optimization algorithms inspired by Darwins theory of evolution and natural selection [67]. Evolutionary algorithms and their applications have been deeply investigated in [67, 89, 90]. In [91] the authors have proposed a genetic programming-based fault diagnosis approach for aircraft jet engines. Using genetic programming the interrelations among different engine parameters during take off and cruise flight phases are derived and is followed by estimating the exit turbine temperature as a significant health parameter of the jet engines.

Despite existing conventional fault diagnosis approaches such as robust observer-based techniques which are working seemingly robust under uncertainties, there still exists the problem of mismatch between the linearized model and the nonlinear model of the system under study. Poster and Passino [67] introduced a genetic adaptive observer approach to cope with this problem. As an efficient optimizer, genetic algorithms have been widely used in combination with other methods such as fuzzy logic-based and neural network-based approaches [92, 93, 94].

1.2.2 Failure Prognostics

Prognostic emerged as an area of interest by the modal analysis community [37]. It was originally dealt with the fracture mechanics and fatigue. Early on, prognostic was about prediction of the remaining useful life (RUL) of the system. Then by developing different techniques in this field, it was also defined as a probability measure which described the probability of a system working without failure for a specified future time [37]. In this

perspective, prognostic has achieved a few acceptance among the researchers and there is a small number of papers based on this definition of prognostics. The prediction part is the common phase of all the mentioned prognostics definitions which is about estimating the RUL of the component or system. One can find other terms in addition to RUL, such as estimated time to failure (ETTF) or probability of the system of interest operating properly and without failure [2].

Failure prognostics has been approached through a number of techniques introduced in the engineering applications (such as gas turbine engines). These techniques encompass a wide range of methodologies and tools such as artificial intelligence methods, probabilistic and statistical methods, Bayesian estimation techniques, adaptive Kalman filtering, time series modeling, stochastic autoregressive integrated moving average models, Weibull models, pattern and cluster search-based approaches, parameter estimation methods, neural networks, etc. [5]. Failure prognostics methods can be divided into three main categories namely, model-based approaches, data-driven-based approaches and experience-based (knowledge-based) approaches [2, 5, 18]. Figure 1.6 depicts different prognostics approaches based on the range of applicability of the systems and also their accuracy and cost. It is worth mentioning that despite the above mentioned generic prognostics approaches, designing a prognostic scheme becomes specific for the application of interest [5].

Model-based prognosis schemes work based on an accurate mathematical model of the system as well as the degradation model. The analytical model demonstrates how the system functions along with the degradation incident [2]. Modeling procedure can be performed at two levels namely, micro and macro. Macro level models represent the mathematical model of the system which demonstrates the relationships among input variables, system state variables and measurement variables or system outputs. Macro level models are simplified forms of representing the system. Then a model uncertainty will

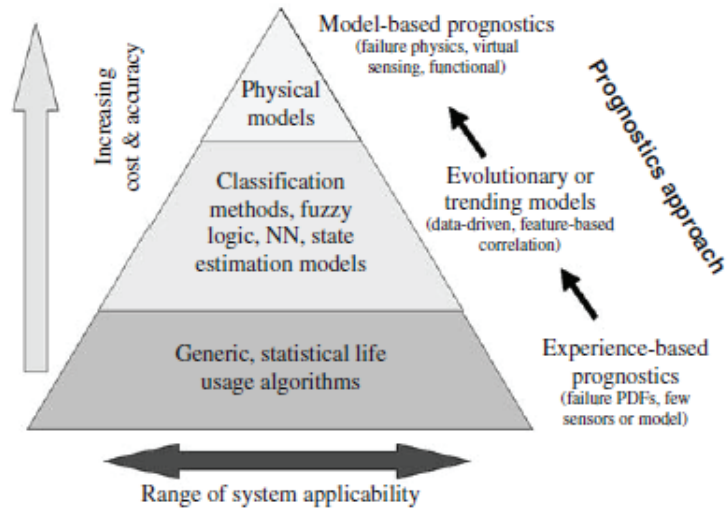


Figure 1.6: Prognostics technical methods [5].

be considered to manage these simplifications. At micro level modeling, relationships between the operational condition of the system and degradation of the system components at a given time are described by a set of dynamical equations associated with their corresponding physical models [95]. For example modeling of the damage propagation is often performed at the micro level modeling.

When a complete understanding of first principles of the system operation are not available or developing an accurate model of the system is expensive due to its complexity, model-based methods are not applicable for prognostic purposes. On the contrary, data-driven methods are capable of predicting the degradation growth trend without requiring to have the degradation mathematical model. Despite the valuable benefit of using data-driven methods, they are less precise than model-based methods and their accuracy is highly dependent on the quantity and quality of the operational data. Utilizing more informative data leads to better results in terms of accuracy and reliability in data-driven based methods. Applicability and easy implementation are other advantages of using data-driven methods [95, 96].

In data-driven prognostics, the data collected by the appropriate sensors installed on the

system for monitoring purposes are taken into an analysis procedure to detect any degradation indication [2]. The measurements usually include parameters such as temperature, pressure, oil debris, currents, voltages, power, vibration and acoustic signals, spectrometric data as well as calibration and calorimetric data, etc. Outcome of the analysis procedure is the prediction of the remaining time before the system fails following the reach of critical parameters of the system to specific values. These specific values can be derived by using either available standards and manuals provided by the manufacturers or failure history of the system of interest. In order to prevent catastrophic failure of the system due to its degradation evolution, the aforementioned predefined final values are defined with enough safe margins [97]. Some other factors that should be taken into account for determining these predefined limits that are so-called "alarm limits" are confidence level required for prognosis, required time for spare parts delivery, extrapolation of the parameters trends and their behavior [97].

For prognostics purposes, to deal with uncertainties associated with the degradation and system models and measurement noise, one determines the confidence intervals besides determining the absolute value of the RUL. Number of methods have been introduced to calculate the confidence intervals. In [97], a number of factors which may have effects on these intervals have been introduced and suggested. Figure 1.7 depicts the RUL and its corresponding confidence. Two types of uncertainties are shown in this figure. One uncertainty is due to the prediction and the other one is associated with the threshold value [2].

In experience-based prognostics, the operational data of the system should be collected over a significant time so that it includes the maintenance and operating data, historical failures, etc. Then the data is used to form some reliability models such as Weibull and exponential models [2]. These models will be used for determining the RUL of the system under investigation [2].

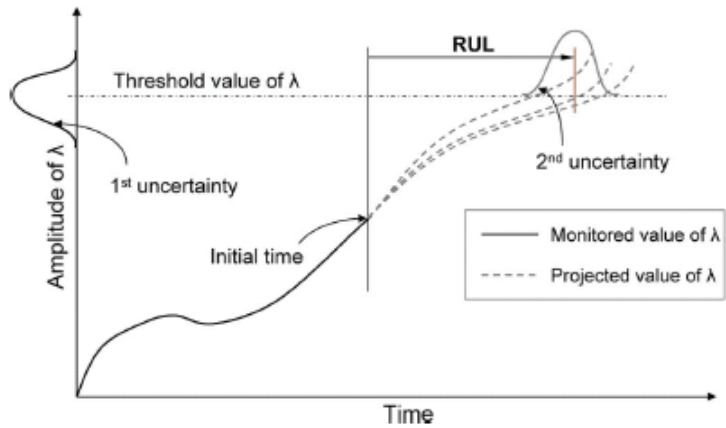


Figure 1.7: Uncertainty associated with RUL [2].

Some of the above mentioned failure prognostics methods in the literature will be presented in the following. References [98, 99] have investigated different prognostics approaches which have been used in the literature for different engineering systems including gas turbine engines.

One of the popular application of model-based prognostics approaches is crack growth modeling [100, 101, 102]. Li *et al.* in [100] have proposed an adaptive model-based approach for predicting the defect growth in rolling element bearing system. They employed vibration measurements and predicted defect sizes for estimating and fine tuning the parameters of the propagation model. In [102] a spur gear fatigue crack prognostic scheme by using Paris crack growth model for crack propagation has been developed for predicting the remaining useful life time of a cracked gear. In [101] Chana *et al.* have investigated a crack propagation in a cyclic engine test and evaluate the accuracy and capability of the tip-timing measurements taken from an eddy current sensor (QinetiQ) and a prognosis software system called "Reasoner". This software has been used to isolate a crack and predict the remaining useful lifetime of the blade. Spey RB168 MK 101 engine with titanium blades has been put under this examination. The tip-timing data coming from the eddy sensors has been used to verify the movement of the blade due to disc crack growth. The

prognosis reasoned software combines the data from the sensors with physics-based models for monitoring the cracks growth and identification purposes. Their results proved the ability of the software for identifying the crack presence, its location, size and determining the remaining useful life time of the blade under study.

Considering the fact that all the subsystems of any complex system are somehow under deterioration, Abbas *et al.* in [103] worked on the interaction of subsystems deterioration on one another and eventually on the failure prognostic problem in the turbofan engine of avionic propulsion systems. This phenomenon accelerates the trend of failure process for the system under study.

In [103] Abbas *et al.* have investigated how the degradation in high pressure compressor (HPC) and low pressure compressor (LPC) influence on creep damage of high pressure turbine blades for an avionic propulsion system of aircraft engine. Creep phenomenon in the HPT blades is considered as one of the major failure causes in the aircraft engines. The results of this investigation have shown that creep damage growth in the HPT is linear as long as other subsystems are operating in healthy condition. This research [103] also showed that the effect of HPC deterioration on HPT creep damage evolution is much higher than the LPC deterioration and their results were supported by using C-MAPSS simulation platform.

Sankavaram *et al.* [104] have proposed an approach for failure prognosis of the coupled systems such as automotive systems incorporating three types of data (failure time data, status parameter and dynamic data). In the proposed data-driven prognosis framework two methods namely soft dynamic multiple fault diagnosis (DMFD) and Cox proportional hazards model (Cox PHM) have been employed for deducing the degraded trends of the components and estimating the components RUL. Also, this approach has been applied for estimating RUL of an automotive electronic throttle control system by using a simulator.

In order to predict the remaining useful life time of an automotive suspension system

which has multiple operational modes Lue *et al.* [105] have proposed a model-based prognostics approach by employing interacting multiple model (IMM) filter for estimating the degradation measure and time-averaged mode probabilities for predicting the remaining useful life time of the system. In [106] a model-based approach for health monitoring of an industrial gas turbine has been introduced. This work developed an extended Kalman filter observer which compensates the effects of the ambient conditions.

Wang and Vachtsevanos [107] have presented a prognosis approach comprising of a dynamic wavelet neural network as a predictor and a static virtual sensor as a mapping gadget between known measurements and faulty data. The dynamic neural network tends to determine the evolution of the failure mode over time and estimate the component's RUL. This prognosis framework has been utilized for a damaged bearing with a crack in its inner race. The damaged bearings or weak mounting screw brings a pump to vibrate and in this approach the vibration measurements are monitored via an accelerometer.

Mejia *et al.* [2] have introduced a data-driven prognostics method which has been verified on real data linked to the bearings. This method works by using a mixture of Gaussian hidden Markov models (MoG-HMM) which are capable of managing complex probability density functions (pdf). In order to extract a proper set of features from the raw collected data, they have used wavelet packet decomposition (WPD) and the pdfs are generated from the obtained features.

In [108] Wenskey *et al.* have investigated the effects of environment on the performance degradation and useful life of the modern aero engines. The authors divided the problem into two areas namely, erosive and anthropogenic areas and their survey was accomplished upon these two categories using engine overhauls data at MTU maintenance. Erosive effects address the most effective natural causes (i.e., dust) on the engine performance. These particles mostly manifest themselves on the HPC by increasing the speed of scrapping the HPC airfoil owing to erosion. Anthropogenic areas address those that are more exposed to

the chemical and industrial pollutants. Considering nitrogen dioxide (outcomes of burning fossil fuels) as a proper indicator for these types of pollutants, scrap growth in the HPT will be accelerated due to the chemical pollutants. In this study the data taken from about 70 engines (General Electric CF6) have been analyzed. Wenskey *et al.* quantified the above environmental effects by using the gradient of delta exhaust gas temperature (dEGT) per cycle. They showed that the interaction of these two environmental factors may double the maintenance cost.

As mentioned earlier, vibration signal analysis is one of the useful monitoring methods especially in CBM of mechanical systems. Any noise added to the vibration signal data can influence the overall performance of the CBM. In order to improve the signal to noise ratio of the data coming from a helicopter gearbox test bed, Zhang *et al.* [38] have introduced a new de-noising procedure. The proposed procedure in [38] consists of a de-convolution de-noising procedure in parallel with an effective feature extraction and modeling the vibration so that informative features can be extracted from the noisy signals.

In [109] Ganguli has developed a fuzzy logic system in order to model the structural damage of a helicopter rotor blade. Using a finite element model of the rotor blade, one is capable of determining the blade frequencies changes and later the changes due to the damage are fuzzified. Ganguli has proposed a fuzzy logic to detect four levels of damage in the rotor blade at five locations across the blade.

In [110] Naeem *et al.* has taken the fuel usage as the most important criteria which highly affects the overall effectiveness of an aircraft as the fuel weight is highly related to the load and passengers number that can be transported. Using a computer program called PYTHIA which is developed by Escher *et al.* [111], consequences of engine degradation based on the fuel consumption are predicted over an assumed military aircraft mission scenario including multiple flight phases. Therefore, predicting the engine degradation leads to making more reasonable decisions about the appropriate time for an aero-engine

to get removed from the aircraft for going through maintenance procedure.

Naeem [112] has accomplished a comprehensive research in quantifying the different degradation effects on the engine of a military aircraft and its components on the HPT blades creep life, HPT blades low cycle fatigue (LCF) life consumption, engine's fuel usage, effectiveness of mission operational and HPT blades thermal fatigue life. The results showed that the take-off phase has the most impact on the missions operational efficiency. Also the HPC has the most impact on the missions operational efficiency in comparison to other engine components such as LPC, low pressure turbine (LPT) and HPT. In addition, HPT deterioration has the most impact on the fuel consumption.

In [113] Abdul *et al.* have investigated the effects of a hot section component's creep life (high pressure turbine) on a single spool turbo-shaft gas turbine engine performance under its different health conditions (such as compressor fouling and turbine erosion) and operating points (such as engine's speed, altitude and ambient temperature). The quantitative value of the creep life is determined based on a model-based creep analysis approach by introducing creep factor that is defined as the ratio between the actual creep life and the reference creep life (this reference or threshold is defined by the user). Their results showed among the engine speed, altitude and ambient temperature, the engine speed has the highest impact on the creep factor and as the degradations have occurred concurrently the impact on the creep factor will be more severe.

An approach towards assessing the general engine performance between two maintenance procedures has been introduced by Ebmeyer *et al.* in [114]. This analytical method consists of two tools namely GasTurbTM and MTU-engine trend monitoring (MTU-ETM) which are thermodynamic gas path models and are modular based. ETM-MTU tool is used for monitoring the in-flight engine parameters and the measured data (also called on-wing data) is transferred into the ground station via aeronautical radio incorporated (ARINC) for analysis purposes. The authors used these two tools, on-wing and off-wing data to

perform the engine on-wing performance degradation. Fan, LPC, HPC, combustor, HPT, LPT and nozzle form the modules and the parameters which have been used for evaluating these modules, and where performances are pressure ratio, isentropic efficiency, change of specific enthalpy and capacity corresponding to a standard day. This approach has been applied to a General Electric CF6 engine.

Number of work and investigations have been accomplished in failure prognosis in the context of discrete-event systems (DES) [115, 15]. In [115] the authors investigated the failure prognosis in real-time discrete-event systems (RTDES) and they modeled the system by timed automata (TA). The proposed approach is based on a diagnosis algorithm which was introduced by these authors before [116]. This prognosis method has been formed by modifying the real-time prognosis problem via employing TA transformation and transferring the real-time prognosis problem into the non-real time prognosis problem. Based on the authors' claims, the state space explosion problem is significantly reduced by using this method as compared to other prognosis methods. State space explosion problem which refers to the case that the state space of the system is very large or even infinite is one of the most serious problems with model checking in practice.

In [117] the growth and evolution of faults are defined by using deterministic or stochastic models, as the faults are considered to change continuously. In order to get benefit of model-based prognostics approaches along with overcoming their drawbacks and in order to increase the reliability and the performance of the prognostics procedures, the hybrid approaches have been extensively used for engineering applications [118, 119]. In [118] the authors have fused monitoring data (vibration features) and fatigue model of the components and utilized it for calculating remaining useful life time of the critical components of the gas turbine engines.

Time-series analysis techniques are another popular data-driven prognostics approaches

which have attracted attention of many researchers in different fields from economic forecasting [120, 121] and biological data analysis [122] to control systems and signal processing domains [123, 124, 125].

Autoregressive moving average (ARMA) models as a time-series-based techniques in prognostics have been used in many practical applications. For example, in the railway industry turnout system is used to determine the direction of a train by moving rails. In [126] the authors have proposed an ARMA model to predict the future health condition of the electro-mechanical turnout system with exponential failure degradation and have determined the remaining useful life time of the system successfully. In [127] the authors have employed two prognostics approaches, namely ARIMA and hidden Markov model-based techniques to detect performance changes of the water level sensor for a steam separator system used in thermal power plants and the results for both approaches were acceptable. However, the results of hidden Markov-model based approach showed better performance in terms of delay time and error probability due to employing cross correlation functions between available measurements of the system such as water level, water and steam flow.

In [14] Marinai has proposed a new method for gas path diagnostics and this method was developed based on fuzzy logic and was tested for the Rolls-Royce Trent 800 engine. Mariani has worked on engine performance analysis based on time-series methods and regression methods and has rendered a prognostics platform in order to perform short-term and long-term predictions considering factors such as maintenance and extra fuel originated from the engine degradation and deterioration. In [128] the authors in order to reduce the cost of maintenance and fuel consumption in turbofan engines have employed two time-series-based techniques namely ARIMA method and regression analysis to perform deterioration in a turbofan engine. Their results have shown that ARIMA method has better performance for shorter term predictions and regression analysis are preferable for long-term predictions.

In order to be able to perform performance prediction with longer horizons for engine systems, Want *et al.* [129] have proposed a method consisting of a Match matrix and auto regressive moving average method. In their approach the feature vectors (a signature describing the engine health status) from past maintenance cycles were used for the new maintenance cycle through this Match matrix which eventually led to better prediction horizon. In [130] the authors have proposed a time-series based prognostics scheme determining the RUL of an autoclave burner which is an industrial equipment by using an artificial neural network and a sliding window technique.

To conclude this section, it is worth mentioning that both data-driven and model-based approaches have been widely used in the literature and practice. However, compared to fault diagnostics, failure prognostics are much less addressed in the literature. Model-based approaches provide more accurate and robust results in comparison with data-driven approaches. Choosing an appropriate approach depends on many factors. Availability of the mathematical models of the system, having a good understanding of the physics of the system under study, feasibility of performing identification procedures such as exciting the system's modes by feeding the system with different inputs and finally cost associated with deriving the mathematical model of the system or degradations are all important factors that determine whether or not a model-based prognostics approach should be utilized.

In contrast, data-driven approaches are more applicable and easier to implement along with lower cost when compared to model-based approaches. In other words, data-driven methods allow one to predict the evolution trend of the degradation of the component or system of interest without any need of having prior mathematical model of the degradation [96]. However, they are less accurate than model-based techniques and are more sensitive to noise which have motivated the researchers toward employing hybrid approaches rather than using pure model-based or data-driven approaches.

1.3 Statement of the Research Problem

The main objective of this thesis is to investigate the degradation prognostics in gas turbine engines by using time-series and fuzzy based methods. Prognostics is one of the inevitable parts of any health monitoring system. An efficient prognostics scheme lets the maintenance team plan maintenance procedure so that it supports a smooth transition from faulty condition to a functional and healthy state. Taking advantage of such a prognostics scheme holds the promise of having a considerable cost saving by avoiding unscheduled maintenance along with boosting the operational safety by employing condition-based maintenance strategies.

The ultimate goal of the prognostics is to answer the question on whether the system under study is able to continue working properly or not and for how long it can function without any problem based on its past and current health condition. The more complex the system is, the more important and challenging the issue becomes. Aircraft engines, power plants, medical equipment are examples of such complex systems as their downtime, availability and safety are critical.

Gas turbine engines as in other mechanical systems which work under different conditions, such as high temperature and stress undergo degradations. For the case of gas turbine engines, these degradations may occur in different paces. Sensors faults, system failures and foreign object damage are considered rapid deteriorations and fouling, erosion, corrosion, mechanical wear are categorized as gradual or slow deteriorations. Fouling and erosion as two important sources of gradual degradations in the gas turbine engines are reflected on the health parameters of the compressor and turbine namely, flow capacity and efficiency. As these health parameters are not measurable directly, we have investigated the effects of fouling and erosion particularly in the compressor and turbine on the measurable parameters of the engine that are obtained from the gas path measurements during its take off mode. Note that the effects of degradations on the engine parameters are manifested

more strongly in the take off mode, since the maximum thrust is expected to be provided in this mode.

Towards this end, two time-series and hybrid fuzzy-time-series approaches to predict the degradation trends in the gas turbine engine are used. Autoregressive integrated moving average (ARIMA), vector autoregressive (VAR) and hybrid fuzzy-time-series approaches have been employed and compared in terms of their effectiveness and prediction horizons. The objective of the above methods is to predict the trends of the gas turbine engine degradation by using the past and the current engine gas path measurements in order to determine whether the engine should go through maintenance procedure or it can continue working for next flights.

1.4 Thesis Contributions

In this thesis, our goal is to develop novel solutions for the problem of gas turbine engine prognostics based on data driven approaches. Towards this end, three different time-series based approaches are employed to address the problem of engine degradation trend prediction due to two physical phenomenon, i.e. fouling and erosion which are considered as main sources of slow degradations in the gas turbine engine. Fouling is related to accumulating and adhering of particles (usually with the size less than 2 to 10 μm) to airfoils and annulus surfaces and erosion is related to removal of the materials from the flow path by hard particles attacking the flow surfaces.

In order to develop an effective prognostics scheme for predicting the health condition of the engine for safe-enough number of flights ahead, various available approaches in the prognostics field have been studied which are relatively a few as compared to the existing fault diagnostics approaches. To the best of the author's knowledge the proposed time-series based approaches that incorporate the two above mentioned degradations have not been introduced in the literature. Moreover, the capability of time-series analysis in

performing trend prediction makes these methods suitable candidates for degradation prognostics of the gas turbine engine. The outcome of the proposed approaches can be used as part of a condition-based monitoring system for the gas turbine engine. The contributions of this thesis in solving the above problem are listed as follows:

First, for obtaining the engine gas path measurements data a Simulink model of a single spool gas turbine engine developed in [13] by Naderi *et al.* is used. This model does not include the governor which controls the fuel flow. Therefore, a controller is developed for the single spool engine model to control the engine pressure ratio (EPR) in the take off mode. One of the challenges in this part is that the engine system is highly nonlinear and cannot be controlled by the conventional linear controllers. To cope with this problem a controller consisting of a feed forward controller (by constructing a look up table) and a negative feedback controller is developed so that the desired EPR is regulated by controlling the fuel flow. Then, the steady state data of the take off mode are captured for prognostics purposes.

Second, since fouling and erosion in the compressor and the turbine lead to increase in turbine exhaust gas temperature, in this thesis this variable is taken as a health measure of the system and its trend is used for degradation prognosis purposes. As mentioned in the previous sections, functionality of the data-driven approaches are dependent on the quality of the data as we are performing prediction procedure based on the past and current data of the system. Therefore, the data from the engine under different degradations with different severities are generated and fed to a time-series based approach namely vector autoregressive (VAR) method in order to predict the engine degradation trend and compared it with the univariate ARIMA model. The data obtained from the engine model (integrated with the degradation models) are validated by the well-known software known as the gas turbine simulation program (GSP) [131]. As mentioned earlier in the literature review section of this thesis, univariate ARIMA models are good predictors for short-term predictions

[128, 129, 130]. In order to improve the prediction accuracy, in addition to the turbine temperature, compressor temperature have also been employed by using the proposed VAR method. By benefiting from more data from the engine, we are able to have longer term predictions along with higher accuracy in terms of the mean and the standard deviation of the prediction errors.

Third, in order to improve the accuracy of the prediction the turbine temperature and the spool speed are fused by using a fuzzy inference engine and a hybrid fuzzy ARIMA model is proposed. This fused data is obtained by feeding the turbine temperature and the spool speed into two Takagi-Sugeno fuzzy engines that represent the turbine temperature in a given spool speed. Our results show that the performance of this approach as compared to the two first methods is improved in terms of prediction horizon and quantitative measures such as the mean and standard deviation of the prediction errors. For all the proposed methods prediction bounds based on the normal theory have been constructed in order to deal with uncertainties associated with prediction.

The capabilities of our proposed approaches are demonstrated under different scenarios and compared in terms of quantitative and qualitative measures. These scenarios which are fully demonstrated in Chapters 3 and 4 in detail entail the engine measurements under different degradation severities. Some of the results of this research have been published in the following work:

1. **M. Gholamhossein**, A. Vatani, N. Daroogeh, and K. Khorasani, "Prediction of the jet engine performance deterioration," in *ASME International Mechanical Engineering Congress and Exposition*, pp. 359-366, 2012.

1.5 Thesis Outline

The remainder of this thesis is organized as follows. In Chapter 2, the background information about the methods that are employed in the later chapters is given. This chapter starts by reviewing the ARIMA and VAR models, different criteria such as the Akaike's information criterion (AIC) and the Bayesian information criterion (BIC) for selecting the order of the models are explained and these are followed by reviewing the fuzzy system structure. Afterwards, the aircraft gas turbine engine model which will be used in this thesis is provided. This chapter concludes by describing the engine degradation models and how they are integrated into the engine model. The generated data from this model will be used for the prediction purpose in the later chapters. Chapter 3 begins by explaining the designed controller for the engine model. Next, the engine degradation trend is predicted by the proposed VAR method under different scenarios which are explained in detail in this chapter and finally these results are compared with the ARIMA method both qualitatively and quantitatively. In Chapter 4, the proposed hybrid fuzzy ARIMA approach is explained and the prognostics performance by using this method is compared with the two other methods. Finally, the conclusion and suggestions for future work are provided in Chapter 5.

Chapter 2

Background Information

In the first chapter of this thesis different prognostics approaches in the literature were reviewed. Also the advantages and drawbacks of both model-based and data-driven prognostics approaches were given. When an accurate mathematical model of the system under study or the degradation evolution model are not available it is preferable to use data-driven techniques. In this thesis, we are aiming to perform degradation prediction for a gas turbine engine where an accurate mathematical model is not available. Therefore, we decided to employ a data-driven approach for this work. Among different data-driven approaches such as artificial neural networks, fuzzy logic and hidden Markov models, time-series techniques are less investigated. The time-series prediction methods are capable of predicting the future incidents based on the known and observed past data points before they are observed and measured [132]. However, studies on empirical systems and specially large-scale ones [133] have shown accuracy of the prediction can be improved by combining different methods. In other words, combining different techniques increases the likelihood of capturing different patterns in the experimental data which eventually leads to a better performance. Inspired by these facts, the main body of the thesis is devoted to use of time series (univariate and bivariate) and a hybrid fuzzy-time series methods as main prognosis tools.

In the following sections, first time-series modeling and prediction methods are reviewed and presented. Then the fuzzy logic will be explained. After that, the gas turbine engine components and their associated equations will be presented. Finally, the degradations in the engine and how these degradations are integrated in the engine model are described.

2.1 Time-Series Modeling and Prediction

A time-series is a collection of quantitative observations over time which are measured sequentially [134, 135]. Daily recorded temperature of a room, daily monitoring price of gas and annual recorded rainfall data are examples of time-series. Figure 2.1 depicts a time-series of measured monthly rainfall for Auckland [6]. Throughout this thesis the realization of a time-series at time t is denoted by x_t and we use $\{x_t\}$ for denoting the time-series process.

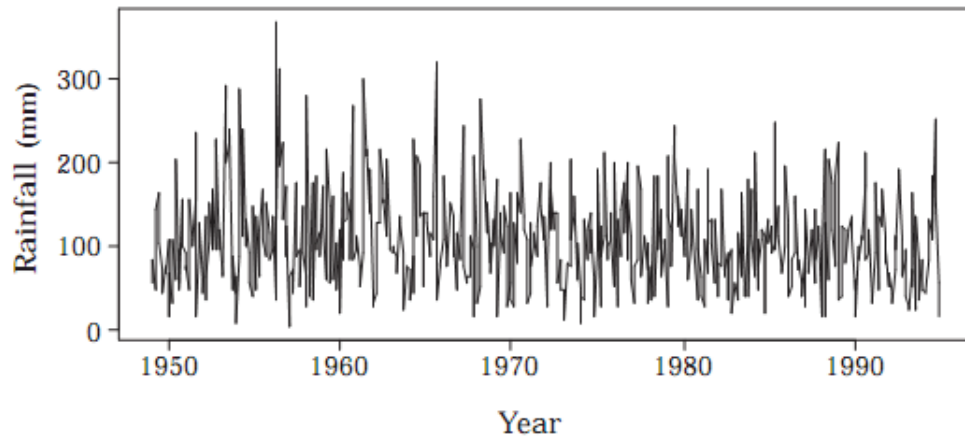


Figure 2.1: Monthly rainfall data for Auckland [6].

Deterministic and Statistical Time-Series

If one can determine the future values of a time-series by adopting a mathematical model, the time-series is called deterministic. Non-deterministic or statistical time-series is the time-series in which its future values are only characterized based on a probabilistic distribution. Figure 2.1 depicts a statistical time-series as it is not possible to predict the exact amount of the rainfall for the next month. One may consider the statistical time-series as a specific realization of a stochastic process based on probabilistic laws of the system under analysis [134].

Stationarity of the Stochastic Processes

A stochastic process is said to be a stationary process if its statistical properties do not change over time. Consider the stochastic process constructed by n observations $x_{t_1}, x_{t_2}, \dots, x_{t_n}$ captured at the times t_1, t_2, \dots, t_n . The joint probability distribution of this stochastic process over the mentioned times should be the same as the joint probability distribution of the process with n observations $x_{t_1+d}, x_{t_2+d}, \dots, x_{t_n+d}$ captured at the times $t_1 + d, t_2 + d, \dots, t_n + d$.

The stationarity properties of a time-series is an important feature in order to fit a model to the time-series under study and its importance will be explained later in this chapter. As indicated in the previous chapter, time-series methods are among one of the approaches that are used in prognosis problems. The problem of time-series prediction deals with using previous and current time-dependent system data to evaluate its future behavior [136].

2.1.1 Autoregressive Integrated Moving Average (ARIMA) Model

Consider the following generalized polynomial model structure [137]:

$$A(z)y(t) = \frac{B(z)}{F(z)}u(t) + \frac{C(z)}{D(z)}e(t) \quad (2.1)$$

where $A(z)$, $B(z)$, $C(z)$, $D(z)$, and $F(z)$ denote the following polynomials:

$$A(z) = 1 + a_1z + \dots + a_{n_a}z^{n_a}$$

$$B(z) = b_1z + \dots + b_{n_b}z^{n_b}$$

$$C(z) = 1 + c_1z + \dots + c_{n_c}z^{n_c}$$

$$D(z) = 1 + d_1z + \dots + d_{n_d}z^{n_d}$$

$$F(z) = 1 + f_1z + \dots + f_{n_f}z^{n_f}$$

where n_a , n_b , n_c , n_d , and n_f denote the order of above polynomials, $y(t)$ denotes the output value at time t , $u(t)$ denotes the value of input signal (control input) at time t , and $\{e(t)\}$ denotes a sequence of independent (identically distributed) random variables, z denotes the backward operator or the delay operator. The model indicated in the equation (2.1) is too general and most often depending on the application some of the above polynomials (A, F, C, and D) would be set to unity.

Among the various available techniques to analyze the data in time domain and frequency domain, the Box-Jenkins models are the most common methods which were developed in 1970 [138] by Box and Jenkins. Because of the high contribution of Box and Jenkins in developing the methodology of the autoregressive moving average (ARMA) models, the ARMA models are also referred to as Box and Jenkins models. A Box-Jenkins model with the order of p and q is denoted by $ARMA(p,q)$ in which p is the order of the autoregressive terms and q is the order of the moving average terms. Both the autoregressive (AR) model with the order of p and the moving average (MA) model with the order of q also fall into the category of Box-Jenkins models and will be explained further in this section. The general form of the $ARMA(p,q)$ model which is a special case of the generalized polynomial model structure shown above can be presented as follows:

$$\varphi(z)x_t = \theta(z)\varepsilon_t \tag{2.2}$$

where p denotes the autoregressive order and q denotes the moving average order of the

model, x_t denotes the value of time-series at the time t , $\{\varepsilon_t\}$ denotes a sequence of independent and identically distributed random variables with zero mean and variance of δ , z denotes the back shift operator such that $zx_t = x_{t-1}$, and $\varphi(z)$ and $\theta(z)$ denote the autoregressive operator and the moving average operator of the forms:

$$\varphi(z) = 1 - \varphi_1 z - \dots - \varphi_p z^p, \quad \theta(z) = 1 + \theta_1 z + \dots + \theta_q z^q$$

In the case that all the θ_i 's are zero, the ARMA model is said to be an autoregressive (AR) model. If all the φ_i 's are zero, the ARMA model is said to be a moving average (MA) model.

Box and Jenkins models are based on the following ARMA difference equation:

$$x_t = \varphi_1 x_{t-1} + \varphi_2 x_{t-2} + \dots + \varphi_p x_{t-p} + \varepsilon_t + \theta_1 \varepsilon_{t-1} + \dots + \theta_q \varepsilon_{t-q} \quad (2.3)$$

where $\theta_1, \dots, \theta_q, \varphi_1, \dots, \varphi_p$ denote the parameters of the model.

Before presenting different approaches for estimating the ARMA model parameters given the measurements x_t , we will be explaining stationarity and invertability conditions of the ARMA model and their importance in the modeling of the time-series data.

Stationarity

In order to study stationarity of an ARMA model, we consider the model as a difference equation in x_t so that $\phi(z)x_t = \theta(z)\varepsilon_t$ is a linear equation between $x_t, x_{t-1}, \dots, x_{t-p}$. It follows that this is the conventional algebraic difference equation except the right hand part of the equation which includes the random terms $\{\varepsilon_t\}$. The general solution of a difference equation comprises of a complementary solution and a particular solution [139]. The complementary solution is the solution of the homogeneous difference equation and the particular solution is any solution to the original difference equation. Let's take the homogeneous ARMA equation which is $\phi(z)x_t = 0$ as follows:

$$x_t - \phi_1 x_{t-1} - \phi_2 x_{t-2} \dots - \phi_p x_{t-p} = 0 \quad (2.4)$$

The solution of the above equation is any function in the form of $x_t = kr^t$ such that $kr^t - k\phi_1 r^{t-1} \dots - k\phi_p r^{t-p} = 0$, where k denotes the constant value which can be calculated by the initial values of x_t . Rearranging the above equation gives us:

$$kr^t \left(1 - \phi_1 \left(\frac{1}{r}\right) \dots - \phi_p \left(\frac{1}{r}\right)^p \right) = kr^t \phi(1/r) = 0 \quad (2.5)$$

From the equation (2.5), a trivial solution is $r = 0$ or r is any solution to $\phi(1/r) = 0$. Therefore, the solution of this homogeneous equation is the reciprocal of the roots of the polynomial $\phi(z)$. Similar to other ordinary difference equations depending on the roots of $\phi(z)$, the complementary function comprises of the linear function of all the solutions to $\phi(z)$ in the following form $k_1 \left(\frac{1}{r_1}\right)^t + k_2 \left(\frac{1}{r_2}\right)^t + \dots + k_p \left(\frac{1}{r_p}\right)^t$, where k_1, \dots, k_p are constants and can be determined by using the initial values x_1, \dots, x_p . Particular solution of the ARMA model is determined as follows:

$$x_t = \phi^{-1}(z)\theta(z)\varepsilon_t \quad (2.6)$$

As mentioned earlier, the model is stationary if its statistical properties such as mean and variance do not change over time. From the general solution to the ARMA model introduced above, the ARMA model is stationary if all the roots of $\phi(z)$ are outside the unit circle [140]. This condition is for ensuring that for large t , x_t is independent of the initial value of x_t and leads to a constant mean. Here, let's take the AR(1) model as an example:

$$x_t = \phi x_{t-1} + \varepsilon_t \quad (2.7)$$

The complementary function $x_t = k\phi^t$ is derived from the corresponding homogeneous

equation, where k is a constant. The particular solution is determined as follows:

$$\begin{aligned}\phi(z)x_t &= \varepsilon_t \\ x_t &= \phi^{-1}(z)\varepsilon_t = \psi(z)\varepsilon_t \\ \phi(z)\psi(z)\varepsilon_t &= \varepsilon_t\end{aligned}\tag{2.8}$$

By equating the coefficients of z from both sides of the above equation, the particular solution of the AR(1) is derived. Finally the general solution to the AR(1) model will be as follows:

$$x_t = k\phi^t + \sum_{j=0}^{\infty} \phi^j \varepsilon_{t-j}\tag{2.9}$$

As seen from the equation (2.9) when $|\phi| < 1$ the complementary function approaches to zero by increasing the t . In other words, in this case the mean of x_t is independent of t , as only the particular solution has remained. Also for the variance of the general solution, it converges when $|\phi| < 1$, [140].

Invertibility

An ARMA model could be presented as an infinite AR representation. Let's take ARMA(1,1) model as an example. In order to determine the infinite AR representation of this model, one can take the following steps:

$$x_t = \phi_1 x_{t-1} + \varepsilon_t + \theta_1 \varepsilon_{t-1}\tag{2.10}$$

$$\varepsilon_t = x_t - \phi_1 x_{t-1} - \theta_1 \varepsilon_{t-1}$$

$$\varepsilon_{t-1} = x_{t-1} - \phi_1 x_{t-2} - \theta_1 \varepsilon_{t-2}\tag{2.11}$$

Substituting ε_{t-1} in the first equation of (2.11) and continuing with this substitution we get:

$$\begin{aligned}\varepsilon_t &= x_t - \phi_1 x_{t-1} - \theta_1 (x_{t-1} - \phi_1 x_{t-2} - \theta_1 \varepsilon_{t-2}) \\ &= x_t - (\phi_1 + \theta_1) x_{t-1} + \theta_1 (\phi_1 + \theta_1) x_{t-2} - \theta_1^2 (\phi_1 + \theta_1) x_{t-3} \dots - (-\theta_1)^{k-1} (\phi_1 + \theta_1) x_{t-k} + \dots\end{aligned}\tag{2.12}$$

From the above equation, it is clear that when $|\theta_1| < 1$ the weights of the coefficients approach to zero and eventually the estimation of ε will converge. For the general ARMA model ($\phi(z)x_t = \theta(z)\varepsilon_t$), similar to the approach which was explained earlier for determining the MA polynomial of an ARMA model (in the form of $x_t = \psi(z)\varepsilon_t$), one can determine the AR polynomial of an ARMA model in the form of $\varepsilon_t = \pi(z)x_t$ and to make sure that the weights are approaching to zero as we go back in time t , all the roots of $\theta(z)$ should be outside of the unit circle. This condition is called invertibility condition [140].

Invertibility is useful for estimation purposes that use least squares estimation. When we have two ARMA models with the same likelihood and the same coefficients for the $\phi(z)$ but different for the $\theta(z)$, in order to choose one model over the other one, invertibility condition should be verified. In other words, the model in which its MA coefficients are invertible distinguish the model. The invertibility condition is necessary as in the estimation stage of the modeling, we choose ε_1 (initial value of ε) arbitrary and under invertibility condition, we make sure that the coefficient of ε_1 decays over increasing the time and this can attenuate the error raised by choosing ε_1 arbitrary.

Model Parameter Estimation Methods

In order to estimate the parameters of an ARMA model i.e. $\phi(z)$ and $\theta(z)$ one can employ different approaches such as [138]:

- Off-line identification methods

- Bayesian approaches for recursive identification
- Stochastic approximation
- Pseudo linear regressions
- Model reference techniques

As mentioned earlier in the first chapter in this thesis we are looking for investigating and modeling the engine performance degradation due to the compressor fouling and the turbine erosion over number of flights and processing of the measurements data from the engine is not online. Therefore, in this thesis we use off-line methods for parameter estimation of the models. Below some common off-line recursive approaches will be explained:

1. Least squares method

Considering $F(z) = D(z) = C(z) = 1$ in equation (2.1) gives $A(z)y(t) = B(z)u(t) + v(t)$ where $v(t)$ is the disturbance. Let's define the vector Θ in terms of $A(z)$ and $B(z)$ parameters and vector $\Phi(t)$ in terms of the regression variables as follows:

$$\begin{aligned}\Theta^T &= (a_1 \dots a_{n_a} b_1 \dots b_{n_b}) \\ \Phi^T(t) &= (-y(t-1) \dots -y(t-n_a) u(t-1) \dots u(t-n_b))\end{aligned}\tag{2.13}$$

From equation (2.13), the difference equation model described by the equation (2.1) can be rearranged as follows:

$$y(t) = \Theta^T \Phi(t) + v(t)\tag{2.14}$$

The goal is estimating the parameters vector Θ from the measurements $y(t)$ by the recursive least squares method. In this method one is trying to estimate the parameters of the model by minimizing the equation error, $y(t) - \Theta^T \Phi(t)$ with respect to the

parameters vector Θ . In other words, the cost function can be defined as follows:

$$V_N(\Theta) = \frac{1}{N} \sum_1^N \alpha_t [y(t) - \Theta^T \Phi(t)]^2 \quad (2.15)$$

where α_t is a parameter that can be set to 1 or it can be chosen according to the variance of the term $v(t)$ and it can be used to give different weights to different measurements and N is the number of measurements used for parameters estimation. As seen from the cost function $V_N(\Theta)$, one is trying to find the best prediction or estimation of the measurements $y(t)$, which is quadratic in Θ and which allows us to minimize it analytically. After taking the derivative of the cost function with respect to Θ , one gets:

$$\hat{\Theta}(N) = \left[\sum_{t=1}^N \alpha_t \Phi(t) \Phi^T(t) \right]^{-1} \sum_{t=1}^N \alpha_t \Phi(t) y(t) \quad (2.16)$$

In the recursive least squares method, equation (2.16) should be expressed in a recursive manner. After some manipulations (see [138] and [141] for more details), the estimated parameters vector $\hat{\Theta}$ can be determined recursively by the following algorithm:

$$\begin{aligned} \hat{\Theta}(t) &= \hat{\Theta}(t-1) + L(t) [y(t) - \hat{\Theta}^T(t-1) \Phi(t)] \\ L(t) &= \frac{P(t-1) \Phi(t)}{1/\alpha_t + \Phi^T(t) P(t-1) \Phi(t)} \\ P(t) &= P(t-1) - \frac{P(t-1) \Phi(t) \Phi^T(t) P(t-1)}{1/\alpha_t + \Phi^T(t) P(t-1) \Phi(t)} \end{aligned} \quad (2.17)$$

It can be shown that by using the recursive least squares algorithm explained above, the estimated parameters $\hat{\Theta}$ converge to the true values Θ_0 only under the following conditions:

- $\{v(t)\}$ is a white noise (sequence of independent random variables with the mean of zero),

- The input control $\{u(t)\}$ should be independent of the noise sequence $\{v(t)\}$ and the regression variables vector $\Phi(t)$ should have only u terms.

2. Instrumental variable method

The instrumental variable method has been developed to modify the short comings of the recursive least squares method which has been mentioned above. The modification has been done by using a vector $\zeta(t)$ in place of $\Phi(t)$ in the equation (2.16) such that $\zeta(t)$ and $v(t)$ are uncorrelated. After this replacement and doing some manipulations we get to the new estimated parameter formula as follows:

$$\hat{\Theta}(N) = \Theta_0 + \left[\frac{1}{N} \sum_{t=1}^N \zeta(t) \Phi^T(t) \right]^{-1} \frac{1}{N} \sum_{t=1}^N \zeta(t) v(t) \quad (2.18)$$

where Θ_0 is the true value of the estimated parameters. The above estimated parameters vector can be rewritten in a recursive manner after some manipulations as follows:

$$\begin{aligned} \hat{\Theta}(t) &= \hat{\Theta}(t-1) + L(t) [y(t) - \hat{\Theta}^T(t-1) \Phi(t)] \\ L(t) &= \frac{P(t-1) \zeta(t)}{1/\alpha_t + \Phi^T(t) P(t-1) \zeta(t)} = P(t) \zeta(t) \\ P(t) &= P(t-1) - \frac{P(t-1) \zeta(t) \Phi^T(t) P(t-1)}{1/\alpha_t + \Phi^T(t) P(t-1) \zeta(t)} \end{aligned} \quad (2.19)$$

The vector $\zeta(t)$ is called the instrumental variables. Under the three conditions below the estimated parameters $\hat{\Theta}(N)$ is approaching to its true values Θ_0 as N goes to infinity using the above algorithm [138]:

- $\zeta(t)$ and $v(t)$ are uncorrelated.
- $v(t)$ should have a zero mean.
- According to equation (2.18), the matrix $\lim_{N \rightarrow \infty} \left[\frac{1}{N} \sum_{t=1}^N \zeta(t) \Phi^T(t) \right]$ should be invertible.

There are many approaches for choosing the instrumental variables $\zeta(t)$ [138], but

in general the instrumental variables should be correlated with $\Phi(t)$ and uncorrelated with the system noise terms. Following vector is an example of a common choice of $\zeta(t)$ [138]:

$$\zeta^T(t) = (-y_M(t-1)\dots - y_M(t-n_a)u(t-1)\dots u(t-n_b)) \quad (2.20)$$

where $y_M(t)$ is the output of a deterministic system with the actual input signal $u(t)$ as follows:

$$y_M(t) + \bar{a}_1 y_M(t-1)\dots + \bar{a}_{n_a} y_M(t-n_a) = \bar{b}_1 u(t-1)\dots \bar{b}_{n_b} u(t-n_b) \quad (2.21)$$

In this approach proposed by Young [142], Mayne [143] and Wong *et al.* [144] the coefficients \bar{a}_i and \bar{b}_i are assumed to be time-dependent. Next, one can use the estimated values of $\hat{a}_i(t)$ and $\hat{b}_i(t)$ from the equation (2.19) in the equation (2.21) which gives us:

$$y_M(t) = \hat{\Theta}^T(t)\zeta(t) \quad (2.22)$$

3. Recursive prediction error method (RPEM)

Both the recursive least squares method and the instrumental variable method are good approaches for estimating the model parameters as long as the cost function is quadratic in terms of Θ . Because when the cost function $V_N(\Theta)$ is a nonlinear function of Θ , it cannot be globally minimized analytically similar to what we did so far. Furthermore, as seen in equation (2.19) in order to perform numerical minimization procedure one needs to pass all the data from $t = 1$ to $t = N$ for several iterations and this can not be used in a recursive algorithm that requires a vector memory with fixed size. In this case we have to determine approximations to $\hat{\Theta}(t)$ in a recursive manner. We define $V_t(\Theta)$ as follows:

$$V_t(\Theta) = \frac{1}{2} \sum_{\tau=1}^t \varepsilon^2(\tau, \Theta) \quad (2.23)$$

In order to take the derivative of the cost function $V_t(\Theta)$, we write the Taylor series expansion of $V_t(\Theta)$ around $\hat{\Theta}(t-1)$ as follows (assuming $\hat{\Theta}(t-1)$ is the optimal estimate of Θ at time $(t-1)$):

$$\begin{aligned} V_t(\Theta) &= V_t(\hat{\Theta}(t-1)) + V_t'(\hat{\Theta}(t-1))[\Theta - \hat{\Theta}(t-1)] \\ &+ \frac{1}{2}[\Theta - \hat{\Theta}(t-1)]^T V_t''(\hat{\Theta}(t-1))[\Theta - \hat{\Theta}(t-1)] + f(|\Theta - \hat{\Theta}(t-1)|^2) \end{aligned} \quad (2.24)$$

where $f(\Theta)$ is a function such that $\lim_{|x| \rightarrow 0} \frac{f(x)}{|x|} \rightarrow 0$.

$$V_t'(\Theta) = V_t'(\hat{\Theta}(t-1)) + \frac{1}{2}(\Theta - \hat{\Theta}(t-1))^T [V_t''(\hat{\Theta}(t-1)) + V_t''(\hat{\Theta}(t-1))^T] = 0 \quad (2.25)$$

Since the second derivative of a scalar function is symmetric, one gets:

$$V_t'(\hat{\Theta}(t-1)) + (\Theta - \hat{\Theta}(t-1))^T V_t''(\hat{\Theta}(t-1)) = 0 \quad (2.26)$$

Solving equation (2.26) with respect to Θ one can approximate $\hat{\Theta}(t)$ as follows:

$$\hat{\Theta}(t) \approx \Theta = \hat{\Theta}(t-1) - [V_t''(\hat{\Theta}(t-1))^T]^{-1} V_t'(\hat{\Theta}(t-1))^T \quad (2.27)$$

As we defined the cost function earlier:

$$V_t(\Theta) = \frac{1}{2} \sum_{\tau=1}^t \varepsilon^2(\tau, \Theta) \quad \Rightarrow \quad V_t'(\Theta) = \sum_{\tau=1}^t \varepsilon(\tau, \Theta) \frac{d\varepsilon(\tau, \Theta)}{d\Theta} \quad (2.28)$$

And by defining the gradient vector ψ such that $\psi(t, \Theta) \stackrel{\text{def}}{=} \left[-\frac{d\varepsilon(t, \Theta)}{d\Theta}\right] = \frac{d\hat{y}(t, \Theta)}{d\Theta}$, equation (2.28) can be rearranged as follows:

$$[V'_t(\Theta)]^T = - \sum_{\tau=1}^t \left(-\frac{d\varepsilon(\tau, \Theta)}{d\Theta}\right)^T \varepsilon(\tau, \Theta) = [V'_{t-1}(\Theta)]^T - \psi(t, \Theta) \varepsilon(t, \Theta) \quad (2.29)$$

For the second derivative of the cost function, we have:

$$[V''_t(\Theta)]^T = [V''_{t-1}(\Theta)]^T + \psi(t, \Theta) \psi^T(t, \Theta) + \varepsilon''(t, \Theta) \varepsilon(t, \Theta) \quad (2.30)$$

In order to minimizing the cost function $V_t(\Theta)$ approximately the following approximations should be taken:

- Assume that the estimate $\hat{\Theta}(t-1)$ and its next estimate $\hat{\Theta}(t)$ are within their small neighborhood when t is large. This implies that $f(|\hat{\Theta}(t) - \hat{\Theta}(t-1)|)$ can be neglected and $V''_t(\hat{\Theta}(t)) = V''_t(\hat{\Theta}(t-1))$
- It is assumed that $\hat{\Theta}(t-1)$ is an optimal estimate of $\Theta(t-1)$ and this implies that $V'_{t-1}(\hat{\Theta}(t-1)) = 0$.
- It is assumed that $\varepsilon''(t, \hat{\Theta}(t-1)) \varepsilon(t, \hat{\Theta}(t-1)) = 0$

Taking the above assumptions into consideration, equation (2.30) can be rewritten as follows:

$$\bar{R}(t) = \bar{R}(t-1) + \psi(t, \hat{\Theta}(t-1)) \psi^T(t, \hat{\Theta}(t-1)) \quad (2.31)$$

where $\bar{R}(t)$ denotes the second derivative of the function $V_t(\Theta)$, i.e. $V''_t(\Theta)$.

Next, from equation (2.29) and the above mentioned assumption $V'_{t-1}(\hat{\Theta}(t-1)) = 0$, one gets:

$$[V'_t(\hat{\Theta}(t-1))]^T = -\psi(t, \hat{\Theta}(t-1)) \varepsilon(t, \hat{\Theta}(t-1)) \quad (2.32)$$

Finally, substituting equation (2.32) into the equation (2.27), one gets:

$$\hat{\Theta}(t) = \hat{\Theta}(t-1) + \bar{R}^{-1}(t-1)\psi(t, \hat{\Theta}(t-1))\varepsilon(t, \hat{\Theta}(t-1)) \quad (2.33)$$

In the prediction stage and the identification part when we employ the least squares methods, evaluating the invertibility condition becomes important. As we do not have access to the past values of x_t for an infinite number of steps, therefore it is necessary that the coefficients of x_t decay to zero over time t , so that our estimation error due to this will be diminished sufficiently.

The ARMA method is only practical when one deals with stationary data. However, in most real-life application cases the observation data is non-stationary. Towards this end, the d th difference of the non-stationary time-series $\{x_t\}$ is written as $(1-z)^d x_t$. Subsequently, the new data become stationary and one can fit an ARMA model into this data. This method is known as autoregressive integrated moving average (ARIMA). The ARIMA model is also known as the Box and Jenkins [134] which in the extended form can be written as:

$$x_t = \varphi_1 x_{t-1} + \varphi_2 x_{t-2} + \dots + \varphi_p x_{t-p} + \varepsilon_t + \theta_1 \varepsilon_{t-1} + \dots + \theta_q \varepsilon_{t-q} \quad (2.34)$$

where $\theta_1, \dots, \theta_q, \varphi_1, \dots, \varphi_p$ denote the parameters of the model. In other words, the ARIMA model can be considered as a combination of a random walk and a random trend model which are finely tuned.

The ARIMA(p, d, q) is one of the most general types of time-series representations for prediction purposes. The stationarization is achieved through differencing and lagging procedure. Depending on the number of the differences taken (d), from the original time-series (before fitting the data into an ARMA model) one is said to have an ARIMA(p, d, q) model as follows [145]:

$$\varphi(z)(1-z)^d x_t = \theta(z)\varepsilon_t \quad (2.35)$$

The first difference ARIMA time-series may be written as follows [145]:

$$\varphi(z)(1-z)x_t = \theta(z)\varepsilon_t \quad (2.36)$$

One can consider a new time-series representation, that is:

$$y_t = (1-z)x_t \quad (2.37)$$

where $\{y_t\}$ denotes the differenced series of $\{x_t\}$. According to the results in [137], the polynomials $\varphi(z)$ and $\theta(z)$ in the ARIMA model must not have any common factors in order to guarantee the identifiability of the selected model. The coefficients $\theta_1, \dots, \theta_q, \varphi_1, \dots, \varphi_p$ are estimated by using the recursive prediction error method known as the RPEM [137, 138] (which was given earlier) that effectively specifies the ARIMA model. One can use the standard training error as a measure to determine the appropriate p and q that gives the best model, fitting to the time-series data.

2.1.2 Vector Autoregressive (VAR) Model

Future values of measurable parameters in a complex system such as a gas turbine engine cannot be accurately predicted from the past measurements. Given that the data sets are non-deterministic due to the parameter uncertainties and system noise, a model that can include this random behavior leads to a better and a more accurate prediction. The ARMA model has the above noted flexibilities by including the random shock terms. In the univariate modeling approach in this thesis we consider only one of the measurable parameters

namely, the turbine exit temperature (TET). Here, the ultimate goal in the time-series analysis is to predict the future behavior of the engine. Therefore, an approach that can enable us to have a longer step-ahead prediction is more preferable due to its resulting possible cost effectiveness and safety improvements. An improved prediction is accomplished by taking advantage of more than one measurement parameter.

The n -variate AR(p) model is given by [146]:

$$\phi(z)X_t = Z_t \quad (2.38)$$

where $X_t = \{x_{1,t}, \dots, x_{n,t}\}$ and $Z_t = \{z_{1,t}, \dots, z_{n,t}\}$ denote the vector of time-series values at time t and the vector of sequences of independent and identically distributed random variables, respectively. Equation (2.38) can be rewritten in an extended form:

$$X_t + \phi_1 X_{t-1} + \dots + \phi_p X_{t-p} = Z_t \quad (2.39)$$

where ϕ_1, \dots, ϕ_p denote $n \times n$ matrices. For example, if $n = 2$ and $p = 1$ then equation (2.39) becomes:

$$\begin{bmatrix} x_{1,t} \\ x_{2,t} \end{bmatrix} = \begin{bmatrix} \phi_{1,11} & \phi_{1,12} \\ \phi_{1,21} & \phi_{1,22} \end{bmatrix} \begin{bmatrix} x_{1,t-1} \\ x_{2,t-1} \end{bmatrix} + \begin{bmatrix} z_{1,t} \\ z_{2,t} \end{bmatrix} \quad (2.40)$$

It can be verified that the current value of x_1 depends on its previous values as well as the previous values of x_2 . Therefore, given that more information from a larger number of parameters are utilized one can expect a longer prediction horizon. For any given data set the target is to determine a proper model for the purpose of farthest future prediction possible. By following the Box and Jenkins [134] modeling procedure one can derive the model of the system under study. This procedure consists of model specification, model parameter estimation, and model checking. For estimating the model parameters one can use the maximum likelihood estimation method which is a commonly used method in the

literature [145, 137]. Akaike's information criterion (AIC) [137], mean and variance of the error are commonly used measures for verifying the model quality.

2.1.3 Time-Series Model Selection

As pointed out in the previous sections in order to fit an ARMA(p, q) model the time-series should be stationary by itself unless we need to differentiate the data until we achieve a stationary time-series. The orders of the model p and q can be selected by using backwards elimination [140]. In the backward elimination procedure, one estimates the model parameters using one of the estimation methods assuming an arbitrary order of the model. Then, the estimated parameters should be verified and the parameters which are too small should be set to zero. Because we are looking for a parsimonious model with the optimal number of lags and the parameters with very small values do not have significant affect on the results and is better to omit them from the model. Next, we estimate the model parameters again with the updated orders p and q . This procedure should be repeated until all the parameters are large enough.

There exist other alternative and widely used quantitative measures to choose the best ARMA model with the fewest parameters which properly describes the data. Akaike's information criterion (AIC) [137, 124] and Bayesian information criterion (BIC) [147, 124] are the common measures when one needs to select the best model among several models which all are fitted to the data. These criteria have been defined based on information theory and address a trade off between the goodness of a fit to the actual data and the order of the model. These two criteria are defined as follows [124]:

$$\begin{aligned}
 AIC &= n \text{Ln}\left(\frac{\hat{\sigma}_e^2}{n}\right) + 2p \\
 BIC &= n \text{Ln}\left(\frac{\hat{\sigma}_e^2}{n}\right) + p + p \text{Ln}(n)
 \end{aligned}
 \tag{2.41}$$

where n denotes the number of data that is used for model fitting, p denotes the number of model parameters and $\hat{\sigma}_e^2$ denotes the sum of squared residuals. A model with smaller AIC or BIC is a better model [140, 137]. Indeed, the penalty terms are associated with these two criteria so that increasing the order of the model will cause an increase in the value of AIC and BIC.

2.1.4 Time-Series Model for Prediction

The goal of prediction is to determine $\hat{x}_t(m)$ by obtaining x_{t+m} given $x_t, x_{t-1}, \dots, x_{t-p+1}$ and $\varepsilon_t, \varepsilon_{t-1}, \dots, \varepsilon_{t-q+1}$ where m denotes the step-ahead lead time. In other words:

$$\hat{x}_t(m) = E[x_{t+m}|x_t, x_{t-1}, \dots] \quad (2.42)$$

As mentioned earlier in equation (2.34), the random shock terms should be normally distributed. In view of this point and replacing $t + 1$ by t in equation (2.34) one gets:

$$x_{t+1} = \varphi_1 x_t + \varphi_2 x_{t-1} + \dots + \varphi_p x_{t-p+1} + \varepsilon_{t+1} + \theta_1 \varepsilon_t + \dots + \theta_q \varepsilon_{t-q+1} \quad (2.43)$$

And taking the expectations of both sides, it yields:

$$\hat{x}_t(1) = \varphi_1 x_t + \varphi_2 x_{t-1} + \dots + \varphi_p x_{t-p+1} + \theta_1 \varepsilon_t + \dots + \theta_q \varepsilon_{t-q+1} \quad (2.44)$$

Knowing that $\varepsilon_{t+1|t}, \varepsilon_{t+2|t}, \dots$ which denote the conditional expectation of $\varepsilon_{t+1}, \varepsilon_{t+2}, \dots$ at time t , are equal to 0, we obtain:

$$\hat{x}_t(2) = \varphi_1 \hat{x}_t(1) + \varphi_2 x_t + \dots + \varphi_p x_{t-p+2} + \theta_2 \varepsilon_t + \dots + \theta_q \varepsilon_{t-q+2} \quad (2.45)$$

$$\hat{x}_t(3) = \varphi_1 \hat{x}_t(2) + \varphi_2 \hat{x}_t(1) + \varphi_3 x_t + \dots + \varphi_p x_{t-p+3} + \theta_3 \varepsilon_t + \dots + \theta_q \varepsilon_{t-q+3} \quad (2.46)$$

And by following the above steps one can obtain $\hat{x}_t(m)$. At time $t + 1$, using x_{t+1} it is possible to obtain ε_{t+1} from equation (2.44) as follows:

$$\varepsilon_{t+1} = x_{t+1} - \hat{x}_t(1) \quad (2.47)$$

2.2 Fuzzy Logic

In recent years employing fuzzy logic as an artificial intelligence method for identification and control of dynamic systems has increased. In 1969, professor Zadeh introduced the concept of the fuzzy sets [8]. A Fuzzy set includes the elements that may have a partially membership of the set. In other words, a fuzzy set does not have a precise and crisp boundary. In general the fuzzy logic is [7]:

- Conceptually easy to be understood by humans.
- Flexible.
- Tolerant against the imprecise data.
- Useful to model any complex nonlinear function.
- A good method to incorporate the knowledge of the expert person to control the system.
- Compatible with the conventional control techniques and can be augmented with them.
- Uses the same basis of the human communication.

Using fuzzy logic allows us to deal with intermediate values that cannot be used in conventional true-false, yes-no, high-low, ... logical systems. So it will be more similar to the human decision making scheme [148].

To explain the fuzzy logic concept an illustrating example is the set of tall people. Here the universe of discourse is the set of all possible human heights. Let us assume that it is the interval of $[1.2, 2.5]$ meters. The linguistic term "tall" does not specify a certain height and it considers a range of heights. If we try to define a tall person as one with height greater than a specific height for example 1.8 meters it is not reasonable to consider some one as a short person and some other one as a tall person because their height difference is as small as 1 millimeter. On the other hand, to deal with this issue we could use a smoothly varying curve to define a tall person instead of using a sharp tall-short definition. Figure 2.2 depicts classical and fuzzy definition of a tall person. In the fuzzy logic terminology these curves are called membership functions and usually are denoted by $\mu(\cdot)$. In a classical set, the membership degree of each element could be either 0 or 1, but in a fuzzy set it could be any real number between 0 and 1. As seen in Figure 2.2, the transition between short and tall in the fuzzy membership function is very smooth which results in a more realistic definition for a tall person [7].

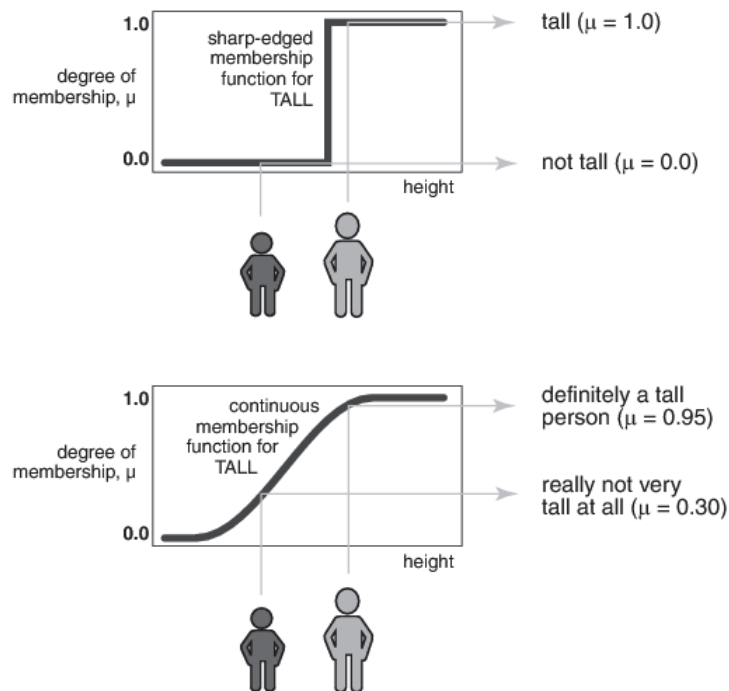


Figure 2.2: Classical and fuzzy definitions of a tall person [7].

2.2.1 Fuzzy Set

Now let us define fuzzy set, universe of discourse and membership functions in more details. The universe of discourse is a classical set of all possible values of the variables and is denoted by \mathcal{X} . The fuzzy set M is defined on \mathcal{X} as follows:

$$M = \{(x, \mu_M(x)) | x \in \mathcal{X}\}$$

where $\mu_M(x) : \mathcal{X} \mapsto [0, 1]$ is the membership function of the fuzzy set M . It is worth to mention that a classical set C can be also represented as a fuzzy set where its membership function $\mu_C(\cdot)$ is defined as follows:

$$\mu_C(x) = \begin{cases} 1, & x \in C \\ 0, & x \notin C \end{cases}$$

For the fuzzy set M the support of M is the set of all $x \in \mathcal{X}$ that $\mu_M(x) > 0$ and the α -cut of M is the set of all $x \in \mathcal{X}$ that $\mu_M(x) > \alpha$. The height of M is $\max_{x \in \mathcal{X}} \mu_M(x)$. Usually the height of fuzzy sets is 1 and in this case it is called a normal fuzzy set. A convex fuzzy set is a fuzzy set that its membership function is a convex function which implies that:

$$\forall x_1, x_2 \in \mathcal{X} \text{ and } 0 < \lambda < 1 \quad \mu_M(\lambda x_1 + (1 - \lambda)x_2) \geq \min\{\mu_M(x_1), \mu_M(x_2)\}$$

The triangular membership function is one of the membership functions which is often used in fuzzy sets and is defined as:

$$\mu(x) = \begin{cases} \frac{1}{w}(x - m + w), & m - w \leq x < m \\ \frac{1}{w}(m + w - x), & m \leq x < m + w \\ 0, & \text{otherwise} \end{cases}$$

Figure 2.3 depicts a plot of the above membership function. The trapezoidal is another

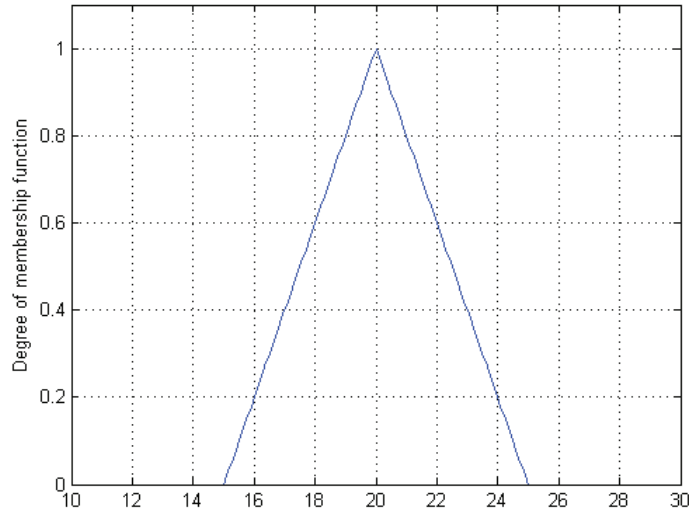


Figure 2.3: Triangular membership function.

commonly used membership function and is defined in equation (2.48) and Figure 2.4 depicts a plot of it.

$$\mu(x) = \begin{cases} \frac{1}{w_1}(x - m_1 + w_1), & m_1 - w_1 \leq x < m_1 \\ 1, & m_1 \leq x < m_2 \\ \frac{1}{w_2}(m_2 + w_2 - x), & m_2 \leq x < m_2 + w_2 \\ 0, & \text{otherwise} \end{cases} \quad (2.48)$$

Another possible membership function that can be used to describe a fuzzy set is the Gaussian membership function of Figure 2.5 and is defined as:

$$\mu(x) = \exp\left(-\frac{1}{2}\left(\frac{x-c}{\sigma}\right)^2\right) \quad (2.49)$$

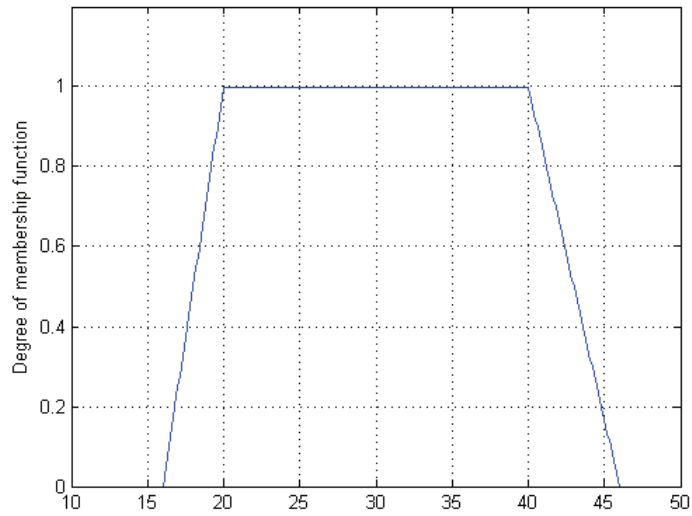


Figure 2.4: Trapezoidal membership function.

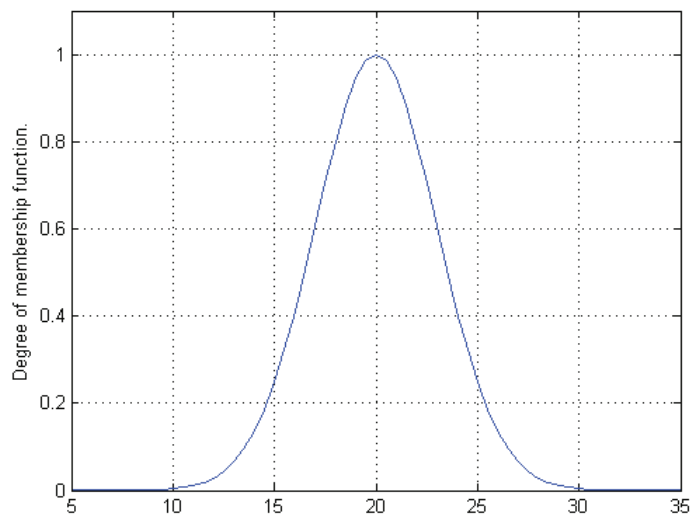


Figure 2.5: Gaussian membership function.

The classical concepts in the set theory are needed to be redefined for fuzzy sets. Assume that M_1 and M_2 are two fuzzy sets on \mathcal{X} and $\mu_1(x)$, $\mu_2(x)$ are their associated membership functions respectively. The fuzzy set M_1 is a subset of M_2 if and only if $\forall x \in \mathcal{X}$, $\mu_1(x) \leq \mu_2(x)$.

The compliment of the fuzzy set M_1 is denoted by fuzzy set \bar{M}_1 and its membership function is:

$$\bar{\mu}_1(x) = 1 - \mu_1(x)$$

The intersection of two fuzzy sets $M_A = M_1 \cap M_2$ can be defined in two different ways. In the first method, it can be defined based on the minimum of the membership function degrees as follows:

$$\mu_A(x) = \min \{ \mu_1(x), \mu_2(x) \}$$

The other way that can be used to define the intersection of two fuzzy sets is using algebraic product. The following formula represents this:

$$\mu_A(x) = \mu_1(x)\mu_2(x)$$

Note that other than min and algebraic product there are other methods to define the intersection operator [9, 149, 150, 151, 152, 153].

To define the union of fuzzy sets it is also possible to use different methods [9, 149, 150]. Let $M_U = M_1 \cup M_2$ be the union of the fuzzy sets M_1 and M_2 and $\mu_U(x)$ denotes its associated membership function. It can be defined based on maximum or algebraic sum operators as follows:

$$\mu_U(x) = \max \{ \mu_1(x), \mu_2(x) \}$$

$$\mu_U(x) = \mu_1(x) + \mu_2(x) - \mu_1(x)\mu_2(x)$$

As an example, let us consider WARM temperature fuzzy set and COLD temperature fuzzy set defined by the following membership functions [8]:

$$\mu_w(T) = \exp\left(-0.5\left(\frac{T-25}{5}\right)^2\right)$$

$$\mu_c(T) = \exp\left(-0.5\left(\frac{T-15}{5}\right)^2\right)$$

Figure 2.6 and Figure 2.7 show the sketch of these two membership functions. We define COLD and WARM temperature fuzzy set as the intersection of the two fuzzy sets of WARM temperature and COLD temperature with the following membership function:

$$\mu_{cw}(T) = \min\{\mu_c(T), \mu_w(T)\}$$

$$\mu_{cw}(T) = \min\left\{\exp\left(-0.5\left(\frac{T-15}{5}\right)^2\right), \exp\left(-0.5\left(\frac{T-25}{5}\right)^2\right)\right\}$$

Figure 2.8 depicts the membership function of the COLD and WARM fuzzy set. The solid line in this figure indicates the membership function μ_{cw} .

Singleton fuzzy set is a fuzzy set that includes only one member with the membership degree of one. Figure 2.9 depicts five singleton fuzzy sets for the VOLTAGE parameter. Positive large (PL), positive small (PS), zero (Z), negative small (NS) and negative large (NL) voltages are defined as exactly 1, 0.5, 0, -0.5, and -1 volts respectively. This type of fuzzy set is widely used for fuzzification.

Fuzzy logic system is a powerful tool for nonlinear mapping of an input vector of a feature of interest into a scalar output [154]. Due to heuristic nature of the fuzzy logic, one can use it to deal with the systems with unknown dynamical model, measurement noise, etc. The heuristic language employs linguistic language to incorporate the expert knowledge,

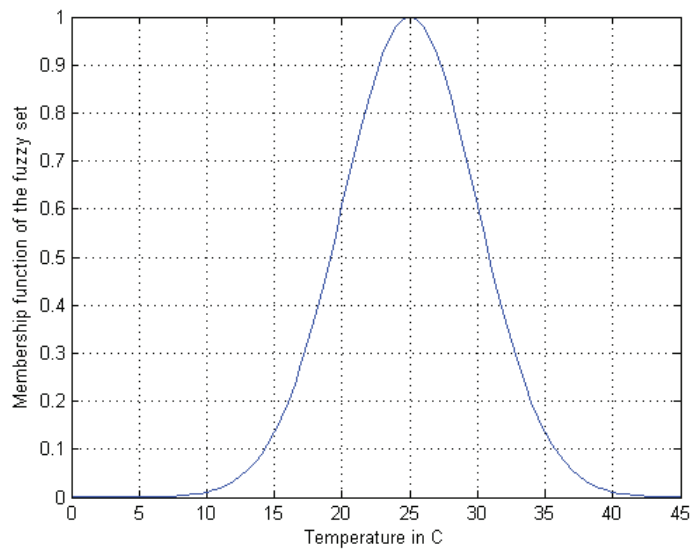


Figure 2.6: Membership function μ_w for the WARM temperature fuzzy set.

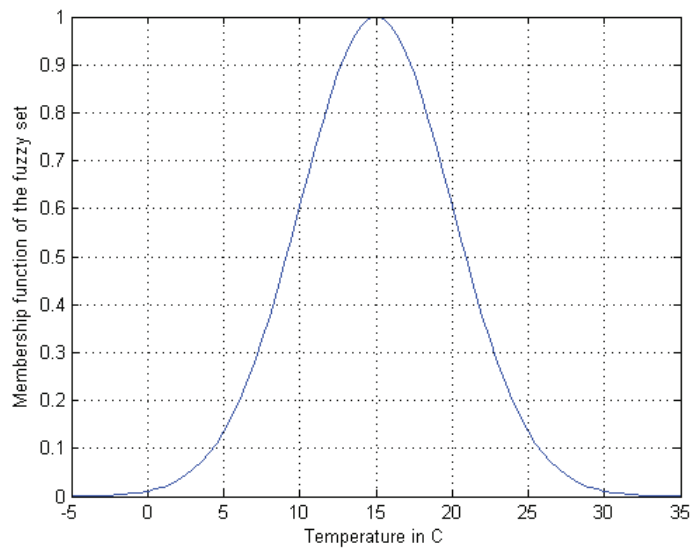


Figure 2.7: Membership function μ_c for the COLD temperature fuzzy set.

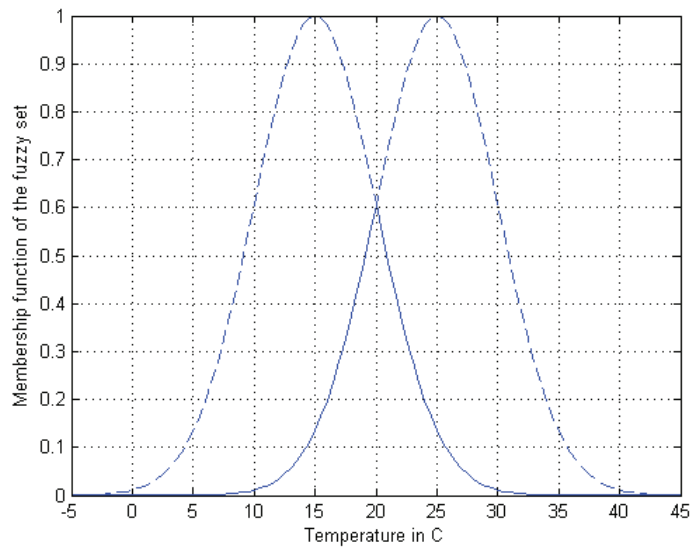


Figure 2.8: Membership function μ_{cw} for the COLD and WARM temperature fuzzy set.

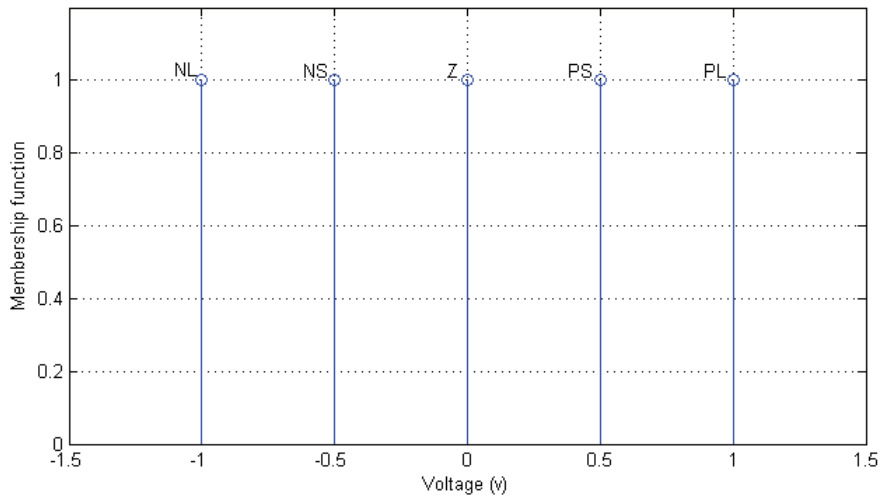


Figure 2.9: Membership functions defining five singleton fuzzy sets [8].

rules of thumb and experience based strategies and resulting with a set of rules in form of *If-Then* rules that allows us to work with fuzzy values instead of working with crisp values for input and output values. For example:

IF input-voltage = Positive large THEN output-voltage = Negative large

As seen this kind of rule can be integrated with human operators strategies and also the assumption of linearity is not necessary [155].

2.2.2 Fuzzy System Structure

A fuzzy system consists of four main parts namely, fuzzification, rule base, inference and defuzzification. Figure 2.10 depicts the structure of a fuzzy system.

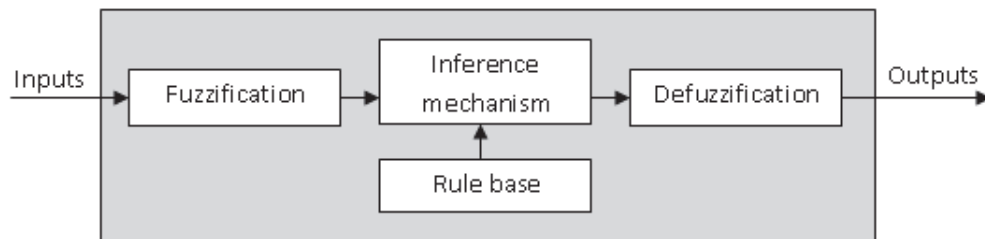


Figure 2.10: Fuzzy system structure [9].

Fuzzification

In the fuzzification stage the actual values of the inputs of the fuzzy system are converted into some fuzzy sets. These fuzzy sets in the inference mechanism are further combined together based on a set fuzzy rules and generate the output fuzzy sets. Here, the fuzzy rules are a combination of the intersection, union and complement operators. At the defuzzification stage the output fuzzy set is mapped to actual values to apply as the outputs of the fuzzy system.

Rule Base

Collection of a number of rules is called a "rule base" and is used to perform a task. A rule base for controlling the temperature of a room could be a good example of this decision making procedure:

1. If TEMPERATURE is LOW & TEMPERATURE VARIATION is POSITIVE , then HEAT UP RATE is SLOW.
2. If TEMPERATURE is LOW & TEMPERATURE VARIATION is ZERO , then HEAT UP RATE is MEDIUM.
3. If TEMPERATURE is LOW & TEMPERATURE VARIATION is NEGATIVE , then HEAT UP RATE is FAST.
4. If TEMPERATURE is MEDIUM & TEMPERATURE VARIATION is NEGATIVE , then HEAT UP RATE is SLOW.
5. If TEMPERATURE is MEDIUM & TEMPERATURE VARIATION is ZERO , then HEAT UP RATE is ZERO.
6. If TEMPERATURE is MEDIUM & TEMPERATURE VARIATION is POSITIVE , then HEAT UP RATE is ZERO.
7. If TEMPERATURE is HIGH then HEAT UP RATE is ZERO.

Inference

Let us take the example of room temperature control which was mentioned earlier. Let T and ΔT denote the temperature and the temperature variation, respectively and $\mu_{LOW}(T)$ represents the membership function of the "LOW" temperature fuzzy set and $\mu_{POS}(\Delta T)$ represents the membership function of the "POSITIVE" temperature variation fuzzy set.

Let y be the heat up rate and $\mu_{SLOW}(y)$ be the membership function of the "SLOW" heat up rate. To inference the first rule first we need to evaluate if the first rule is fired or not. In the crisp notion of the rules it can be either on or off but in fuzzy it is represented by a fuzzy set called the "premise fuzzy set" for that rule. Here its membership function is as follows:

$$\mu_1(T, \Delta T) = \mu_{LOW}(T) \wedge \mu_{POS}(\Delta T)$$

Also an "implied fuzzy" set is defined for the rule output and its membership function as follows:

$$\hat{\mu}_{SLOW}(y) = \mu_{SLOW}(y) \wedge \mu_1(T, \Delta T)$$

Now let us denote the membership function of premise fuzzy set of the i^{th} rule by $\mu_i(x)$ where x is the vector of the inputs of the fuzzy system and let us denote the membership function of the output of the rule by $\mu_{Q_i}(y)$ where y denotes the output of the fuzzy system. Then, the membership function of the implied fuzzy set is defined as follows:

$$\mu_{\hat{Q}_i}(y) = \mu_{Q_i}(y) \wedge \mu_i(x) \quad (2.50)$$

Having R rules in a rule base generates R implied fuzzy sets $\mu_{\hat{Q}_i}, i = 1, 2, \dots, R$ defined by the membership function of the equation (2.50).

Defuzzification

As explained above, in the inference step of the fuzzy system, first we need to find the degree of the firing of each rule in the rule base of interest and then provide the implied fuzzy sets of each rule according to the degree of firing of that rule.

In order to map the output of the fuzzy system into a crisp output, one can use different available methods of defuzzification, such as center of gravity (COG), center average (CA),

bisector of area (BOA), mean of maximum (MOM), smallest of maximum (SOM) and largest of maximum (LOM) defuzzification techniques. Here two of the above mentioned techniques which are employed mostly in practice are explained in more details.

1. Center of gravity (COG) defuzzification

Having $\mu_{Q_i}(y)$ as the membership function of the output of the rule i . The "center of area" of $\mu_{Q_i}(y)$, point C_i is a point such that:

$$\int_{-\infty}^{C_i} \mu_{Q_i}(y) dy = \int_{C_i}^{\infty} \mu_{Q_i}(y) dy$$

Therefore, the corresponding crisp output of the fuzzy system is determined as follows:

$$y_{crisp} = \frac{\sum_{i=1}^R C_i \int \mu_{\hat{Q}_i}}{\sum_{i=1}^R \int \mu_{\hat{Q}_i}}$$

2. Center average (CA) defuzzification

Similar to the COG defuzzification technique, for performing the CA defuzzification technique the following formula can be used:

$$y_{crisp} = \frac{\sum_{i=1}^R C_i \max_y \{ \mu_{\hat{Q}_i}(y) \}}{\sum_{i=1}^R \max_y \{ \mu_{\hat{Q}_i}(y) \}}$$

There are two main types of fuzzy systems named, Mamdani [9] and Takagi-Sugeno (TS) [156].

- Mamdani fuzzy system

The explanation presented so far was for Mamdani fuzzy systems which let us to model the system more intuitively and human like manner.

- Takagi-Sugeno fuzzy system

Takagi-Sugeno fuzzy systems is very similar to the Mamdani fuzzy system, except for the rule base part of the system. In Mamdani fuzzy system, both inputs and outputs of the rules constructed by the fuzzy sets. On the contrary, the output of the rules are constructed by memoryless functions $f_i(\cdot)$ in TS fuzzy system by the following form of rule:

$$\text{If } x_1 \text{ is } P_1 \ \& \ x_2 \text{ is } P_2 \ \& \ \dots, \text{ then } C_i = f_i(\cdot)$$

where P_1 and P_2 denote the input fuzzy sets.

The consequence of the rules in the TS fuzzy system are mathematical descriptions and can be any function of the input variables. That's why the TS fuzzy systems are less intuitive than the Mamdani fuzzy systems.

For the defuzzification stage of the TS fuzzy systems, similar to what we explained for the Mamdani fuzzy systems, one can determine the crisp output of the system as follows:

$$y_{crisp} = \frac{\sum_{i=1}^R C_i \mu_{\hat{Q}_i}}{\sum_{i=1}^R \mu_{\hat{Q}_i}}$$

Compared to the Mamdani fuzzy systems, TS fuzzy systems work better with linear techniques such as PID control and have better performance in fuzzy identification of dynamic systems. TS fuzzy systems are also better to mathematical analysis [157, 8].

2.3 Aircraft Gas Turbine Engine

Gas turbines are machines which are widely used for delivering power, heat or thrust. In industrial or stationary gas turbine engines, the goal is delivering the shaft power for electricity production or other purposes. In aircraft gas turbines, the goal is providing the thrust or propulsion power. Depending on the application, other names are also used for the gas turbine engines. The gas turbine engine for electrical power generation purposes are also

called "combustion turbine" or "turboshaft engine". In aviation domain the gas turbine engine is also called a "jet engine" and depending on its specific usage it may be called "turbojet", "turboprop", "turbofan" or "ramjet" [10]. Figure 2.11 depicts the block diagrams of an aircraft jet engine and a stationary gas turbine engine. As seen in this figure the hot air flow passing through the turbine is accelerated into the air via the nozzle and the reaction of this produced thrust will cause the aircraft move forward. For the stationary gas turbine engine, the accelerated hot air flow is used as an output shaft power to derive an electrical generator or other devices [158].

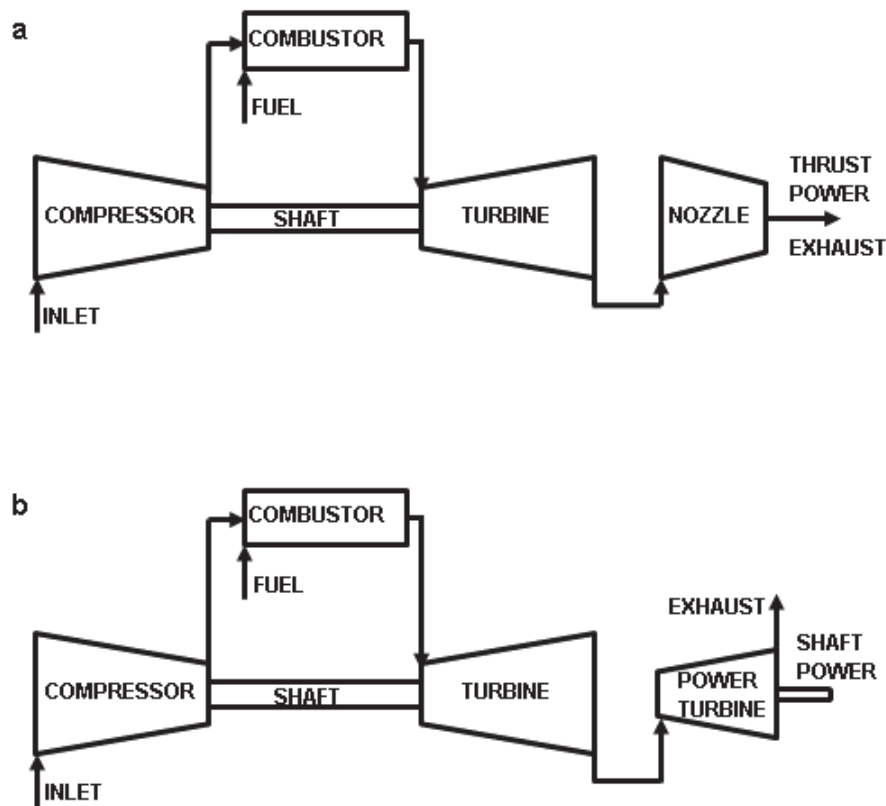


Figure 2.11: Block diagram of an aircraft gas turbine engine (a) and a stationary gas turbine engine (b) [10].

Figure 2.12 depicts the schematic of a single spool jet engine. All the jet engines work based on the same basis. Surrounding air is taken through the intake part of the engine

and is compressed in the compressor. The pressurized air is directed into the combustion chamber to burn with the fuel. Therefore, the energy will be absorbed by the fluid (here air) as heat. Then, this heated air is expanded in the turbine followed by the combustion chamber and then passes through the nozzle to generate thrust which leads to push the plane forward. A portion of the gas which is expanded in the turbine is employed to derive the compressor via a shaft [159, 11].

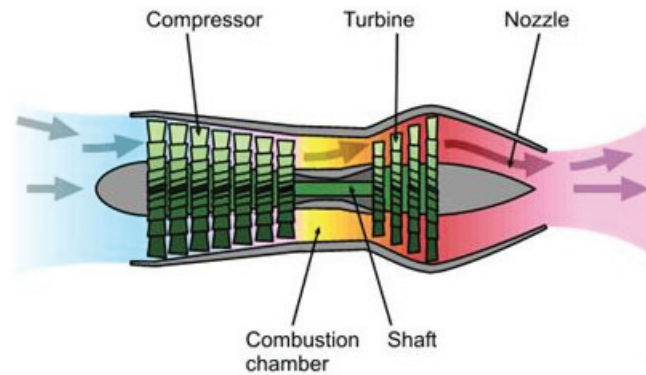


Figure 2.12: Schematic of a single spool jet engine [11].

2.3.1 Gas Turbine Cycles

A gas turbine cycle explains the status of the air in terms of the volume of the air occupied and its correspondent pressure throughout its path in the engine. The working cycle or Brayton cycle is also shown in Figure 2.13. As demonstrated in this figure, in the compressor the air is compressed so that its pressure increases and its volume decreases. Then, in the combustion chamber, the pressure is kept almost the same and the volume will be increased. In the turbine and the nozzle, the expansion phase of the cycle, the volume increases and the pressure drops.

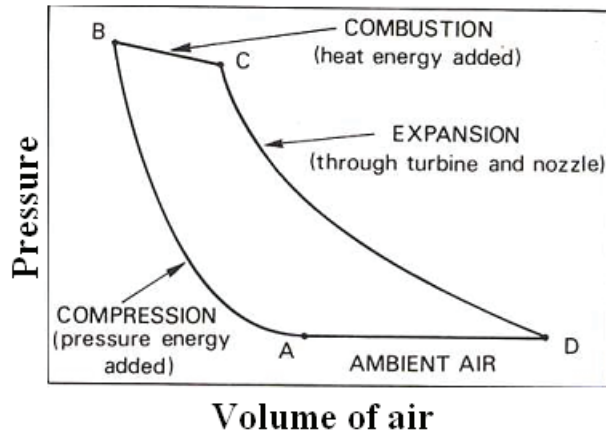


Figure 2.13: Working cycle pressure-volume graph in the gas turbine engine [12].

2.3.2 Aircraft Gas Turbine Engine Mathematical Model

Mathematical representation of the gas turbine engines have been investigated by a number of authors in the literature [160, 71, 161]. The model of the engine which is used in this thesis is the nonlinear model of a single spool jet engine which has been developed in Matlab Simulink software by Naderi *et. al* [13]. The model represents the relationships between different engine variables such as the turbine temperatures, pressures, and gas flow rates, etc.

In this model, the compressor and turbine components are modeled by the performance maps adopted from a commercial software GSP 11 [131]. Also the derived model in the work of Naderi *et. al* has been validated by GSP. In the remainder of this section, the detailed mathematical expressions defining the dynamics of the engine components are presented. Figure 2.14 depicts the information flow between the engine modules in the Simulink model of the single spool engine.

In order to derive the mathematical model of the jet engine, one needs to identify the dynamics of the rotor, volume and heat transfer of the jet engine for transient response. In this model, the heat transfer dynamics of the system is neglected as compared to the rotor and volume dynamics, as the effect of heat transfer dynamics is negligible. Refer to the

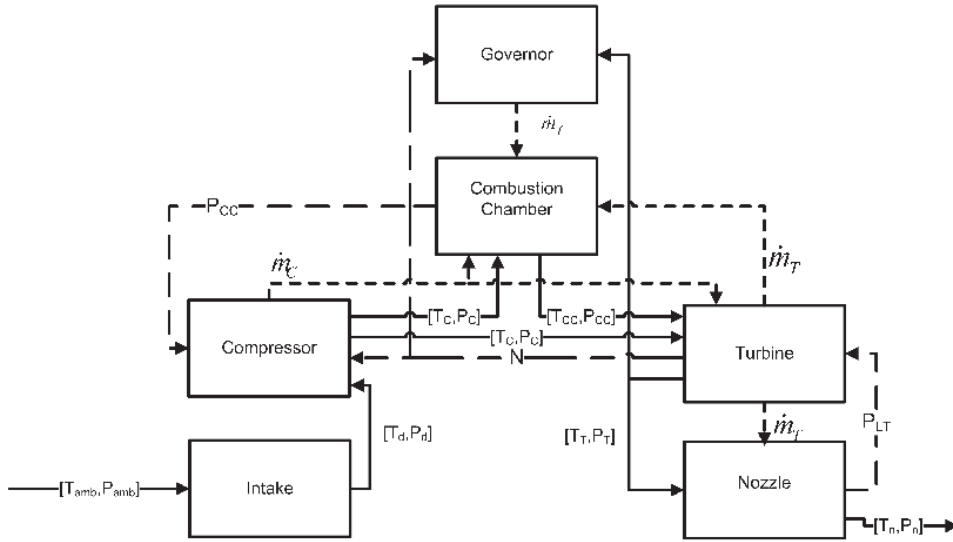


Figure 2.14: Flow diagram and interdependencies of different modules of the jet engine dynamics [13].

nomenclature section for definitions of the variables and terms.

Rotor Dynamics

The rotors connecting the pairs of turbine and compressor might be accelerated or decelerated due to the existing power imbalance between the turbine and the compressor. Therefore the energy balance between the compressor and the shaft or spool should be modeled as follows:

$$\frac{dE}{dt} = \eta_{mech} W_T - W_C \quad (2.51)$$

where $E = \frac{J \left(\frac{N2\pi}{60} \right)^2}{2}$.

Volume Dynamics

Any mass flow unbalance through the engine components may lead to changes in pressure of volumes and should be taken into consideration as volume dynamics. Volume dynamics with the assumption that the gas with the homogeneous properties has zero speed is given as follows:

$$\dot{P} = \frac{RT}{V} (\sum \dot{m}_{in} - \sum \dot{m}_{out}) \quad (2.52)$$

Components - Intake

Assuming adiabatic process (a process in which the net heat transfer to or from the working fluid (e.g. gas) is zero), the pressure and the temperature of the engine intake are determined by the following formulae:

$$\frac{P_d}{P_{amb}} = \left[1 + \eta_d \frac{\gamma - 1}{2} M^2 \right]^{\frac{\gamma}{\gamma - 1}} \quad (2.53)$$

$$\frac{T_d}{T_{amb}} = 1 + \frac{\gamma - 1}{2} M^2 \quad (2.54)$$

Components - Compressor

As mentioned earlier for modeling the compressor behavior, compressor performance map taken from the commercial software GSP has been used [131]. In order to determine the efficiency (η_C) and mass flow rate ($\dot{m}_C \frac{\sqrt{\theta}}{\delta}$) of the compressor by having the pressure ratio (π_C) and the corrected rotational speed ($\frac{N}{\sqrt{\theta}}$) one needs to employ an interpolation technique, so that $\theta = \frac{T_i}{T_o}$ and $\delta = \frac{P_i}{P_o}$. In other words, $\dot{m}_C \frac{\sqrt{\theta}}{\delta} = f_{\dot{m}_C} \left(\frac{N}{\sqrt{\theta}}, \pi_C \right)$ and $\eta_C = f_{\eta_C} \left(\frac{N}{\sqrt{\theta}}, \pi_C \right)$. Using the determined compressor efficiency and mass flow rate, the mechanical power and compressor temperature increase can be obtained by the following formulae:

$$T_o = T_i \left[1 + \frac{1}{\eta_C} (\pi_C^{\frac{\gamma-1}{\gamma}} - 1) \right] \quad (2.55)$$

$$W_C = \dot{m}_C c_p (T_o - T_i) \quad (2.56)$$

Components - Combustion Chamber

The combustion chamber manifests both the volume dynamics and energy cumulation between the turbine and the compressor simultaneously which eventually have the following relationships:

$$\dot{P}_{CC} = \frac{P_{CC}}{T_{CC}} \dot{T}_{CC} + \frac{\gamma R T_{CC}}{V_{CC}} (\dot{m}_C + \dot{m}_f - \dot{m}_T) \quad (2.57)$$

$$\dot{T}_{CC} = \frac{1}{c_v m_{CC}} \left[(c_p T_C \dot{m}_C + \eta_{CC} H_u \dot{m}_f - c_p T_{CC} \dot{m}_T) - c_v T_{CC} (\dot{m}_C + \dot{m}_f - \dot{m}_T) \right] \quad (2.58)$$

Components - Turbine

As mentioned earlier for modeling the turbine behavior, turbine performance map taken from the commercial software GSP has been used [131]. In order to determine the efficiency (η_T) and mass flow rate ($\dot{m}_T \frac{\sqrt{\theta}}{\delta}$) of the turbine by having the pressure ratio (π_T) and the corrected rotational speed ($\frac{N}{\sqrt{\theta}}$) one needs to employ an interpolation technique, so that $\theta = \frac{T_i}{T_o}$ and $\delta = \frac{P_i}{P_o}$. In the other words $\dot{m}_T \frac{\sqrt{\theta}}{\delta} = f_{\dot{m}_T} \left(\frac{N}{\sqrt{\theta}}, \pi_T \right)$ and $\eta_T = f_{\eta_T} \left(\frac{N}{\sqrt{\theta}}, \pi_T \right)$. Using the determined turbine efficiency and mass flow rate, the mechanical power and turbine temperature decrease can be obtained by the following formulae:

$$T_o = T_i \left[1 - \eta_T (1 - \pi_T^{\frac{\gamma-1}{\gamma}}) \right] \quad (2.59)$$

$$W_T = \dot{m}_T c_p (T_o - T_i) \quad (2.60)$$

The mass flow rate of the nozzle is obtained by the following formula:

$$\frac{\dot{m}_n \sqrt{T_{n_i}}}{P_{n_i}} = \begin{cases} \frac{u}{\sqrt{T_{n_i}}} \frac{A_n}{R} \frac{P_{amb}}{P_{n_i}} \frac{T_{n_i}}{T_{no}}, & \frac{P_{amb}}{P_{n_i}} < \left[1 + \frac{1-\gamma}{\eta_n(1+\gamma)}\right]^{\frac{\gamma}{\gamma-1}} \\ \frac{u}{\sqrt{T_{n_i}}} \frac{A_n}{R} \frac{P_{crit}}{P_{n_i}} \frac{T_{n_i}}{T_{crit}}, & \text{otherwise} \end{cases} \quad (2.61)$$

where $\frac{u}{T_{n_i}} = \sqrt{2c_p \eta_n \left(1 - \frac{P_{amb}}{P_{n_i}} \frac{\gamma-1}{\gamma}\right)}$, $\frac{T_{no}}{T_{n_i}} = 1 - \eta_n \left(1 - \left(\frac{P_{amb}}{P_{n_i}}\right)^{\frac{\gamma-1}{\gamma}}\right)$, $\frac{P_{crit}}{P_{n_i}} = \left(1 - \frac{1}{\eta_n} \left(\frac{\gamma-1}{\gamma+1}\right)\right)^{\frac{\gamma}{\gamma-1}}$, $\frac{u}{T_{n_i}} = \frac{2\gamma R}{\gamma+1}$ and $\frac{T_{crit}}{T_{n_i}} = \frac{2}{\gamma+1}$, where P_{n_i} is equal to the turbine pressure P_T and T_{n_i} is equal to the mixer temperature T_M . Using the energy balance in the mixer gives the mixer temperature as follows:

$$T_M = \frac{\dot{m}_T T_T + \beta \dot{m}_C T_C}{\dot{m}_T + \beta \dot{m}_C} \quad (2.62)$$

Set of Governing Nonlinear Equations

Finally the aforementioned process and dynamics of a single spool jet engine can be summarized by the following set of governing nonlinear equations [13]:

$$\begin{aligned} \dot{T}_{CC} &= \frac{1}{c_v m_{CC}} \left[(c_p T_C \dot{m}_C + \eta_{CC} H_u \dot{m}_f - c_p T_{CC} \dot{m}_T) - c_v T_{CC} (\dot{m}_C + \dot{m}_f - \dot{m}_T) \right] \\ \dot{N} &= \frac{\eta_{mech} \dot{m}_T c_p (T_{CC} - T_T) - \dot{m}_{CC} c_p (T_C - T_d)}{JN \left(\frac{\pi}{30}\right)^2} \\ \dot{P}_T &= \frac{RT_M}{V_M} (\dot{m}_T + \frac{\beta}{\beta+1} \dot{m}_C - \dot{m}_n) \\ \dot{P}_{CC} &= \frac{P_{CC}}{T_{CC}} \dot{T}_{CC} + \frac{RT_{CC}}{V_{CC}} (\dot{m}_C + \dot{m}_f - \dot{m}_T) \end{aligned} \quad (2.63)$$

where η_{mech} and J denote the mechanical efficiency and the inertia of the spool. The dynamics of the fuel flow rate is described by the following expression [13]:

$$\tau \frac{d}{dt} \dot{m}_f + \dot{m}_f = G u_{fd} \quad (2.64)$$

where τ denotes the time constant, G and u_{fd} denote the gain associated with the fuel valve and the required fuel.

2.3.3 Degradations in the Engine

Gas turbine engines like any other complex system contain a lot of elements and each of these elements might fail in variety of manners. A faulty element does not only affect that element's normal behavior but due to existing action and reaction between this element and other system's elements, it can affect normal behavior of other system's elements. Obviously the severity of these effects on other system's elements can be different. It is possible that the subsequent faults are different from the primary faults in both severity and propagation dynamics point of views. In other words, in some cases, the faults arise due to a non-serious primary fault by itself are critical and damaging to the engine. Compressor fouling is a good example of this type. Compressor fouling fault is not considered as a critical and serious fault for the engine, but it can lead to blades degradation and eventually to the engine failure [103]. In general, every engine can be considered as a collection of three main sets as follows [30]:

- Accessory equipment consisting of components such as fuel pump, fuel control, engine air bleed, and lubrication and ignition systems.
- Thermodynamic gas path components entailing the compressor, the gas containment path, the burner and the turbine.
- Rotational mechanical equipment including rotors, engine bearings and gear trains.

Engine degradation can be initiated from different sources such as fouling, blade erosion and corrosion, worn seals and excessive blade tip clearance that can induce gradual

degradation in the performance of the engine [14, 162]. References [163] and [164] have investigated several degradation mechanisms in the gas turbines.

Types of Degradation in the Engine

Generally engine degradations can be categorized in to three main categories as follows [112]:

- Recoverable degradation

Particles such as dust, dirt, soot might be accumulated on the gas path surfaces and compressor airfoils due to the engines normal operation. Permeation of oil particles into the compressor input with the incoming air flow can work as glue, consequently the dirt particles stick to compressors airfoils. In addition, at the end of the compressor module these oily particles can be baked due to the high temperature of that area and they can form a non-uniform and thick coating. Depending on the amount and type of these particles the engine will be subjected to performance degradation. A proper cleaning or washing procedure can recover the engine from this type of deterioration [112].

- Non-recoverable degradation

Despite going through maintenance, the degraded engine may not be recovered completely. This can happen due to the surface deposit that is not removed by washing procedure. Basically any surface erosion or corrosion, increasing of tip and seal clearance and many other causes will not be retrieved employing washing procedure [112].

- Permanent performance degradation

Purpose of the maintenance procedure is restituting the engine to its normal condition as much as possible. Therefore, during the maintenance procedure some of the damaged parts

will be replaced, the eroded airfoils get recoated. Despite all this, after a major maintenance or overhaul, the engine performance will not be restored to its new condition. This can be due to increasing the roughness of the gas path components surfaces, or cylinder distortion [112].

An engine model derived by using accurate definition of engine components characteristics can be used for evaluating the engine performance. One can express the engine performance in terms of dependent measurable parameters and independent parameters which are not measurable [114]. Dependent parameters are addressing the parameters such as fuel flows, thrust, spool speeds, turbine and compressor temperatures and pressures of compressor and turbine. Independent parameters (performance parameters) or engine health parameters are referring to flow capacities and efficiencies of the engine rotating elements and discharge coefficient of the propelling nozzles [14]. One can perform analysis and assess the changes in the engine performance based on the dependent parameters from the engine's gas path. Figure 2.15 depicts different connections in the mentioned performance analysis [14].

As shown in Figure 2.15 performance changes due to the gas path components degradation could have originated from physical faults such as blade tip clearance because of erosion and wearing, fouling, corrosion, hot end component damage, foreign object damage (FOD), etc. The physical faults are the results of variations in the gas turbine thermodynamic performances which are unavoidable for any mechanical equipment such as an aero engine [14, 28]. Components flow capacities and efficiencies are employed for determining these performances. Flow capacity and efficiency (performance parameters) changes reflects on engine parameters such as pressure, temperature, spools speeds, and fuel flow. Using the engine parameters which convey the degraded performance of the engine components, one can detect, isolate the faulty components [28].

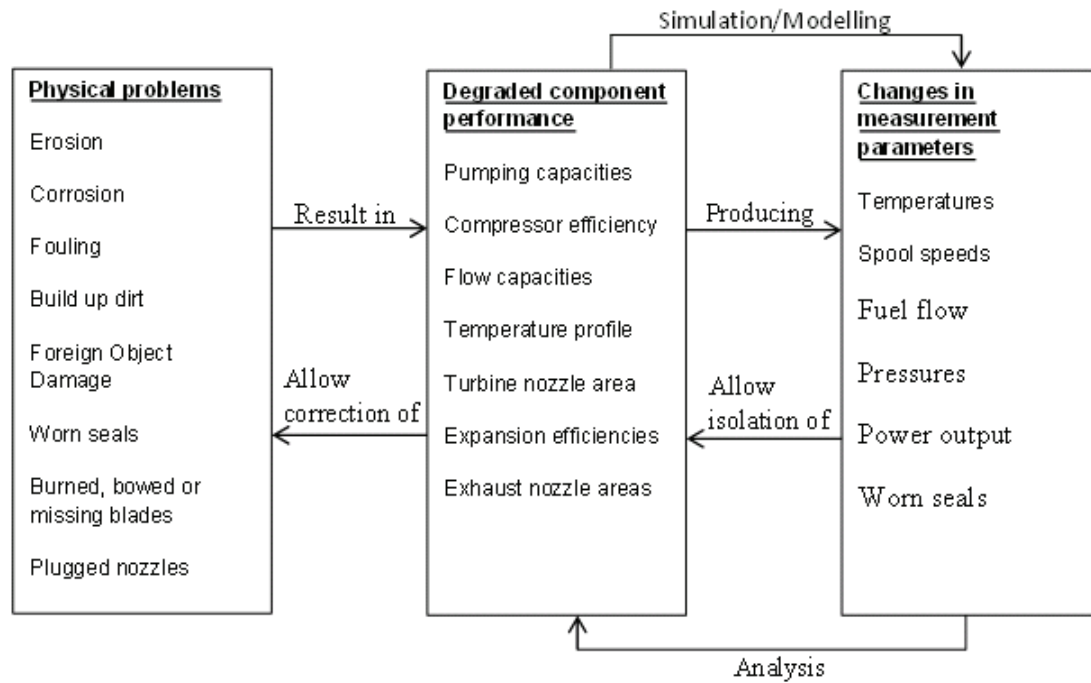


Figure 2.15: Gas Turbine Engine Performance Analysis [14],[15].

The main moving subsystems of a jet engine are fan, low pressure compressor (LPC), high pressure compressor (HPC), high pressure turbine (HPT), and finally low pressure turbine (LPT) and operating conditions of engine are namely ambient temperature, inlet air pressure and aircraft speed [103].

A non-rigorous definition of the engine deterioration is an increased level of losses in the components of the engine and it is reflected in the overall performance of the engine such as decreases in the engine thrust and increases in the specific fuel consumption. In the following a brief description of main sources of deterioration in the gas turbine engines will be presented [27, 165, 166, 167]:

- When dust and external particles accumulate on the airfoils and interior surfaces of the engine, it is called fouling and results in increasing the surface roughness and changing shape of the blades. The effect of fouling can be seen in Figure 2.16.

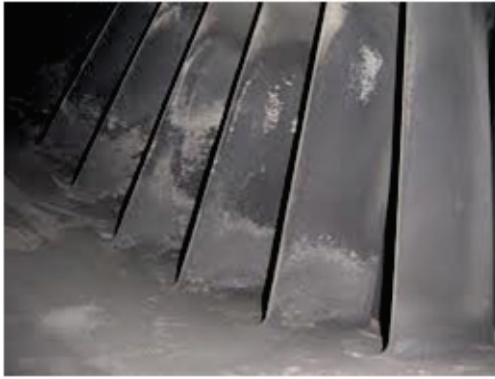


Figure 2.16: The blade fouling in the compressor [16].

- In the case of collision between a solid particle suspended in the inlet air or gas and the engine's blade, it is possible that some material from blades are removed. We call this phenomenon erosion. Figure 2.17 shows the blade erosion in an engine.

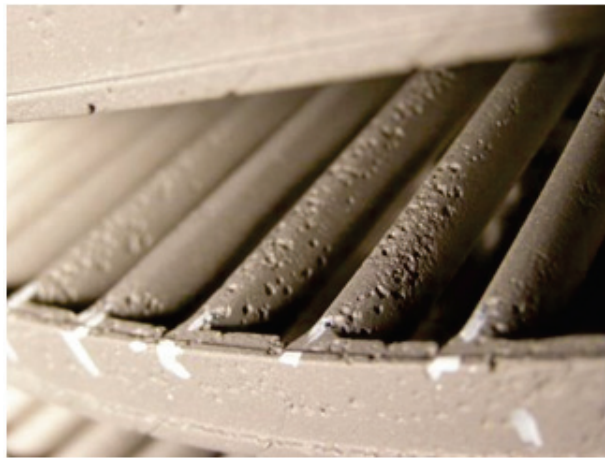


Figure 2.17: The blade erosion [17].

- If the removal of material from the rotor blades is caused by physical contact between the rotor components and the stator parts it is called abrasion or rubbing-wear and it naturally happens during the engine running-in period before establishing proper clearances. It also occurs due to the loss of the engine bearings stiffness as engine ages.

- Corrosion in the engine components is the loss of material caused by chemical reactions between the component material and the air/gas fluids contamination such as salts or reactive gases and usually occurs at high temperatures.
- In general, if the failure in a component is severe it is called damage. There are different source for damage including foreign object damage such as the bird strike, and domestic object damage such as a piece of seal impacting a downstream component [27].

There are different sources that may cause gradual deterioration in the engine during its normal operation but mainly they are fouling, erosion and corrosion. In [168] the effects of these factors on different components of the engine are described. These factors lead to increase in tip clearance and change in the geometry and surface structure of the airfoils in the compressor and cause reduction in the compressor efficiency, flow capacity and its work capacity. Except for the severe cases such as plugged fuel injector, the combustion chamber is not subject to gradual deterioration and its efficiency does not decrease [27]. However, in case of combustor deterioration the temperature of exiting gases is fluctuated and the peak temperatures may result in damages in turbine components. The mechanism of effects of the above factors on the turbine are similar to those of the compressor and cause the reduction in efficiency and increase flow capacity. These facts are supported by analysis of operational data of engine in [27].

Although the mechanisms that cause engine deterioration are known, due to their dependence on some extent of factors such as usage, environment and time, they are not purely deterministic and each engine experiences a unique degradation profile. [27].

2.3.4 Flight Phases

In general, each flight consists of five main phases namely, take off, climb, cruise, descent and landing. Take off is the part of the flight that aircraft goes through a transition from

ground to flying in the air and its engine is working under full power in order to produce the necessary thrust. Climb is the next phase of the flight and it starts from retracting the wheels into the aircraft. During the climb phase, aircraft should reach to altitude (typically 10Km). After the climb phase, aircraft goes through the cruise phase at this altitude which is more economic in terms of fuel consumption. Commercial aircraft engines are designed such that they function optimally in the cruise phase as it is the longest phase of the flight [169].

During the flight, whenever the aircraft decreases the altitude, it is called descent. Descent is a necessary phase of the flight before the last phase, landing. The other situations that the aircraft may go through descent phase are for avoiding traffic, air conditions, clouds or entering into warm weather. The last phase of the flight is landing in which the aircraft speed down to return to the ground. In order to perform a smooth landing, this speed reduction is performed by a decrease in the speed combining with inducing a larger drag value (this can be done by employing landing gear, flaps and air brakes) [169].

2.4 Integrating Engine Degradation into the Engine Model

In this thesis, we have investigated the effects of the compressor fouling and the turbine erosion as two main soft degradation causes of the gas turbine engines. In order to quantitatively represent the effects of the turbine erosion and compressor fouling on the engine performance, we introduce an erosion factor denoted by $0 \leq E_i < 1$ and a fouling factor denoted by $0 \leq F_i < 1$. Based on the approach presented in [112, 162] the dynamics of the

engine is affected by F_i and E_i as follows:

$$\begin{aligned}
 \dot{m}_C &= \left(1 - \frac{1}{2}F_i\right)\dot{m}_C^* \\
 \eta_C &= (1 - F_i)\eta_C^* \\
 \dot{m}_T &= \left(1 + \frac{1}{2}E_i\right)\dot{m}_T^* \\
 \eta_T &= (1 - E_i)\eta_T^*
 \end{aligned} \tag{2.65}$$

where \dot{m}_C^* , η_C^* , \dot{m}_T^* and η_T^* denote mass flow rate and efficiency of the compressor and the turbine of the healthy engine, respectively.

To model the degradation of engine different scenarios are considered and based on each scenario F_i and E_i are calculated in each take off simulation cycle. For example in fouling scenario with fouling index FI the fouling factor F_i at cycle n is computed as:

$$F_i(n) = \frac{n}{Total\ flight\ cycles} FI$$

and in the erosion scenario with erosion index EI at n^{th} simulation cycle $E_i(n) = \frac{n}{Total\ flight\ cycles} EI$.

Other considered scenarios and their details are presented in Chapter 3. The model which is used in this work for generating the healthy and degraded data (process parameters) is taken from the work of Naderi *et al.* [13]. The degraded data as indicated above are due to the injection of physical faults, compressor fouling and turbine erosion. The model is a single spool turbojet engine which also includes degradations in the system health parameters, i.e. the mass flow rate and the efficiency of both the compressor and the turbine. It should be noted that the aforementioned degradation model with its validation procedure presented in this section had been accomplished in cooperation with the author of this thesis and some of these results have been published in the following conference:

1. N. Daroogheh, A. Vatani, **M. Gholamhossein** and K. Khorasani, "Engine life evaluation based on a probabilistic approach," in *ASME International Mechanical Engineering Congress and Exposition*, pp. 347-358, 2012.

In order to validate the accuracy of the numerical model in presence of compressor fouling and turbine erosion, first the fouling scenario with different FI 1%, FI 2% and FI 3% is considered for 100 flight cycles. At each flight cycle the value of F_i is computed and based on that numerical simulation using our Simulink model and GSP software are performed. Figure 2.18 shows the compressor temperature, turbine temperature, spool speed and fuel consumption of the engine that result by our Simulink model. As shown the compressor fouling decrease the compressor efficiency and mass flow rate and its ratio is 1:2. It also shows the fouling caused increase in the turbine temperature and despite increase in mass flow rate the engine spool speed is decreased. The quantitative comparison of our model and GSP is presented in Table 2.1. Although it shows some discrepancies in the data due to difference in compressor and turbine mapping functions, the trend is the same.

In the second step the erosion scenario for 200 flight cycles and EI 1%, 2% and 3% is considered and both our Simulink model and GSP software are used to perform numerical simulations. The results obtained from our engine model software are presented in Figure 2.19. As shown the erosion caused increase in the turbine temperature and decrease in compressor temperature and spool speed. It is worth mentioning the erosion has more effect on engine states and the trend is more nonlinear. The quantitative results for both our Simulink model and GSP software simulation results are presented in Table 2.2. Here again, the results show the same trend for both cases despite some discrepancies.

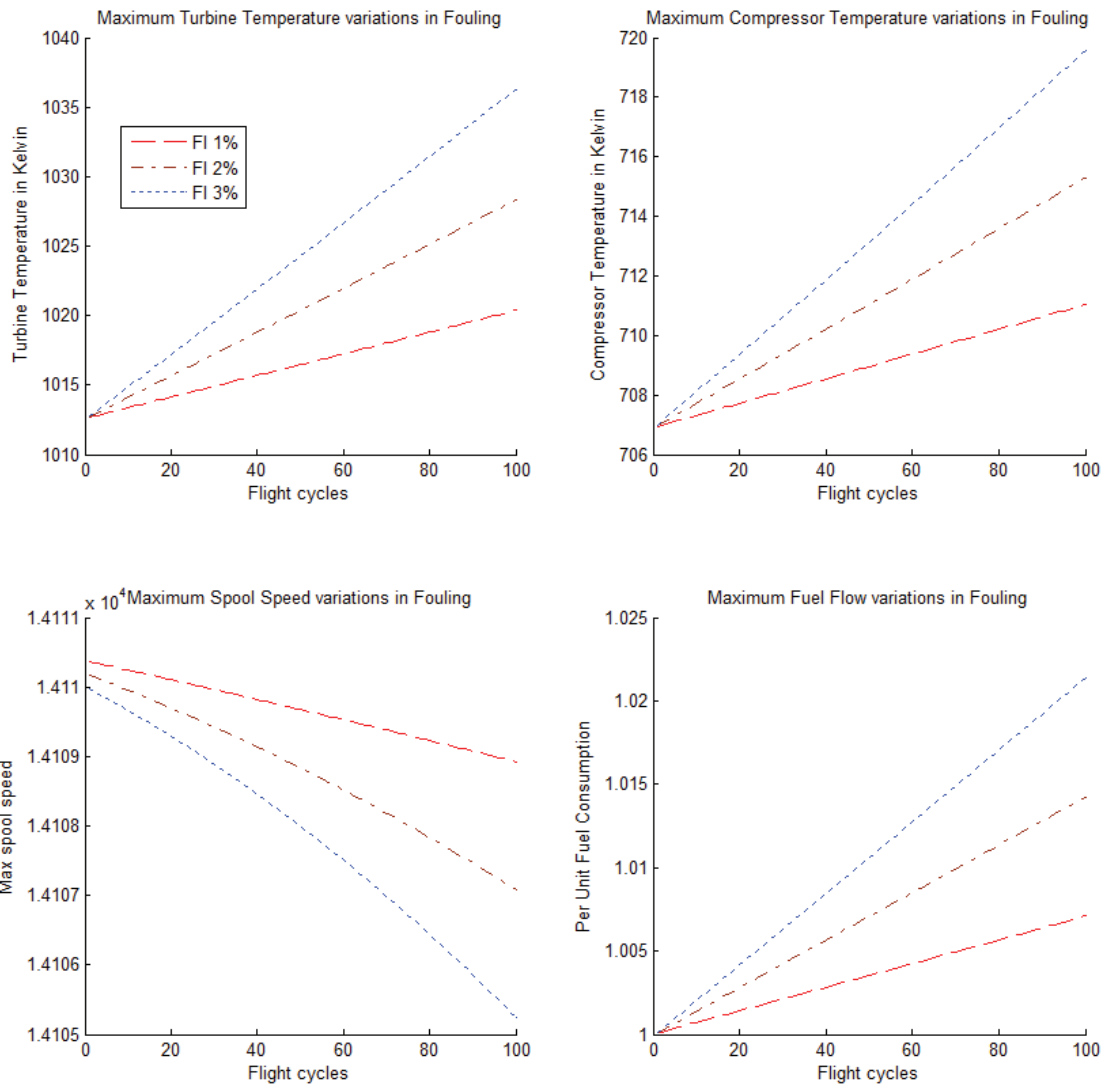


Figure 2.18: The outputs of the degraded model associated with the fouling degradation [18].

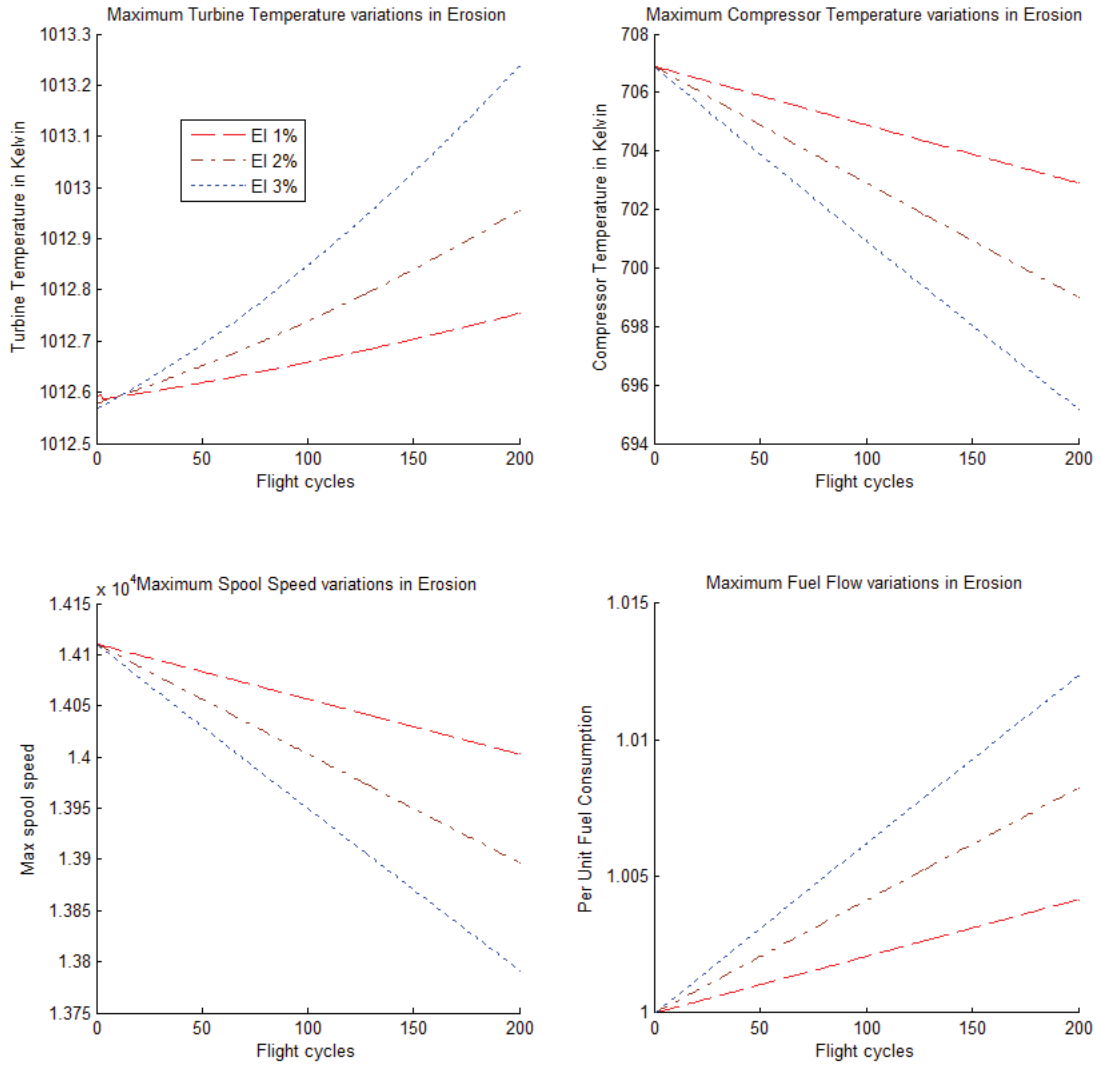


Figure 2.19: The outputs of the degraded model associated with the erosion degradation [18].

Table 2.1: Per unit changes in the engine parameters corresponding to the fouling scenarios.

Engine Parameter	Per Unit Change in Our Model	Per Unit Change in the GSP [131]
Fuel Flow consumption in FI 1%	0.0699	0.01678
Fuel Flow Consumption in FI 2%	0.04855	0.02368
Fuel Flow Consumption in FI 3%	0.02127	0.03210
Compressor Temperature in FI 1%	0.05798	0.03817
Compressor Temperature in FI 2%	0.03287	0.08371
Compressor Temperature in FI 3%	0.01776	0.01187
Turbine Temperature in FI 1%	0.093	0.01151
Turbine Temperature in FI 2%	0.0652	0.02370
Turbine Temperature in FI 3%	0.02839	0.03255
Spool Speed in FI 1%	-0.007087	-0.01456
Spool Speed in FI 2%	-0.02325	-0.02795
Spool Speed in FI 3%	-0.03543	-0.04016

Table 2.2: Per unit changes in the engine parameters corresponding to the erosion scenarios.

Engine Parameter	Per Unit Change in Our Model	Per Unit Change in the GSP [131]
Fuel Flow consumption in EI 1%	0.04181	0.01763
Fuel Flow consumption in EI 2%	0.08272	0.03367
Fuel Flow consumption in EI 3%	0.01236	0.04949
Compressor Temperature in EI 1%	-0.05626	-0.04173
Compressor Temperature in EI 2%	-0.01112	-0.07378
Compressor Temperature in EI 3%	-0.01648	-0.09640
Turbine Temperature in EI 1%	0.0568	0.01771
Turbine Temperature in EI 2%	0.01086	0.03352
Turbine Temperature in EI 3%	0.01632	0.05396
Spool Speed in EI 1%	-0.07583	-0.01029
Spool Speed in EI 2%	-0.01502	-0.01854
Spool Speed in EI 3%	-0.02246	-0.02500

2.5 Summary

In this chapter, first the time-series modeling and prediction focused on ARIMA and VAR methods were presented. AIC and BIC as two widely used criteria for model selection have also been explained. Fuzzy logic structure and its components were reviewed. The aircraft gas turbine engine components, its components and flight phases were reviewed. This was followed by reviewing the degradation in the engine and finally we explained how the degradations models were integrated into the engine model.

Chapter 3

VAR a Time-series Approach

In this chapter, first the designed controller for generating the data will be explained. Then, two time-series based models employed for predicting the deterioration trend of a single-pool gas turbine engine performance will be described. The proposed time-series methods are applied to certain engine measurable variables namely, the turbine and the compressor temperatures. Finally, the two methods are compared at the end of this chapter.

3.1 Gas Turbine Engine Controller

The data used in this thesis are generated by the Simulink model that was explained in previous chapter. The data is captured at the time when the maximum thrust is applied to the engine in the take off mode. The take off time for each flight is 20 seconds. Therefore, we keep one data from each cycle for each parameter. The reason that the engine degradation is investigated in the take off mode is that the effects of the degradation on the engine parameters are manifested more strongly in the take off mode, since the maximum thrust is expected to be provided in this mode. A feed forward and a negative feedback controller have been designed to control the amount of the fuel flow of the engine to keep the thrust at the desired level. In order to find out the fuel range of the engine under study, first the

fuel has been increased until the turbine temperature does not exceed its maximum value and the spool speed is still within its normal range. This gives us the maximum value of the fuel. In order to find the minimum amount of the fuel for the engine, the fuel should be decreased until the engine is not going to its idle mode.

Engine pressure ratio (EPR) is the ratio of the engine exhaust pressure to the intake pressure into the gas turbine engine and it is proportional to the engine thrust. To make sure that the collected data is suitable for further analysis in each cycle, engine EPR should follow its desired value despite any changes in its efficiency as a result of the fouling and erosion. To achieve this goal a controller is needed to keep the EPR value at the desirable value.

In order to generate the required data for degradation trend modeling purposes, one needs to capture the steady state data of the Simulink model. Therefore, the objective of this controller under all possible engine health conditions are set as follows:

- Settling time as small as 0.5 second.
- Steady state error less than 1%.

Engine is a nonlinear system. To deal with its nonlinearity first a feed-forward controller is designed. The idea is to find a mapping function between the amount of the fuel and the steady state value of the EPR for the healthy engine. For any desired engine EPR value we could provide the feed-forward fuel input of the engine. Hence, the engine can be considered as a linear system around that operating point and a linear feedback controller could be used to force the error to approach to zero. In order to implement the feed-forward controller for some EPR desired values, the amount of input fuel in the Simulink model is manually adjusted until the engine EPR reaches its desired value. After that, the look-up table block of Simulink is used to interpolate the other mapping points. Finally a proportional controller is used to implement the linear control part. It is worth mentioning that a saturation block is also used to guarantee that the fuel input of the engine always remains

Table 3.1: Steady state error % and settling time of the controller response under different engine conditions

Engine condition	Steady state error %	Settling time (second)
Healthy	2.95e-4	0.14
EI1%	0.012	0.14
EI3%	0.038	0.15
FI1%	0.0198	0.14
FI3%	0.0605	0.14
FI3% EI3%	0.09	0.15

in its acceptable range and the engine does not exceed its limitations. Figure 3.1 depicts the diagram of the controller in the Simulink and Table 3.1 depicts how the controller meets the above objectives. As seen in this table, steady state error of the controller for the healthy condition of the engine is close to zero and it increases as the engine gets eroded or fouled but still remains in its acceptable region. The settling time remains almost the same under different engine conditions.

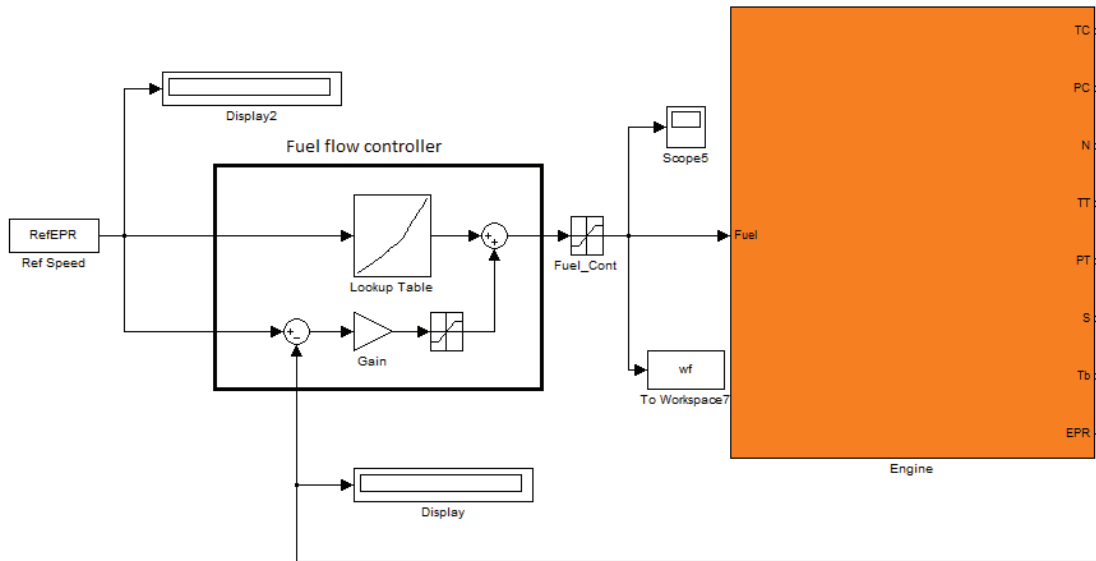


Figure 3.1: Schematic of the fuel flow controller for the gas turbine engine.

Furthermore, to show the effectiveness of the aforementioned controller, the EPR output, tracking error and the control input of the engine are shown in Figures 3.2-3.4, respectively.

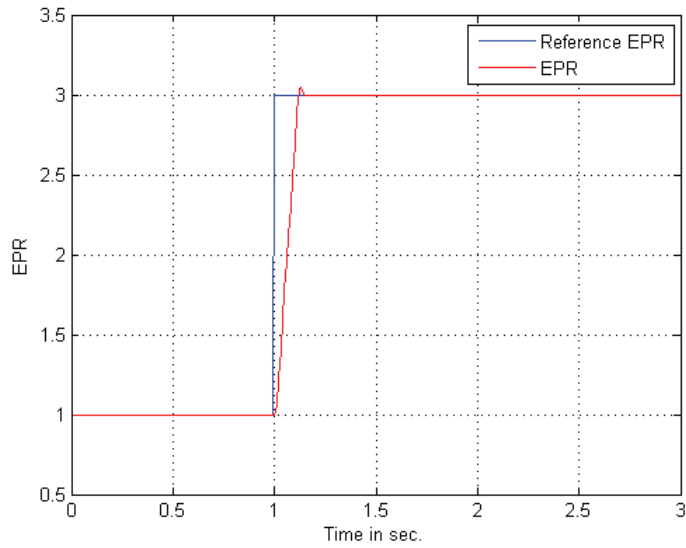


Figure 3.2: Tracking the desired engine pressure ratio using the feed-forward and negative feedback controllers in the healthy condition.

Figures 3.5-3.10 depict the controller performance in presence of the turbine erosion, compressor fouling and both of them, respectively.

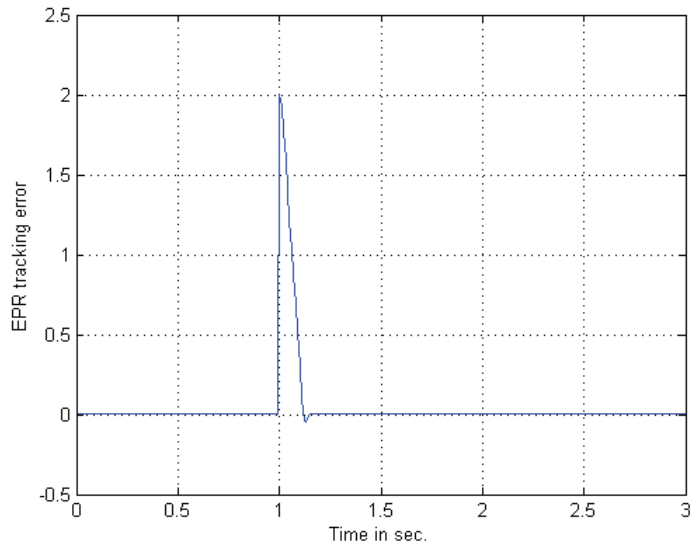


Figure 3.3: Tracking error in the healthy condition.

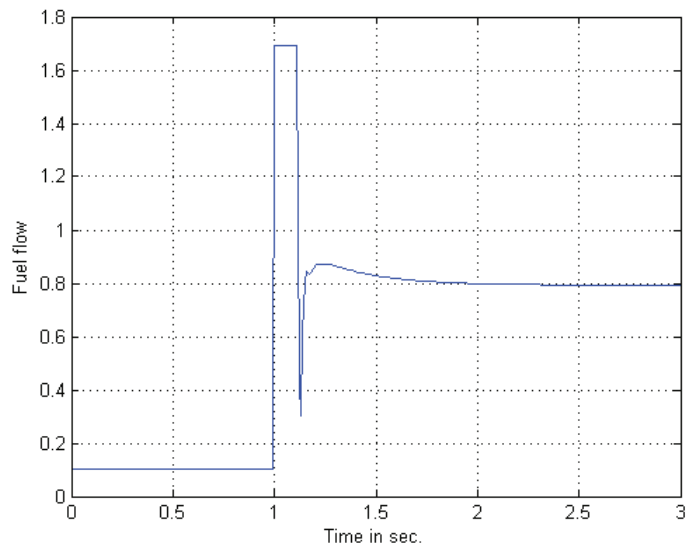


Figure 3.4: The control input of the engine in the healthy condition.

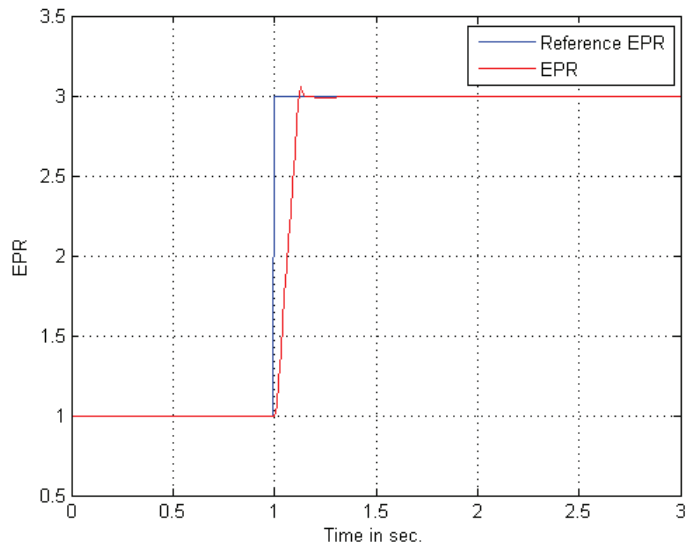


Figure 3.5: Tracking the desired engine pressure ratio using a feed-forward and negative feedback in the presence of the compressor fouling.

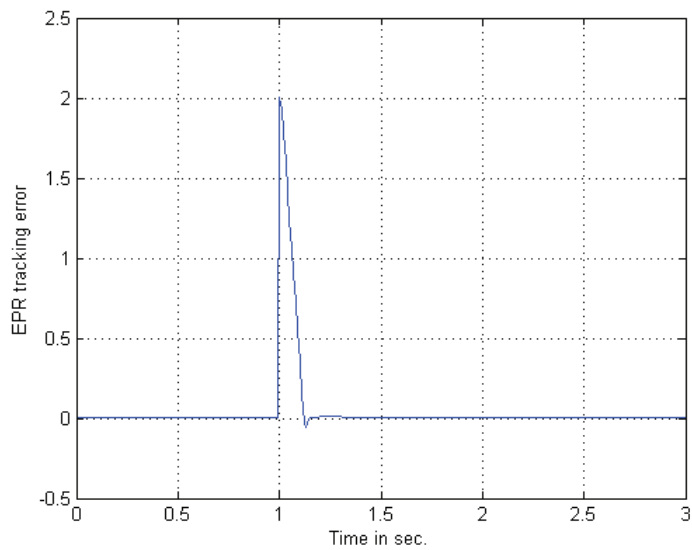


Figure 3.6: Tracking error in the presence of the compressor fouling.

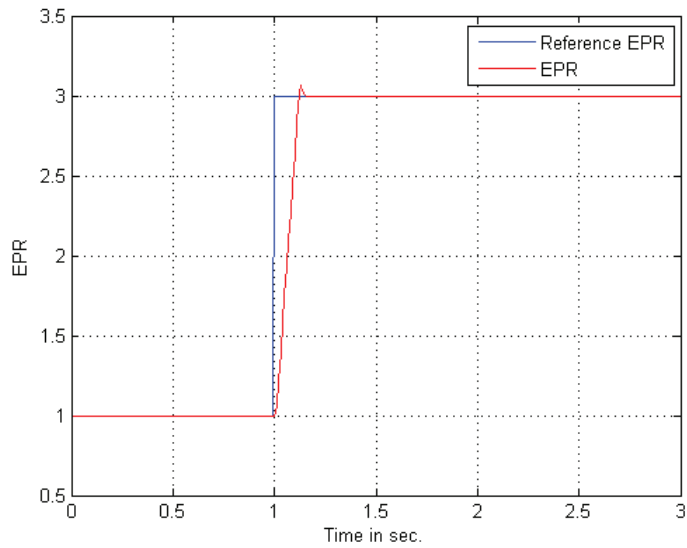


Figure 3.7: Tracking the desired engine pressure ratio using a feed-forward and negative feedback in the presence of the turbine erosion.

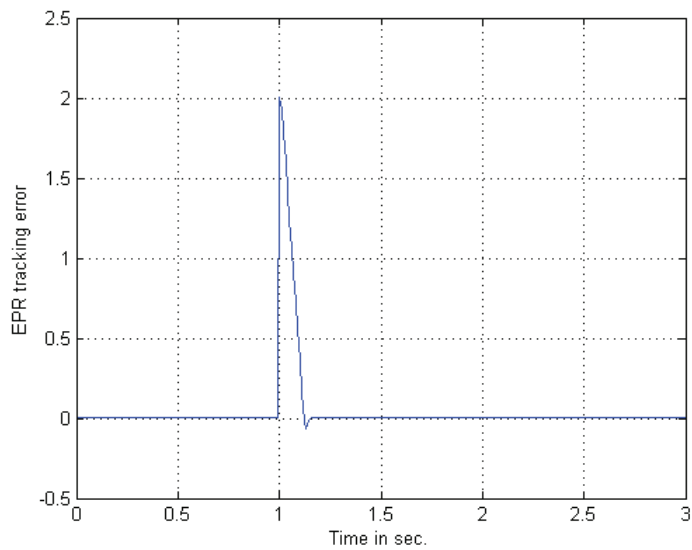


Figure 3.8: Tracking error in the presence of the turbine erosion.

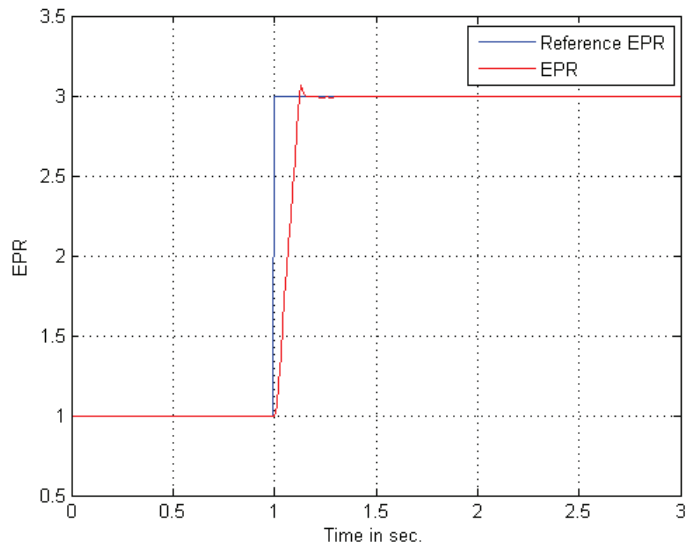


Figure 3.9: Tracking the desired engine pressure ratio using a feed-forward and negative feedback in the presence of both fouling and erosion.

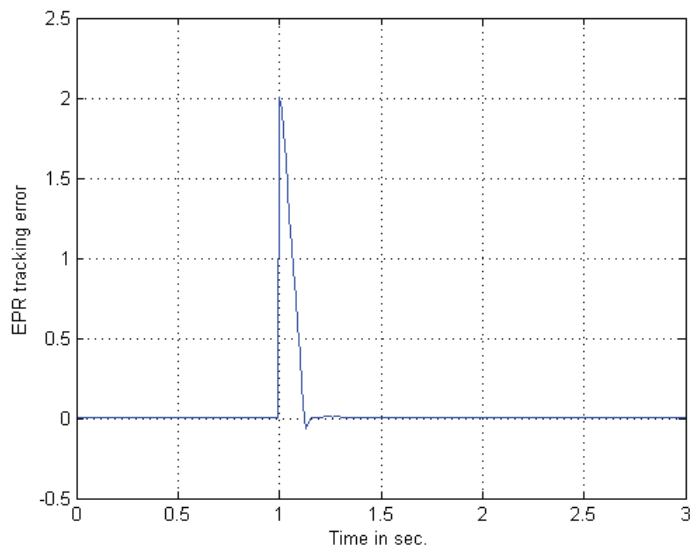


Figure 3.10: Tracking error in the presence of both fouling and erosion.

3.2 ARIMA and VAR Model Selection

In order to find the appropriate order of the model, different scenarios have been applied to different orders of the model. Using the mean and standard deviation of the prediction errors, AIC and BIC criteria, which were explained in the second chapter, one can select the best model. Tables 3.2 to 3.5 depict some selected results of the simulations which are employed for choosing the order of the ARIMA model and the VAR model, respectively. Tables 3.2 and 3.3 shows the BIC and AIC values associated with different orders of ARIMA and VAR models in presence of the compressor fouling (FI 1%), turbine erosion (EI 1%) and both of them (FI 1% and EI 1%). Tables 3.4 and 3.5 show the mean and standard deviation of the prediction errors for different orders of ARIMA and VAR models in presence of the compressor fouling (FI 1%), turbine erosion (EI 1%) and both of them (FI 1% and EI 1%). As shown in these four tables, ARIMA(4,5) and VAR(6) have been selected as the appropriate models which fit better overall to the data and eventually lead to better predictions for different degradations.

Table 3.2: BIC and AIC values for different orders of the ARIMA model in the presence of compressor fouling (FI 1%), Erosion (EI 1%) and both of them (FI 1% and EI 1%).

In the presence of compressor fouling		
ARIMA(p,q)	BIC	AIC
(2,1)	459.58	466.75
(3,1)	448.54	459.27
(3,2)	455.18	465.91
(3,6)	463.71	474.34
(4,5)	441.44	455.66
(5,3)	444.21	461.97
In the presence of the turbine erosion		
ARIMA(p,q)	BIC	AIC
(2,1)	549.28	466.45
(3,1)	448.16	458.88
(3,2)	455.05	465.77
(3,6)	464.34	474.97
(4,5)	447.23	461.51
(5,3)	444.01	461.78
In the presence of both fouling and erosion		
ARIMA(p,q)	BIC	AIC
(2,1)	423.91	431.07
(3,1)	414.01	424.74
(3,2)	414.75	425.48
(3,6)	404.21	414.84
(4,5)	404.19	418.41
(5,3)	408.38	426.15

Table 3.3: BIC and AIC values for different orders of the VAR model in the presence of compressor fouling (FI 1%), Erosion (EI 1%) and both of them (FI 1% and EI 1%).

In the presence of compressor fouling		
VAR(p)	BIC	AIC
(3)	893.05	886.00
(4)	883.70	876.65
(5)	875.49	868.44
(6)	867.54	860.50
(7)	867.03	859.99
(8)	865.26	858.22
(9)	864.52	857.48
In the presence of the turbine erosion		
VAR(p)	BIC	AIC
(3)	1075.5	1065.4
(4)	1054.0	1047.0
(5)	1032.8	1025.7
(6)	1024.8	1017.8
(7)	1023.5	1016.5
(8)	1020.1	1013.1
(9)	1018.7	1011.7
In the presence of both fouling and erosion		
VAR(p)	BIC	AIC
(3)	616.95	609.91
(4)	582.05	575.00
(5)	581.68	574.43
(6)	567.37	560.33
(7)	566.57	559.53
(8)	566.07	559.03
(9)	565.04	557.10

Table 3.4: The description of the mean and the standard deviation of the prediction errors for different orders of the ARIMA model for ten steps ahead prediction in the presence of compressor fouling (FI 1%), Erosion (EI 1%) and both of them (FI 1% and EI 1%).

In the presence of compressor fouling		
ARIMA(p,q)	Mean	Standard deviation
(2,1)	1.5527	2.8238
(2,5)	1.5729	2.8278
(3,2)	1.5817	2.8549
(3,5)	1.5673	2.8265
(4,3)	1.5902	2.8702
(4,5)	1.5469	2.8222
In the presence of the turbine erosion		
ARIMA(p,q)	Mean	Standard deviation
(2,1)	1.2835	1.9674
(2,5)	1.3084	1.9836
(3,2)	1.3177	1.9799
(3,5)	1.3297	2.0165
(4,3)	1.2926	1.9664
(4,5)	1.2830	1.9704
In the presence of both fouling and erosion		
ARIMA(p,q)	Mean	Standard deviation
(2,1)	1.5953	2.8381
(2,5)	1.5943	2.8266
(3,2)	1.6159	2.8541
(3,5)	1.6145	2.8437
(4,3)	1.5793	2.8139
(4,5)	1.5934	2.8235
(5,2)	1.5527	2.8238

Table 3.5: The description of the mean and the standard deviation of the prediction errors for different order of the VAR model for ten steps ahead prediction in the presence of compressor fouling (FI 1%), Erosion (EI 1%) and both of them (FI 1% and EI 1%).

In the presence of compressor fouling		
VAR(p)	Mean	Standard deviation
(3)	1.6606	2.6335
(4)	1.5811	2.6882
(5)	1.5369	2.7125
(6)	1.5734	2.7857
(7)	1.5894	2.8435
(8)	1.6171	2.9180
(9)	1.5527	2.8238
In the presence of the turbine erosion		
VAR(p)	Mean	Standard deviation
(3)	1.3654	1.8437
(4)	1.2420	1.8345
(5)	1.2648	1.8121
(6)	1.2332	1.8463
(7)	1.2502	1.8642
(8)	1.2561	1.8838
(9)	1.2629	1.9484
In the presence of both fouling and erosion		
VAR(p)	Mean	Standard deviation
(3)	1.9601	2.7923
(4)	1.7842	2.7809
(5)	1.6130	2.8520
(6)	1.6319	2.7897
(7)	1.6884	2.9344
(8)	1.8198	3.0075
(9)	1.8308	2.8810

3.3 Case Study Scenarios

Given that the data sets are non-deterministic due to parameter uncertainties and system noise, a model that can include this random behavior results in a better and a more accurate prediction. The ARMA model has the above noted flexibilities by including the random shock terms. In the univariate modeling approach in this thesis we consider only one of the measurable parameters, namely the turbine exit temperature (TET). In order to verify the effectiveness of the ARIMA and VAR models in terms of the prediction horizons and accuracy, different case study scenarios are applied to each of these models. The prediction of the gas turbine performance degradation is then obtained which can be used to schedule maintenance actions for a jet engine. The take off time for each flight is 20 seconds. In each take off cycle, we capture the data at the steady state point. Therefore we keep one data from each cycle for each parameter. Each scenario consists of 250 points that form the time-series data we are working with. In Table 3.6, the details of the scenarios are given.

In the first scenario, the engine is considered to start operating from healthy condition, then the compressor is injected with fouling for the next 120 cycles to reach to the FI of 3%. Then the compressor gets washed through the maintenance procedure and the engine continues working for 10 cycles in the healthy condition. Afterwards, it is injected with fouling for the next 70 cycles to reach FI of 2%. Then the engine gets washed so that it starts working for 50 cycles and the FI reaches to 1%.

In the second scenario, the effects of the turbine erosion on the engine is investigated. In this scenario, the engine is considered to start operating from healthy condition, then the engine is injected with erosion for the next 125 cycles to reach to the of EI 3%. Then the turbine goes through the maintenance procedure and the engine continues working for 25 cycles under healthy condition. Afterwards, it is injected with erosion for the next 60 cycles to reach EI of 2%. Then the engine goes through the maintenance and starts working for 40 cycles and the EI reaches to 1%.

In the third scenario, the effects of both the turbine erosion and compressor fouling on the engine are investigated. In this scenario, the engine is considered to start operating from healthy condition, then the compressor is injected with fouling for the next 100 cycles to reach to the FI of 2%. For the next 50 cycles while compressor fouling is increasing to reach to the FI of 3%, the turbine gets eroded with EI of 1%. Then the engine goes through the maintenance procedure and the engine continues working from healthy condition and the compressor is injected with fouling for the next 70 cycles to reach FI of 1%. After the 180th cycle the turbine is injected with erosion and compressor continues getting fouled and eventually they reach to the FI of 2% and EI of 2% at the 250th cycle.

Table 3.6: The description of the scenarios that are considered for conducting simulations.

First Scenario				
Engine Condition	FI 3%	Healthy	FI 2%	FI 1%
Number of Cycles	120	10	70	50
Second Scenario				
Engine Condition	EI 3%	Healthy	EI 2%	EI 1%
Number of Cycles	125	25	60	40
Third Scenario				
Engine Condition	FI 2%	FI 3% and EI 1%	FI 1%	FI 3% and EI 2%
Number of Cycles	100	50	30	70

3.4 Simulation Results

3.4.1 ARIMA Model

The ARIMA model that was described in the previous section is applied to the Turbine Exit Temperature (TET) which is one of the most important health parameters of the engine [170]. In real life prognostic problems dealing with uncertainties is inevitable. These uncertainties could be originated from insufficient data and changing operating conditions. Taking the above facts into account, it may not be practical to obtain or be concerned with an exact prediction point. Therefore, one needs to construct instead confidence bounds that

give a realistic boundary for the prediction. When a specified upper bound threshold is met one may determine and declare that the engine should be taken for maintenance. To determine the confidence bounds for evaluating the prediction performance of the model, Monte Carlo simulations are performed and according to normal theory a multiple of the standard deviations of the prediction error (for a given confidence level, that is 95%) is added and subtracted from the actual values.

Data Preprocessing

Figure 3.11 depicts the results of the prediction for a ten step ahead using ARIMA(4,5). The dashed lines show our upper and lower prediction intervals. The star points in the figure represent actual data values and the circle points indicate the predicted temperatures. All the figures shown in this thesis depict the prediction portion of the scenario, since certain parts of the data were used for testing. It should be mentioned that from the available measurements for the ARIMA method, we used 40% of the measurements for model parameters estimation. The remaining measurement points are used for testing and evaluating the prediction performance. As seen in Figure 3.11 between the 120th to the 130th cycles and also at the 200th cycle, the prediction error is significantly large due to the maintenance that was performed at the cycles 120 and 200. Clearly the data before the maintenance action is not sufficient to allow for a reliable prediction subsequent to this action. Despite this, even after 10 cycles (number of steps ahead for this case) prediction error is significantly large and this occurs when there is gap between the values of the captured data. These gaps can be originated from possible dramatically degradation changes or post maintenance capturing data. To cope with this problem and achieving a better and more acceptable prediction in terms of accuracy, in this thesis a compensation method in the form of data preprocessing has been conducted.

In order to identify the gap between the values of the measurement points, the difference

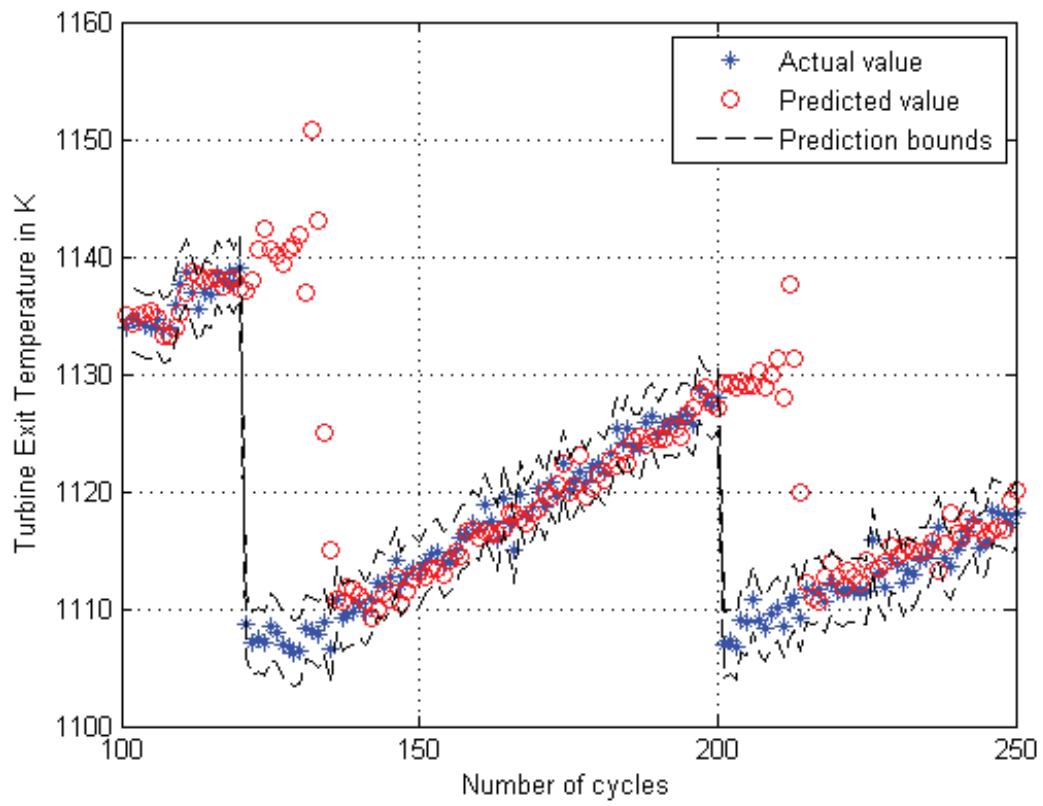


Figure 3.11: Ten step ahead prediction results by using the ARIMA(4,5) model without compensator for the first scenario.

of the data will be verified and when the difference of the two consequent data exceeds a specified value, the algorithm takes these two points as a gap. After finding all the gaps, the average of the specified window of the data before and after the gap point is calculated and depending on the gap direction, all the data values after the gap point will be added or subtracted by the difference of two average values. Finally, when the prediction procedure is finished, this modifier value will be extracted from the results. Figure 3.13 shows the results of the prediction for the same scenario with the mentioned compensator.

Subsequently, the aforementioned compensator will be applied to all the simulations throughout this section.

Scenario 1

The detailed description of the first scenario was presented earlier in the section Case Study Scenarios. The standard deviation of the measurement noise is considered as 1 (0.097 percent of the nominal value of the turbine temperature [13]). Figures 3.12-3.15 depict the results of the prediction in the presence of the same level of measurement noise. The dashed lines show our upper and lower prediction intervals. The star points represent actual data values and the circle points indicate the predicted temperatures. Table 3.7 shows the mean and the standard deviation of the prediction errors for different number of steps ahead in presence of the measurement noise with the standard deviation of 1.

In order to investigate the effects of measurement noise on the prediction results, each scenario has been repeated for different value of measurement noise. Figures 3.16-3.18 depict the results of the prediction in presence of the same level of measurement noise with the standard deviation of 2. Table 3.8 represents the mean and the standard deviation of the prediction errors for different number of steps ahead in presence of the measurement noise with the standard deviation of 2.

Figures 3.19-3.21 depict the results of the prediction in presence of the same level of

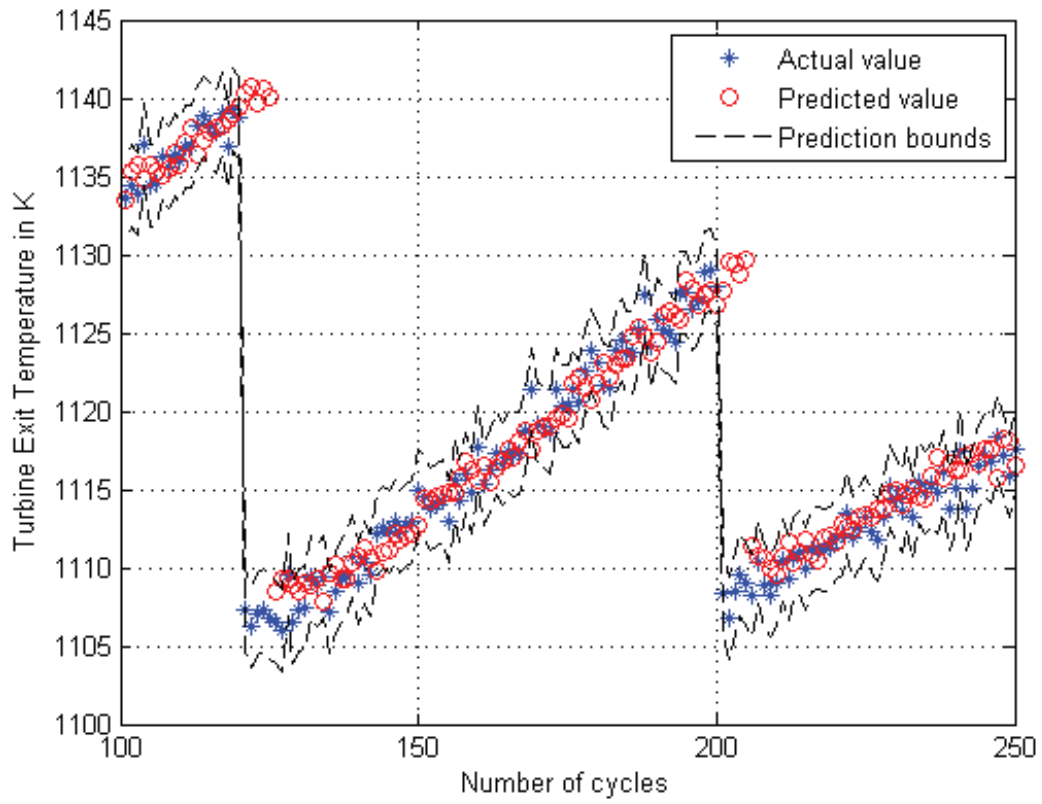


Figure 3.12: Five step ahead prediction results by using the univariate ARIMA(4,5) model for the first scenario in presence of the measurement noise with the standard deviation of 1.

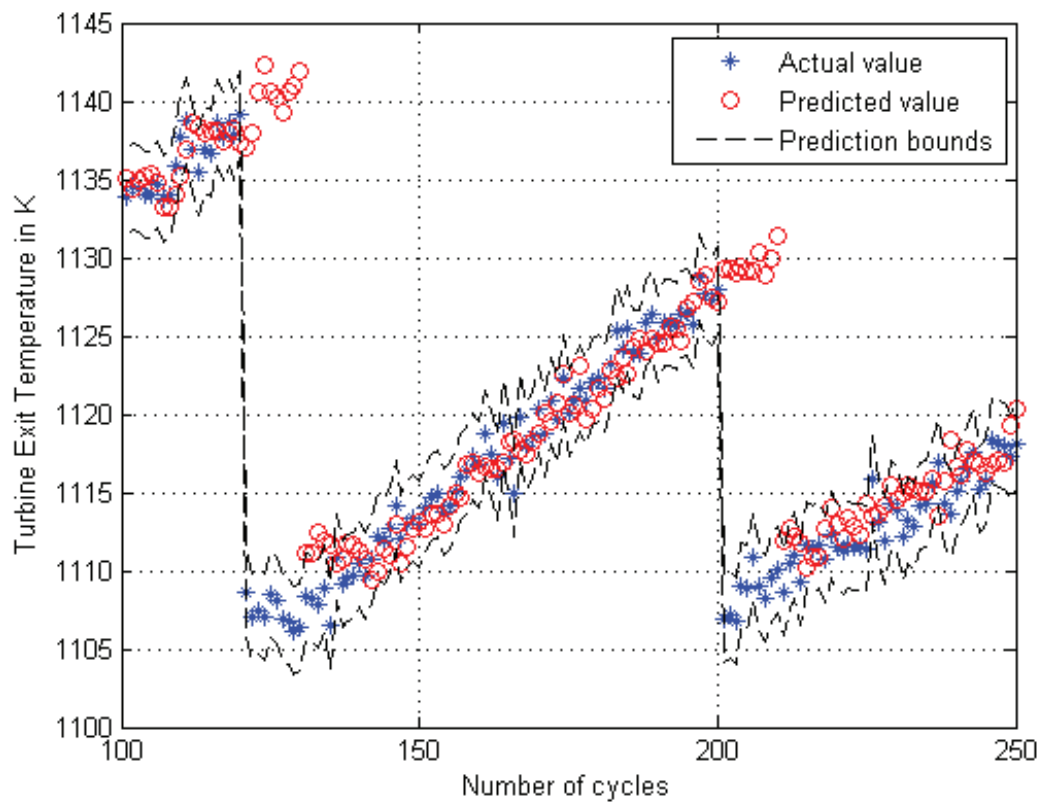


Figure 3.13: Ten step ahead prediction results by using the ARIMA(4,5) model including compensator for the first scenario in presence of the measurement noise with the standard deviation of 1.

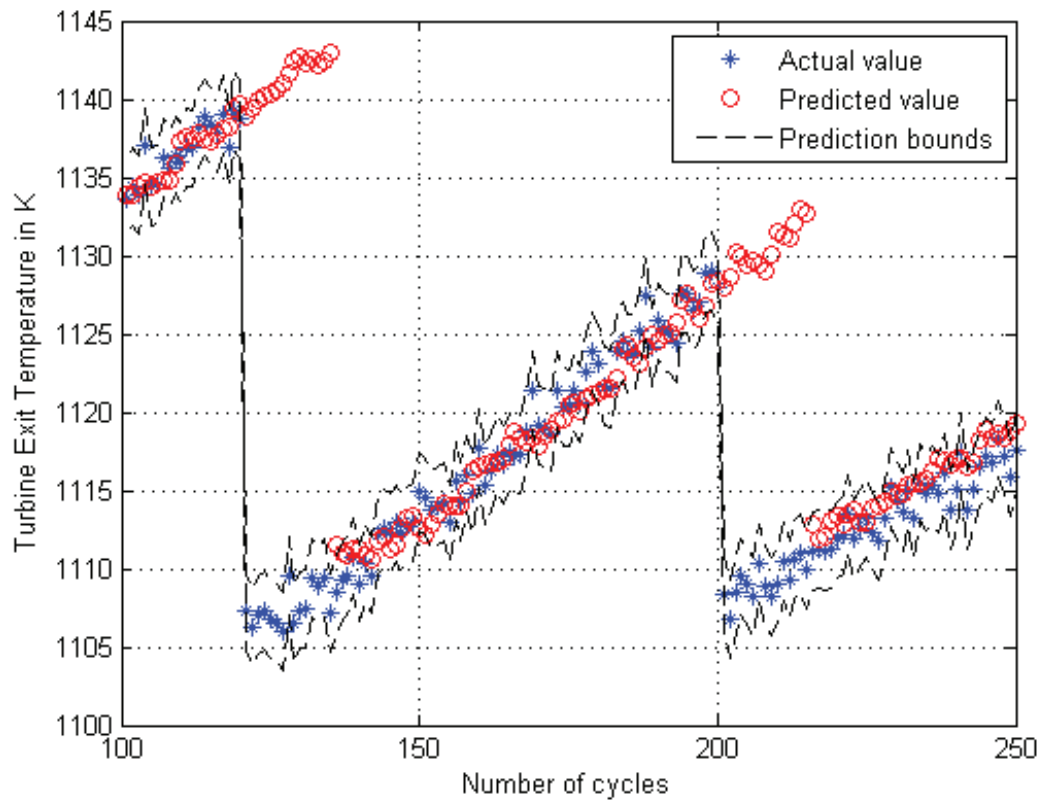


Figure 3.14: Fifteen step ahead prediction results by using the univariate ARIMA(4,5) model for the first scenario in presence of the measurement noise with the standard deviation of 1.

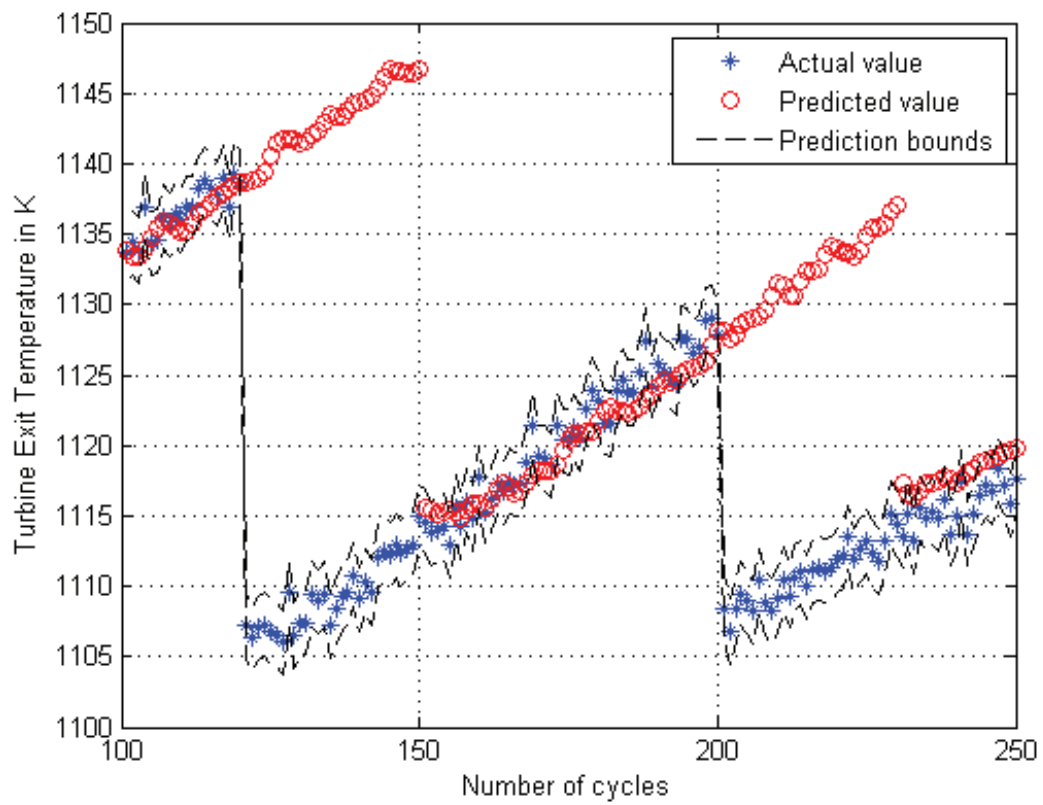


Figure 3.15: Thirty step ahead prediction results by using the univariate ARIMA(4,5) model for the first scenario in presence of the measurement noise with the standard deviation of 1.

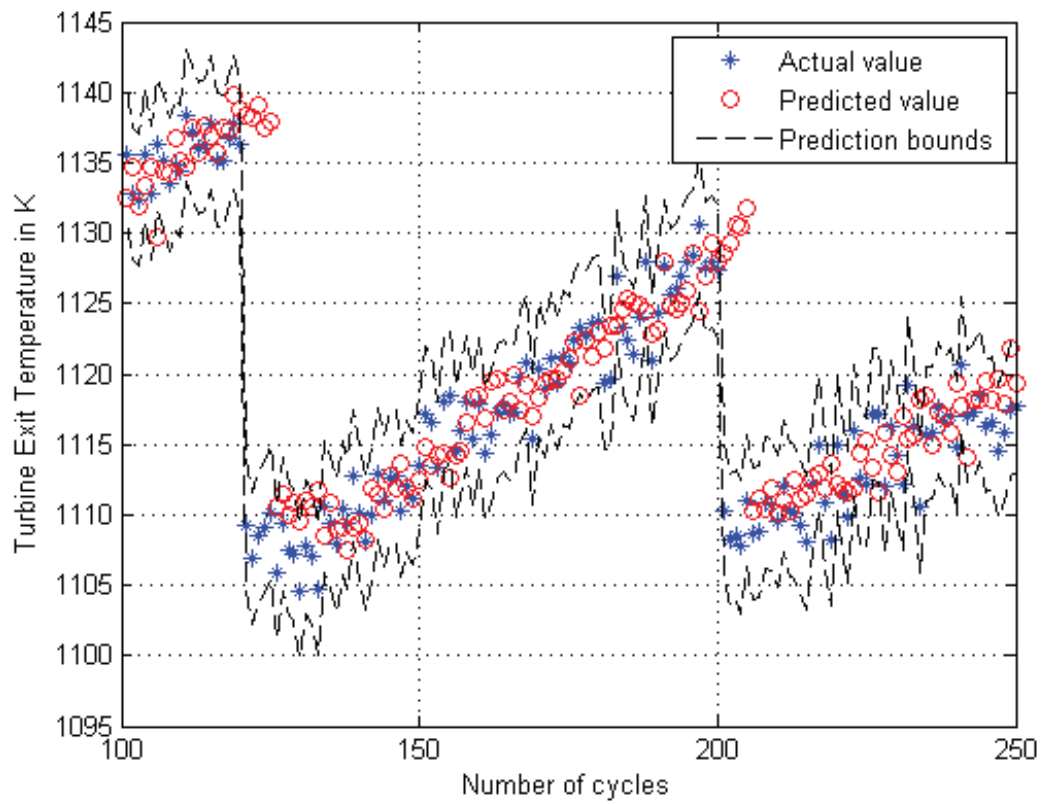


Figure 3.16: Five step ahead prediction results by using the univariate ARIMA(4,5) model for the first scenario in presence of the measurement noise with the standard deviation of 2.

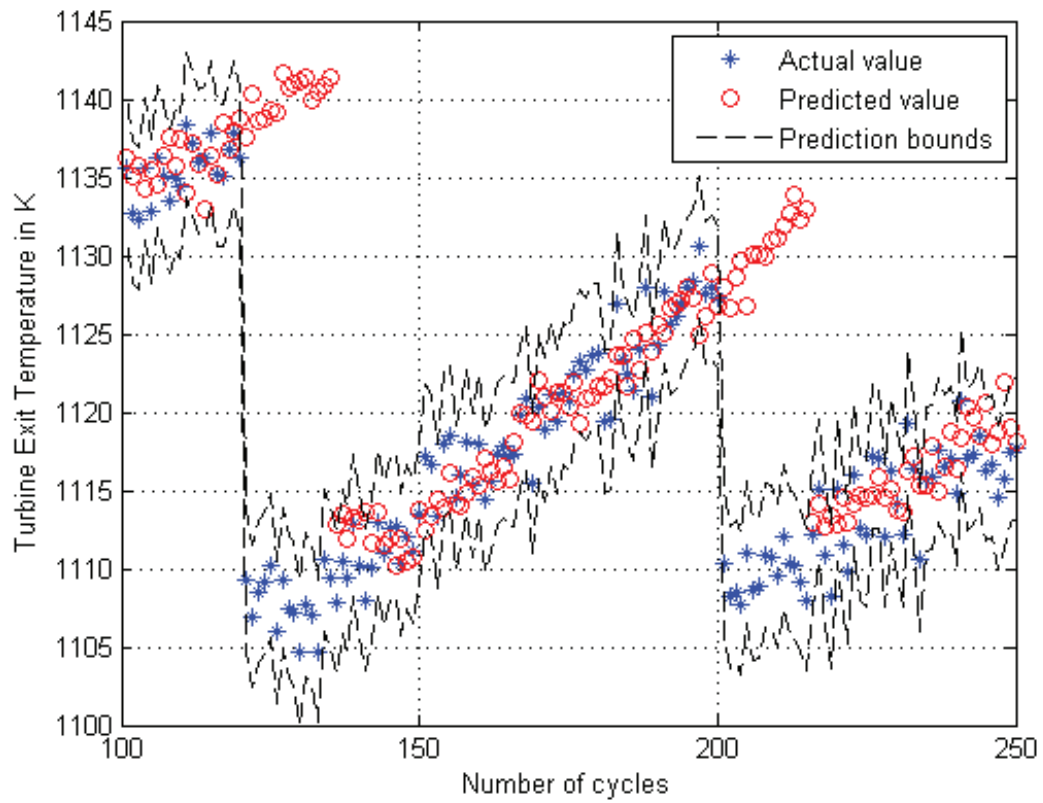


Figure 3.17: Fifteen step ahead prediction results by using the univariate ARIMA(4,5) model for the first scenario in presence of the measurement noise with the standard deviation of 2.

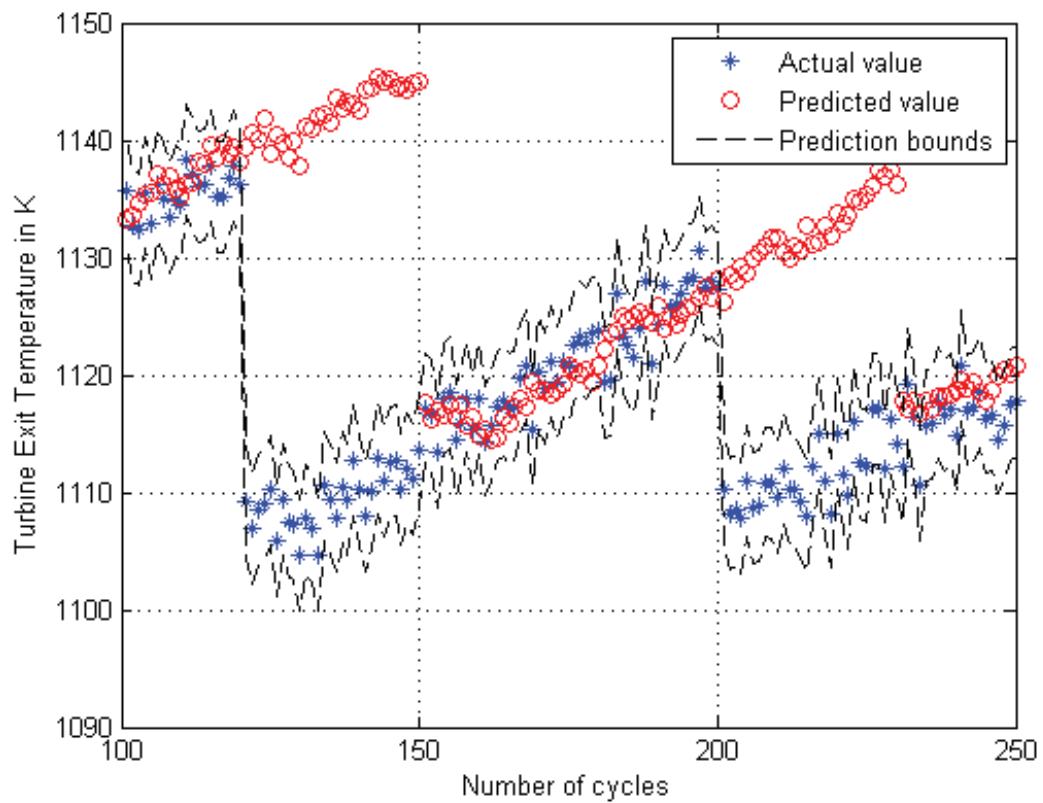


Figure 3.18: Thirty step ahead prediction results by using the univariate ARIMA(4,5) model for the first scenario in presence of the measurement noise with the standard deviation of 2.

Table 3.7: Mean and standard deviation of the prediction errors for the ARIMA model for the first scenario in presence of the measurement noise with the standard deviation of 1.

Number of steps ahead	Mean	Standard deviation
3	1.9746	5.5320
5	2.7945	7.0279
10	4.5364	9.6166
15	6.3432	11.3959
20	8.2333	12.7161
25	10.0870	13.6326
30	11.8863	14.2086

Table 3.8: Mean and standard deviation of the prediction errors for the ARIMA model for the first scenario in presence of the measurement noise with the standard deviation of 2.

Number of steps ahead	Mean	Standard deviation
3	2.8909	5.5274
5	3.6079	6.8187
10	5.1188	9.2927
15	6.8562	11.0814
20	8.5631	12.2012
25	10.2439	13.0616
30	11.9772	13.7022

measurement noise with the standard deviation of 5. Table 3.9 shows the mean and the standard deviation of the prediction errors for different number of steps ahead in presence of the measurement noise with the standard deviation of 5.

As seen in Figure 3.12, all the predicted values are within the defined boundaries. At 120th and 200th flight cycles for 5 flight cycles, the predicted values are outside the boundaries. This happens because of the maintenance that was performed at the cycles 120 and 200 in the first scenario and the compressor got washed. Clearly the data before the maintenance action is not sufficient to allow for a reliable prediction subsequent to this action. As the prediction horizon increases to ten, as seen in Figure 3.13, the predicted values are still within the boundaries but it takes a few more cycles for the model to perform enough accurate prediction after the maintenance at the cycles 120 and 200. When the number of

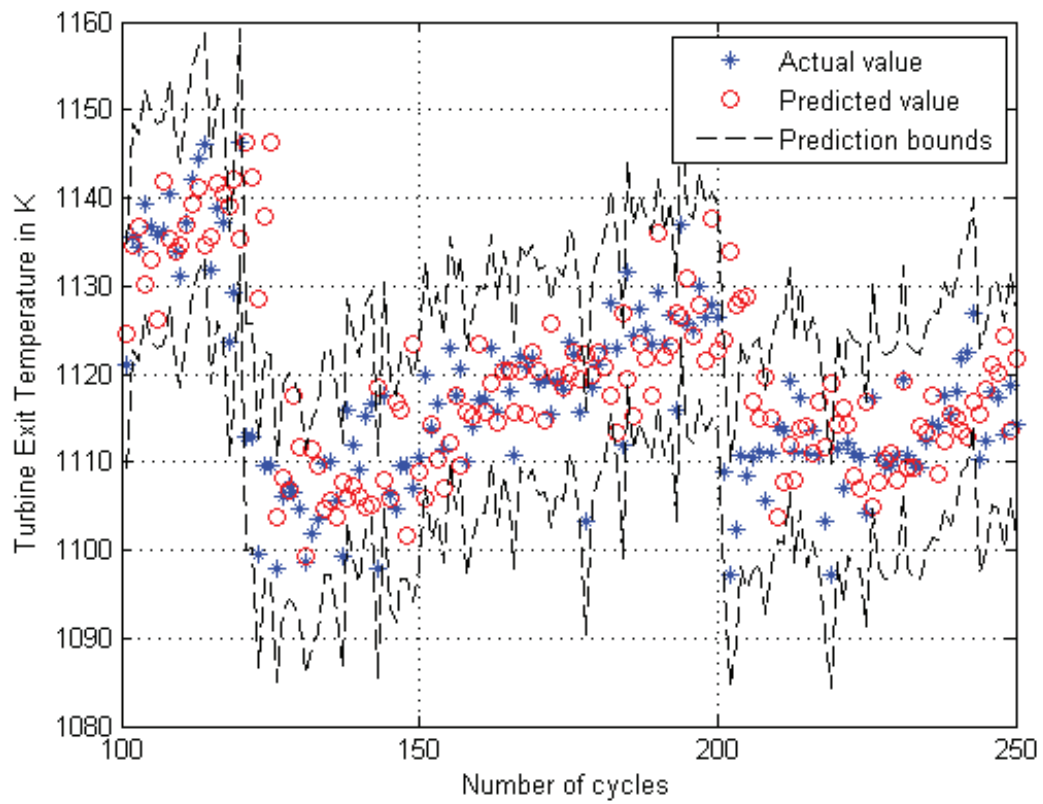


Figure 3.19: Five step ahead prediction results by using the univariate ARIMA(4,5) model for the first scenario in presence of the measurement noise with the standard deviation of 5.

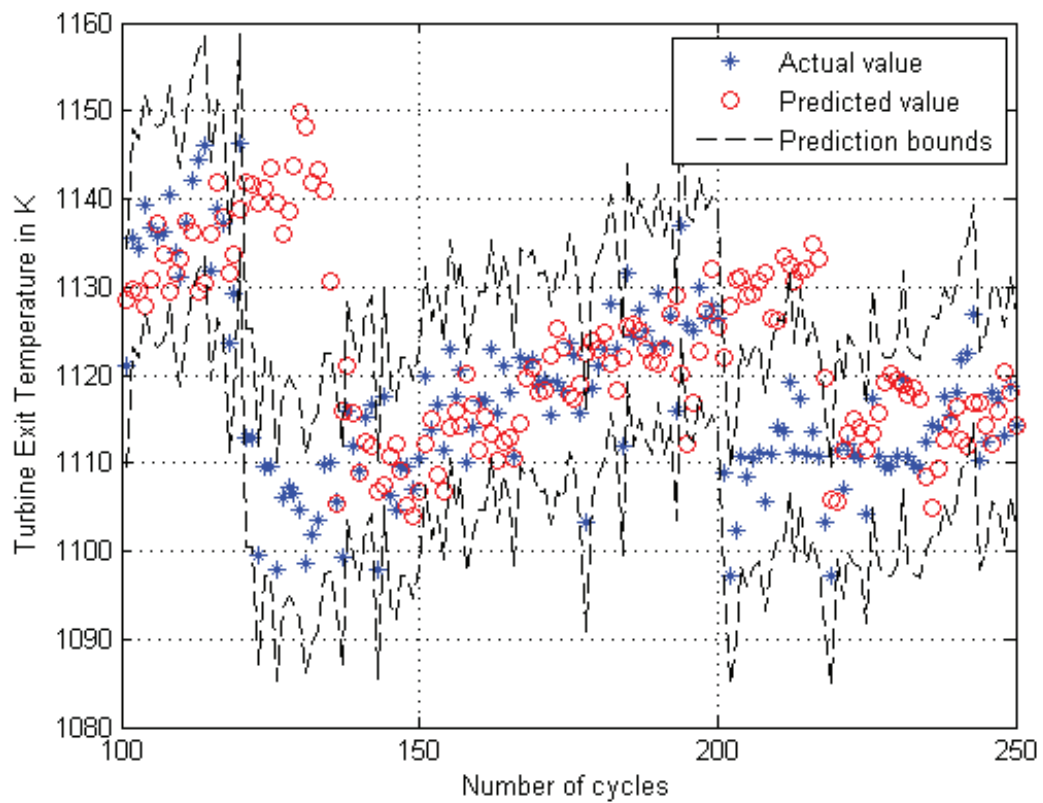


Figure 3.20: Fifteen step ahead prediction results by using the univariate ARIMA(4,5) model for the first scenario in presence of the measurement noise with the standard deviation of 5.

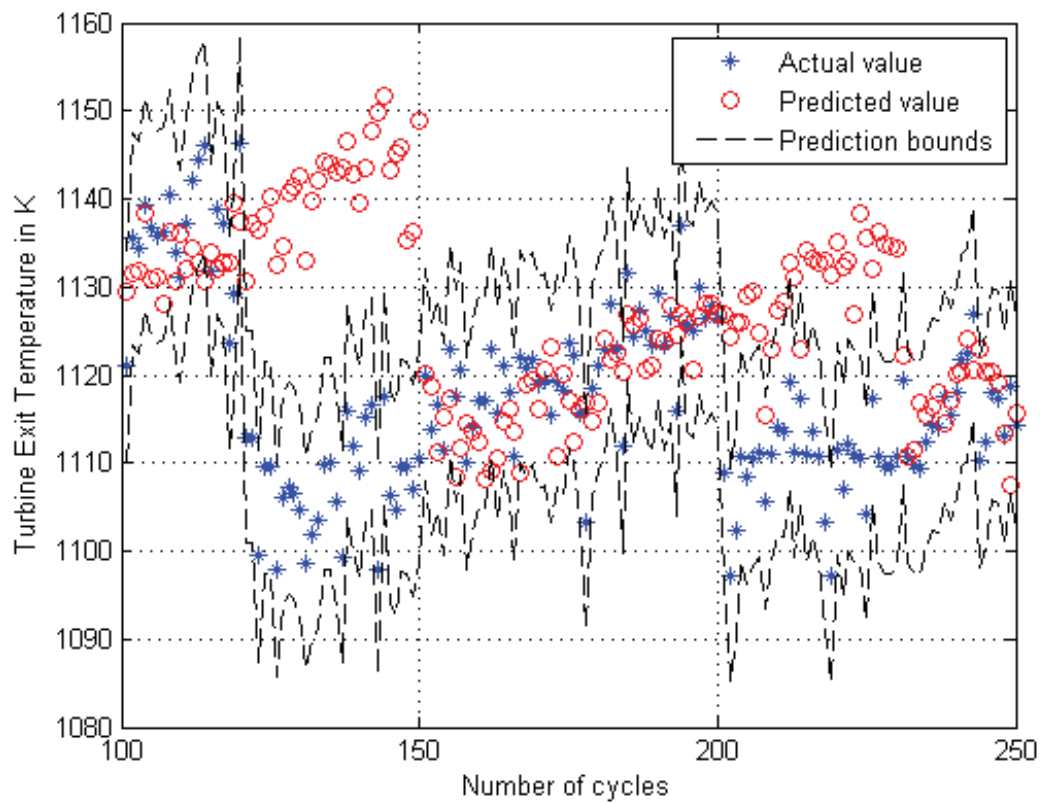


Figure 3.21: Thirty step ahead prediction results by using the univariate ARIMA(4,5) model for the first scenario in presence of the measurement noise with the standard deviation of 5.

Table 3.9: Mean and standard deviation of the prediction errors for the ARIMA model for the first scenario in presence of the measurement noise with the standard deviation of 5.

Number of steps ahead	Mean	Standard deviation
3	6.2754	8.4807
5	7.1134	9.9517
10	8.5847	12.0376
15	10.1466	13.7248
20	11.7623	14.9629
25	12.4388	15.2695
30	13.7327	15.8727

steps ahead reaches to 30, the predicted values are marginally within the boundaries. Figures 3.16-3.18 depict the same scenario in presence of the measurement noise with standard deviation of 2. By increasing the measurement noise level, the accuracy of the prediction decreases in comparison to cases with the same number of step ahead predictions. Figures 3.19-3.21 depict the same scenario in presence of the measurement noise with standard deviation of 5. Due to the high level noise associated with the measurement data, the predicted values are more scattered and marginally within the boundaries. By increasing the number of steps ahead prediction the predicted data maintain the trend and even for the thirty steps ahead in Figure 3.21 the predicted values are still within the boundaries. However, the prediction accuracy is not as good as before.

Scenario 2

The detailed description of the second scenario was presented in the section Case Study Scenarios. The standard deviation of the measurement noise is considered as 1 (0.097 percent of the nominal value of the turbine temperature [13]). Figures 3.22-3.24 depict the results of the prediction in presence of the same level of measurement noise. The dashed lines show our upper and lower prediction intervals. The star points in the figure represent the actual data values and the circle points indicate the predicted temperatures. Table 3.10 shows the mean and the standard deviation of the prediction errors for different number of

steps ahead in presence of the measurement noise with the standard deviation of 1.

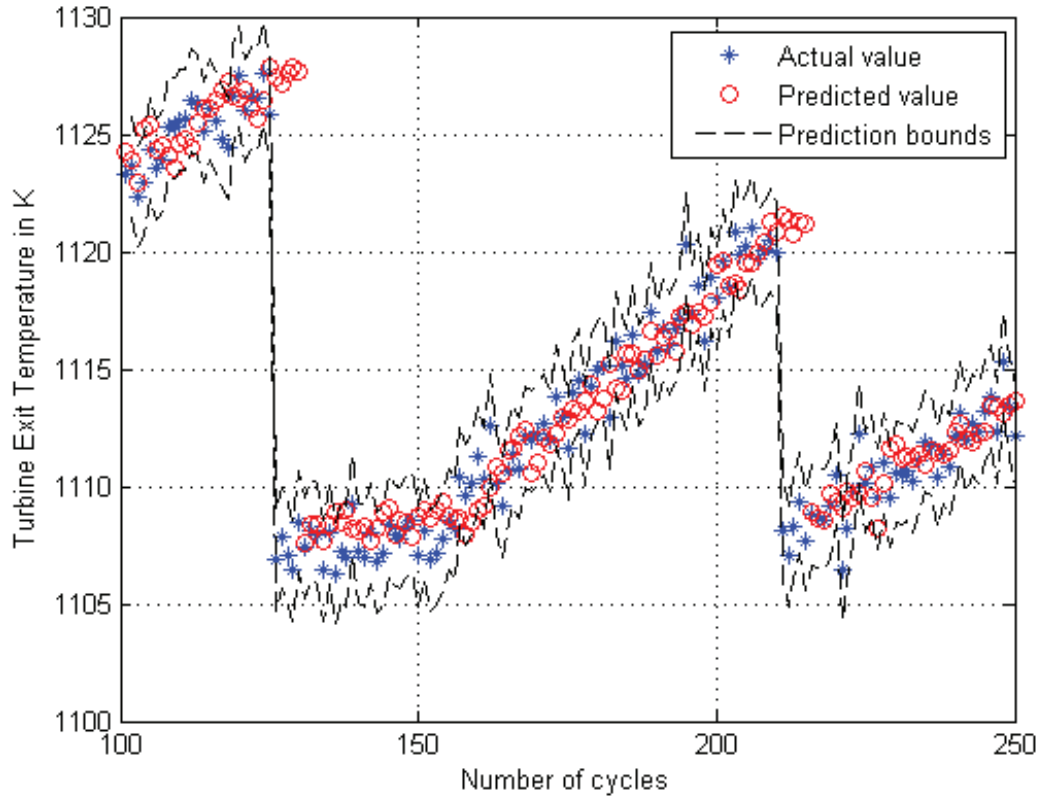


Figure 3.22: Five step ahead prediction results by using the univariate ARIMA(4,5) model for the second scenario in presence of the measurement noise with the standard deviation of 1.

Figures 3.25-3.27 depict the results of the prediction for the second scenario in presence of the same level of measurement noise with the standard deviation of 2. Table 3.11 shows the mean and the standard deviation of the prediction errors for different number of steps ahead in presence of the measurement noise with the standard deviation of 2.

Figures 3.28-3.30 depict the results of the prediction in presence of the same level of measurement noise with the standard deviation of 5. Table 3.12 shows the mean and the standard deviation of the prediction errors for different number of steps ahead in presence of the measurement noise with the standard deviation of 5.

As seen in Figure 3.22, all the predicted values are within the defined boundaries. At

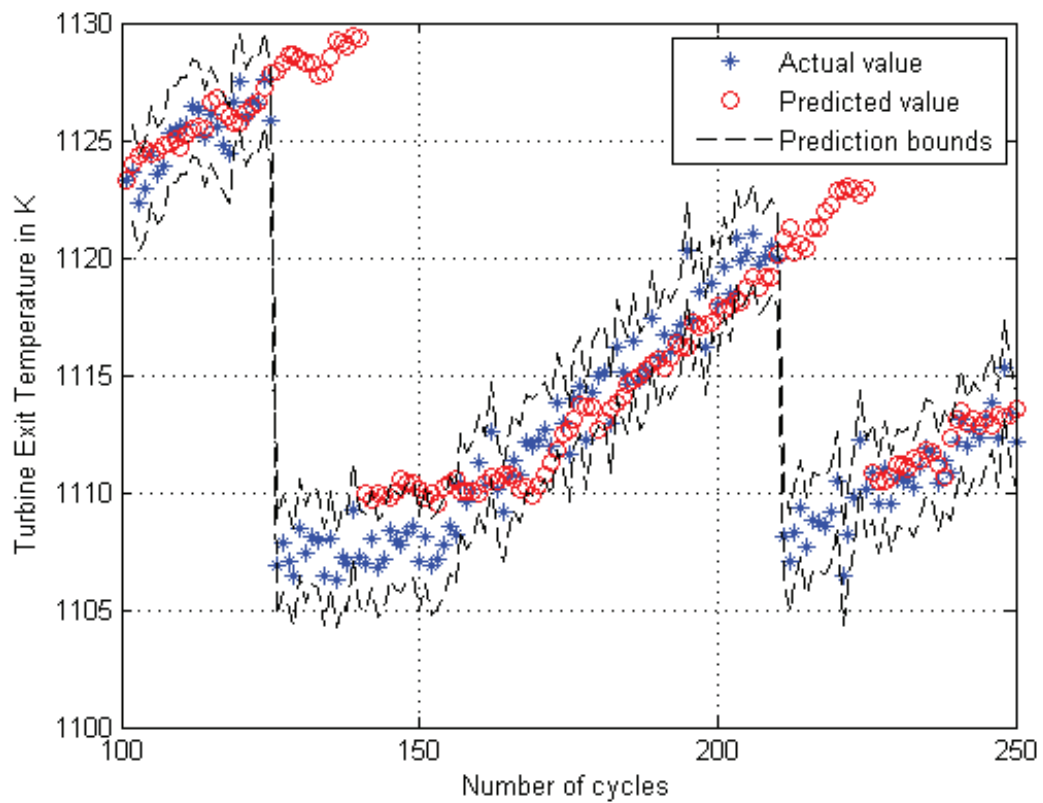


Figure 3.23: Fifteen step ahead prediction results by using the univariate ARIMA(4,5) model for the second scenario in presence of the measurement noise with the standard deviation of 1.

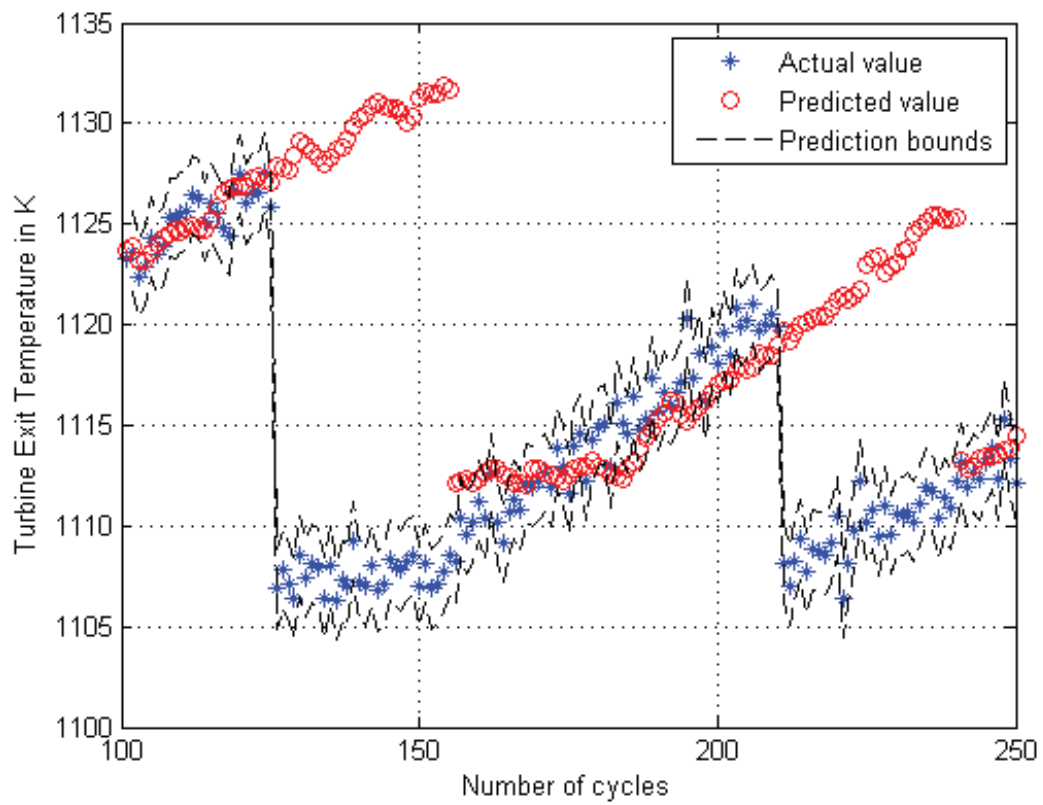


Figure 3.24: Thirty step ahead prediction results by using the univariate ARIMA(4,5) model for the second scenario in presence of the measurement noise with the standard deviation of 1.

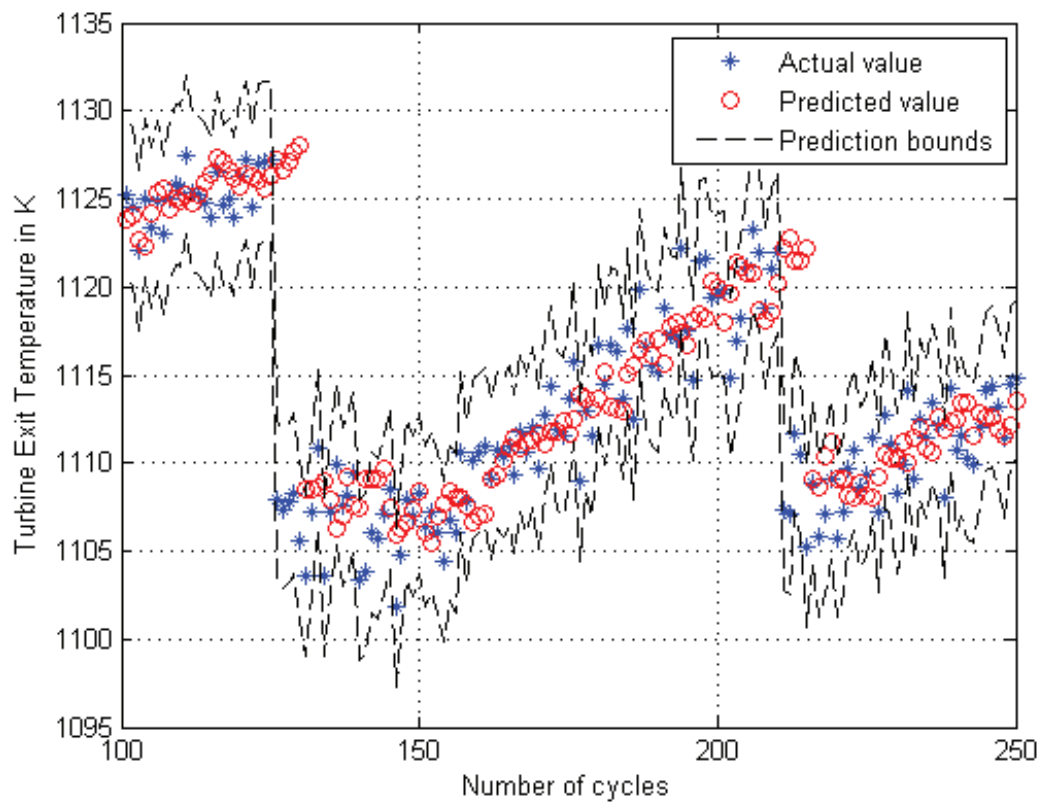


Figure 3.25: Five step ahead prediction results by using the univariate ARIMA(4,5) model for the second scenario in presence of the measurement noise with the standard deviation of 2.

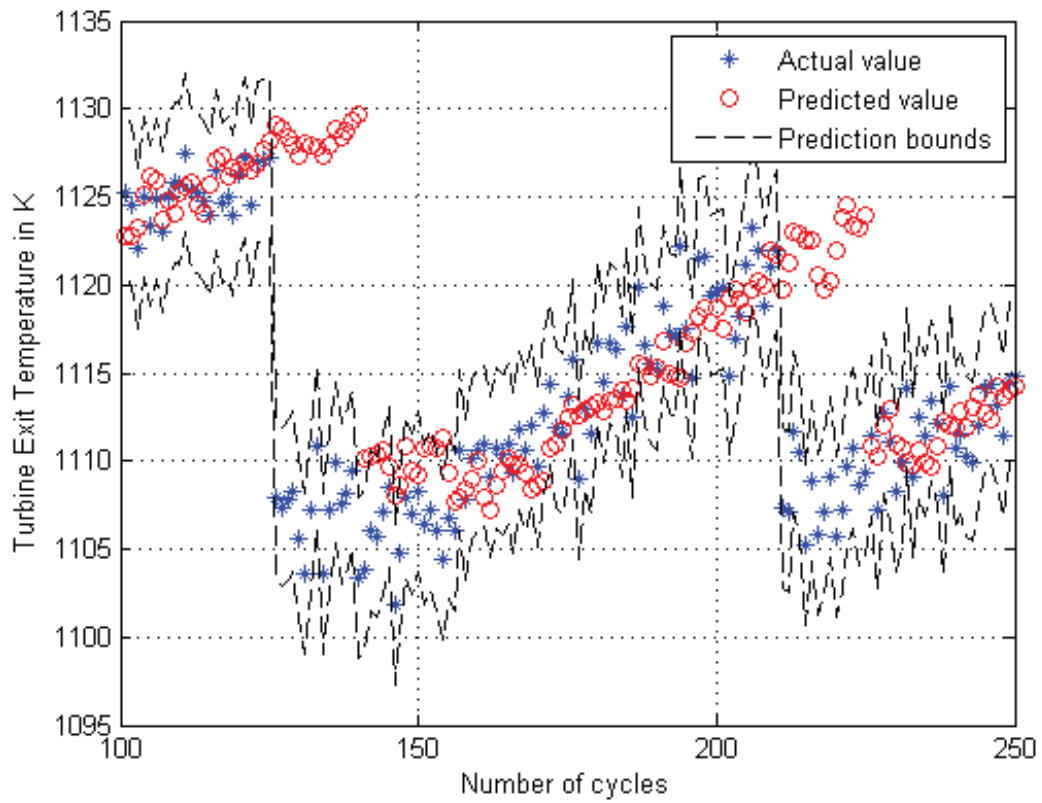


Figure 3.26: Fifteen step ahead prediction results by using the univariate ARIMA(4,5) model for the second scenario in presence of the measurement noise with the standard deviation of 2.

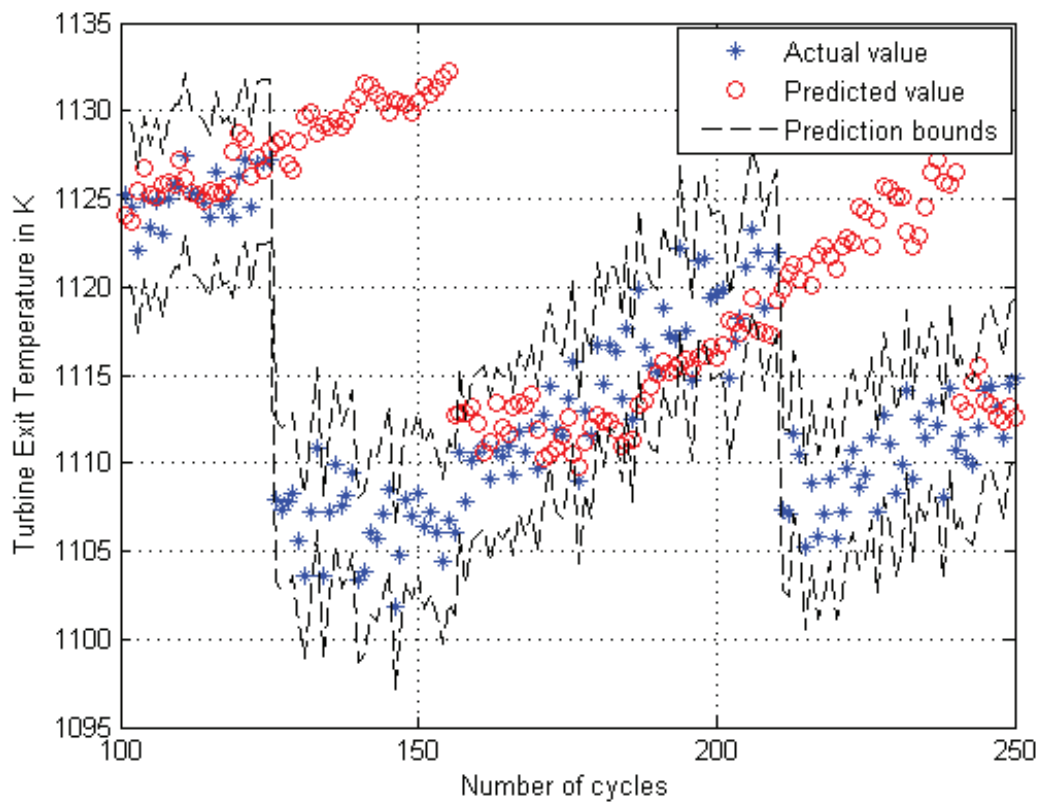


Figure 3.27: Thirty step ahead prediction results by using the univariate ARIMA(4,5) model for the second scenario in presence of the measurement noise with the standard deviation of 2.

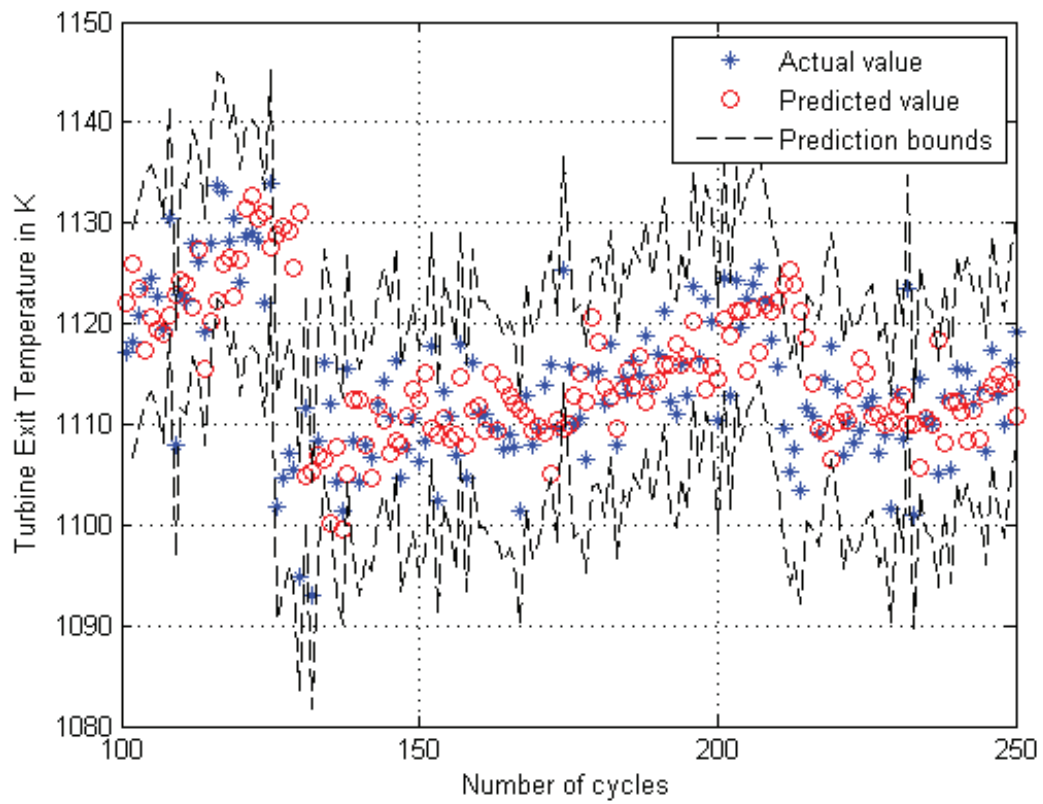


Figure 3.28: Five step ahead prediction results by using the univariate ARIMA(4,5) model for the second scenario in presence of measurement noise with the standard deviation of 5.

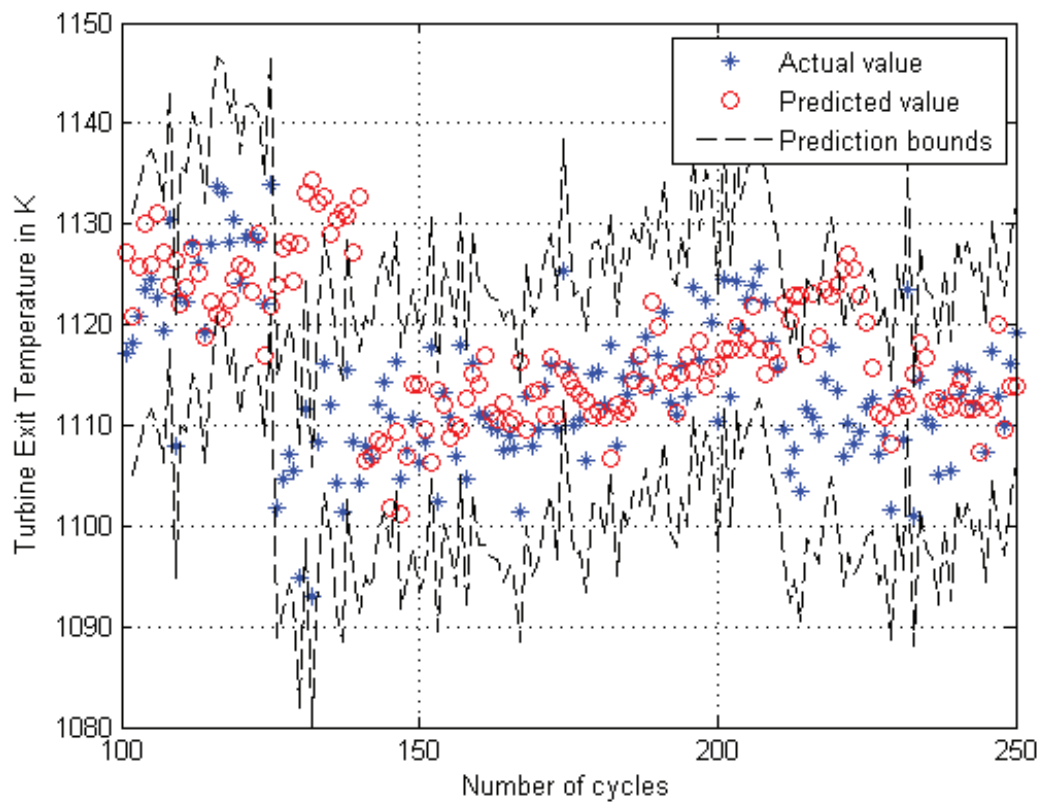


Figure 3.29: Fifteen step ahead prediction results by using the univariate ARIMA(4,5) model for the second scenario in presence of the measurement noise with the standard deviation of 5.

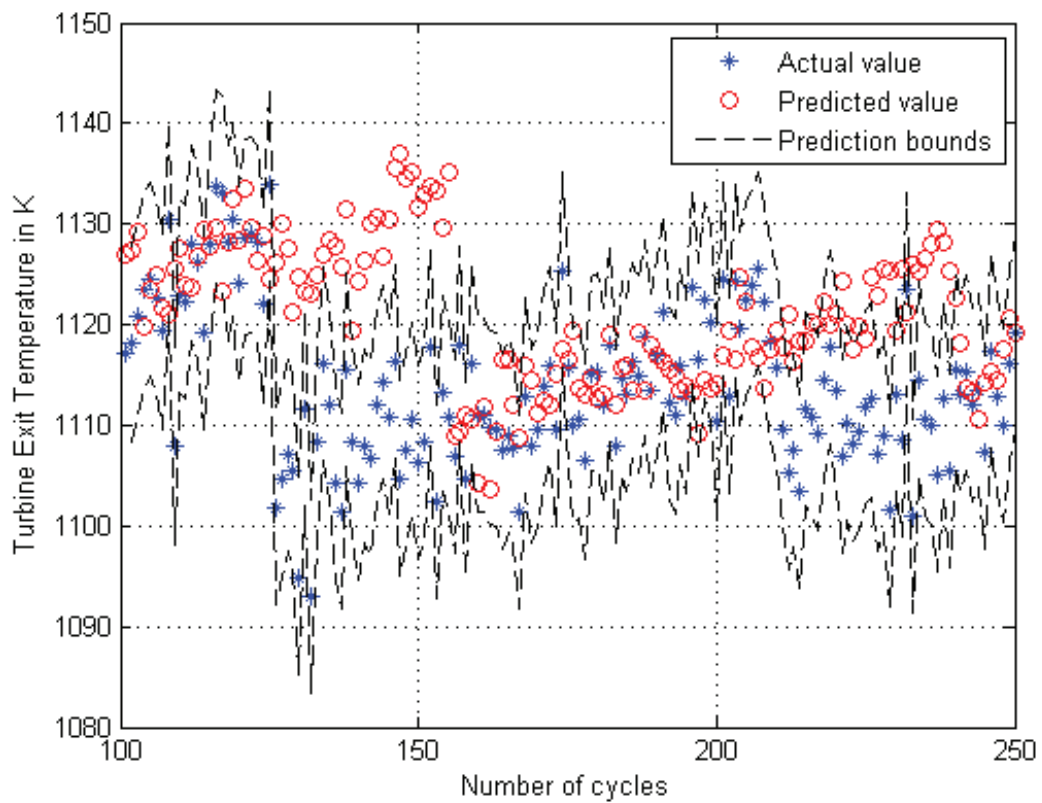


Figure 3.30: Thirty step ahead prediction results by using the univariate ARIMA(4,5) model for the second scenario in presence of the measurement noise with the standard deviation of 5.

Table 3.10: Mean and standard deviation of the prediction errors for the ARIMA model for the second scenario in presence of the measurement noise with the standard deviation of 1.

Number of steps ahead	Mean	Standard deviation
3	1.5527	3.5020
5	2.0285	4.4178
10	3.0963	5.9582
15	4.3212	7.2008
20	5.4455	8.0721
25	6.6459	8.7613
30	7.7710	9.3717

Table 3.11: Mean and standard deviation of the prediction errors for the ARIMA model for the second scenario in presence of measurement noise with the standard deviation of 2.

Number of steps ahead	Mean	Standard deviation
3	2.3321	3.9033
5	2.8696	4.8410
10	3.8452	6.4152
15	5.1542	7.6210
20	6.3336	8.7144
25	7.5401	9.4937
30	8.7345	10.1242

125th and 210th flight cycles for 5 flight cycles, the predicted values are outside the boundaries. This happens because of the maintenance that was performed at the cycles 125 and 210 in the second scenario and the eroded components have been changed with the new ones. Clearly the data before the maintenance action is not sufficient to allow for a reliable prediction subsequent to this action. As the prediction horizon increases to fifteen, as seen in Figure 3.23, the predicted values are still within the boundaries but it takes a few more cycles for the model to perform enough accurate prediction after the maintenance at the cycles 125 and 210. When the number of steps ahead reaches to 30 in the second scenario, the predict values are marginally within the boundaries and their predicted values are outside of the boundaries. Figures 3.25-3.27 depict the same scenario in presence of the measurement noise with the standard deviation of 2. By increasing the measurement noise level, the accuracy of prediction decreases in comparison to cases with the same number of step

Table 3.12: Mean and standard deviation of the prediction errors for the ARIMA model for the second scenario in presence of the measurement noise with the standard deviation of 5.

Number of steps ahead	Mean	Standard deviation
3	5.2366	6.9094
5	5.6643	7.8375
10	6.2346	8.8596
15	7.3275	9.7231
20	8.2246	10.0577
25	8.4377	10.0574
30	9.4644	10.2106

ahead predictions and for thirty steps ahead the predicted values are accurate enough. In Figures 3.28-3.30 the prediction results have been shown for the same scenario in presence of the measurement noise with standard deviation of 5. Due to the high level noise associated with the measurement data, the predicted values are more scattered and marginally within the boundaries as compared to the measurement noise with the standard deviations of 1 and 2. By increasing the number of steps ahead prediction the predicted data maintain the trend and even for the thirty steps ahead in Figure 3.30 the predicted values are barely within the boundaries.

Scenario 3

The detailed description of the third scenario was presented in the section Case Study Scenarios. The standard deviation of the measurement noise is considered as 1 (0.097 percent of the nominal value of the turbine temperature [13]). Figures 3.31-3.33 depict the results of the prediction in presence of the same level of measurement noise. The dashed lines show our upper and lower prediction intervals. The star points in the figure represent actual data values and the circle points indicate the predicted temperatures. Table 3.13 shows the mean and the standard deviation of the prediction errors for different number of steps ahead in presence of the measurement noise with the standard deviation of 1.

Figures 3.34-3.36 depict the results of the prediction for the third scenario in presence

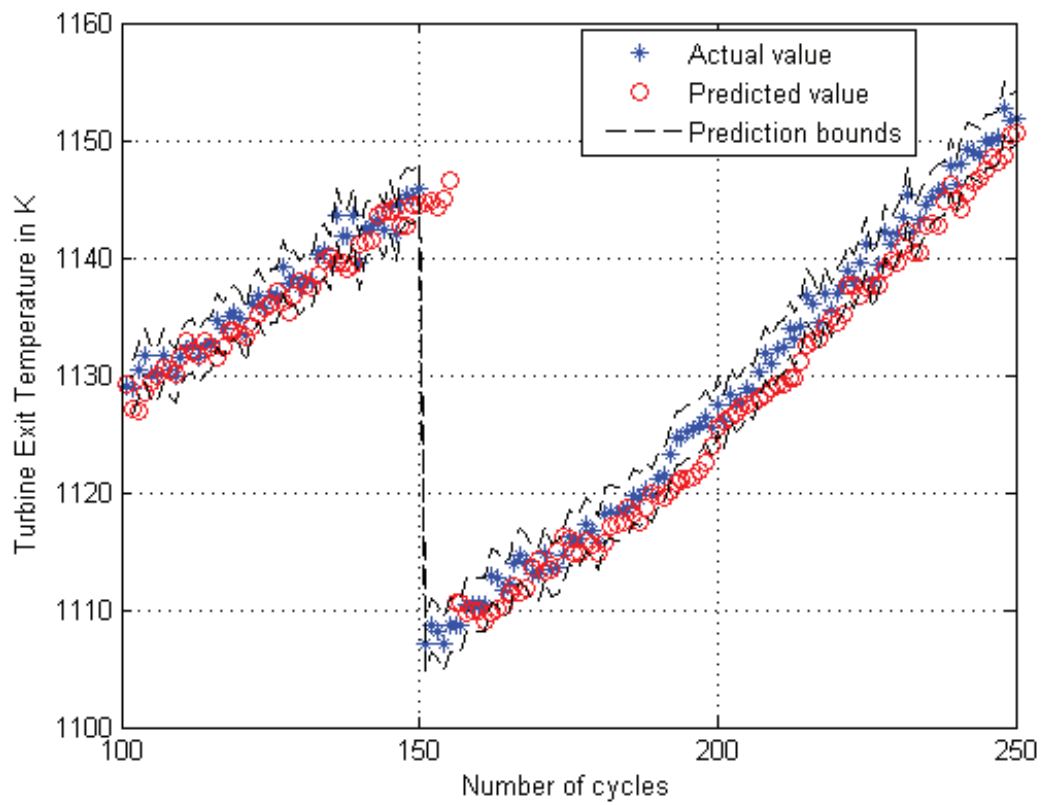


Figure 3.31: Five step ahead prediction results by using the univariate ARIMA(4,5) model for the third scenario in presence of the measurement noise with the standard deviation of 1.

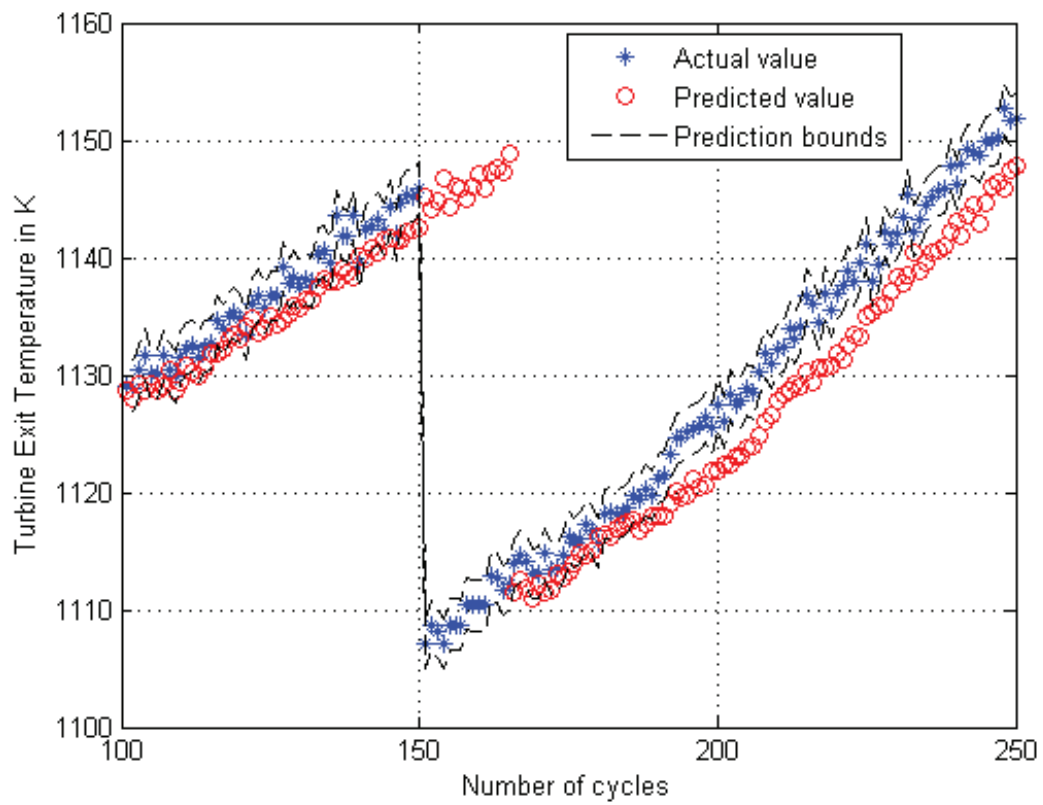


Figure 3.32: Fifteen step ahead prediction results by using the univariate ARIMA(4,5) model for the third scenario in presence of the measurement noise with the standard deviation of 1.

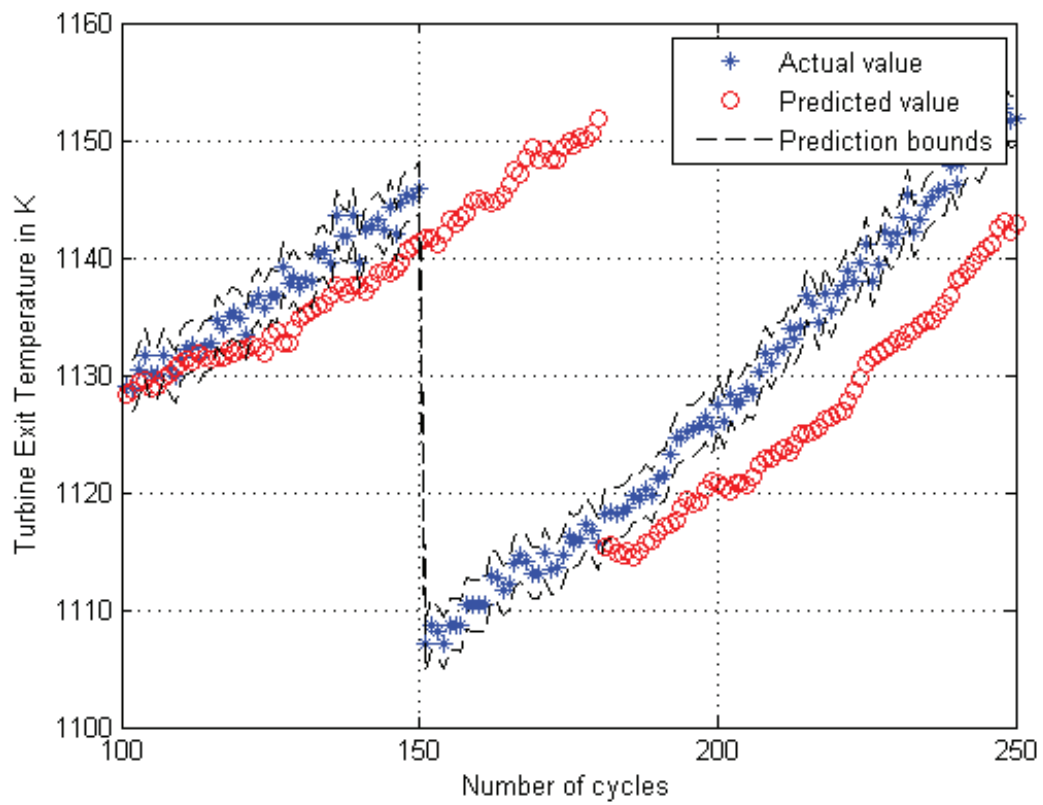


Figure 3.33: Thirty step ahead prediction results by using the univariate ARIMA(4,5) model for the third scenario in presence of the measurement noise with the standard deviation of 1.

Table 3.13: Mean and standard deviation of the prediction errors for the ARIMA model for the third scenario in presence of measurement noise with the standard deviation of 1.

Number of steps ahead	Mean	Standard deviation
3	1.8533	5.5818
5	2.9440	7.1066
10	4.5461	9.8598
15	6.6062	12.0289
20	8.3154	13.6296
25	9.9066	15.0818
30	11.5437	16.3052

Table 3.14: Mean and standard deviation of the prediction errors for the ARIMA model for the third scenario in presence of measurement noise with the standard deviation of 2.

Number of steps ahead	Mean	Standard deviation
3	2.8051	5.5696
5	3.5618	7.1859
10	4.7961	9.5748
15	6.4305	11.4981
20	8.0404	13.2292
25	9.5016	14.6031
30	10.9545	15.8002

of the same level of measurement noise with the standard deviation of 2. Table 3.14 shows the mean and the standard deviation of the prediction errors for different number of steps ahead in presence of measurement noise with the standard deviation of 2.

Figures 3.37-3.39 depict the results of the prediction in presence of the same level of measurement noise with the standard deviation of 5. Table 3.15 shows the mean and the standard deviation of the prediction errors for different number of steps ahead in presence of the measurement noise with the standard deviation of 5.

As seen in Figures 3.31, 3.34 and 3.37 showing the prediction results under three different measurement noise with standard deviations of 1, 2 and 5 for the five steps ahead, the predicted values are marginally within the boundaries. However, the prediction accuracy decreases as noise level increases. At 150th flight cycle for 5 flight cycles, the predicted

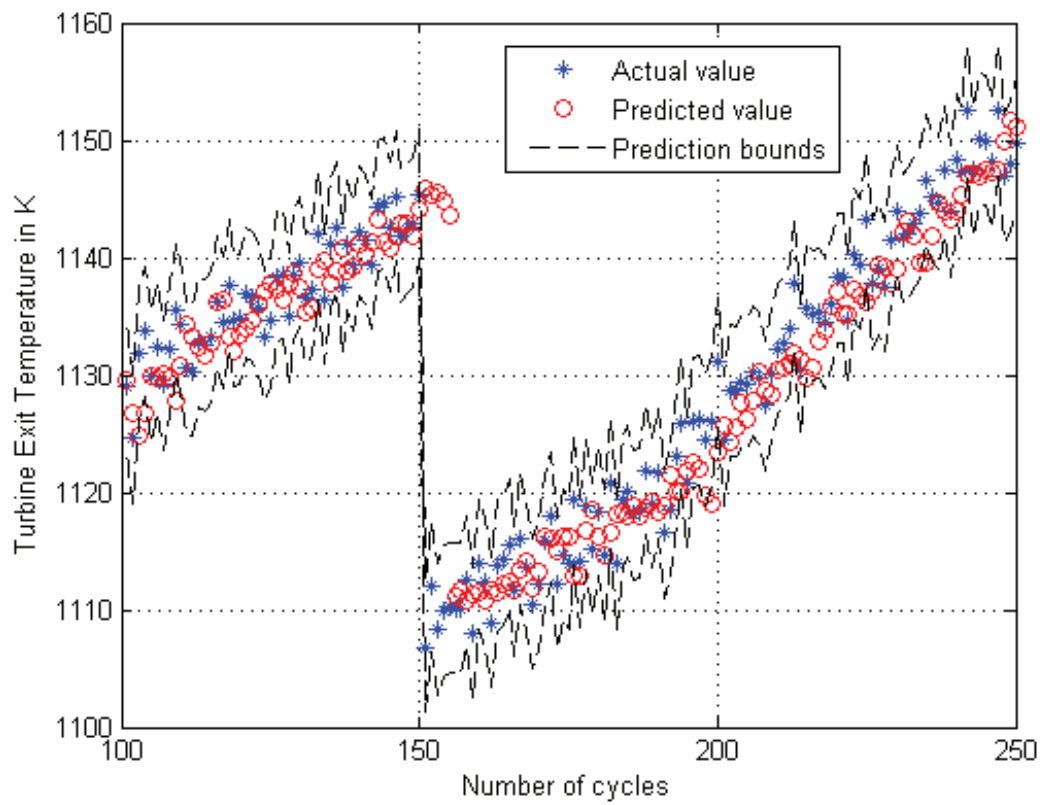


Figure 3.34: Five step ahead prediction results by using the univariate ARIMA(4,5) model for the third scenario in presence of the measurement noise with the standard deviation of 2.

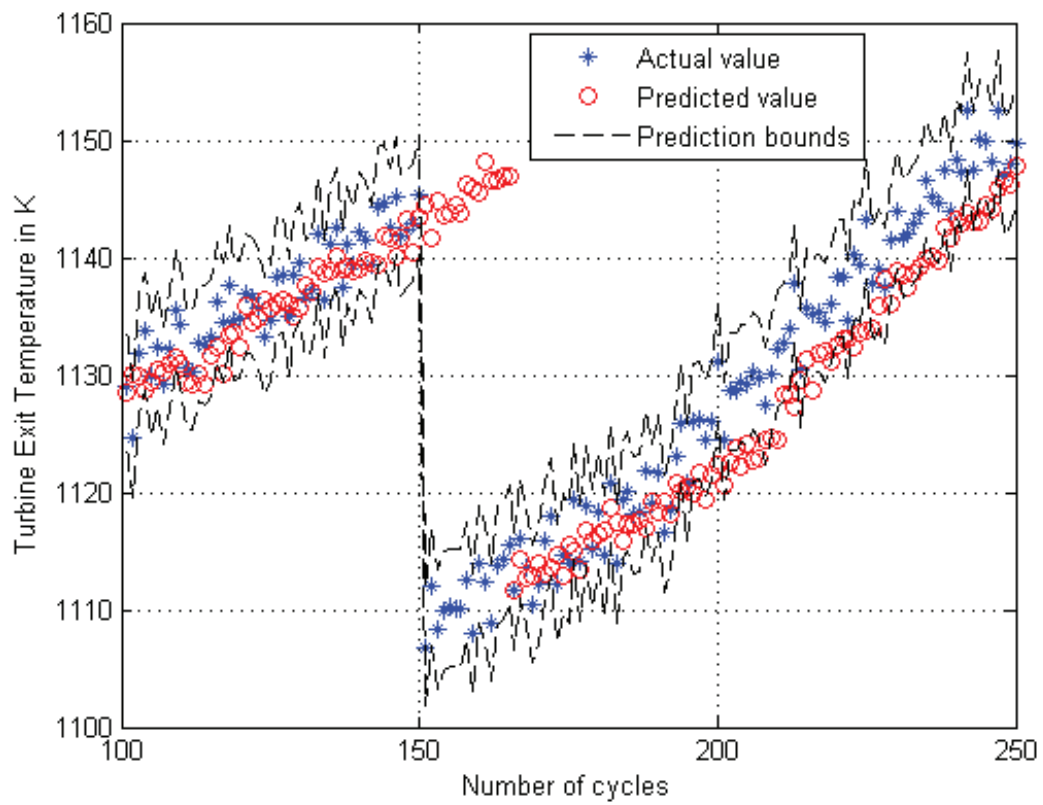


Figure 3.35: Fifteen step ahead prediction results by using the univariate ARIMA(4,5) model for the third scenario in presence of the measurement noise with the standard deviation of 2.

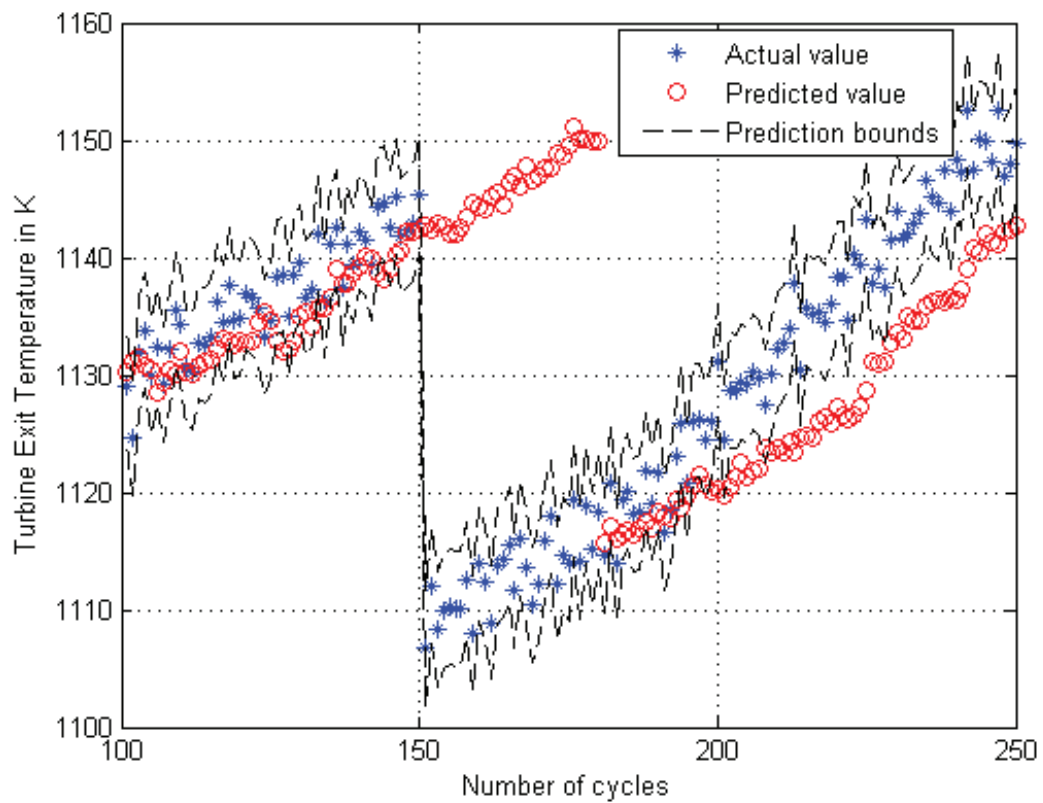


Figure 3.36: Thirty step ahead prediction results by using the univariate ARIMA(4,5) model for the third scenario in presence of the measurement noise with the standard deviation of 2.

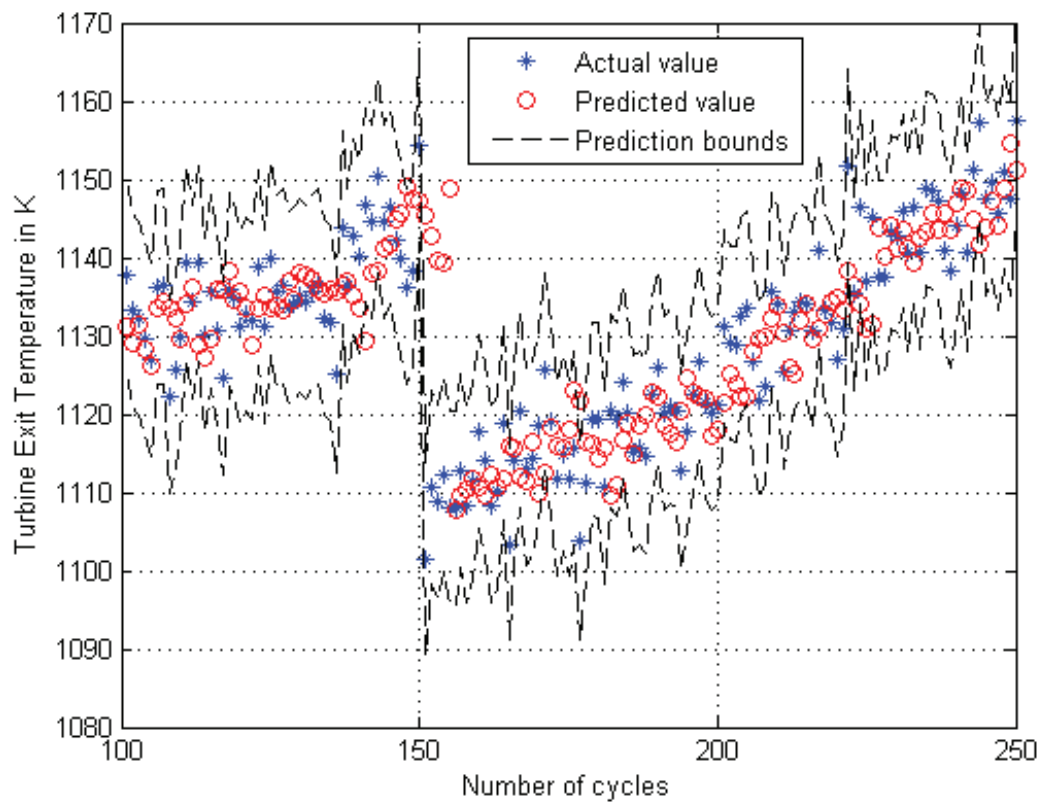


Figure 3.37: Five step ahead prediction results by using the univariate ARIMA(4,5) model for the third scenario in presence of the measurement noise with the standard deviation of 5.

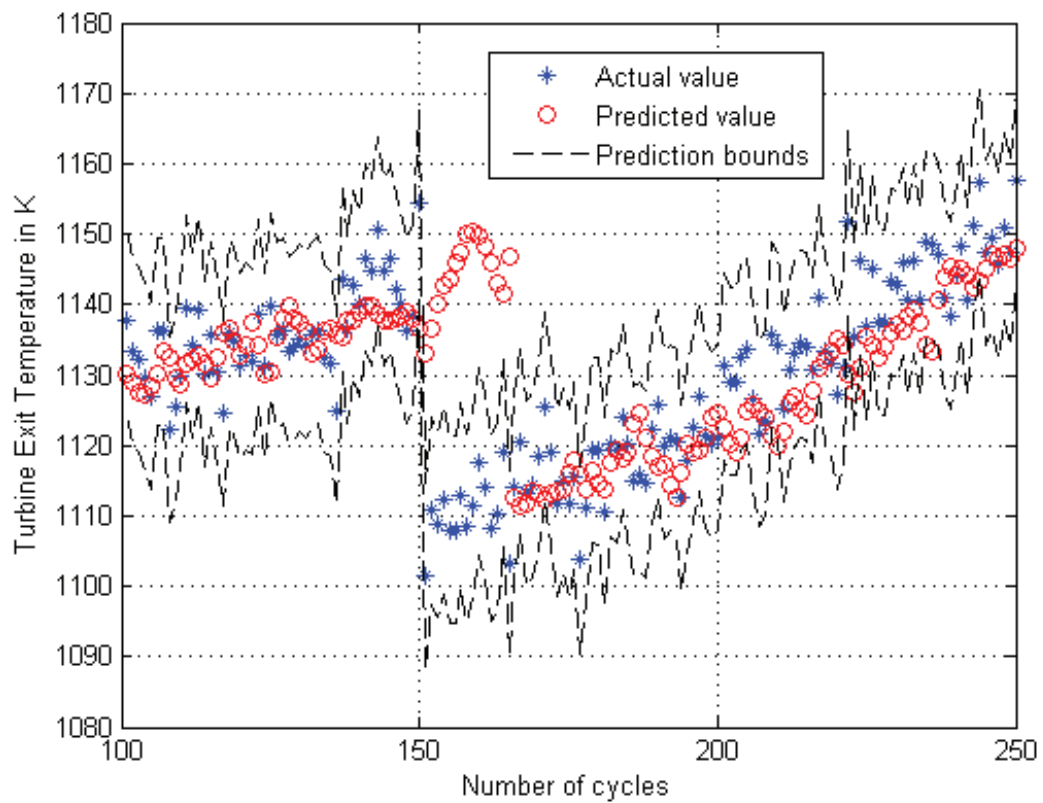


Figure 3.38: Fifteen step ahead prediction results by using the univariate ARIMA(4,5) model for the third scenario in presence of the measurement noise with the standard deviation of 5.

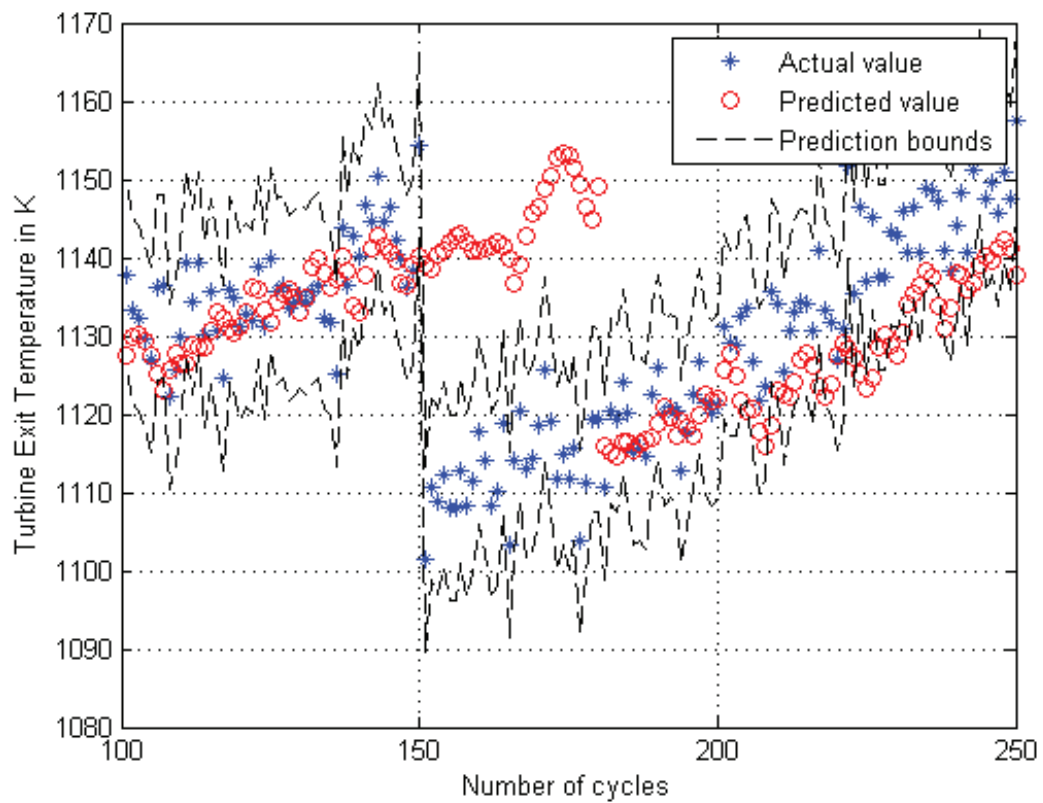


Figure 3.39: Thirty step ahead prediction results by using the univariate ARIMA(4,5) model for the third scenario in presence of the measurement noise with the standard deviation of 5.

Table 3.15: Mean and standard deviation of the prediction errors for the ARIMA model for the third scenario in presence of measurement noise with the standard deviation of 5.

Number of steps ahead	Mean	Standard deviation
3	5.3217	7.6909
5	5.8700	8.9263
10	6.8720	11.1903
15	8.2628	12.6852
20	9.0866	13.4829
25	10.3172	14.7415
30	11.5288	16.0321

values are outside the boundaries. This happens because of the maintenance that was performed at the cycle 150 in the third scenario and the compressor got washed and the turbine eroded blades were changed. Clearly, the data before the maintenance action is not sufficient to allow for a reliable prediction subsequent to this action. As seen in Figures 3.32, 3.35, 3.33 and 3.36 the prediction accuracy is not acceptable and considerable parts of the predicted values are outside the boundaries.

3.4.2 VAR Model

VAR(6) model is fitted into the vector of time-series entailing the turbine exit temperature (TET) and the compressor temperature. In this thesis, as given in equation (2.40), the non-diagonal elements of the matrix ϕ_1 ($\phi_{1,12}$ and $\phi_{1,21}$) show the effect of the past values of the two time-series on each other present values. By using the VAR model, one takes advantage of this characteristic for prediction purposes. Similar to what was accomplished for meeting the required prediction performance, Monte Carlo simulations are conducted with confidence levels of 95% that are implemented according to the normal theory. It should be noted that from the 250 available measurements in the VAR method we used 40% of the measurements for model parameters estimation and the remaining points are used for testing and evaluating the prediction performance of the model.

Data Preprocessing

Figure 3.40 depicts the results of the prediction for a ten step ahead for the VAR(6) model. The dashed lines show our upper and lower prediction intervals. The star points in the figure represent actual data values and the circle points indicate the predicted temperatures. All the figures depict the prediction portion of the scenario, since certain parts of the data were used for testing as mentioned earlier.

As seen in Figure 3.40, between the 120th to the 130th cycles and also at the 200th cycle, the prediction error is significantly large due to the maintenance that was performed at the cycles 120 and 200. Clearly the data before the maintenance action is not sufficient to allow for a reliable prediction subsequent to this action. Despite this even after 10 cycles (number of steps ahead for this case) prediction error is significantly large and this occurs when there is a gap between the values of the captured data. These gaps can be originated from possible dramatically degradation changes or post maintenance capturing data. To cope with this problem and achieving a better and more acceptable predictions in terms of accuracy, in this thesis a compensation method in the form of data preprocessing has been conducted. The procedure is similar to the one that is used for ARIMA model and it has been demonstrated earlier in this section. Figure 3.43 shows the results of the prediction for the same scenario with the above mentioned compensator. Subsequently, the aforementioned compensator will be applied to all the simulations throughout this section.

Scenario 1

The detailed description of the first scenario was presented in the section Case Study Scenarios. The standard deviation of the measurement noise is considered as 1. Figures 3.41-3.45 depict the results of the prediction in presence of the same level of measurement noise for both turbine and compressor temperatures. The dashed lines show our upper and lower prediction intervals. The star points in the figure represent actual data values and the circle

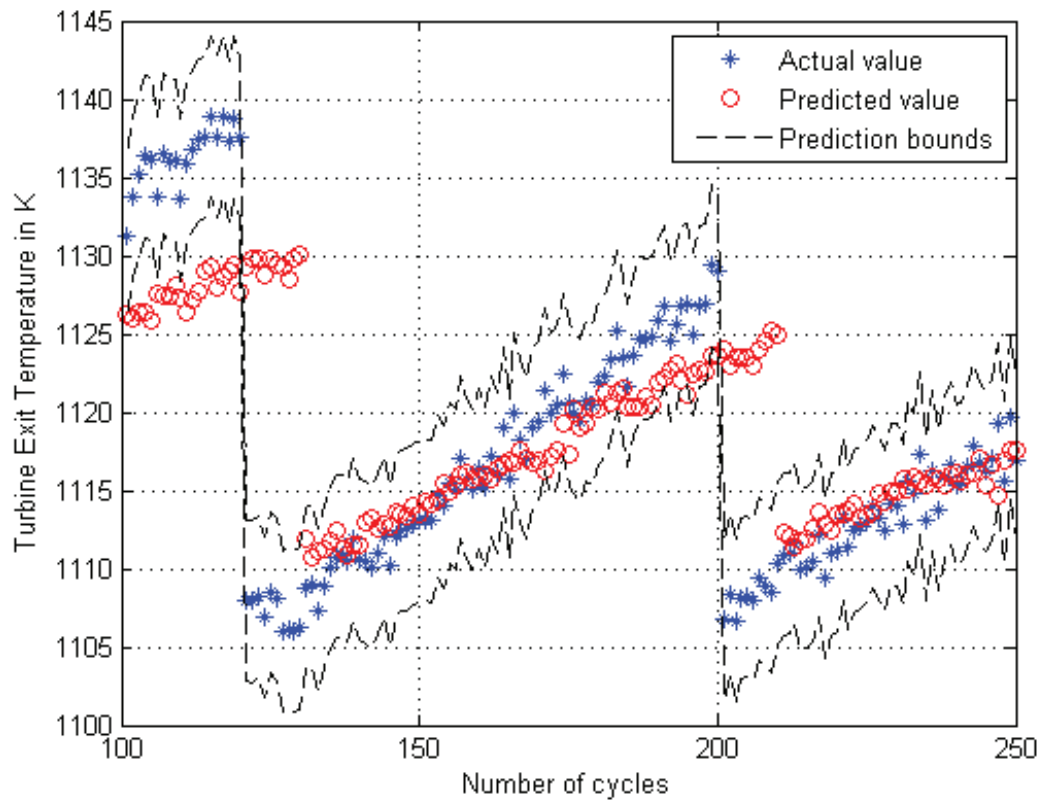


Figure 3.40: Ten step ahead prediction results by using the VAR(6) model without compensator for the first scenario in presence of measurement noise with the standard deviation of 1.

points indicate the predicted temperatures. Table 3.16 represents the mean and the standard deviation of the prediction errors for different number of steps ahead in presence of measurement noise with the standard deviation of 1.

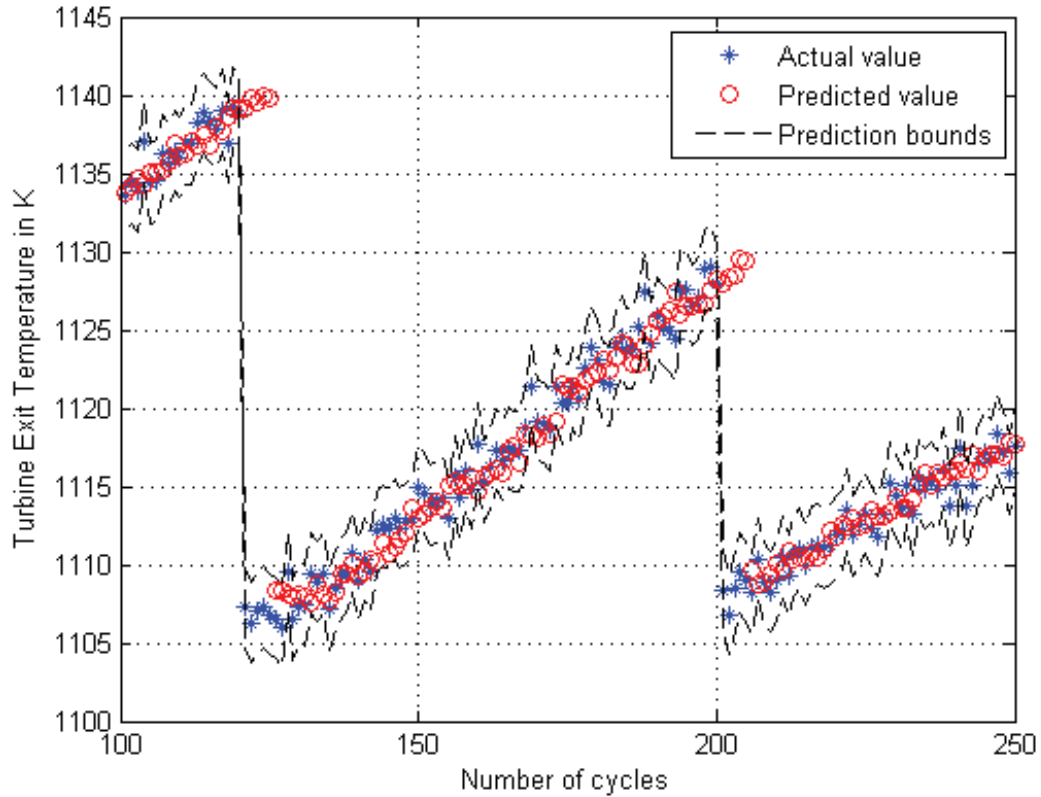


Figure 3.41: Five step ahead turbine temperature prediction results by using the bivariate VAR(6) model for the first scenario in presence of measurement noise with the standard deviation of 1.

In order to investigate the effects of measurement noise on the prediction results, each scenario has been repeated for different value of measurement noise. Figures 3.46-3.49 depict the results of the prediction in presence of the same level of measurement noise with the standard deviation of 2. Table 3.17 represents the mean and the standard deviation of the prediction error for different number of steps ahead in presence of measurement noise with the standard deviation of 2.

Figures 3.50-3.53 depict the results of the prediction in presence of the same level of

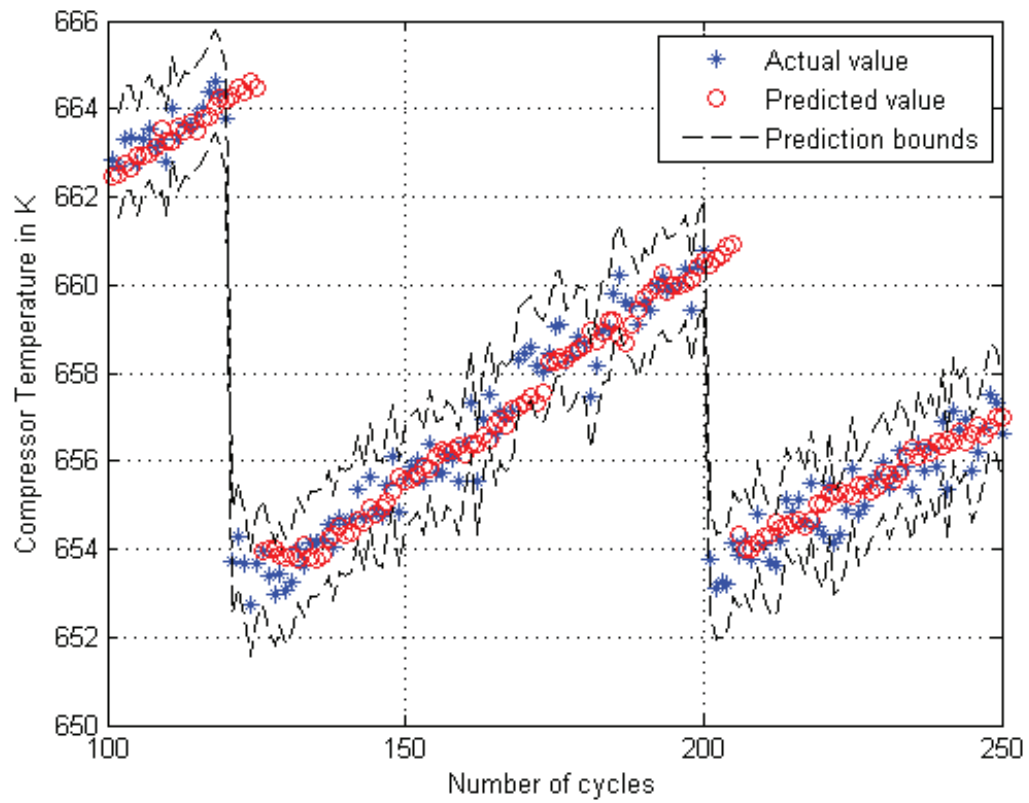


Figure 3.42: Five step ahead compressor temperature prediction results by using the bivariate VAR(6) model for the first scenario in presence of measurement noise with the standard deviation of 1.

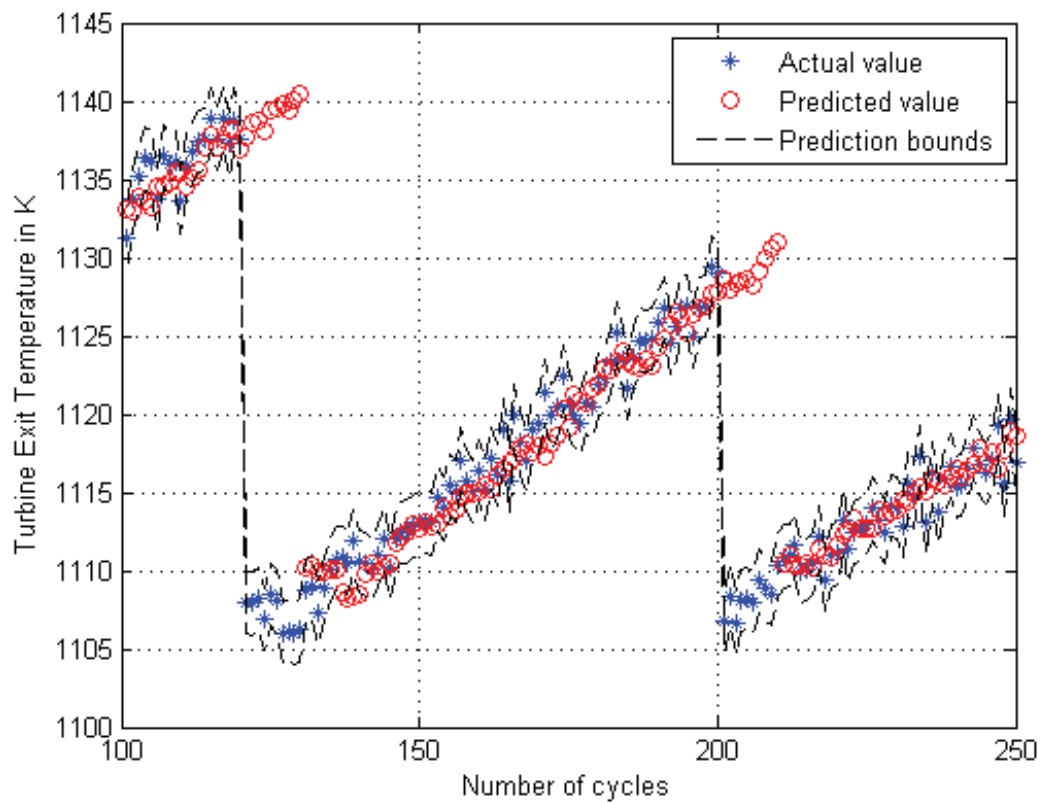


Figure 3.43: Ten step ahead prediction results by using the VAR(6) model including compensator for the first scenario in presence of measurement noise with the standard deviation of 1.

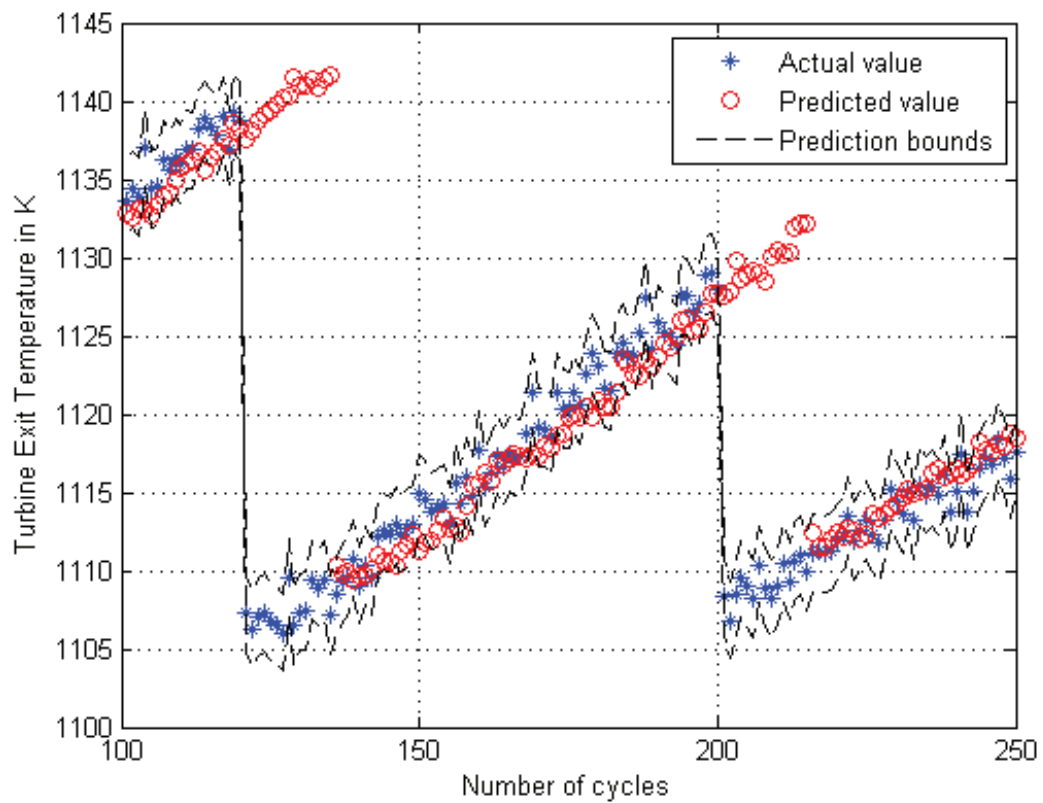


Figure 3.44: Fifteen step ahead turbine temperature prediction results by using the bivariate VAR(6) model for the first scenario in presence of measurement noise with the standard deviation of 1.

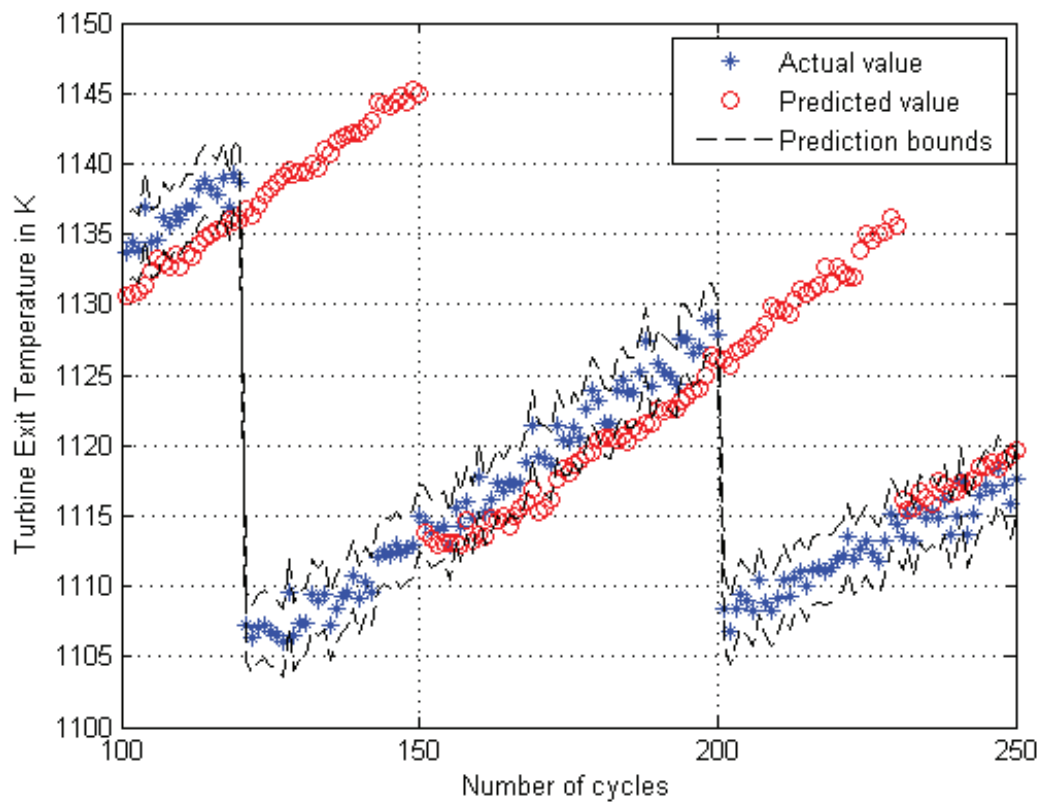


Figure 3.45: Thirty step ahead turbine temperature prediction results by using the bivariate VAR(6) model for the first scenario in presence of measurement noise with the standard deviation of 1.

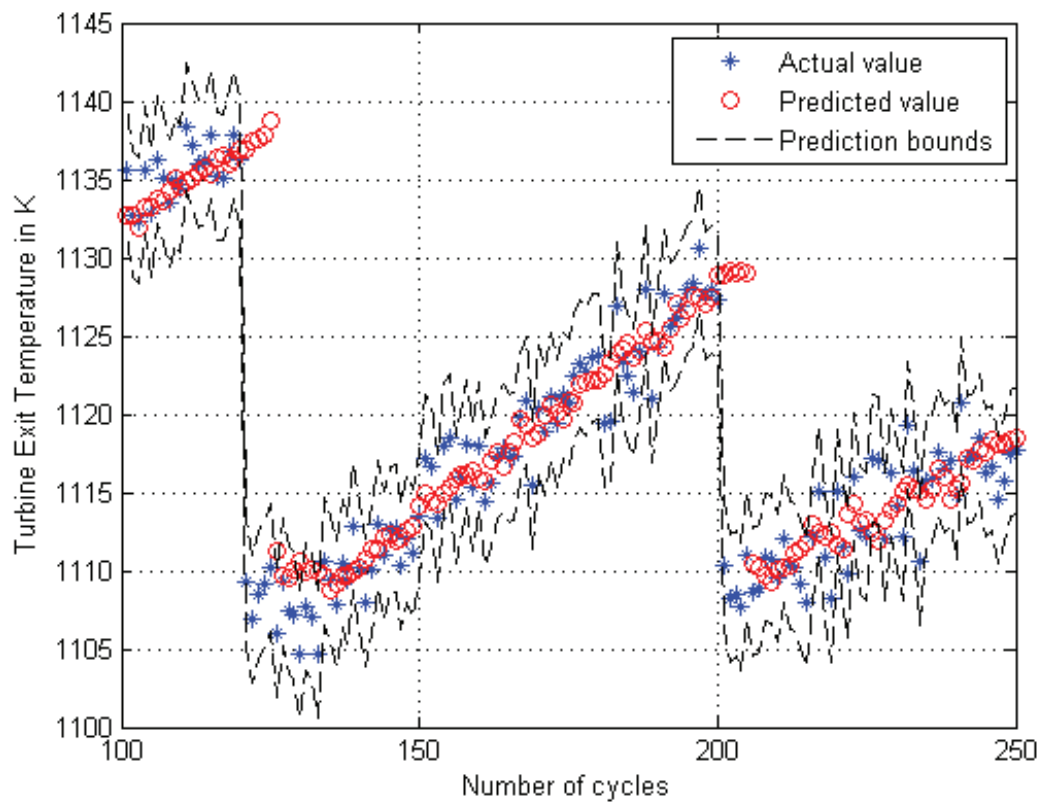


Figure 3.46: Five step ahead turbine temperature prediction results by using the bivariate VAR(6) model for the first scenario in presence of measurement noise with the standard deviation of 2.

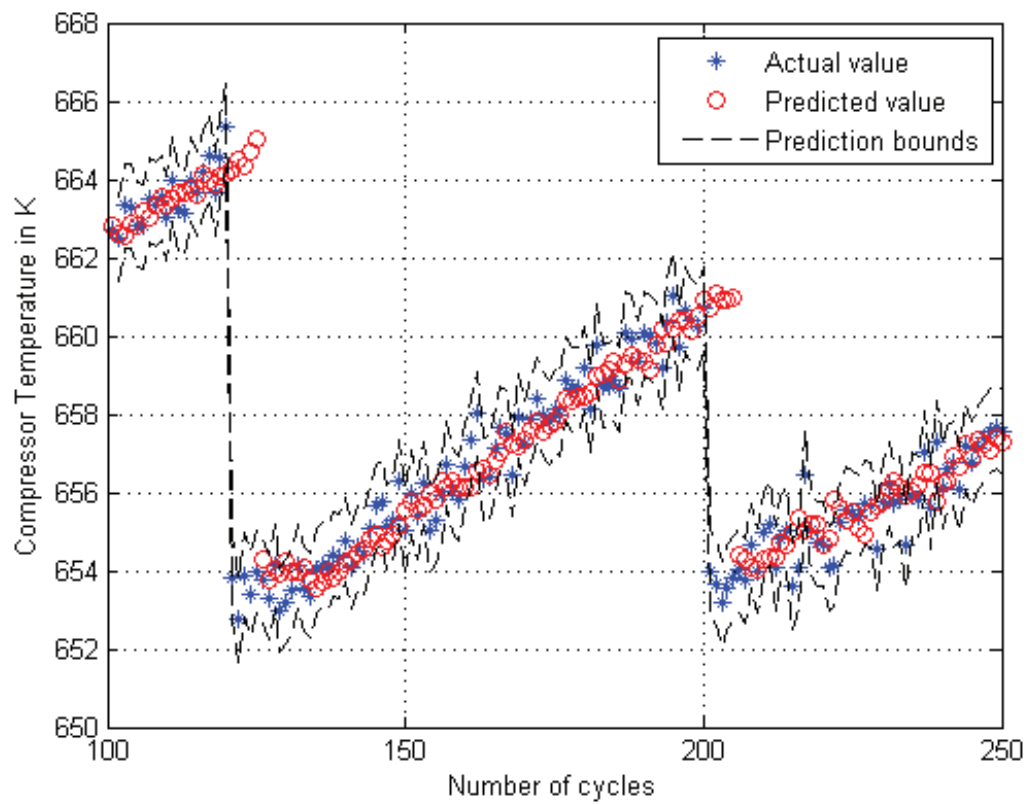


Figure 3.47: Five step ahead compressor temperature prediction results by using the bivariate VAR(6) model for the first scenario in presence of measurement noise with the standard deviation of 2.

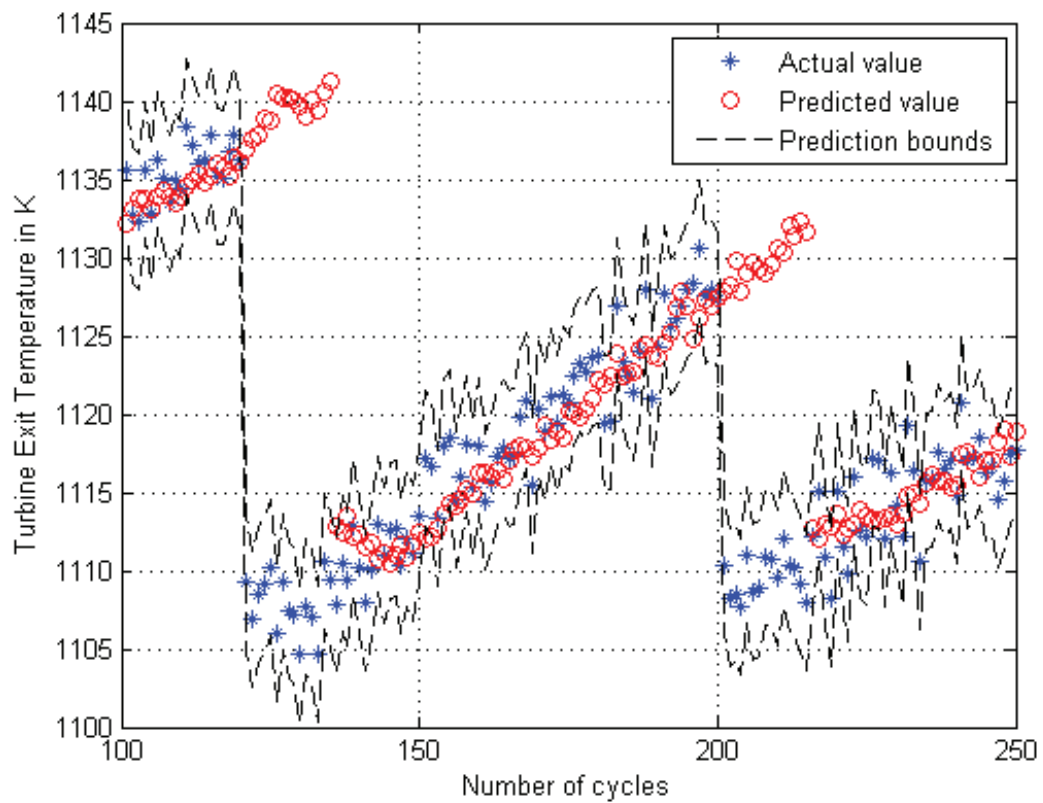


Figure 3.48: Fifteen step ahead turbine temperature prediction results by using the bivariate VAR(6) model for the first scenario in presence of measurement noise with the standard deviation of 2.

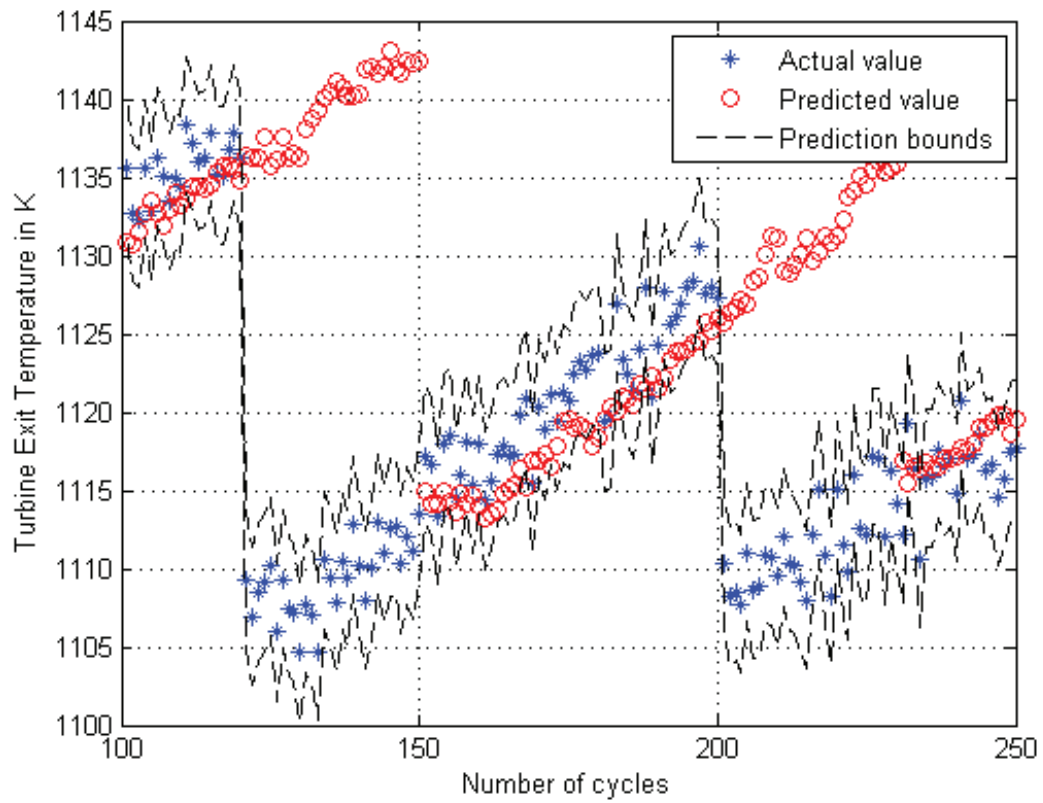


Figure 3.49: Thirty step ahead turbine temperature prediction results by using the bivariate VAR(6) model for the first scenario in presence of measurement noise with the standard deviation of 2.

Table 3.16: Mean and standard deviation of the prediction errors for the VAR model for the first scenario in presence of measurement noise with the standard deviation of 1.

Number of steps ahead	Turbine temperature		Compressor temperature	
	Mean	Standard deviation	Mean	Standard deviation
3	1.9478	5.5505	0.8001	1.8626
5	2.6303	6.9669	1.0118	2.3819
10	4.4182	9.6522	1.6163	3.2421
15	6.3504	11.3587	2.3058	4.0714
20	8.2984	12.7969	2.8375	4.2897
25	10.1600	13.7229	3.4659	4.5876
30	11.8872	14.2123	4.1713	4.9759

Table 3.17: Mean and standard deviation of the prediction errors for the VAR model for the first scenario in presence of measurement noise with the standard deviation of 2.

Number of steps ahead	Turbine temperature		Compressor temperature	
	Mean	Standard deviation	Mean	Standard deviation
3	2.4927	5.2811	0.8112	1.9906
5	3.1609	6.5429	1.0383	2.4193
10	4.8167	9.0826	1.6608	3.3662
15	6.6294	11.1476	2.2862	3.8679
20	8.3792	12.2241	3.0280	4.5164
25	9.7858	12.9092	3.3897	4.5970
30	11.4435	13.6340	4.0244	4.8319

measurement noise with the standard deviation of 5. Table 3.18 shows the mean and the standard deviation of the prediction error for different number of steps ahead in presence of measurement noise with the standard deviation of 5.

As seen in Figure 3.41, all the predicted values are completely within the defined boundaries and the accuracy of the prediction is satisfactory. At 120th and 200th flight cycles for 5 flight cycles, the predicted values are outside the boundaries. This happens because of the maintenance that was performed at the cycles 120 and 200 in the first scenario and the compressor got washed. Clearly, the data before the maintenance action is not sufficient to allow for a reliable prediction subsequent to this action. As the prediction horizon increases

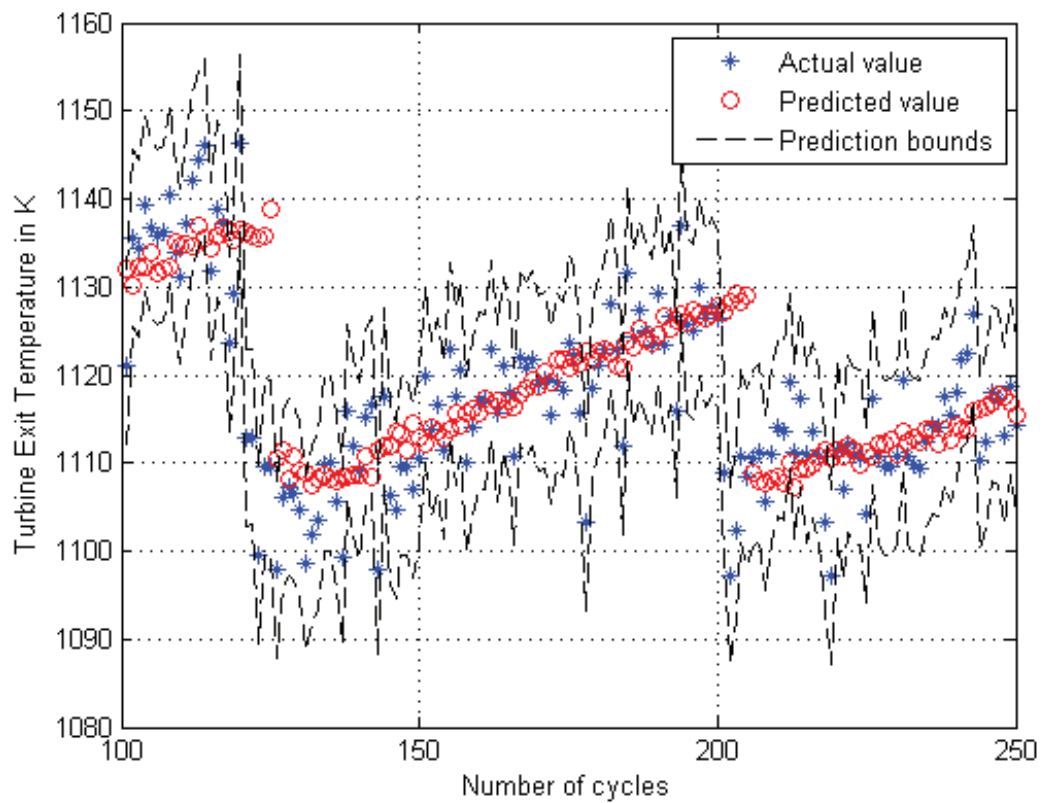


Figure 3.50: Five step ahead turbine temperature prediction results by using the bivariate VAR(6) model for the first scenario in presence of measurement noise with the standard deviation of 5.

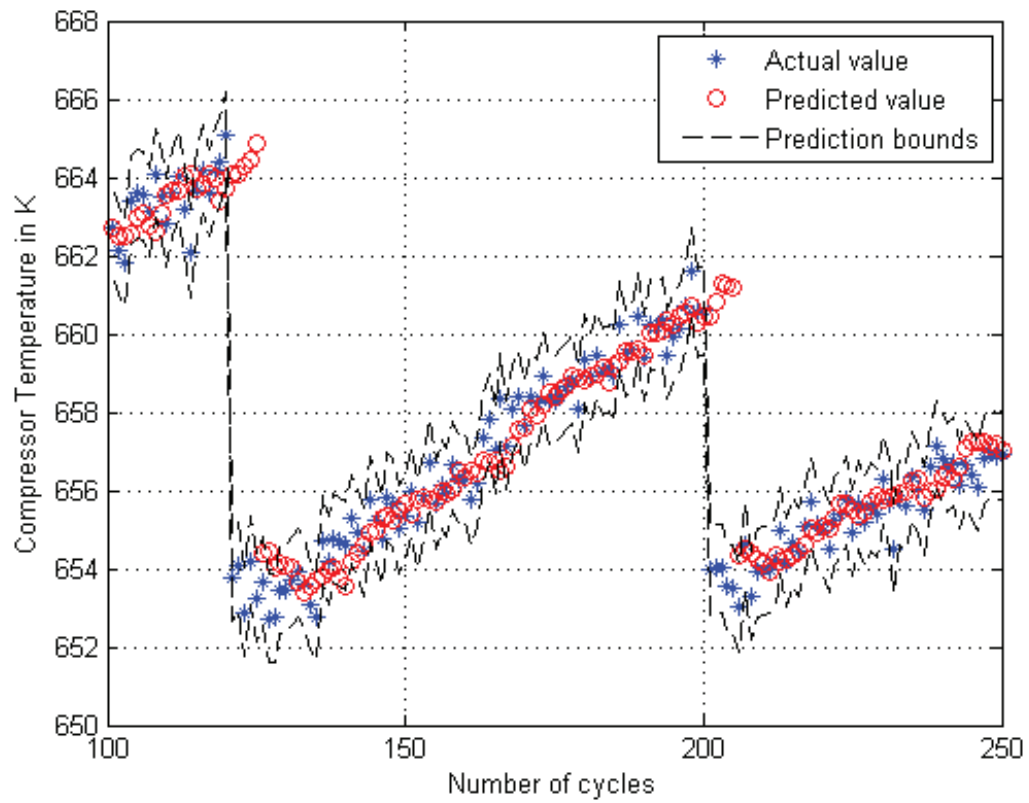


Figure 3.51: Five step ahead compressor temperature prediction results by using the bivariate VAR(6) model for the first scenario in presence of measurement noise with the standard deviation of 5.

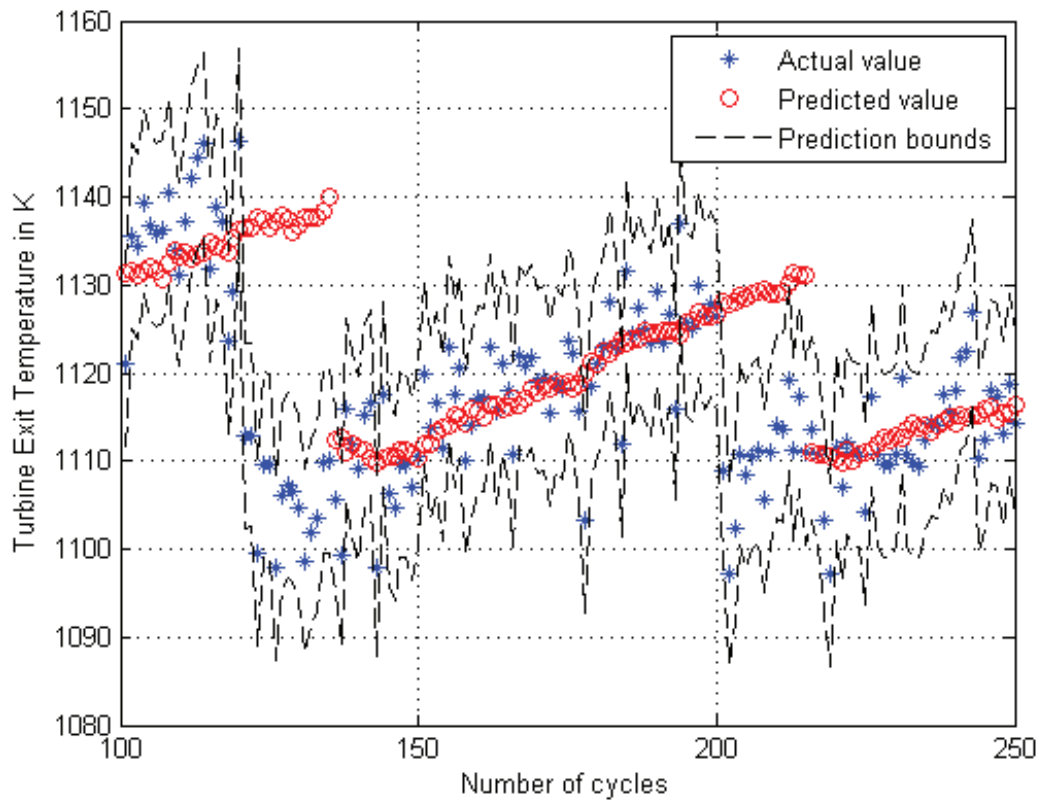


Figure 3.52: Fifteen step ahead turbine temperature prediction results by using the bivariate VAR(6) model for the first scenario in presence of measurement noise with the standard deviation of 5.

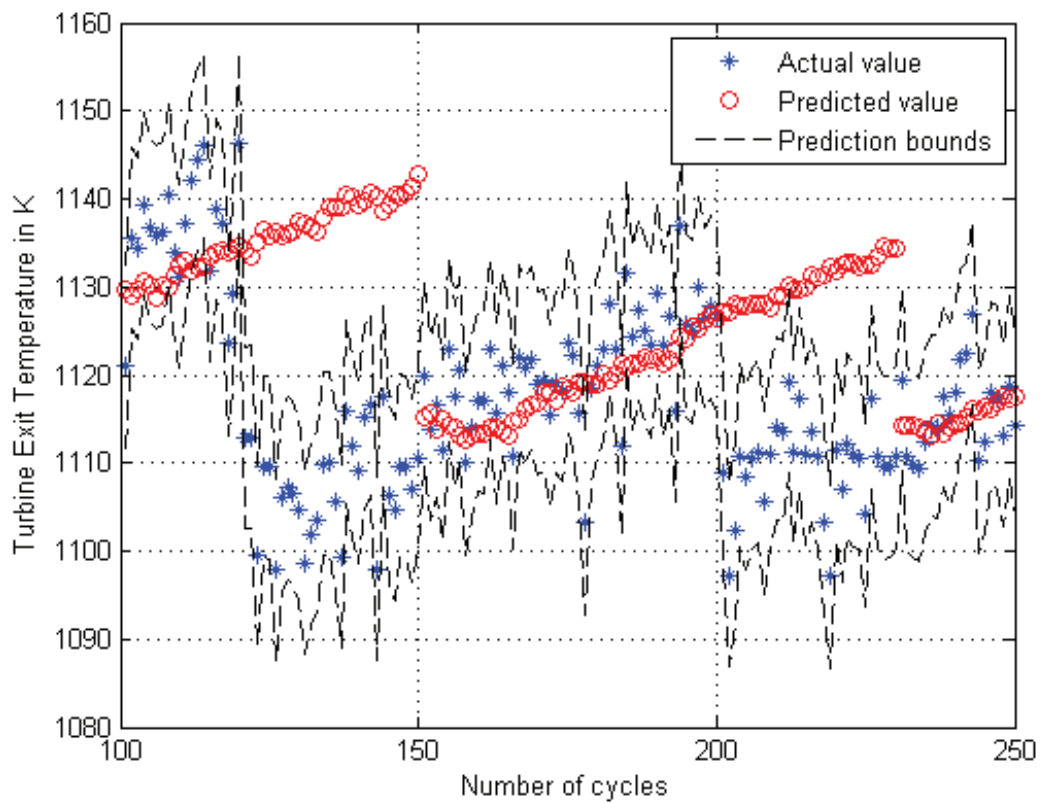


Figure 3.53: Thirty step ahead turbine temperature prediction results by using the bivariate VAR(6) model for the first scenario in presence of measurement noise with the standard deviation of 5.

Table 3.18: Mean and standard deviation of the prediction errors for the VAR model for the first scenario in presence of measurement noise with the standard deviation of 5.

Number of steps ahead	Turbine temperature		Compressor temperature	
	Mean	Standard deviation	Mean	Standard deviation
3	5.0315	7.5360	0.7906	1.8871
5	5.6436	8.4000	1.0523	2.3827
10	7.1729	10.5646	1.6907	3.3197
15	8.4105	11.9981	2.3020	4.0000
20	9.9438	13.3387	2.9267	4.3895
25	11.5522	14.2821	3.5319	4.6882
30	13.1832	15.1653	4.1582	4.9308

to fifteen, as seen in Figure 3.44, the predicted values are within the boundaries with acceptable accuracy. When the number of steps ahead reaches to 30, the prediction accuracy is not acceptable and there are many predicted values outside the boundaries. Figures 3.46 and 3.50 depict the same scenario in presence of the measurement noise with standard deviation of 2 and 5 for five steps ahead. Despite the high level of the measurement noise the predicted values are completely within the boundaries and the prediction accuracy is completely satisfactory. Figures 3.48 and 3.52 show the predicted values for fifteen steps ahead under the measurement noise with the standard deviations of 2 and 5. The predicted values are within the boundaries and the prediction accuracy is good. As seen in Figures 3.49 and 3.53 many of the predicted values are outside of the boundaries and the prediction accuracy is not acceptable.

Scenario 2

The detailed description of the second scenario was presented in the section Case Study Scenarios. The standard deviation of the measurement noise is considered as 1. Figures 3.54-3.57 depict the results of the prediction in presence of the same level of measurement noise. The dashed lines show our upper and lower prediction intervals. The star points

in the figure represent actual data values and the circle points indicate the predicted temperatures. Table 3.19 shows the mean and the standard deviation of the prediction errors for different number of steps ahead in presence of measurement noise with the standard deviation of 1. Figures 3.58-3.61 depict the results of the prediction in presence of the

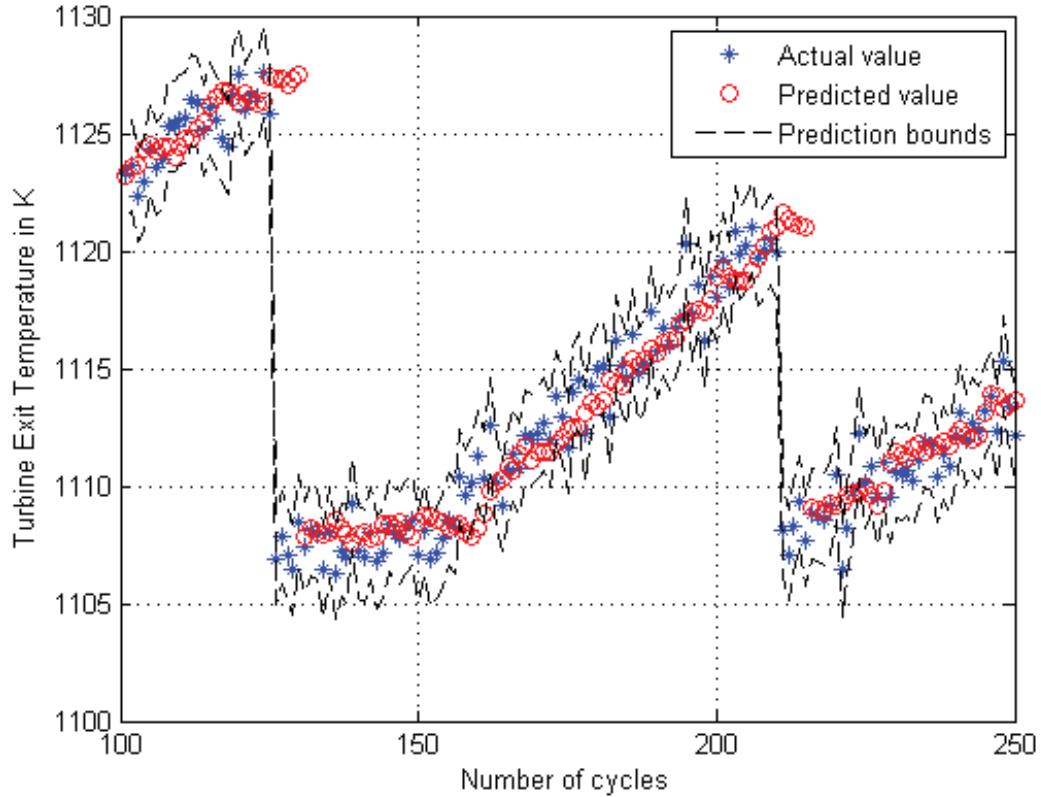


Figure 3.54: Five step ahead turbine temperature prediction results by using the bivariate VAR(6) model for the second scenario in presence of measurement noise with the standard deviation of 1.

same level of measurement noise with the standard deviation of 2. Table 3.20 shows the mean and the standard deviation of the prediction error for different number of steps ahead in presence of measurement noise with the standard deviation of 2.

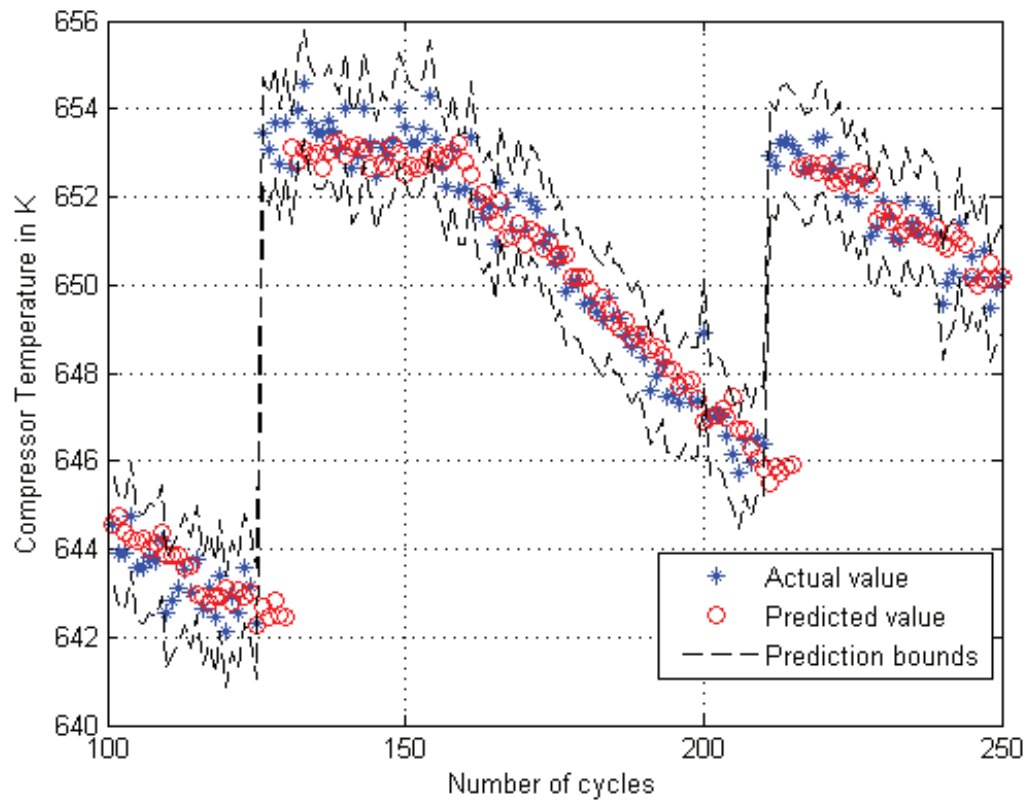


Figure 3.55: Five step ahead compressor temperature prediction results by using the bi-variate VAR(6) model for the second scenario in presence of measurement noise with the standard deviation of 1.

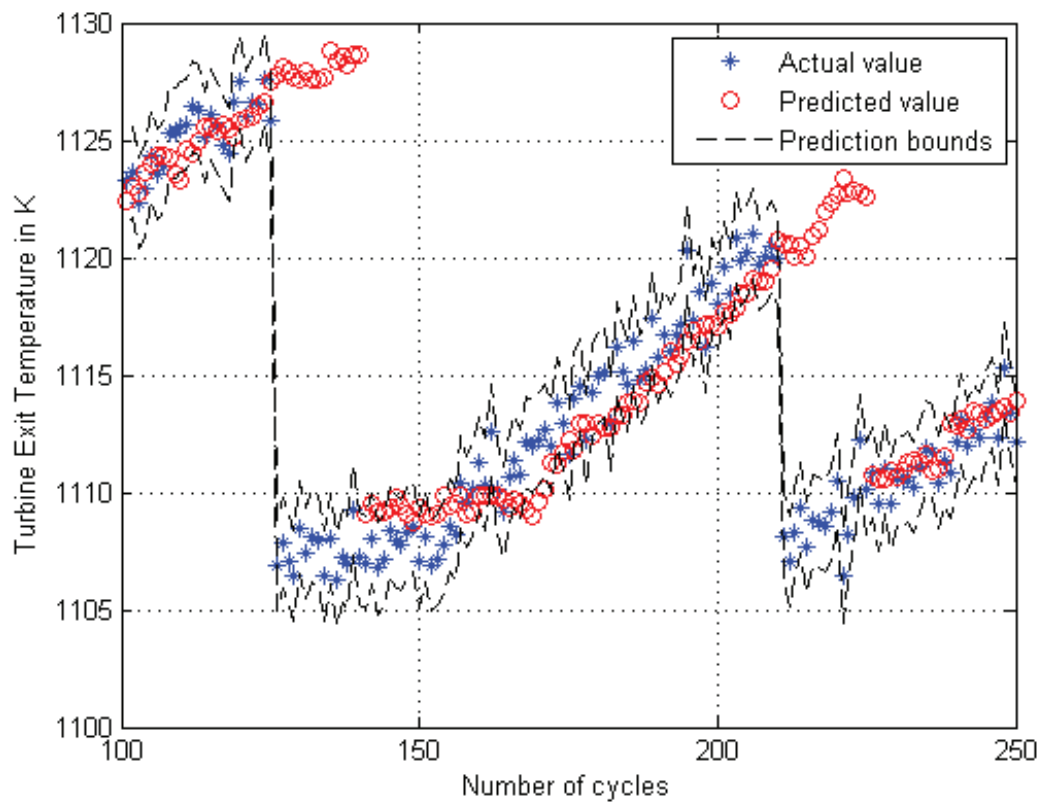


Figure 3.56: Fifteen step ahead turbine temperature prediction results by using the bivariate VAR(6) model for the second scenario in presence of measurement noise with the standard deviation of 1.

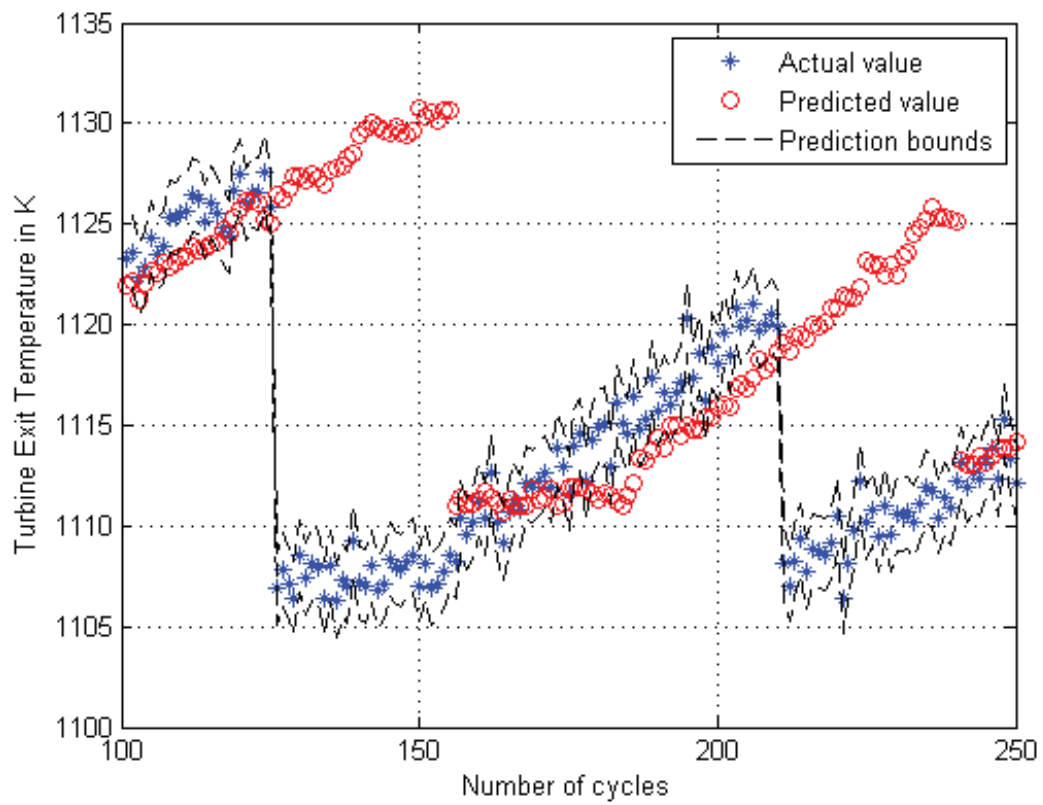


Figure 3.57: Thirty step ahead turbine temperature prediction results by using the bivariate VAR(6) model for the second scenario in presence of measurement noise with the standard deviation of 1.

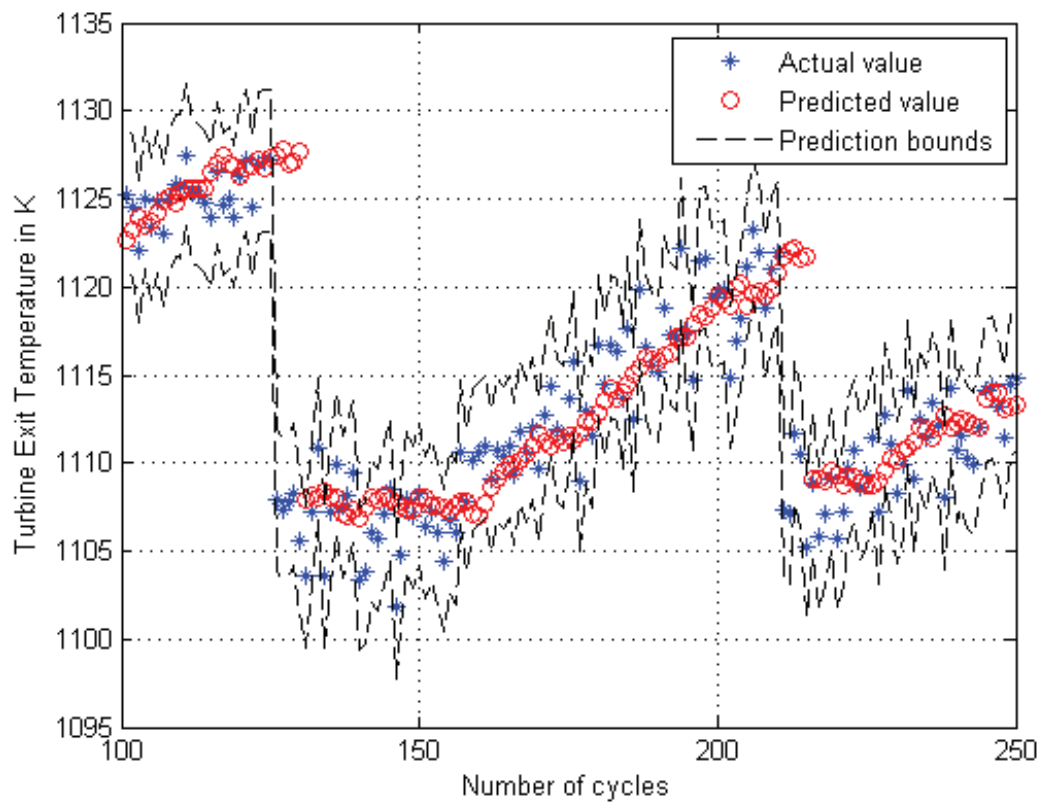


Figure 3.58: Five step ahead turbine temperature prediction results by using the bivariate VAR(6) model for the second scenario in presence of measurement noise with the standard deviation of 2.

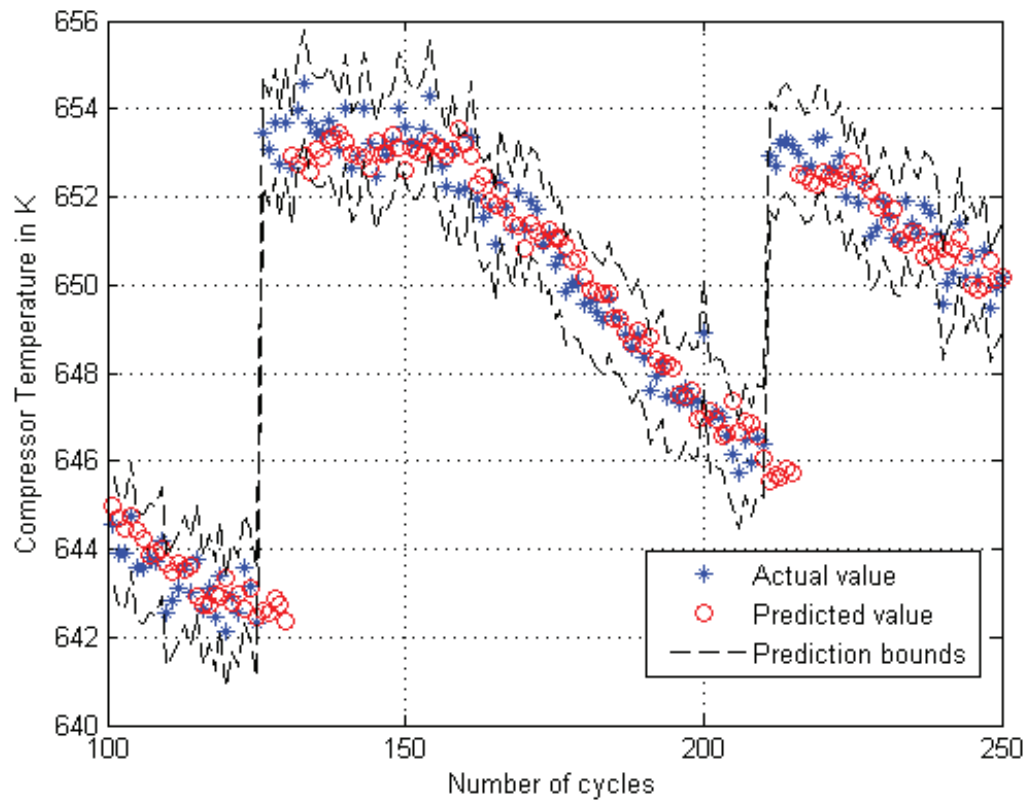


Figure 3.59: Five step ahead compressor temperature prediction results by using the bi-variate VAR(6) model for the second scenario in presence of measurement noise with the standard deviation of 2.

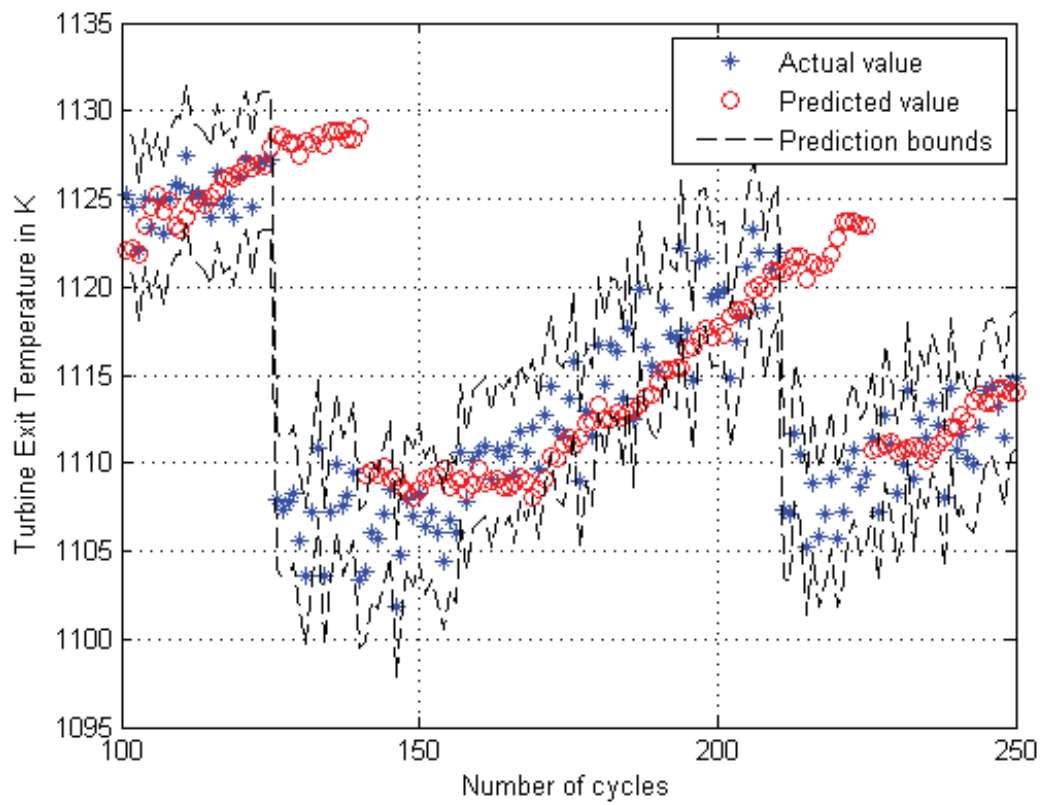


Figure 3.60: Fifteen step ahead turbine temperature prediction results by using the bivariate VAR(6) model for the second scenario in presence of measurement noise with the standard deviation of 2.

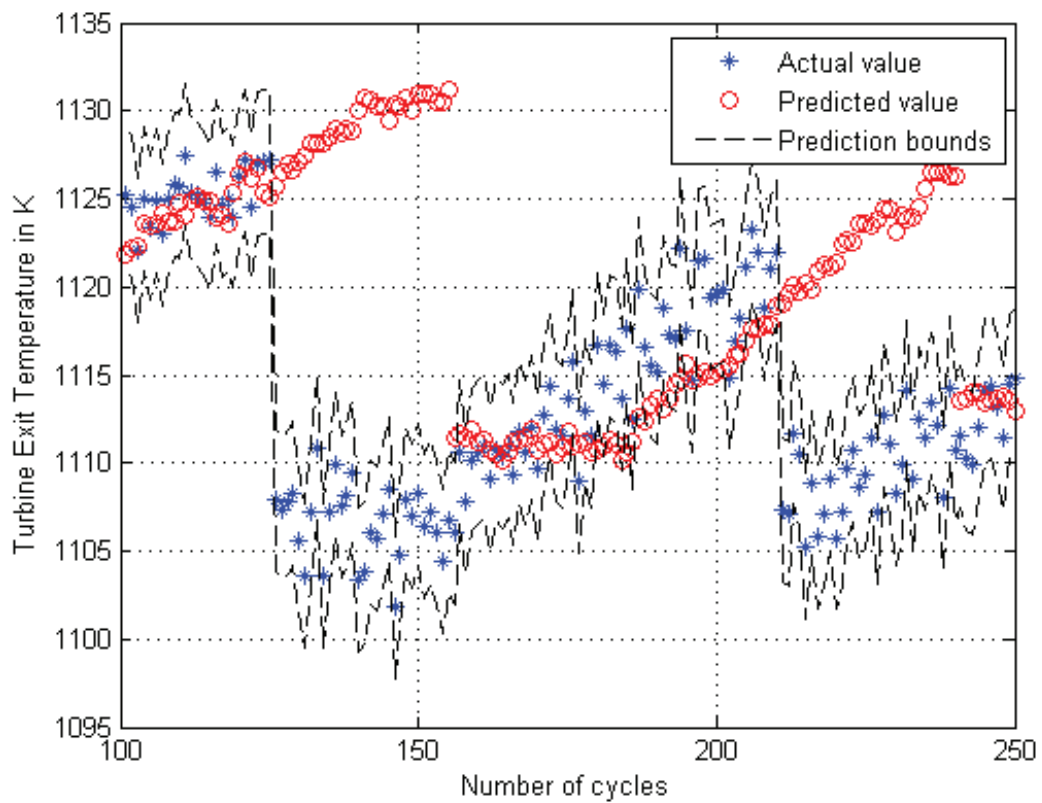


Figure 3.61: Thirty step ahead turbine temperature prediction results by using the bivariate VAR(6) model for the second scenario in presence of measurement noise with the standard deviation of 2.

Table 3.19: Mean and standard deviation of the prediction errors for the VAR model for the second scenario in presence of measurement noise with the standard deviation of 1.

Number of steps ahead	Turbine temperature		Compressor temperature	
	Mean	Standard deviation	Mean	Standard deviation
3	1.4601	3.4640	0.7801	1.8545
5	1.9611	4.4107	1.0530	2.3785
10	3.0882	5.9786	1.7424	3.3318
15	4.3240	7.2258	2.3885	4.0081
20	5.4897	8.1474	3.0695	4.4746
25	6.6794	8.8692	3.7350	4.8713
30	7.7611	9.3436	4.7078	5.5034

Table 3.20: Mean and standard deviation of the prediction errors for the VAR model for the second scenario in presence of measurement noise with the standard deviation of 2.

Number of steps ahead	Turbine temperature		Compressor temperature	
	Mean	Standard deviation	Mean	Standard deviation
3	2.1943	3.7853	0.7923	1.8640
5	2.6711	4.7678	1.0571	2.3939
10	3.8798	6.5545	1.7517	3.3384
15	5.1290	7.7681	2.4380	4.0514
20	6.2943	8.8394	3.1454	4.5527
25	7.4938	9.6679	3.8159	4.9678
30	8.5734	10.2989	4.4443	5.2903

Figures 3.62-3.65 depict the results of the prediction in presence of the same level of measurement noise with the standard deviation of 5. Table 3.21 shows the mean and the standard deviation of the prediction error for different number of steps ahead in presence of measurement noise with the standard deviation of 5.

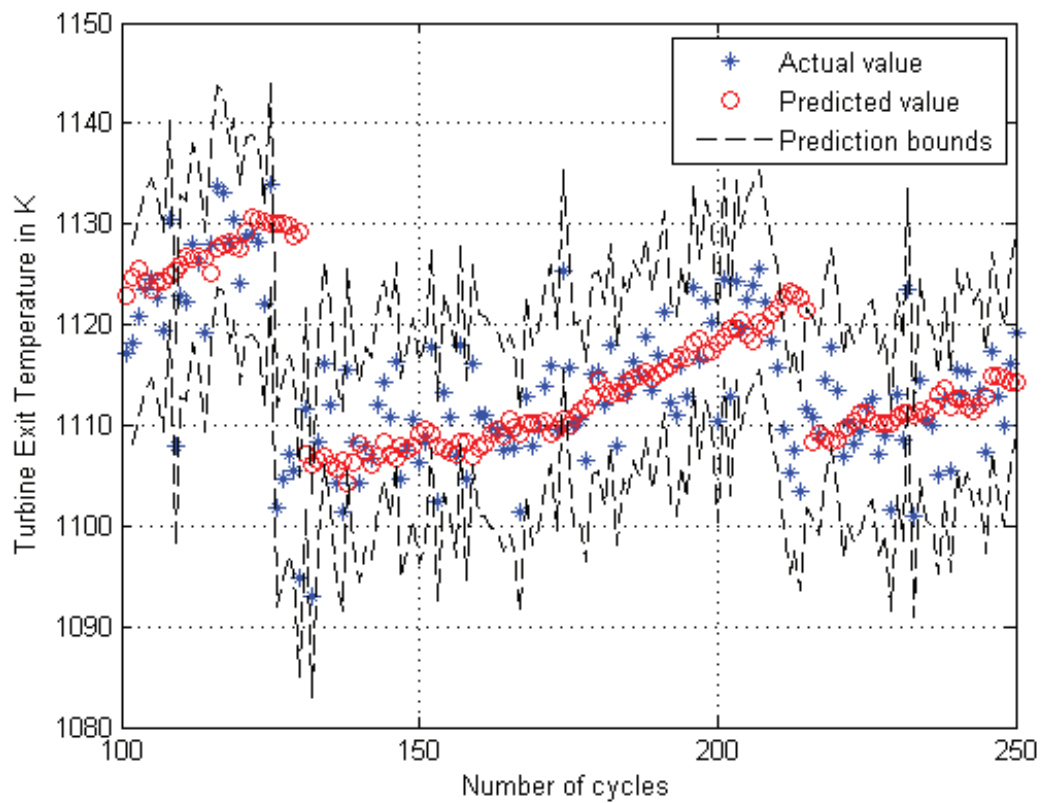


Figure 3.62: Five step ahead turbine temperature prediction results by using the bivariate VAR(6) model for the second scenario in presence of measurement noise with the standard deviation of 5.

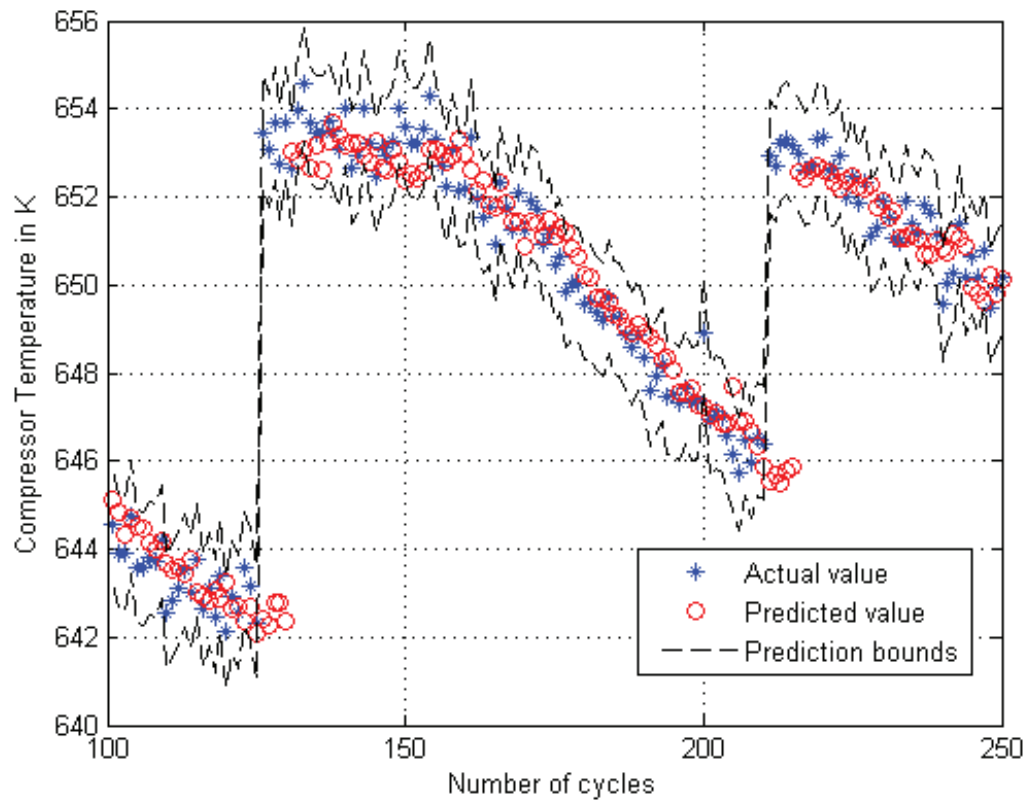


Figure 3.63: Five step ahead compressor temperature prediction results by using the bi-variate VAR(6) model for the second scenario in presence of measurement noise with the standard deviation of 5.

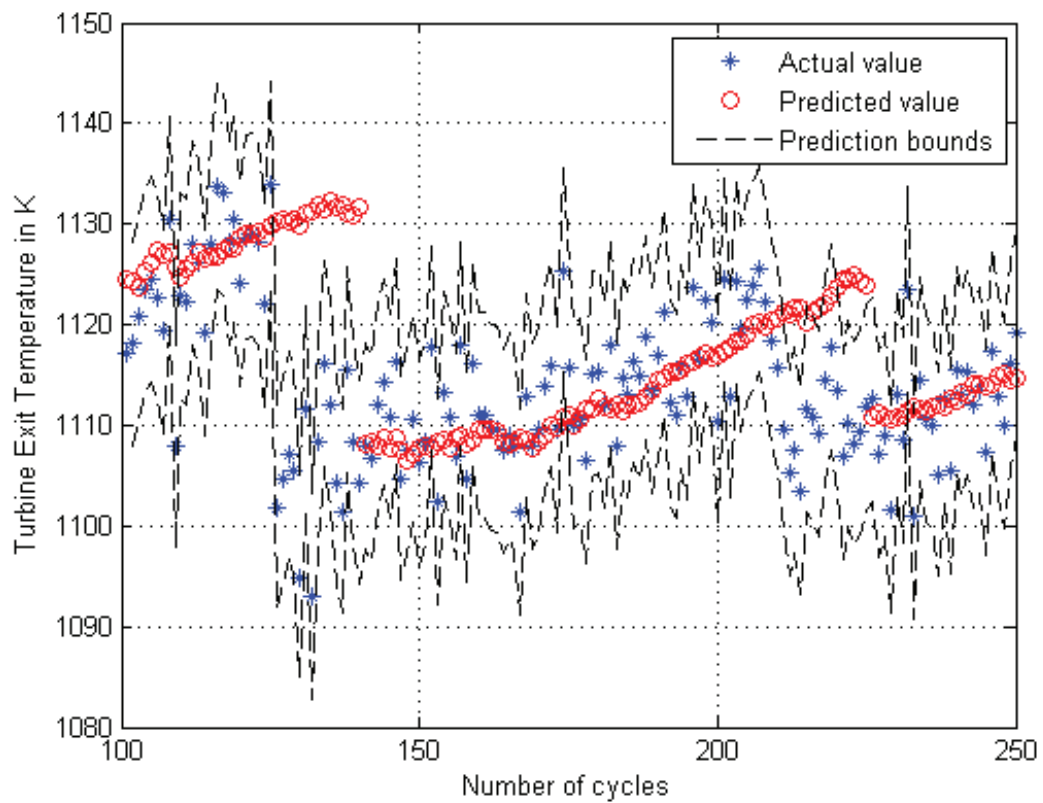


Figure 3.64: Fifteen step ahead turbine temperature prediction results by using the bivariate VAR(6) model for the second scenario in presence of measurement noise with the standard deviation of 5.

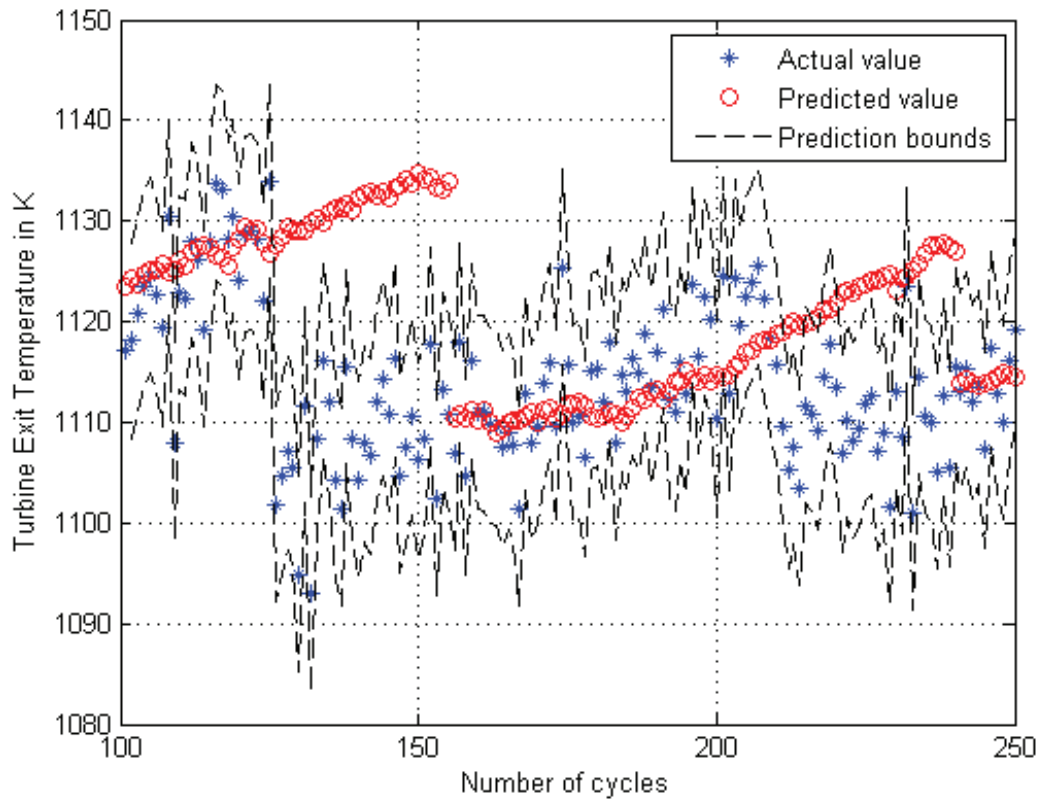


Figure 3.65: Thirty step ahead turbine temperature prediction results by using the bivariate VAR(6) model for the second scenario in presence of measurement noise with the standard deviation of 5.

Figure 3.54 shows how all the predicted values are completely within the defined boundaries and the accuracy of the prediction is satisfactory. At 125th and 210th flight cycles for 5 flight cycles, the predicted values are outside the boundaries. This happens because of the maintenance that was performed at the cycles 125 and 210 in the second scenario and the eroded components have been changed with the new ones. Clearly, the data before the maintenance action is not sufficient to allow for a reliable prediction subsequent to this action. Figures 3.58 and 3.62 depict the same scenario in presence of the measurement noise with standard deviation of 2 and 5 for five steps ahead. Despite the high level of the measurement noise the predicted values are completely within the boundaries and the

Table 3.21: Mean and standard deviation of the prediction errors for the VAR model for the second scenario in presence of measurement noise with the standard deviation of 5.

Number of steps ahead	Turbine temperature		Compressor temperature	
	Mean	Standard deviation	Mean	Standard deviation
3	4.5991	6.4320	0.8161	1.8782
5	5.0112	7.4119	1.1052	2.4194
10	5.6431	8.4561	1.8723	3.3960
15	6.7597	9.5686	4.0771	5.0997
20	7.9426	10.3890	3.1389	4.5545
25	8.7901	10.8835	3.8049	4.9484
30	9.8141	11.3199	4.3949	5.2620

prediction accuracy is completely satisfactory. As the prediction horizon increases to fifteen, as seen in Figure 3.56 the predicted values are within the boundaries with acceptable accuracy. When the number of steps ahead reaches to 30, the prediction accuracy is not acceptable and there are many predicted values outside the boundaries. Figures 3.60 and 3.64 depict the predicted values for fifteen steps ahead under the measurement noise with the standard deviations of 2 and 5. The predicted values are within the boundaries and the prediction accuracy is good. As seen in Figures 3.61 and 3.65 many of the predicted values are outside of the boundaries and the prediction accuracy is not acceptable.

Scenario 3

The detailed description of the third scenario was presented in the section Case Study Scenarios. The standard deviation of the measurement noise is considered as 1. Figures 3.66-3.69 depict the results of the prediction in presence of the same level of measurement noise. The dashed lines show our upper and lower prediction intervals. The star points in the figure represent actual data values and the circle points indicate the predicted temperatures. Table 3.22 shows the mean and the standard deviation of the prediction errors for different number of steps ahead in presence of measurement noise with the standard deviation of 1.

Figures 3.70-3.73 depict the results of the prediction in presence of the same level of

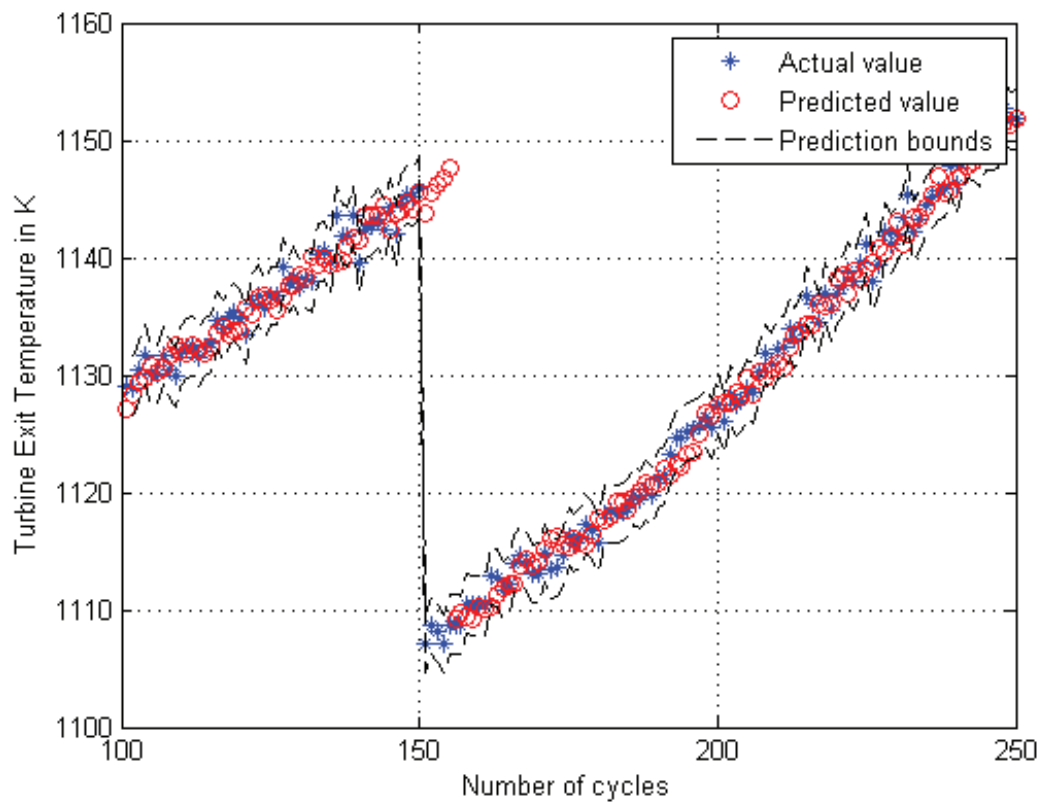


Figure 3.66: Five step ahead turbine temperature prediction results by using the bivariate VAR(6) model for the third scenario in presence of measurement noise with the standard deviation of 1.

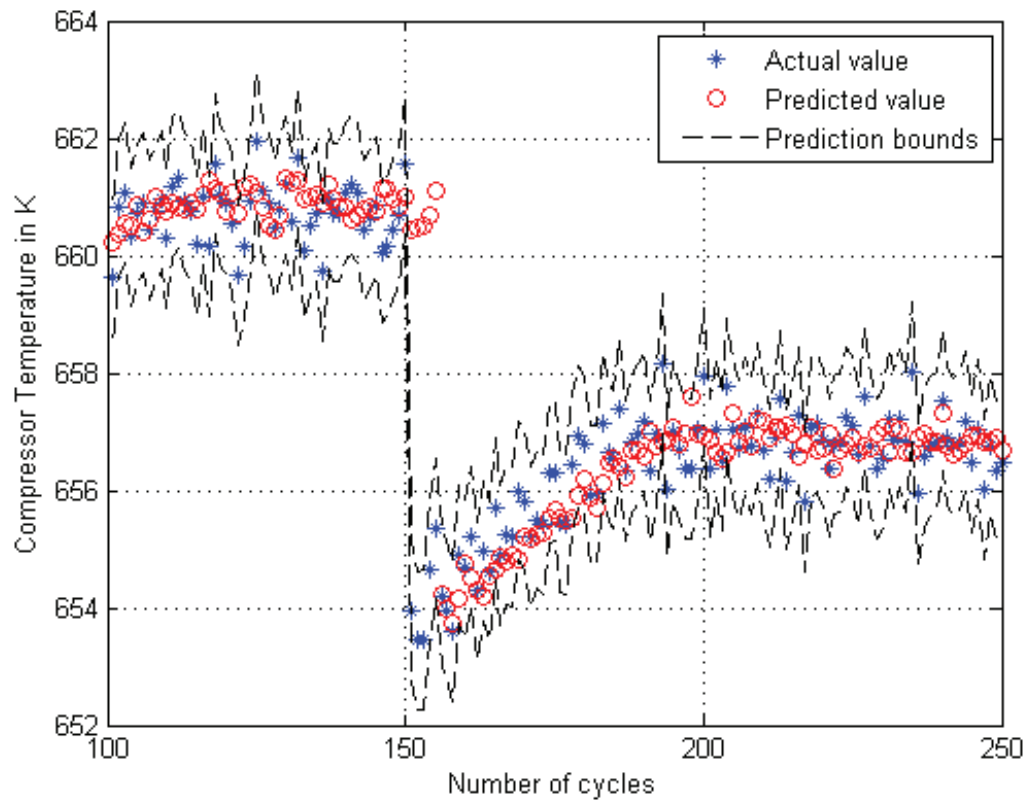


Figure 3.67: Five step ahead compressor temperature prediction results by using the bi-variate VAR(6) model for the third scenario in presence of measurement noise with the standard deviation of 1.

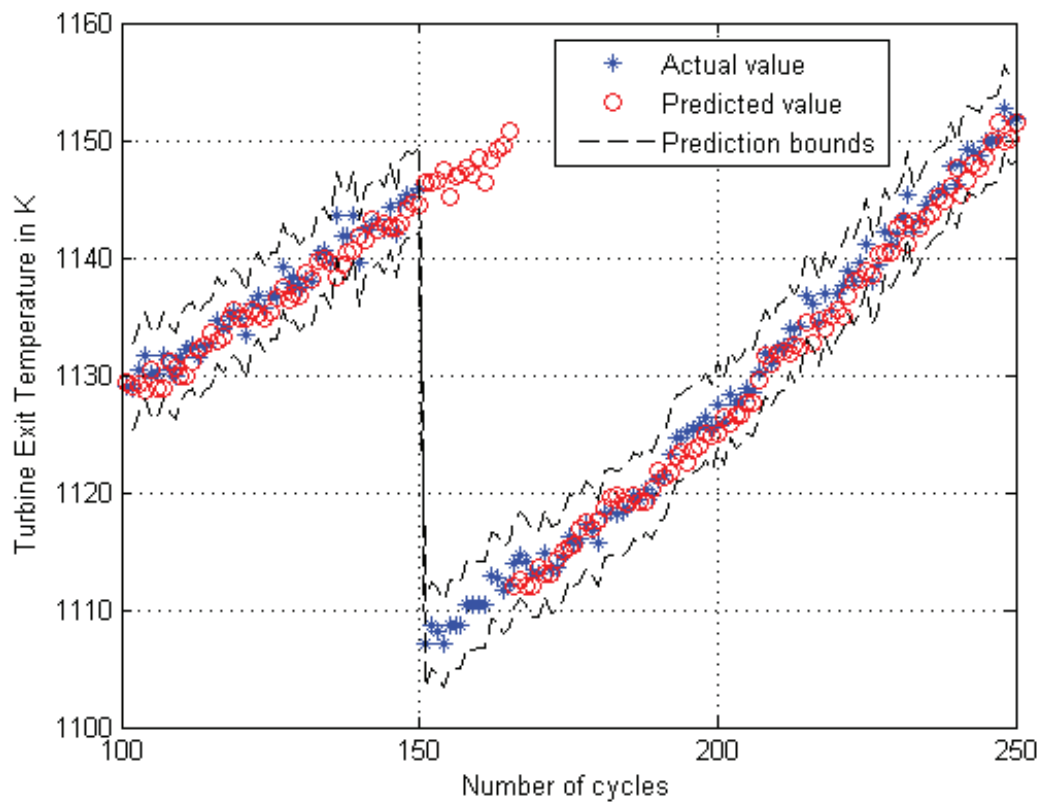


Figure 3.68: Fifteen step ahead turbine temperature prediction results by using the bivariate VAR(6) model for the third scenario in presence of measurement noise with the standard deviation of 1.

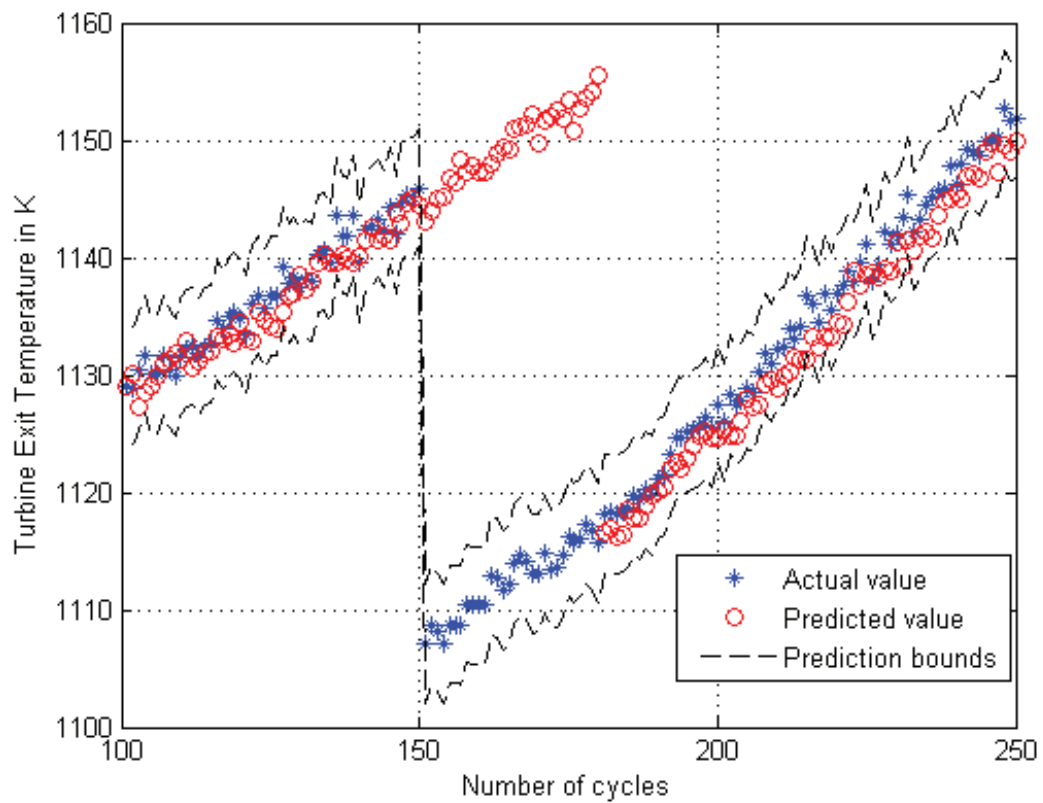


Figure 3.69: Thirty step ahead turbine temperature prediction results by using the bivariate VAR(6) model for the third scenario in presence of measurement noise with the standard deviation of 1.

Table 3.22: Mean and standard deviation of the prediction errors for the VAR model for the third scenario in presence of measurement noise with the standard deviation of 1.

Number of steps ahead	Turbine temperature		Compressor temperature	
	Mean	Standard deviation	Mean	Standard deviation
3	1.6645	5.5288	0.5561	1.1305
5	2.2883	7.0135	0.6183	1.2922
10	3.5866	9.6792	0.9352	1.8238
15	4.8393	11.6567	1.1934	2.1362
20	6.1417	13.1343	1.4363	2.4041
25	7.4556	14.5035	1.6639	2.6296
30	8.8546	15.6309	1.8733	2.7872

Table 3.23: Mean and standard deviation of the prediction errors for the VAR model for the third scenario in presence of measurement noise with the standard deviation of 2.

Number of steps ahead	Turbine temperature		Compressor temperature	
	Mean	Standard deviation	Mean	Standard deviation
3	2.5578	5.5233	0.5650	1.1230
5	3.0537	6.8401	0.6253	1.2863
10	4.2235	9.3211	0.9306	1.8142
15	5.5481	11.1124	1.1894	2.1245
20	6.8053	12.6884	1.4273	2.3923
25	7.9559	14.0237	1.6652	2.6247
30	9.2560	15.1058	1.8800	2.7799

measurement noise with the standard deviation of 2. Table 3.23 shows the mean and the standard deviation of the prediction error for different number of steps ahead in presence of measurement noise with the standard deviation of 2.

Figures 3.74-3.77 depict the prediction results in presence of the same level of measurement noise with the standard deviation of 5. Table 3.24 shows the mean and the standard deviation of the prediction error for different number of steps ahead in presence of measurement noise with the standard deviation of 5.

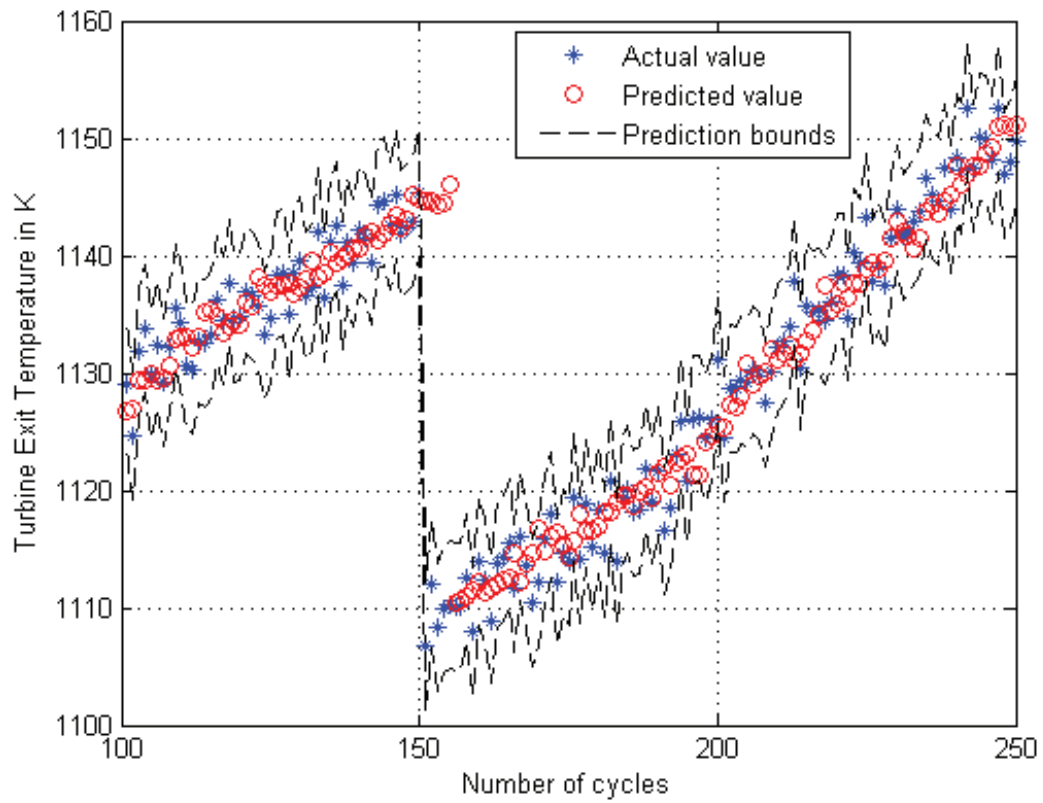


Figure 3.70: Five step ahead turbine temperature prediction results by using the bivariate VAR(6) model for the third scenario in presence of measurement noise with the standard deviation of 2.

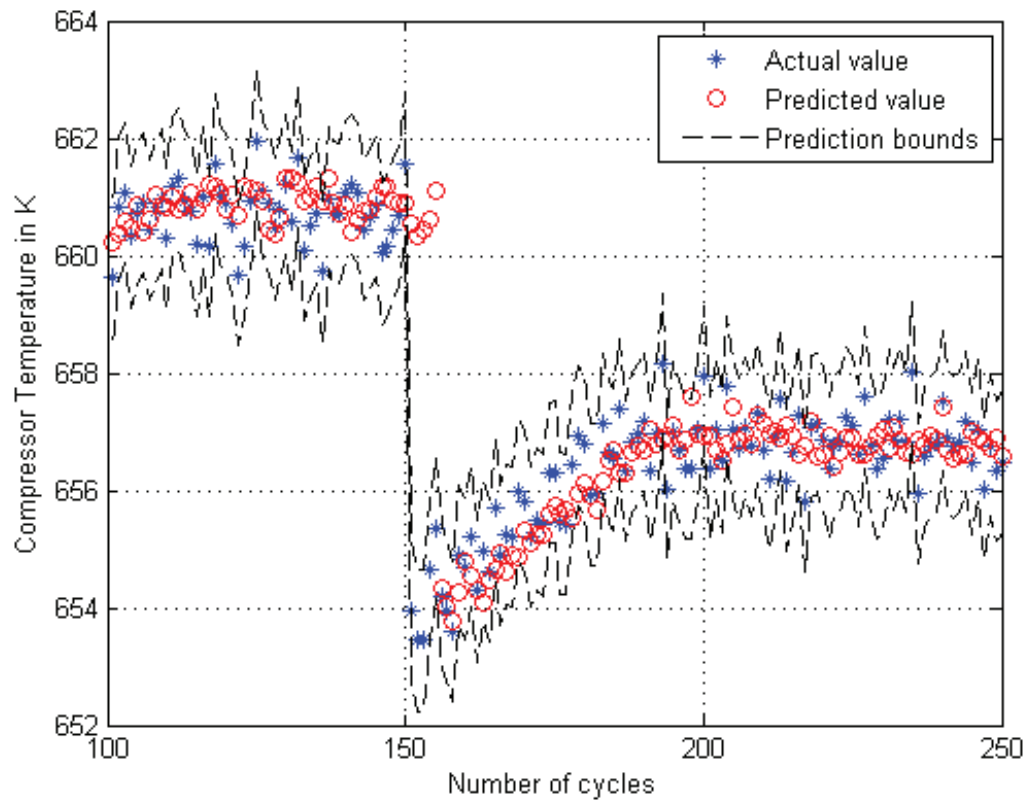


Figure 3.71: Five step ahead compressor temperature prediction results by using the bi-variate VAR(6) model for the third scenario in presence of measurement noise with the standard deviation of 2.

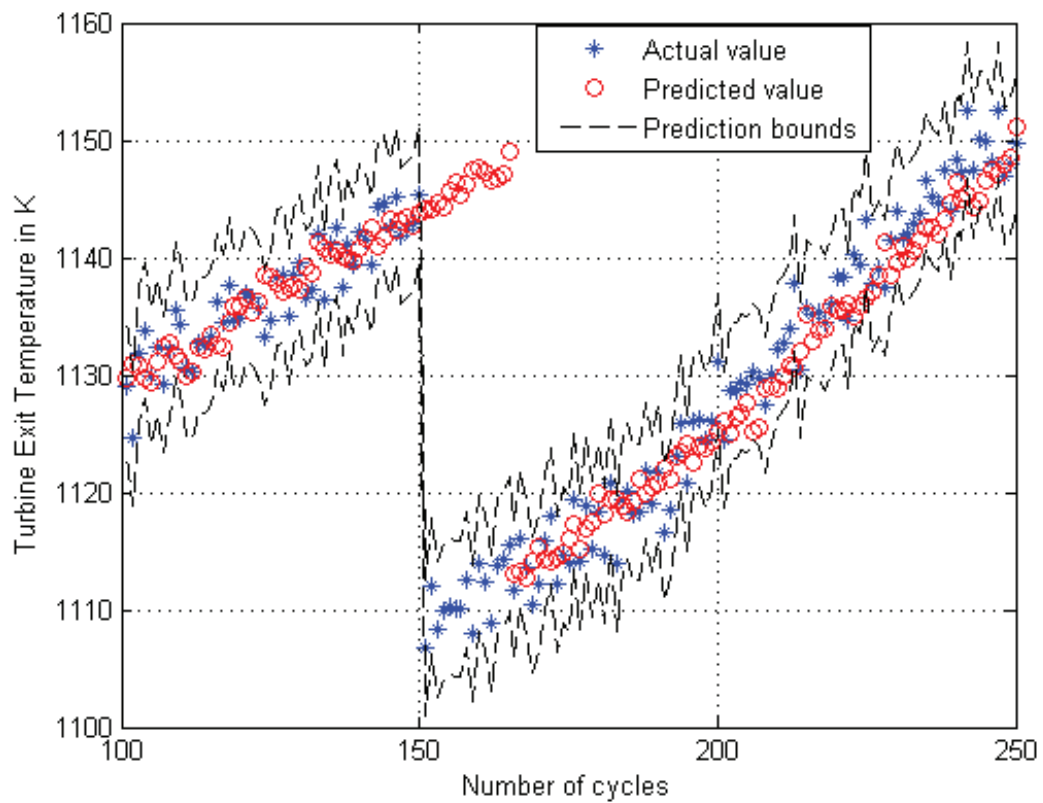


Figure 3.72: Fifteen step ahead turbine temperature prediction results by using the bivariate VAR(6) model for the third scenario in presence of measurement noise with the standard deviation of 2.

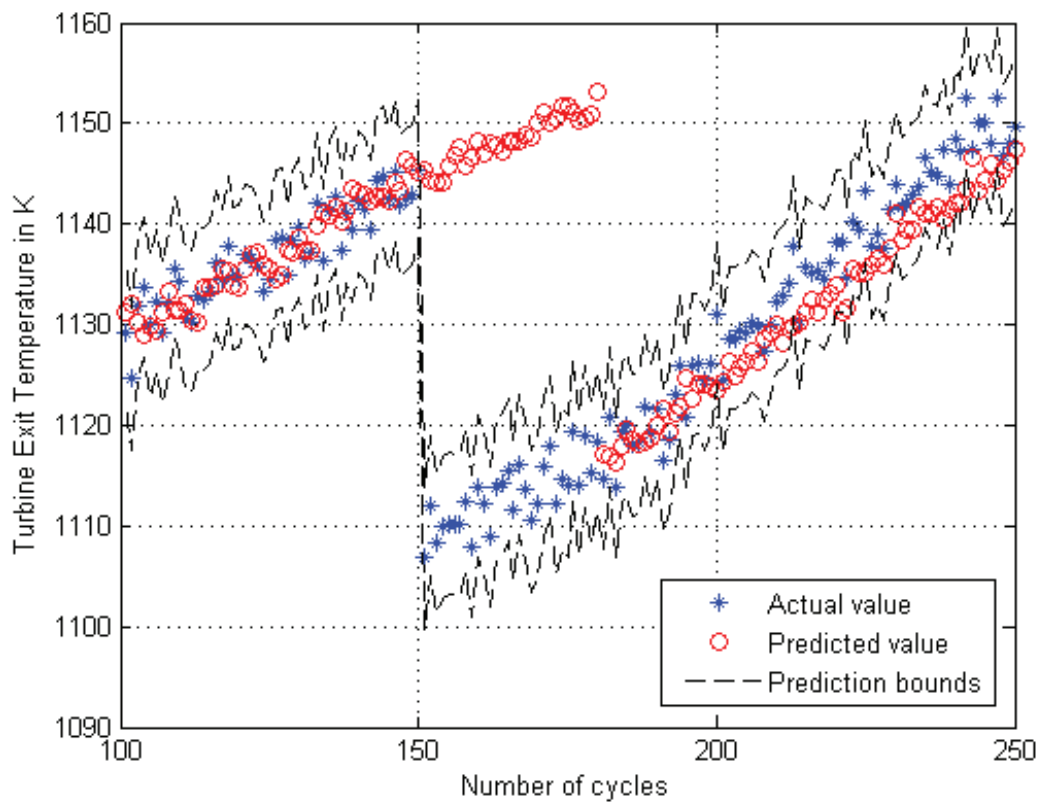


Figure 3.73: Thirty step ahead turbine temperature prediction results by using the bivariate VAR(6) model for the third scenario in presence of measurement noise with the standard deviation of 2.

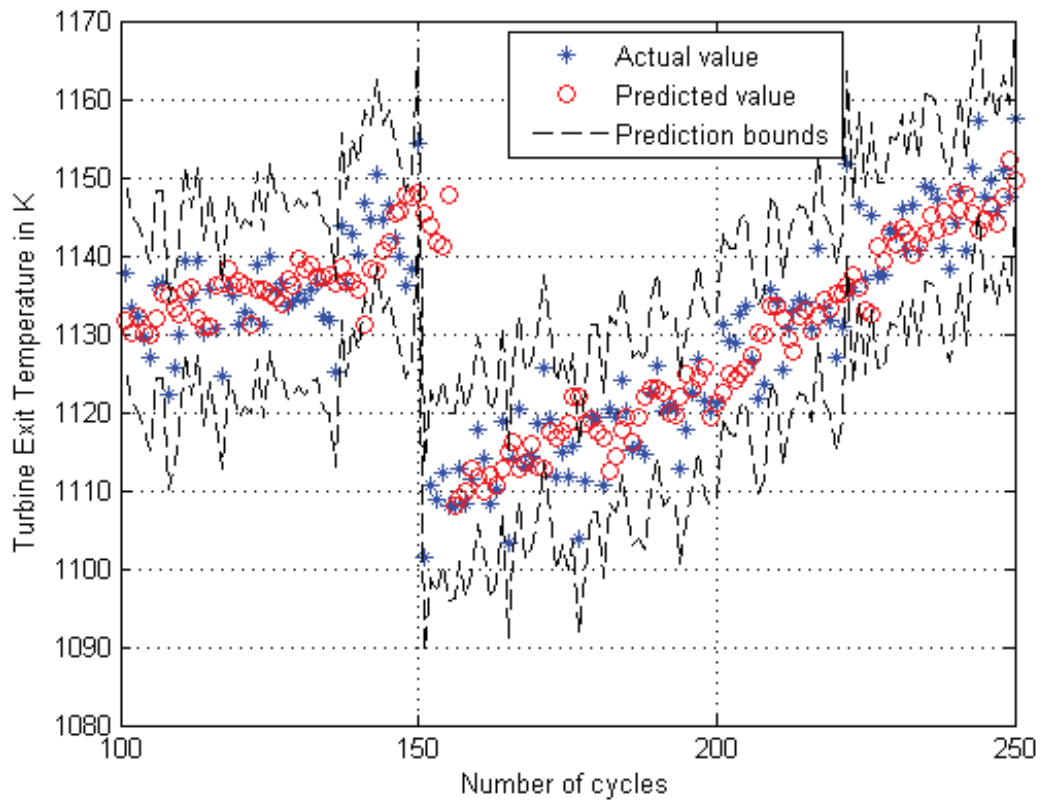


Figure 3.74: Five step ahead turbine temperature prediction results by using the bivariate VAR(6) model for the third scenario in presence of measurement noise with the standard deviation of 5.

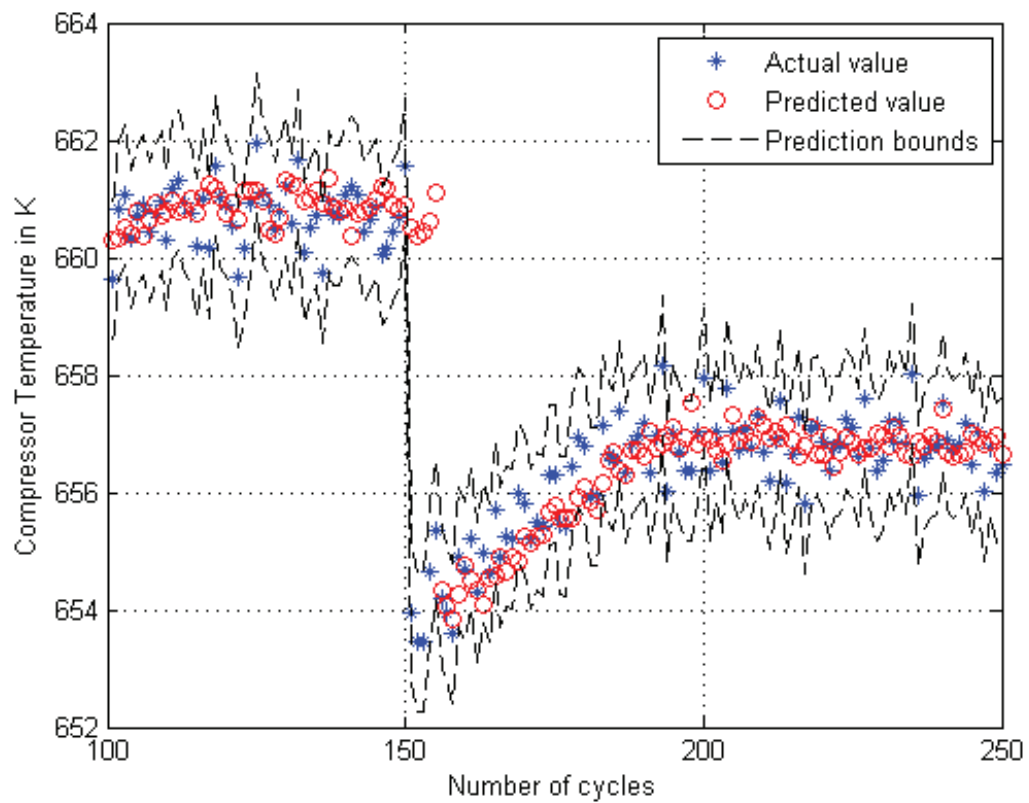


Figure 3.75: Five step ahead compressor temperature prediction results by using the bi-variate VAR(6) model for the third scenario in presence of measurement noise with the standard deviation of 5.

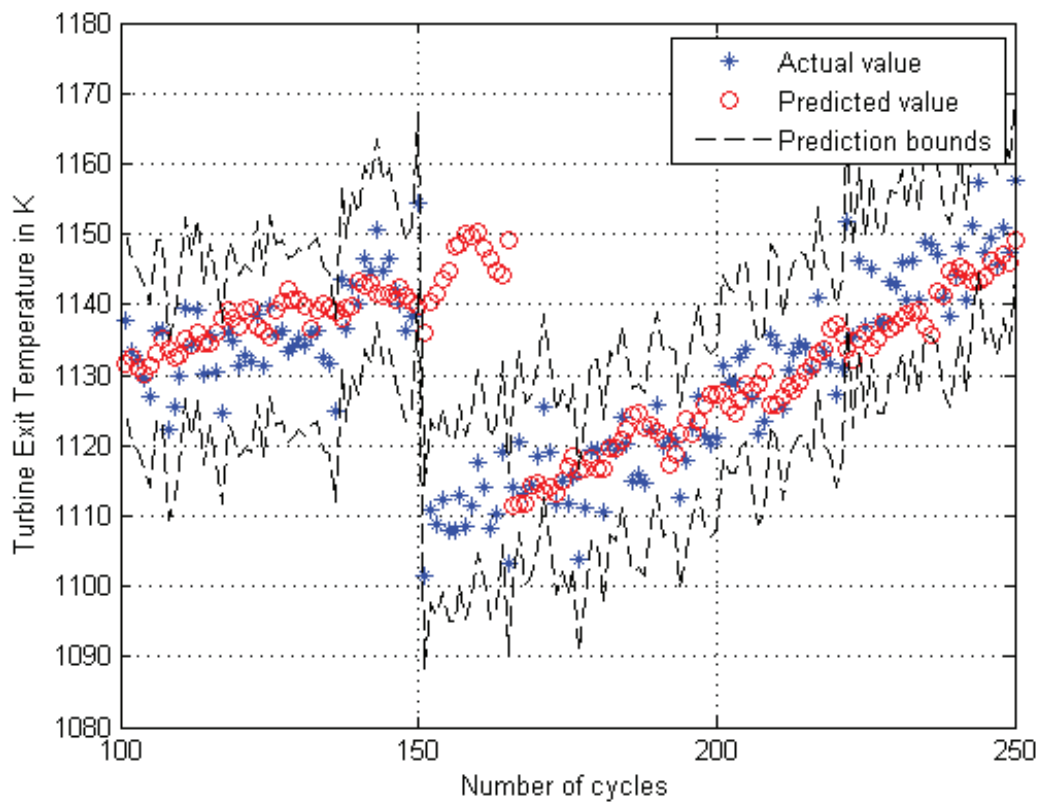


Figure 3.76: Fifteen step ahead turbine temperature prediction results by using the bivariate VAR(6) model for the third scenario in presence of measurement noise with the standard deviation of 5.

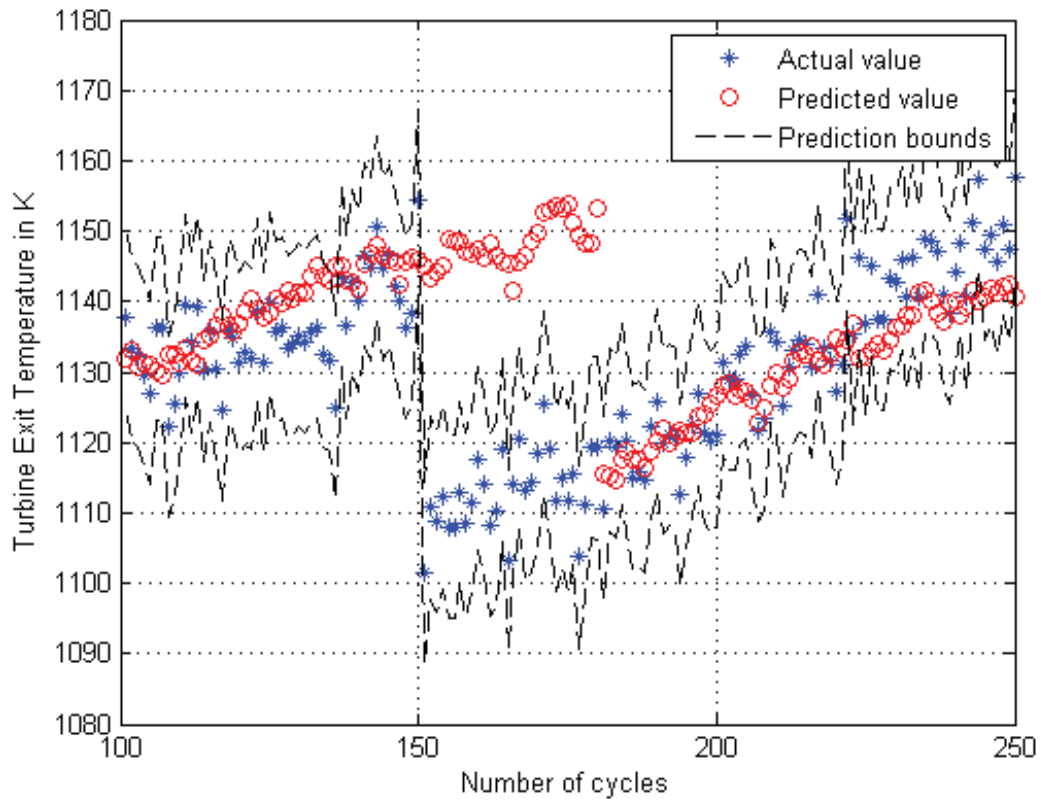


Figure 3.77: Thirty step ahead turbine temperature prediction results by using the bivariate VAR(6) model for the third scenario in presence of measurement noise with the standard deviation of 5.

Figures 3.66, 3.70 and 3.74 demonstrate how all the predicted values are completely within the defined boundaries and the accuracy of the prediction is satisfactory with all the three noise levels for the five steps ahead. At 150th flight cycle for 5 flight cycles, the predicted values are outside the boundaries. This happens because of the maintenance that was performed at the cycle 150 in the third scenario and the compressor got washed and the turbine eroded blades were changed. Clearly, the data before the maintenance action is not sufficient to allow for a reliable prediction subsequent to this action. As seen in Figures 3.68 and 3.69 as opposed to the ARIMA model, all the predicted values for both the 15 and 30 number of steps ahead are within the boundaries and the accuracy is satisfactory. The same superiority is observed for the higher level of noise for the third scenario.

Table 3.24: Mean and standard deviation of the prediction errors for the VAR model for the third scenario in presence of measurement noise with the standard deviation of 5.

Number of steps ahead	Turbine temperature		Compressor temperature	
	Mean	Standard deviation	Mean	Standard deviation
3	5.2095	7.5972	0.5690	1.1281
5	5.6308	8.7208	0.6208	1.2847
10	6.5119	10.8720	0.9298	1.8112
15	7.9286	12.3199	1.1881	2.1288
20	8.9548	13.2670	1.4176	2.3964
25	9.9981	14.4545	1.6510	2.6221
30	11.1494	15.7134	1.8639	2.7771

3.5 Comparison of VAR and ARIMA Models

In this chapter, in order to generate data from the engine Simulink model, an EPR controller has been designed. Three different scenarios are considered:

- Scenario 1 including compressor fouling with different severities.
- Scenario 2 including turbine erosion with different severities.
- Scenario 3 including both compressor fouling and turbine erosion with different severities.

For three different levels of measurement noise (low, medium and high) time-series data are generated. In order to select the order of ARIMA and VAR models based on Monte Carlo simulation approach for each different model AIC, BIC, mean and standard deviation of the prediction errors have been computed and are presented in Tables 3.2 and 3.5. ARIMA(4,5) and VAR(6) were selected based on the derived results.

The selected ARIMA and VAR models have been applied to time-series generated for the above mentioned scenarios and noise levels. For each time-series different numbers of step ahead prediction horizons are considered and the qualitative results are presented in Figures 3.12-3.77 and the quantitative results are presented in Tables 3.7-3.24.

Based on the outcome of the simulations and in order to show the effectiveness of the two presented methods the mean and the standard deviation of the prediction errors are evaluated. In the first scenario, the performance of VAR model is better than the ARIMA model except in presence of the low noise level and higher number of steps ahead. In the second scenario, for all noise levels the VAR model performance is better than ARIMA model in lower number of steps ahead. On the contrary, for all noise levels the ARIMA model performance is better than the VAR model in higher numbers of steps ahead. In the third scenario for all of the cases VAR model performance is better than the ARIMA model.

In general, the performance of the VAR model is better than the ARIMA model. However, for the scenarios 1 and 2 in which only the fouling or erosion is considered, the ARIMA model performance is better than the VAR model in predicting higher steps ahead. This result is reasonable as the performance of simpler models for longer prediction horizons and simpler scenarios is better than more complex models. However, the precision of the prediction for smaller prediction horizons and more complex scenarios is poor.

In order to benefit from the long term prediction along with high precision for complex scenarios, we are proposing a hybrid fuzzy ARIMA model which will be presented in the next chapter.

3.6 Summary

In this chapter, first the specifications of the designed controller for the gas turbine engine model have been explained. Next, ARIMA and VAR model selection procedures based on AIC and BIC criteria were given. The case study scenarios including fouling and erosion degradations are presented in detail and this section was followed by the simulation results showing the prediction performance of these methods.

At the end of this chapter the effectiveness of the engine degradation prognostics (prediction) performance of the proposed VAR model as compared to the ARIMA method was investigated. Qualitative results are shown in the figures of this chapter by depicting that the predicted values are within the defined boundaries based on the normal theory with a given confidence level of 95%. Defining the upper and lower bounds instead of emphasizing on the exact predicted values are more realistic. Quantitative results of the prediction namely, mean and standard deviation of the prediction errors are given in tables for both ARIMA and VAR models for all the scenarios. From both qualitative and quantitative perspectives VAR method achieves better results in complex scenarios including both erosion and fouling degradations. The VAR method has been developed by the author in [162].

Chapter 4

Hybrid Fuzzy ARIMA Approach

In this chapter a single spool gas turbine engine performance degradation trend based on another novel approach namely, hybrid fuzzy autoregressive integrated moving average (ARIMA) is proposed. In the previous chapter the ARIMA and VAR methods were applied to perform the engine performance prediction under different scenarios including fouling and erosion and their combinations. In this chapter, in order to improve the prediction effectiveness a hybrid fuzzy ARIMA approach is introduced by considering the turbine exit temperature (TET) and the spool speed (N) as the measuring parameters of the engine. Three scenarios are considered to demonstrate the effectiveness of the proposed method. The results show a better performance of the hybrid method in terms of mean and standard deviation of the prediction errors. The simulation results are followed by a comparison of the hybrid fuzzy ARIMA model with the VAR and ARIMA models.

4.1 Hybrid Fuzzy ARIMA Modeling

In the ARIMA method, one of the system measurements can be used for prediction purposes. Since the dynamical model of the engine is nonlinear, using ARIMA method results in poor prediction accuracy of the turbine temperature. Therefore, using the VAR method,

that can use more than one measurement of the system boosts the prediction performance and the results presented in [162] support this. In this chapter, a hybrid fuzzy approach is applied to fuse different measurements of the systems into a single one to use as ARIMA method input. To compare the performance of the proposed hybrid fuzzy ARIMA method and that of the VAR method, three different scenarios are considered and the results of the numerical simulations are presented.

Towards this end, the turbine exit temperature denoted by T and the spool speed denoted by N of the engine are fused by employing the fuzzy inference engine. The fuzzy inference engine used in this work consists of two Takagi-Sugeno (TS) fuzzy functions [156]. One named, $\alpha(N)$, employs 14 rules and the other one, named $\beta(N)$ uses 18 rules which are adjusted based on the simulation data. The fused data denoted by f is computed by the following equation:

$$f = \alpha(N) \left(\frac{T}{\beta(N)} - 1 \right) \quad (4.1)$$

The time-series resulting from the fused data is denoted by f_t that is fed to an ARIMA model for prediction purposes. In the ARIMA(p,q) model, p and q are set to 4 and 5, respectively. The coefficients of the ARIMA model are determined by the recursive prediction error method. More information about the details of this identification method is available in [138].

For the prediction step, one determines $\hat{f}_t(m)$ by obtaining f_{t+m} given $f_t, f_{t-1}, \dots, f_{t-h}$ where m and h denote the step-ahead lead time and prediction window respectively. In the other words:

$$\hat{f}_t(m) = E[f_{t+m} | f_t, f_{t-1}, \dots, f_{t-h}] \quad (4.2)$$

In every prediction iteration the prediction error E_t is computed by using equation (4.3),

$$E_t = \hat{f}_{(t-m)}(m) - f_t \quad (4.3)$$

and the prediction horizon h is increased by one so that we can get more benefit from the longer number of data as we go forward in the prediction step. Moreover, the moving average of the prediction errors denoted by Th is calculated for a window size of $3m$ at each iteration. In order to improve the prediction performance in this work we reset the value of h to the value of m whenever the prediction error exceeds the value of Th as an adaptive threshold for m consequent times.

After predicting \hat{f}_t , using the following equation the prediction values of the turbine temperature T are reconstructed as:

$$\hat{T}_t(m) = \beta(N) \left(\frac{\hat{f}_t(m)}{\alpha(N)} + 1 \right) \quad (4.4)$$

As mentioned in the previous chapter the fuzzy logic system is a powerful tool for nonlinear mapping of an input vector of a feature of interest into a scalar output [154]. Due to heuristic nature of the fuzzy logic, one can use it to deal with systems with unknown dynamical model, measurement noise, etc. A fuzzy system consists of fuzzy rules, fuzzifier, inference engine, defuzzifier. There are two main types of defuzzifier, Mamdani [9] and Takagi-Sugeno (TS) [156]. Depending on the application, one may employ one of these systems. For example, for classification and controller design problems Mamdani systems are widely used due to their intuitive nature and their capability to deal with multiple output systems. On the other hand, TS systems are more flexible than Mamdani systems which allow several parameters in the output as the output is expressed as a mathematical function that can consist of several inputs and parameters. Moreover, TS systems are more flexible than Mamdani systems in terms of less complexity of the defuzzification process which makes TS systems computationally faster and more efficient than Mamdani systems. Since in this thesis we are dealing with quantitative data and given that TS fuzzy systems are more suitable for mathematical analysis [157, 8], we choose TS method to implement the fuzzy inference engine.

Fuzzy rules consist of several IF-THEN statements that are usually provided by the expert or numerical data. In this thesis we used 14 rules for α and 18 rules for β which have the following format:

$$\text{Rule } i : \quad \text{if } (N \in M_i) \text{ then } y_i = a_i(N - N_i) + b_i$$

where the fuzzy set M_i and parameters a_i and b_i should be adjusted by using numerical simulation data. By increasing the number of rules, one may achieve more accurate results. However, this increase in the accuracy is achieved at the cost of increase in design complexity and computational time. In order to determine proper number of rules we employed different number of rules for both functions $\alpha(N)$ and $\beta(N)$ and evaluated the prediction results in terms of the mean and the standard deviation of prediction error. Table 4.1 shows these results in which it follows that by exceeding the number of rules from 14 and 18 the result is not improved. Therefore, we have selected 14 and 18 rules for the functions $\alpha(N)$ and $\beta(N)$ in this chapter.

Table 4.1: Mean and standard deviation of the prediction errors for the hybrid fuzzy ARIMA model for 10 steps ahead for different number of fuzzy rules.

Number of rules for $\alpha(N)$	Number of rules for $\beta(N)$	Mean	Standard deviation
6	8	2.8889	8.4541
8	8	2.8881	8.4507
8	10	2.8672	8.3604
10	10	2.8752	8.3933
10	12	2.8593	8.3246
12	12	2.8598	8.3265
12	14	2.8478	8.2748
14	14	2.8420	8.2506
14	16	2.8115	8.0862
14	18	2.8055	8.0850
16	18	2.8054	8.0848
16	20	2.8054	8.0830

There are different types of membership functions that one may use such as triangular, trapezoidal, piece-wise linear or Gaussian functions. Different membership functions such

as triangular, square, step could be considered as special cases of the trapezoidal function and noting that trapezoidal membership functions are easy to implement and modification and fast in computing, therefore, we used trapezoidal function in this thesis. In order to obtain the numerical values of $\alpha(N)$ and $\beta(N)$, first for each rule the spool speed is fuzzified by using the trapezoidal membership functions $\mu(M_i)$. These membership functions are depicted in Figures 4.1 and 4.2, respectively. In the next step for each fuzzy rule the value of the associated function is computed and weighted based on the degree of membership of the fuzzy rule. Finally, in defuzzification step the weighted average of the associated function values are evaluated [156].

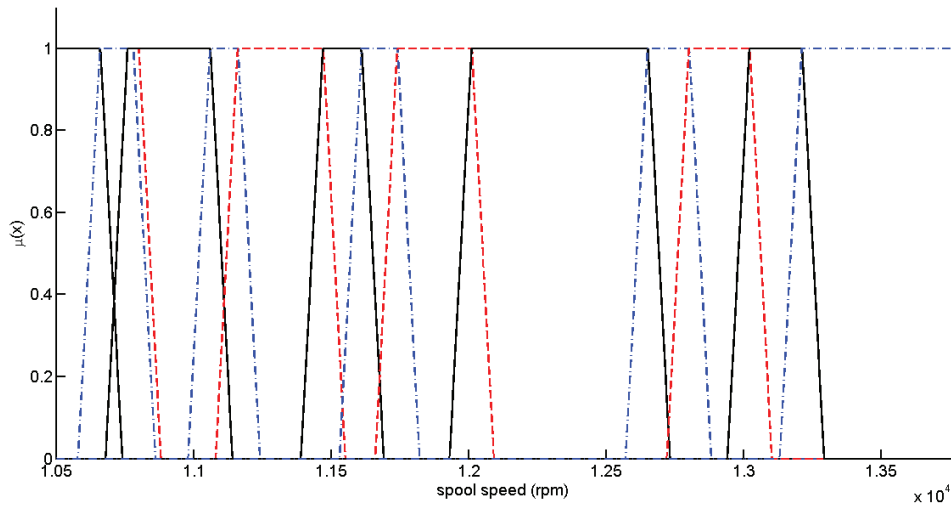


Figure 4.1: Trapezoidal functions defining the degree of memberships for $\alpha(N)$.

The fuzzy rules of $\beta(N)$ are defined by using the engine turbine temperature under healthy condition. We start this procedure by setting N_1 to the lowest acceptable spool speed and simulate the healthy engine for several times and set b_1 to the average value of turbine temperatures. In the next step we perform simulations to obtain the average turbine temperature for a spool speed N slightly larger than N_1 and try to adjust a_1 such that $y_1 = a_1(N - N_1) + b_1$ be close to the turbine temperature average value as much as possible. We use the average of the turbine temperature for the sake of minimizing the

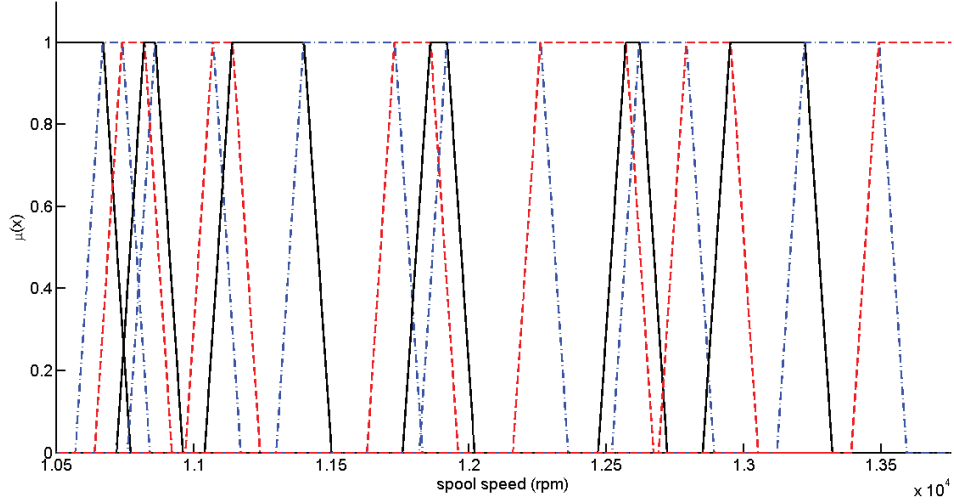


Figure 4.2: Trapezoidal functions defining the degree of memberships for $\beta(N)$.

effects of measurement noise. If the difference between y_1 and the average value of the turbine temperature is small enough we repeat this step with a slightly larger spool speed until selecting a proper value for a_1 is not possible longer.

At this stage we select N_2 approximately as $2N - N_1$ and adjust b_2 and a_2 by following along the same steps and repeat the procedure until at step n the value of $2N - N_n$ is larger than the maximum acceptable spool speed. After selecting all N_i, a_i and b_i for $i = 1, \dots, n$ we set the parameters of trapezoidal membership functions μ_{M_i} such that $\mu_{M_i}(N_i) = 1$ for $i = 1, \dots, n$, $\mu_{M_i}(\frac{N_i + N_{i+1}}{2}) = \frac{1}{2}$ for $i = 1, \dots, n - 1$ and $\mu_{M_n}(N_{\max}) = 1$.

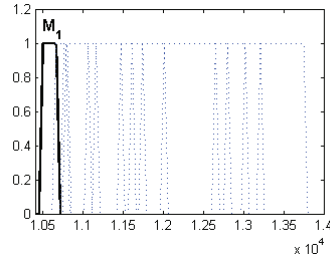
In the final step we adjust the slope of the trapezoidal edges of the membership functions such that for any spool speed in the acceptable range, $\beta(N)$ is close to the average of engine turbine temperature under healthy condition as much as possible. Similar approach is also employed to adjust the fuzzy rules of $\alpha(N)$. Towards this end, we consider a non-healthy model of the engine and start the procedure from the minimum acceptable spool speed of the engine. At each step the average turbine temperature denoted by T_i from repeated simulation results are determined and we set b_i such that $b_i \left(\frac{T_i}{\beta(N_i)} - 1 \right)$ is constant for all N_i .

We employ the average of the turbine temperature by repeating the simulations for the sake of minimizing the effects of measurement noise. Next, we choose a slightly larger spool speed and adjust a_i as much as possible. Then, we choose $2N - N_i$ as N_{i+1} for the next rule. Finally, we set the trapezoidal membership functions and adjust the slopes of trapezoids edges such that at any spool speed N in the acceptable range the value of $\alpha(N) \left(\frac{T}{\beta(N)} - 1 \right)$ is the same constant.

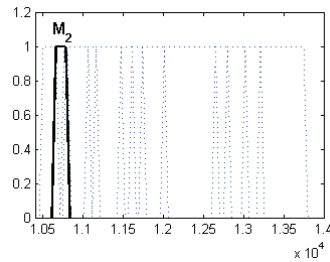
By applying the above procedure we set the fuzzy rules that are required to compute the value of functions $\alpha(N)$ and $\beta(N)$ as presented in Tables 4.2 and 4.3, respectively.

Table 4.2: Rule base of $\alpha(N)$

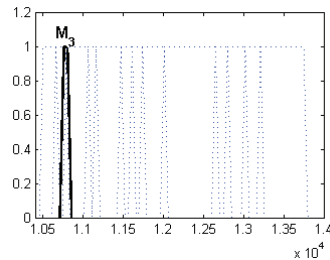
if $N \in M_1$ then $y = 1.1875e-4 N + 0.1771$



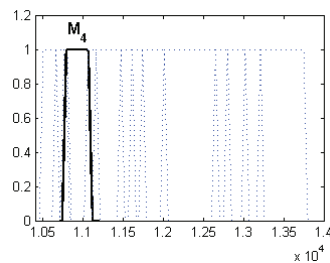
if $N \in M_2$ then $y = -5.8333e-5 N + 2.0648$



if $N \in M_3$ then $y = 1.2500e-4 N + 0.0870$



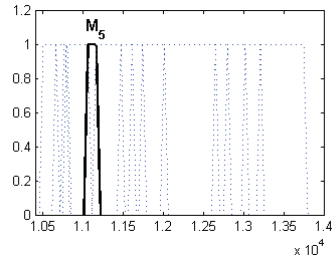
if $N \in M_4$ then $y = -2.3667e-4 N + 3.9785$



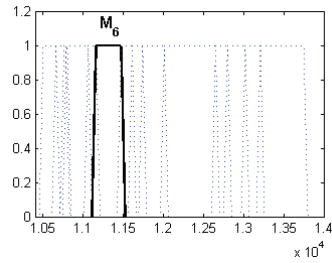
if $N \in M_5$ then $y = -4.6000e-4 N + 6.4486$

Continued on next page

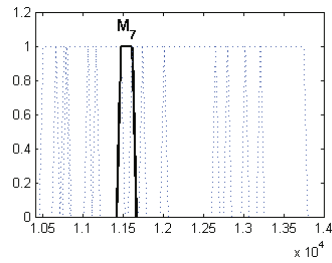
Table 4.2: Rule base of $\alpha(N)$



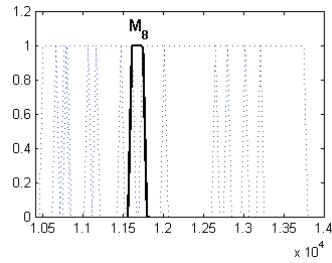
if $N \in M_5$ then $y = -1.7097e-4 N + 3.2230$



if $N \in M_6$ then $y = -4.7143e-4 N + 6.6693$



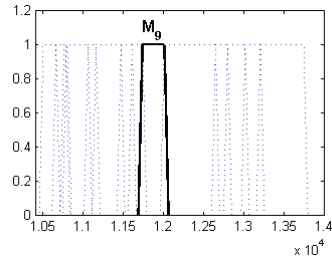
if $N \in M_7$ then $y = -1.6923e-4 N + 3.1608$



if $N \in M_8$ then $y = 4.4444e-5 N + 0.6522$

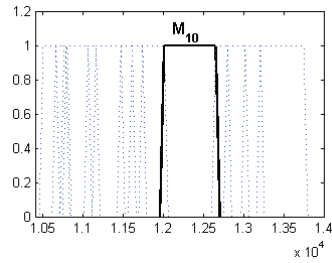
Continued on next page

Table 4.2: Rule base of $\alpha(N)$



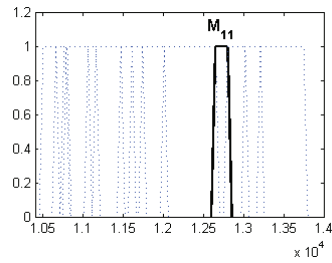
if $N \in M_{10}$

then $y = -1.0781e-4 N + 2.4808$



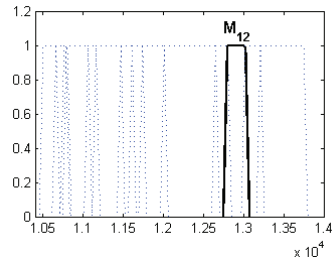
if $N \in M_{11}$

then $y = -6.6000e-4 N + 9.4660$



if $N \in M_{12}$

then $y = -9.4091e-5 N + 2.2224$

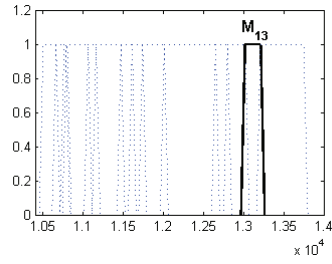


if $N \in M_{13}$

then $y = -1.7421e-4 N + 3.2655$

Continued on next page

Table 4.2: Rule base of $\alpha(N)$



if $N \in M_{14}$

then $y = -1.1648e-4 N + 2.5029$

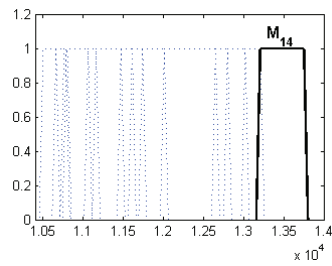
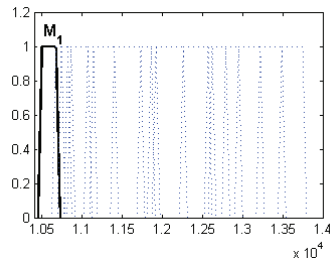


Table 4.3: Rule base of $\beta(N)$

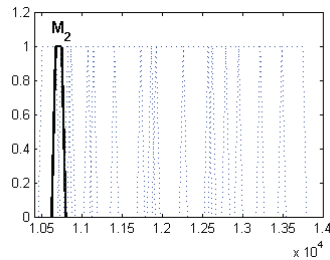
if $N \in M_1$

then $y = 0.1541 N - 993.4353$



if $N \in M_2$

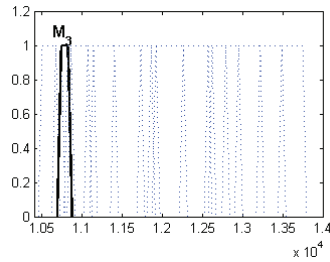
then $y = 0.2557 N - 2077.5$



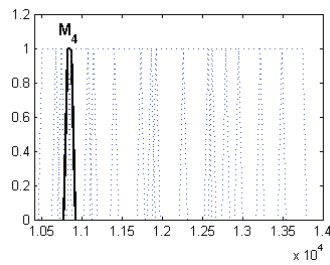
Continued on next page

Table 4.3: Rule base of $\beta(N)$

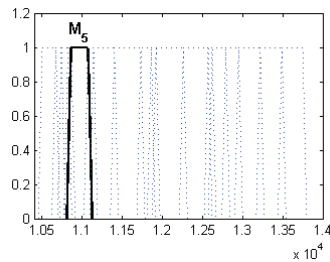
if $N \in M_3$ then $y = 0.2413 N - 1922.1$



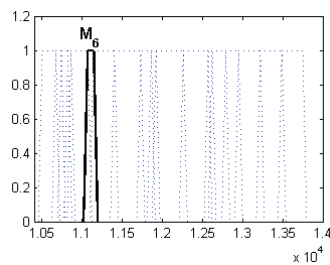
if $N \in M_4$ then $y = 0.1800 N - 12594$



if $N \in M_5$ then $y = 0.2067 N - 1549.0$



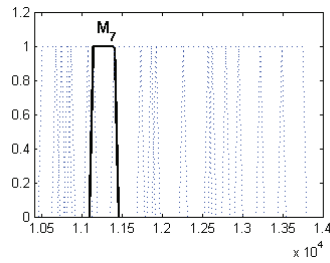
if $N \in M_6$ then $y = 0.3714 N - 3372.9$



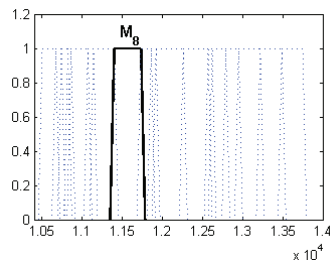
if $N \in M_7$ then $y = 0.1258 N - 636.2692$

Continued on next page

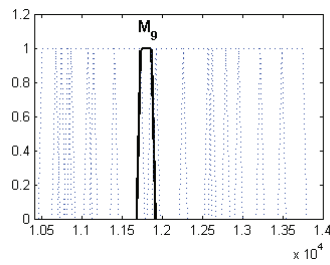
Table 4.3: Rule base of $\beta(N)$



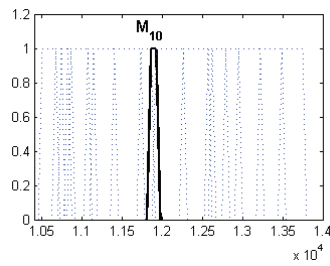
if $N \in M_8$ then $y = 0.0994 N - 335.5909$



if $N \in M_9$ then $y = 0.1662 N - 1118.7$



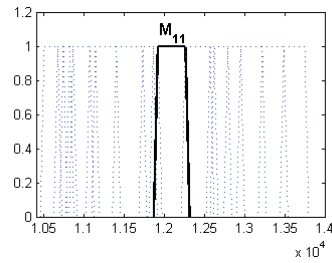
if $N \in M_{10}$ then $y = 0.1383 N - 788.7333$



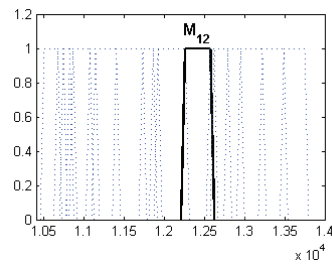
if $N \in M_{11}$ then $y = 0.1462 N - 882.2235$

Continued on next page

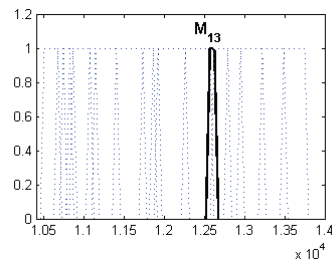
Table 4.3: Rule base of $\beta(N)$



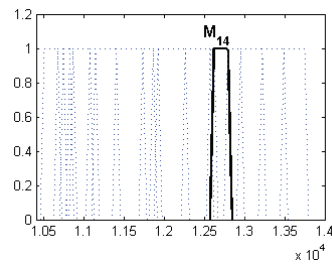
if $N \in M_{11}$ then $y=0.1619 N - 1075.4$



if $N \in M_{12}$ then $y= 0.1900 N - 1428.2$



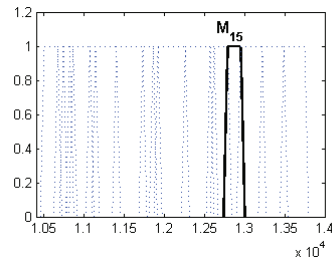
if $N \in M_{13}$ then $y=0.1782 N - 1279.7$



if $N \in M_{14}$ then $y=0.2256 N - 1885.8$

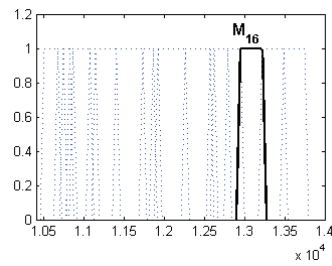
Continued on next page

Table 4.3: Rule base of $\beta(N)$



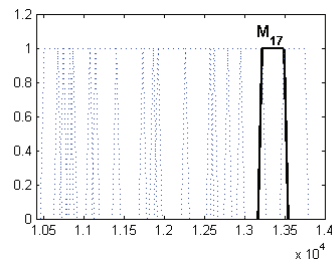
if $N \in M_{16}$

then $y=0.2296 N - 1937.7$



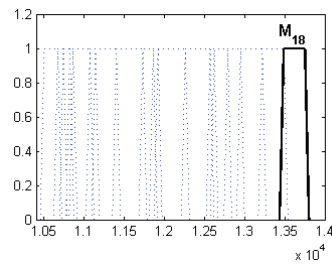
if $N \in M_{17}$

then $y=0.2963 N - 2819.0$



if $N \in M_{18}$

then $y=0.3346 N - 3336.0$



4.2 Case Study Scenarios

In order to compare the prediction performance of the hybrid fuzzy ARIMA method with that of the other methods, the dynamical model of a single spool turbojet engine presented in Naderi *et al.* [13] is used for numerical simulation purposes. In the following simulations the compressor fouling and the turbine erosion faults with different severities are injected to the numerical model at different flight numbers. The detailed description of the scenarios that are used in this chapter has been presented in the previous chapter in the section Case Study Scenarios.

4.3 Simulation Results

Scenario 1

The standard deviation of the measurement noise is considered as 1 (0.097 percent of the nominal value of the turbine temperature [13]). Figures 4.3-4.5 depict the results of the prediction in presence of the same level of measurement noise. The dashed lines show our upper and lower prediction intervals. The star points in the figure represent actual data values and the circle points indicate the predicted temperatures. Table 4.4 shows the mean and the standard deviation of the prediction errors for different number of steps ahead in presence of measurement noise with the standard deviation of 1.

In order to investigate the effect of measurement noise on the prediction results, each scenario has been repeated for different value of measurement noise. Figures 4.6-4.8 depict the results of the prediction in presence of the same level of measurement noise with the standard deviation of 2. Table 4.5 represents the mean and the standard deviation of the prediction errors for different number of steps ahead in presence of measurement noise with the standard deviation of 2.

Figures 4.9-4.11 depict the results of the prediction in presence of the same level of

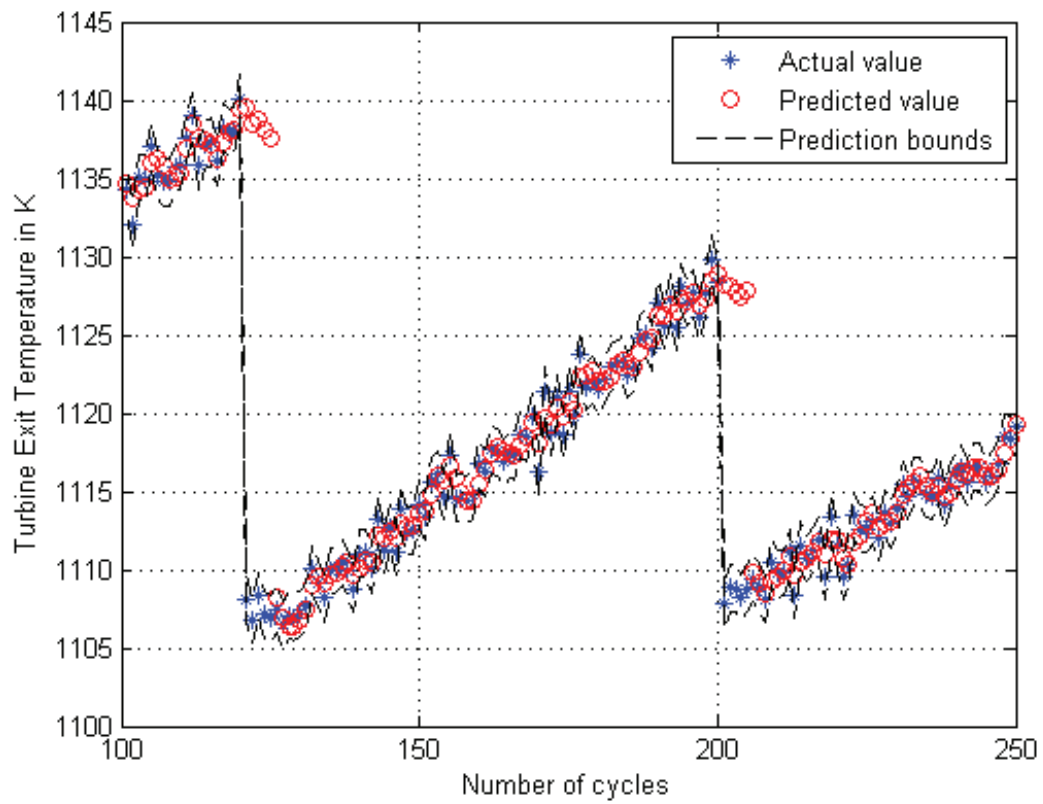


Figure 4.3: Five step ahead prediction results by using the hybrid fuzzy ARIMA(4,5) model for the first scenario in presence of measurement noise with the standard deviation of 1.

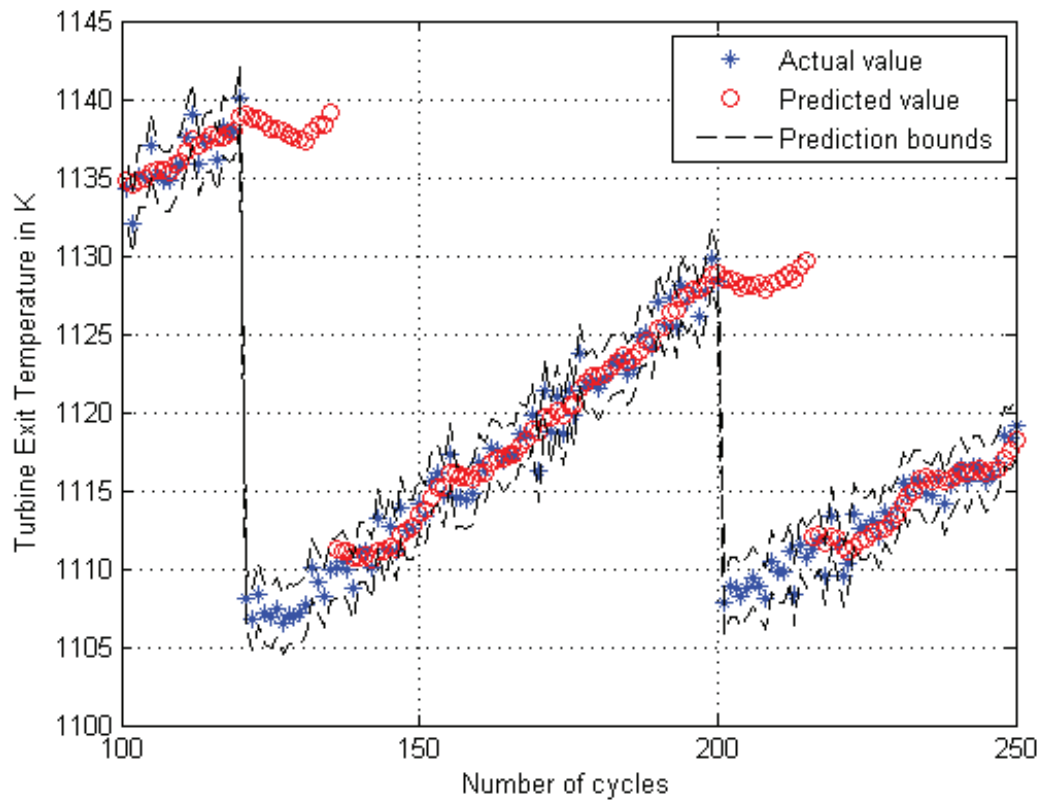


Figure 4.4: Fifteen step ahead prediction results by using the hybrid fuzzy ARIMA(4,5) model for the first scenario in presence of measurement noise with the standard deviation of 1.

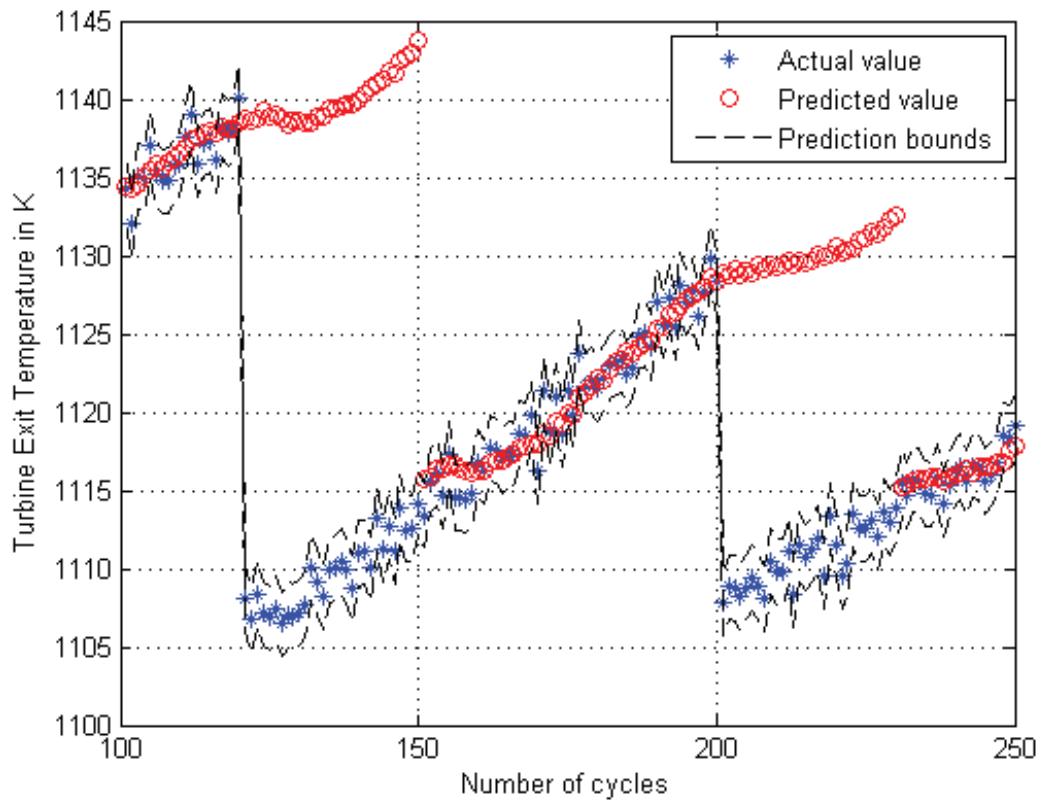


Figure 4.5: Thirty step ahead prediction results by using the hybrid fuzzy ARIMA(4,5) model for the first scenario in presence of measurement noise with the standard deviation of 1.

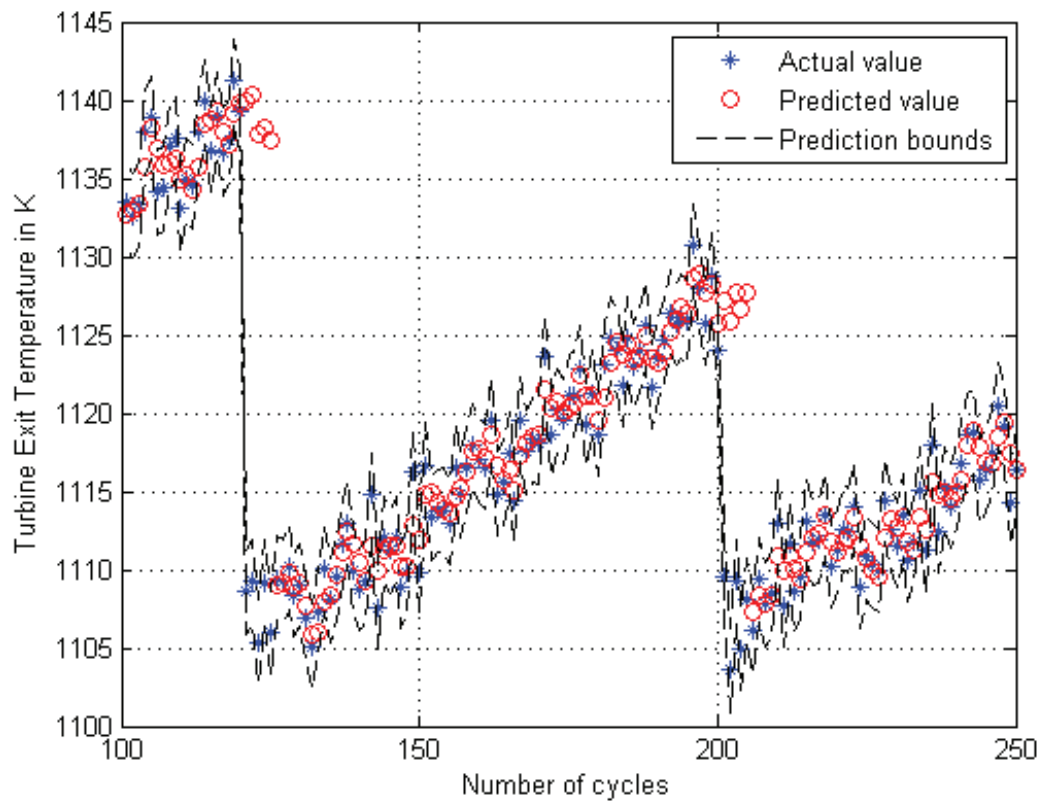


Figure 4.6: Five step ahead prediction results by using the hybrid fuzzy ARIMA(4,5) model for the first scenario in presence of measurement noise with the standard deviation of 2.

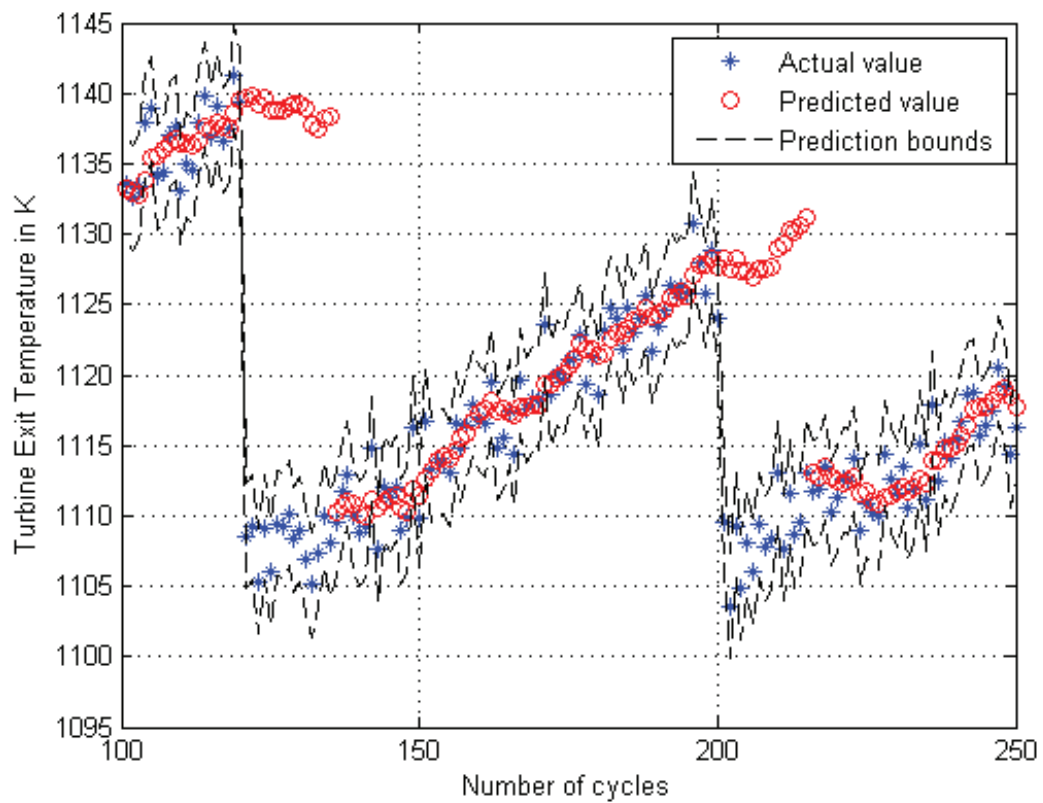


Figure 4.7: Fifteen step ahead prediction results by using the hybrid fuzzy ARIMA(4,5) model for the first scenario in presence of measurement noise with the standard deviation of 2.

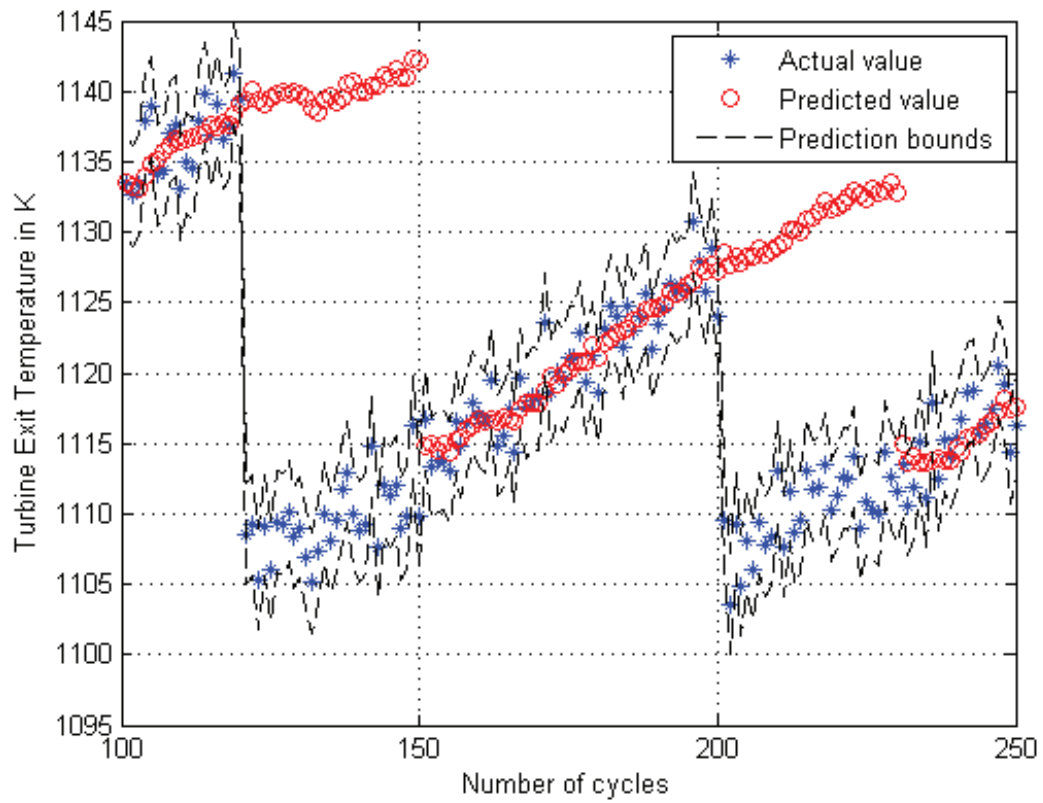


Figure 4.8: Thirty step ahead prediction results by using the hybrid fuzzy ARIMA(4,5) model for the first scenario in presence of measurement noise with the standard deviation of 2.

Table 4.4: Mean and standard deviation of the prediction errors for the hybrid fuzzy ARIMA model for the first scenario in presence of measurement noise with the standard deviation of 1.

Number of steps ahead	Mean	Standard deviation
3	1.5898	5.3050
5	2.2132	6.5357
10	3.9363	8.7927
15	5.5561	10.2953
20	7.2075	11.4131
25	8.7952	12.1921
30	10.4087	12.6988

Table 4.5: Mean and standard deviation of the prediction errors for the hybrid fuzzy ARIMA model for the first scenario in presence of measurement noise with the standard deviation of 2.

Number of steps ahead	Mean	Standard deviation
3	2.0553	5.4522
5	2.6387	6.6727
10	4.4626	8.8844
15	6.1130	10.5990
20	7.7925	11.6746
25	9.4988	12.5560
30	11.0795	13.1747

measurement noise with the standard deviation of 5. Table 4.6 shows the mean and the standard deviation of the prediction errors for different number of steps ahead in presence of measurement noise with the standard deviation of 5.

As seen in Figures 4.3, 4.6 and 4.9 showing 5 steps ahead prediction results all the predicted values are within the defined boundaries for all the three level noises. At 120th and 200th flight cycles for 5 flight cycles, the predicted values are outside the boundaries. This happens because of the maintenance that was performed at the cycles 120 and 200 in the first scenario and the compressor got washed. Clearly, the data before the maintenance action is not sufficient to allow for a reliable prediction subsequent to this action. As the prediction horizon increases even to thirty, as seen in Figures 4.4 and 4.5 the predicted values are completely within the boundaries. The same observation is valid for the other

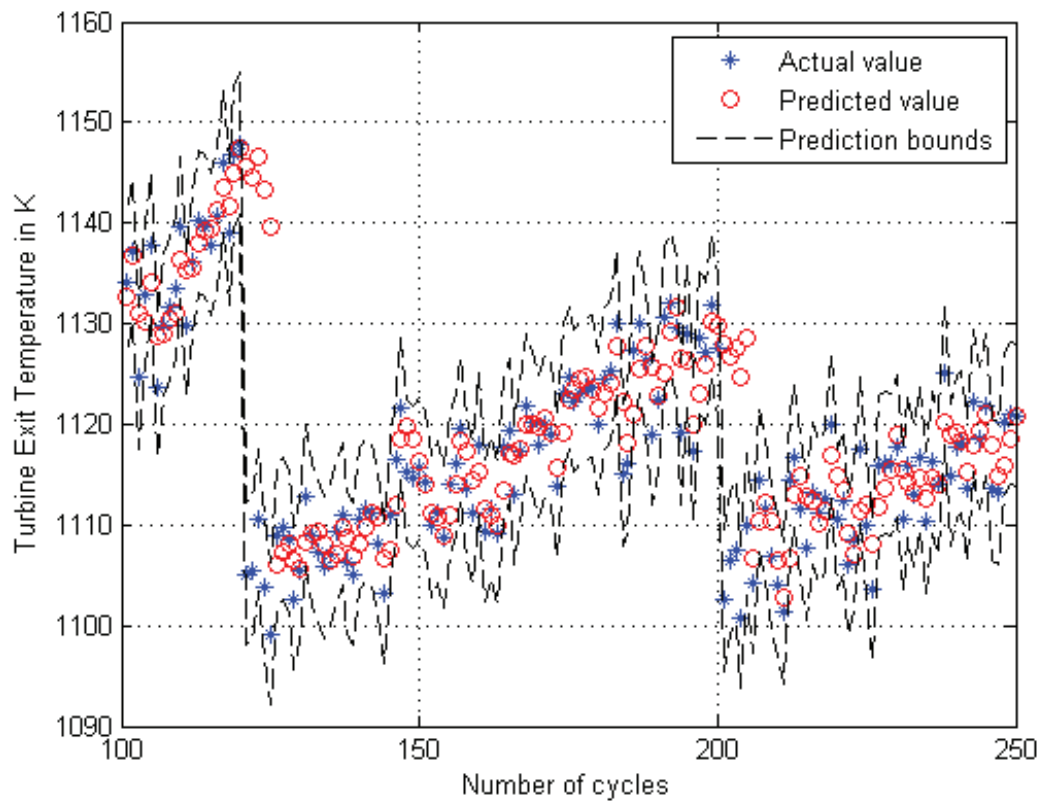


Figure 4.9: Five step ahead prediction results by using the hybrid fuzzy ARIMA(4,5) model for the first scenario in presence of measurement noise with the standard deviation of 5.

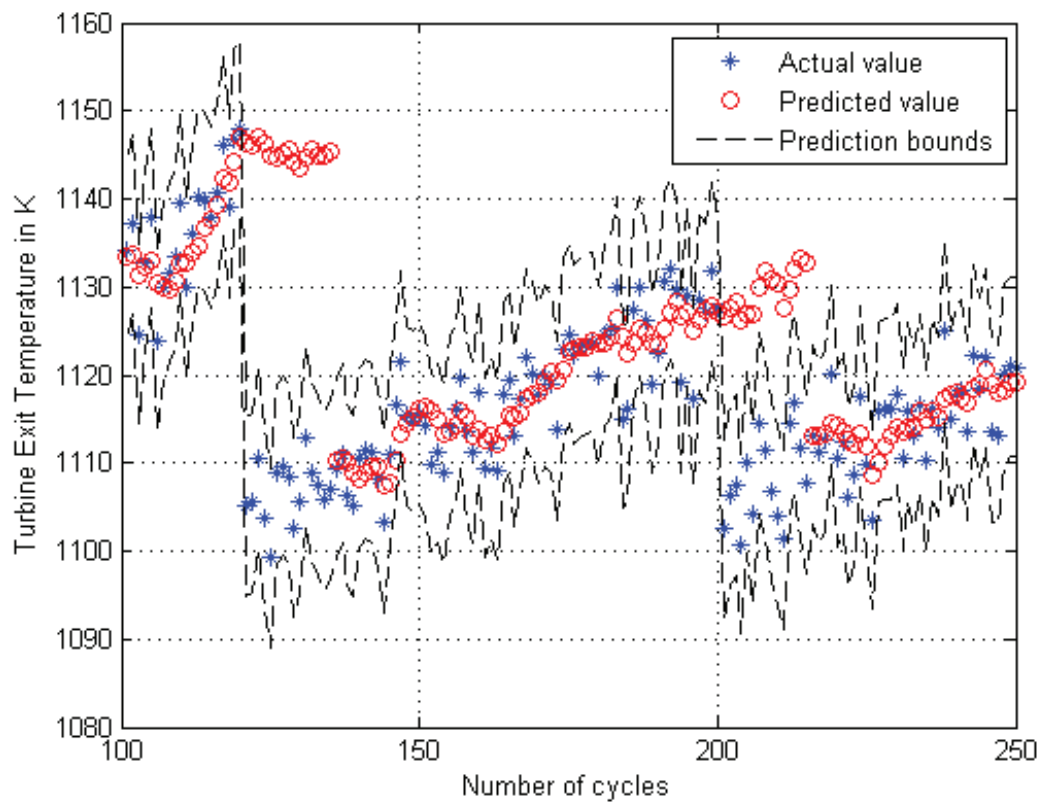


Figure 4.10: Fifteen step ahead prediction results by using the hybrid fuzzy ARIMA(4,5) model for the first scenario in presence of measurement noise with the standard deviation of 5.

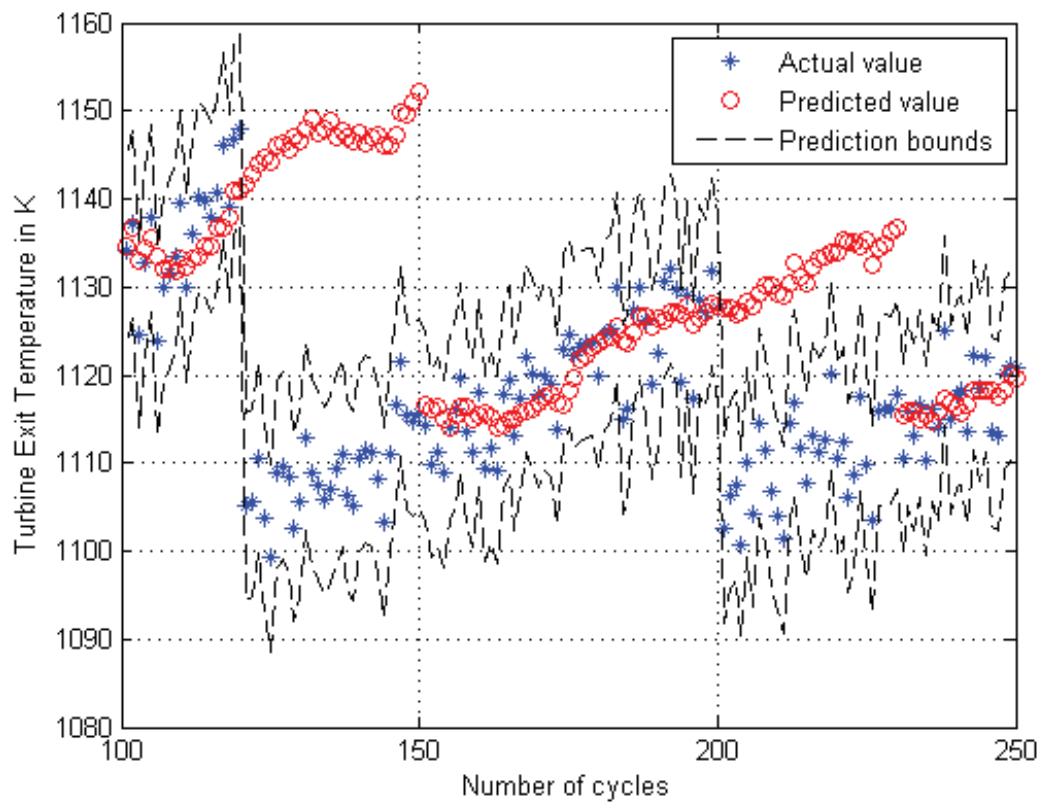


Figure 4.11: Thirty step ahead prediction results by using the hybrid fuzzy ARIMA(4,5) model for the first scenario in presence of measurement noise with the standard deviation of 5.

Table 4.6: Mean and standard deviation of the prediction errors for the hybrid fuzzy ARIMA model for the first scenario in presence of measurement noise with the standard deviation of 5.

Number of steps ahead	Mean	Standard deviation
3	3.6567	7.0307
5	4.2665	8.4764
10	6.4593	11.2734
15	8.3005	13.1829
20	10.2857	14.6583
25	12.2357	15.7905
30	13.6965	16.0877

noise levels. However, by increasing the noise level the predicted values become more scattered within the boundaries.

As compared to the prediction results of the ARIMA and VAR models, hybrid fuzzy ARIMA model are more accurate even for higher number of steps ahead predictions.

Scenario 2

Figures 4.12-4.14 depict the results of the prediction for the second scenario in presence of the same level of measurement noise. The dashed lines show our upper and lower prediction intervals. The star points in the figure represent actual data values and the circle points indicate the predicted temperatures. Table 4.7 shows the mean and the standard deviation of the prediction errors for different number of steps ahead in presence of measurement noise with the standard deviation of 1.

Figures 4.15-4.17 depict the results of the prediction in presence of the same level of measurement noise with the standard deviation of 2. Table 4.8 shows the mean and the standard deviation of the prediction errors for different number of steps ahead in presence of measurement noise with the standard deviation of 2.

Figures 4.18-4.20 depict the results of the prediction in presence of the same level of measurement noise with the standard deviation of 5. Table 4.9 shows the mean and the

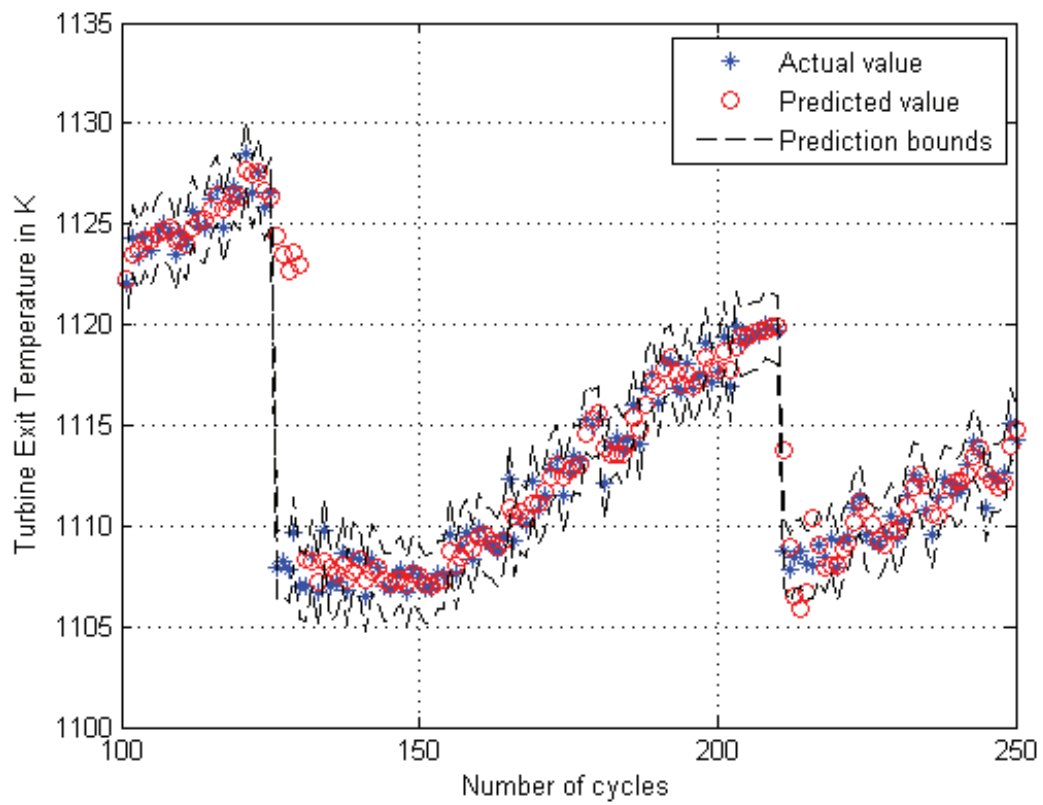


Figure 4.12: Five step ahead prediction results by using the hybrid fuzzy ARIMA(4,5) model for the second scenario in presence of measurement noise with the standard deviation of 1.

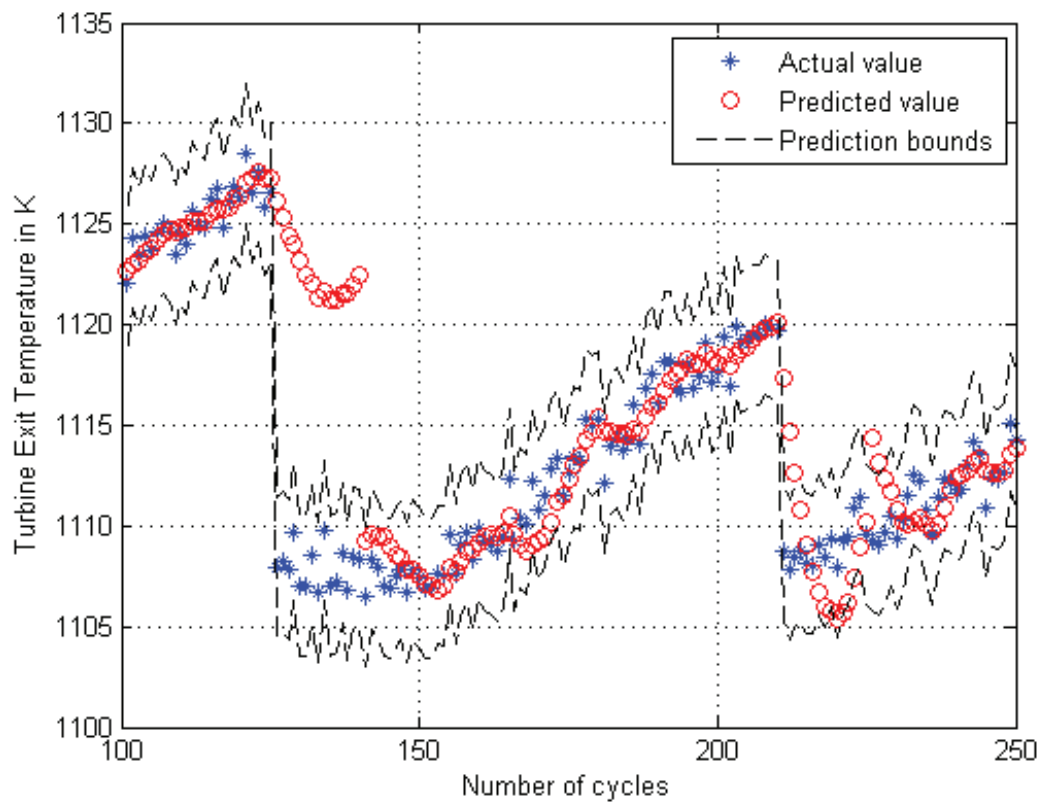


Figure 4.13: Fifteen step ahead prediction results by using the hybrid fuzzy ARIMA(4,5) model for the second scenario in presence of measurement noise with the standard deviation of 1.

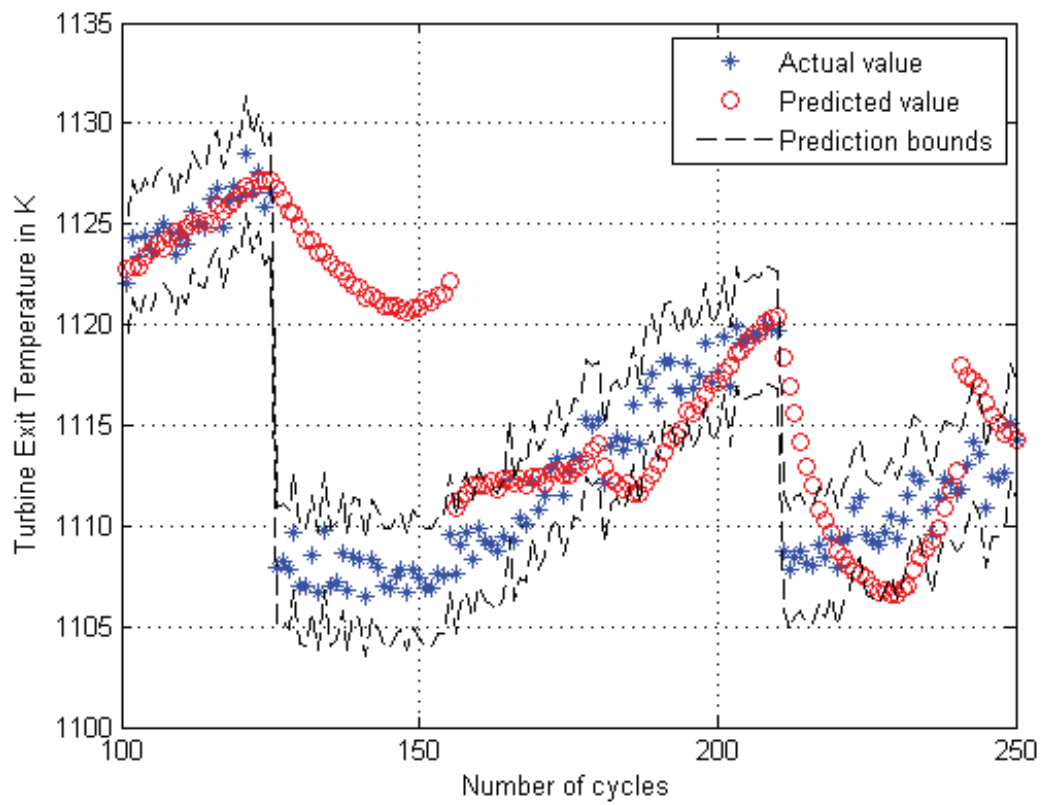


Figure 4.14: Thirty step ahead prediction results by using the hybrid fuzzy ARIMA(4,5) model for the second scenario in presence of measurement noise with the standard deviation of 1.

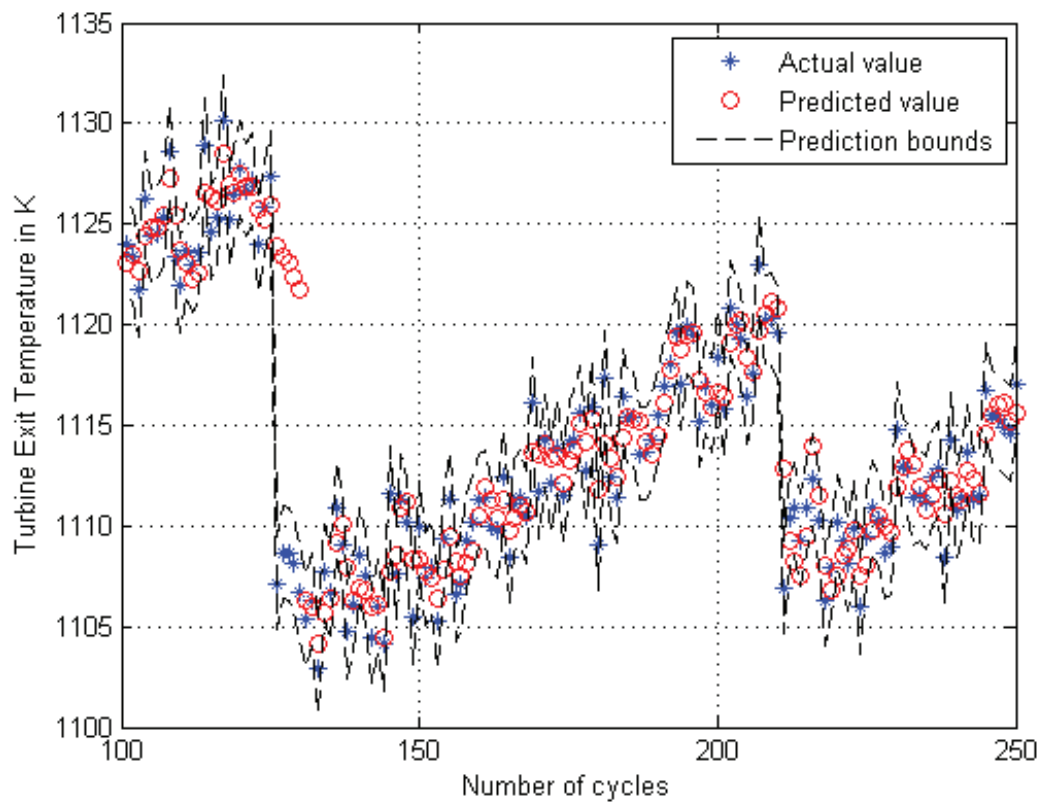


Figure 4.15: Five step ahead prediction results by using the hybrid fuzzy ARIMA(4,5) model for the second scenario in presence of measurement noise with the standard deviation of 2.

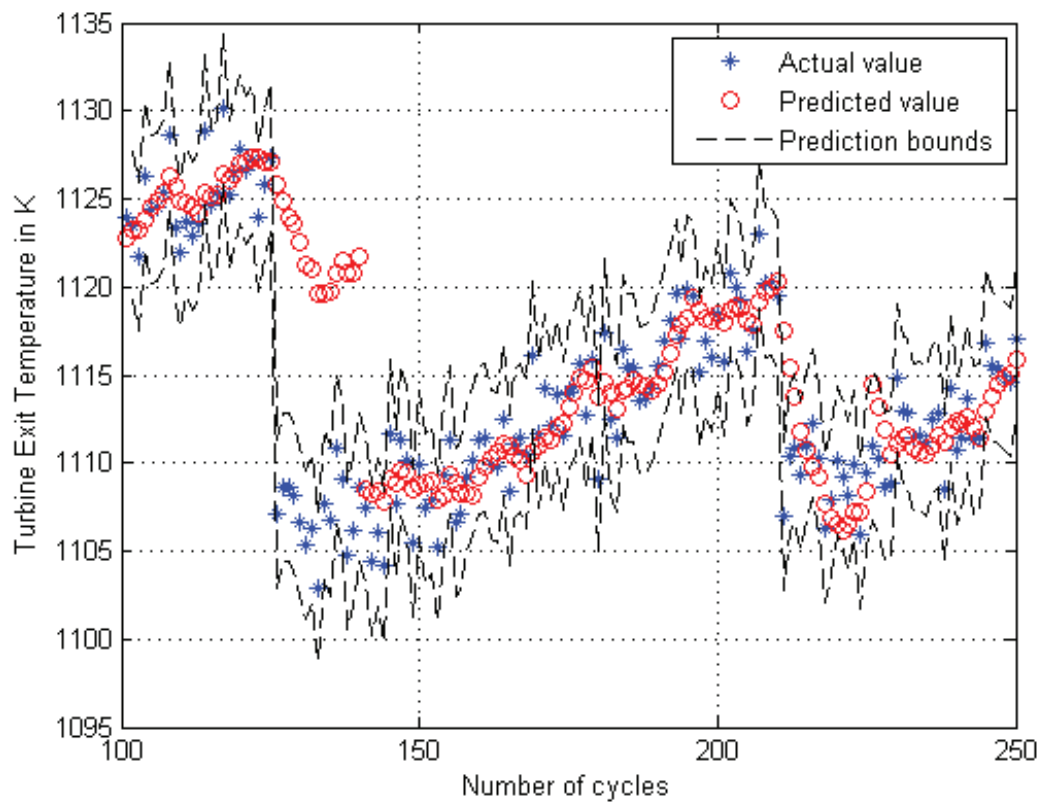


Figure 4.16: Fifteen step ahead prediction results by using the hybrid fuzzy ARIMA(4,5) model for the second scenario in presence of measurement noise with the standard deviation of 2.

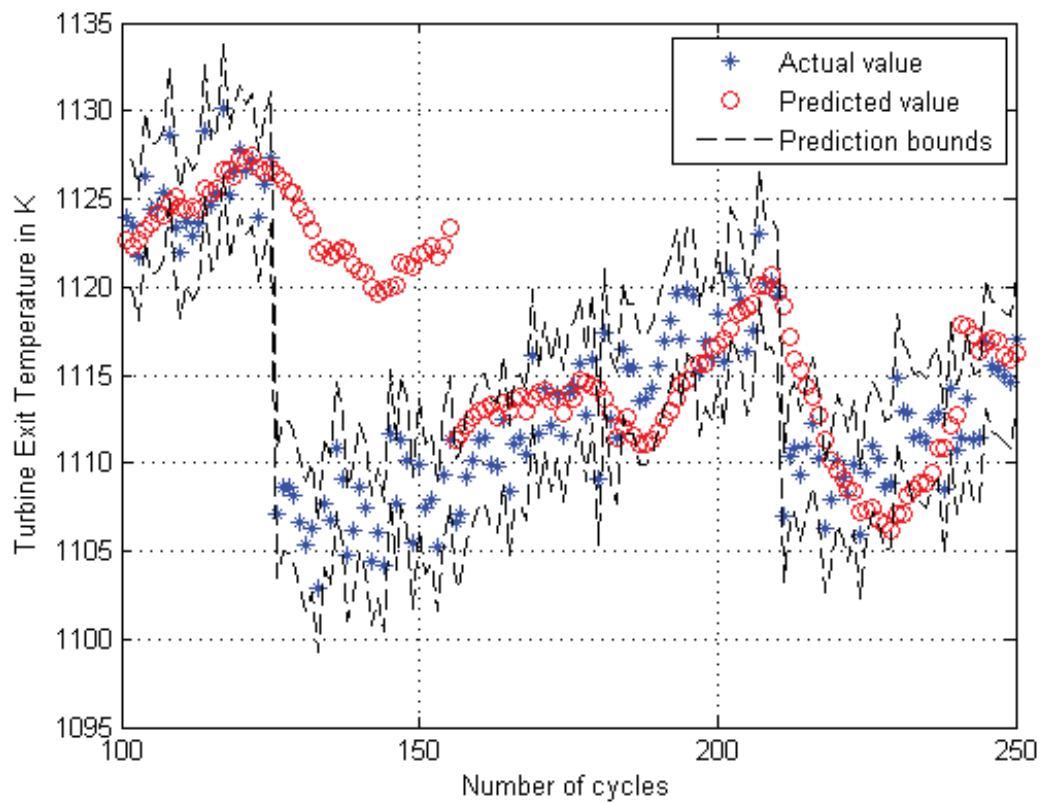


Figure 4.17: Thirty step ahead prediction results by using the hybrid fuzzy ARIMA(4,5) model for the second scenario in presence of measurement noise with the standard deviation of 2.

Table 4.7: Mean and standard deviation of the prediction errors for the hybrid fuzzy ARIMA model for the second scenario in presence of measurement noise with the standard deviation of 1.

Number of steps ahead	Mean	Standard deviation
3	0.9031	2.4771
5	1.0732	2.8795
10	1.7391	3.9105
15	2.5186	4.7608
20	3.2054	5.4570
25	3.8379	5.9854
30	4.5490	6.4551

Table 4.8: Mean and standard deviation of the prediction errors for the hybrid fuzzy ARIMA model for the second scenario in presence of measurement noise with the standard deviation of 2.

Number of steps ahead	Mean	Standard deviation
3	1.4130	2.6614
5	1.5810	3.0653
10	2.2954	4.1520
15	2.9529	4.9162
20	3.5983	5.6059
25	4.1214	6.0914
30	4.8638	6.5893

standard deviation of the prediction errors for different number of steps ahead in presence of measurement noise with the standard deviation of 5.

As seen in Figures 4.12, 4.15 and 4.18 showing 5 steps ahead prediction results all the predicted values are within the defined boundaries for all the three levels of noise. At 125th and 210th flight cycles for 5 flight cycles, the predicted values are outside the boundaries. This happens because of the maintenance that was performed at the cycles 125 and 210 in the second scenario and the eroded components have been changed with the new ones. Clearly, the data before the maintenance action is not sufficient to allow for a reliable prediction subsequent to this action. In the second scenario, as the prediction horizon increases to thirty, as shown in Figures 4.4 and 4.5 the predicted values are within the boundaries although not as good as the first scenario results. The same observation is

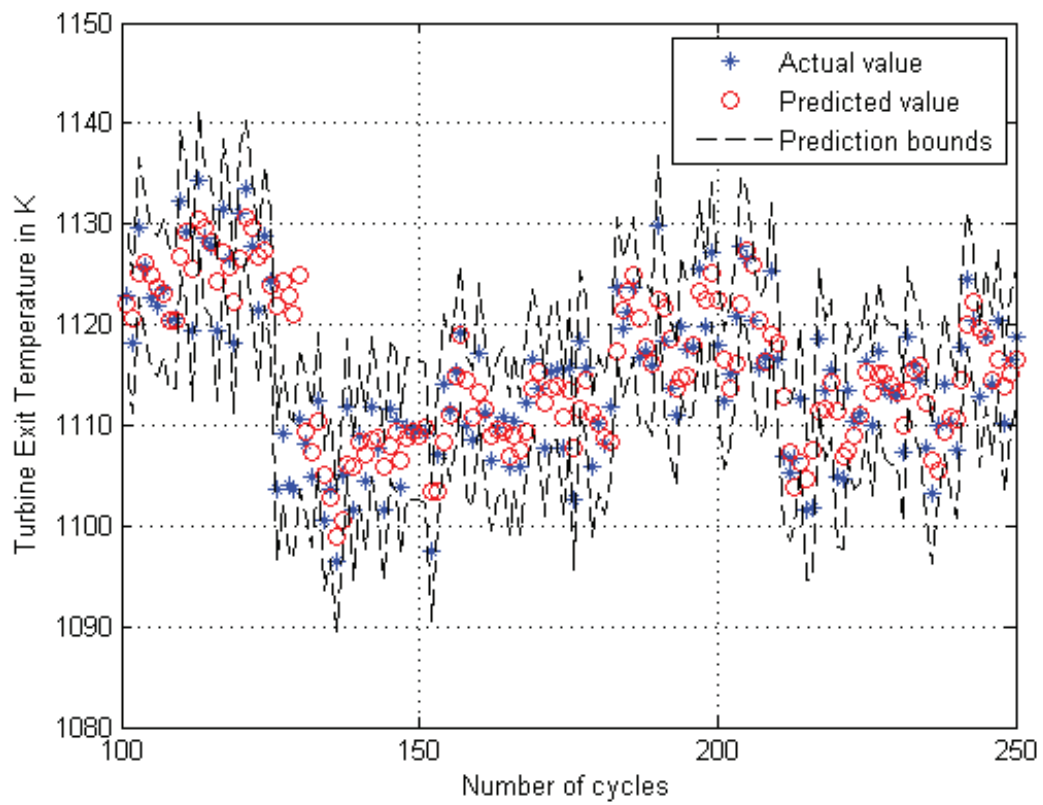


Figure 4.18: Five step ahead prediction results by using the hybrid fuzzy ARIMA(4,5) model for the second scenario in presence of measurement noise with the standard deviation of 5.

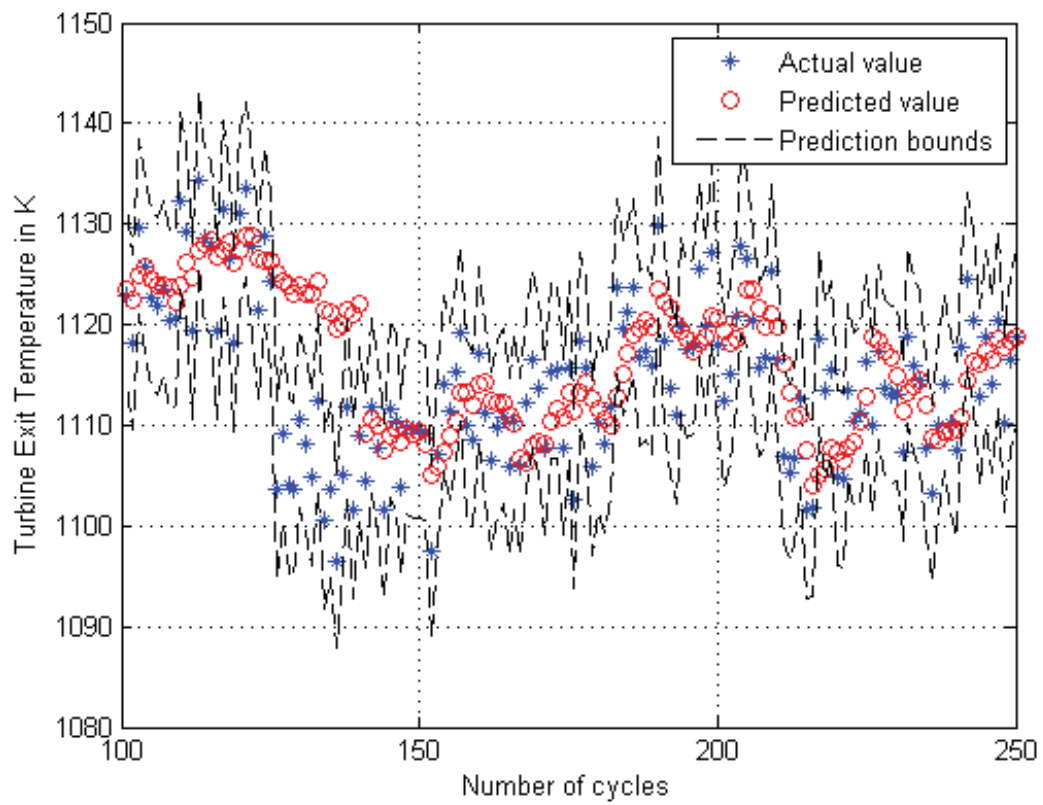


Figure 4.19: Fifteen step ahead prediction results by using the hybrid fuzzy ARIMA(4,5) model for the second scenario in presence of measurement noise with the standard deviation of 5.

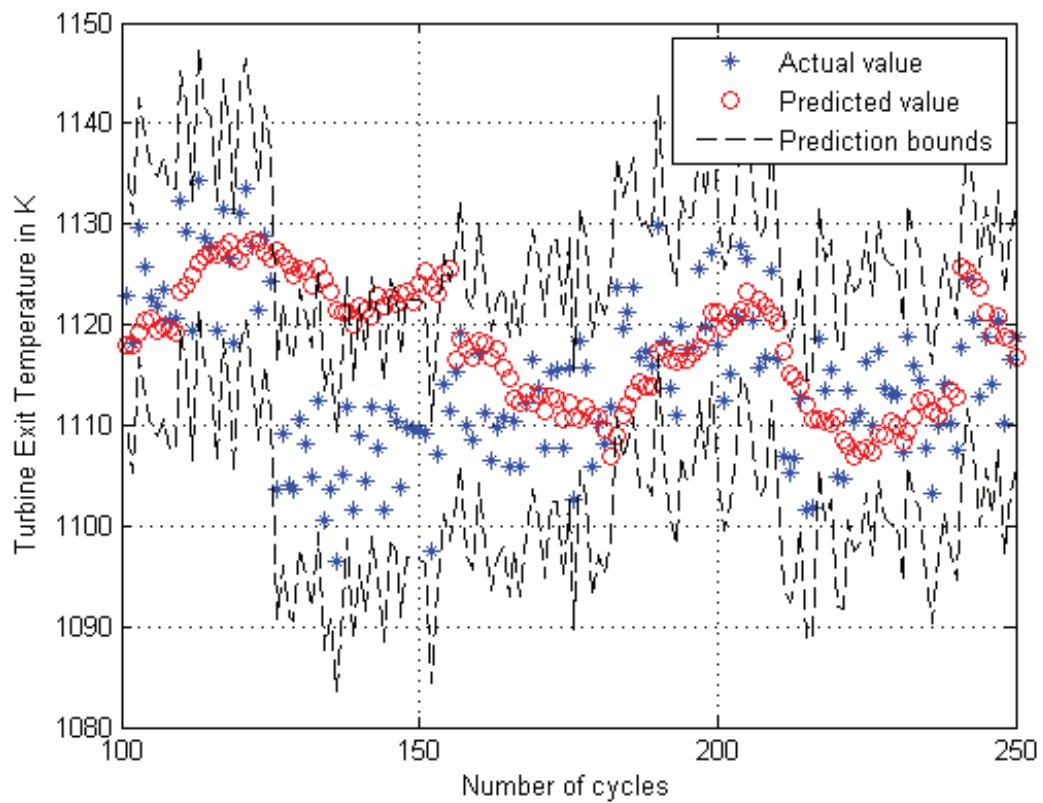


Figure 4.20: Thirty step ahead prediction results by using the hybrid fuzzy ARIMA(4,5) model for the second scenario in presence of measurement noise with the standard deviation of 5.

Table 4.9: Mean and standard deviation of the prediction errors for the hybrid fuzzy ARIMA model for the second scenario in presence of measurement noise with the standard deviation of 5.

Number of steps ahead	Mean	Standard deviation
3	3.0261	4.1686
5	3.2116	4.5132
10	4.3561	6.0054
15	5.1270	6.8436
20	5.6638	7.3866
25	6.3850	8.0841
30	7.1244	8.6652

valid for the other noise levels. However, by increasing the noise level the predicted values become more scattered within the boundaries.

Similar to the first scenario, as compared to the prediction results of the ARIMA and VAR models, the hybrid fuzzy ARIMA model is more accurate even for higher number of steps ahead predictions.

Scenario 3

Figures 4.21-4.23 depict the results of the prediction for the third scenario in presence of the same level of measurement noise. The dashed lines show our upper and lower prediction intervals. The star points in the figure represent actual data values and the circle points indicate the predicted temperatures. Table 4.10 shows the mean and the standard deviation of the prediction errors for different number of steps ahead in presence of measurement noise with the standard deviation of 1.

Figures 4.24-4.26 depict the results of the prediction in presence of the same level of measurement noise with the standard deviation of 2. Table 4.11 shows the mean and the standard deviation of the prediction errors for different number of steps ahead in presence of measurement noise with the standard deviation of 2.

Figures 4.27-4.29 depict the results of the prediction in presence of the same level of

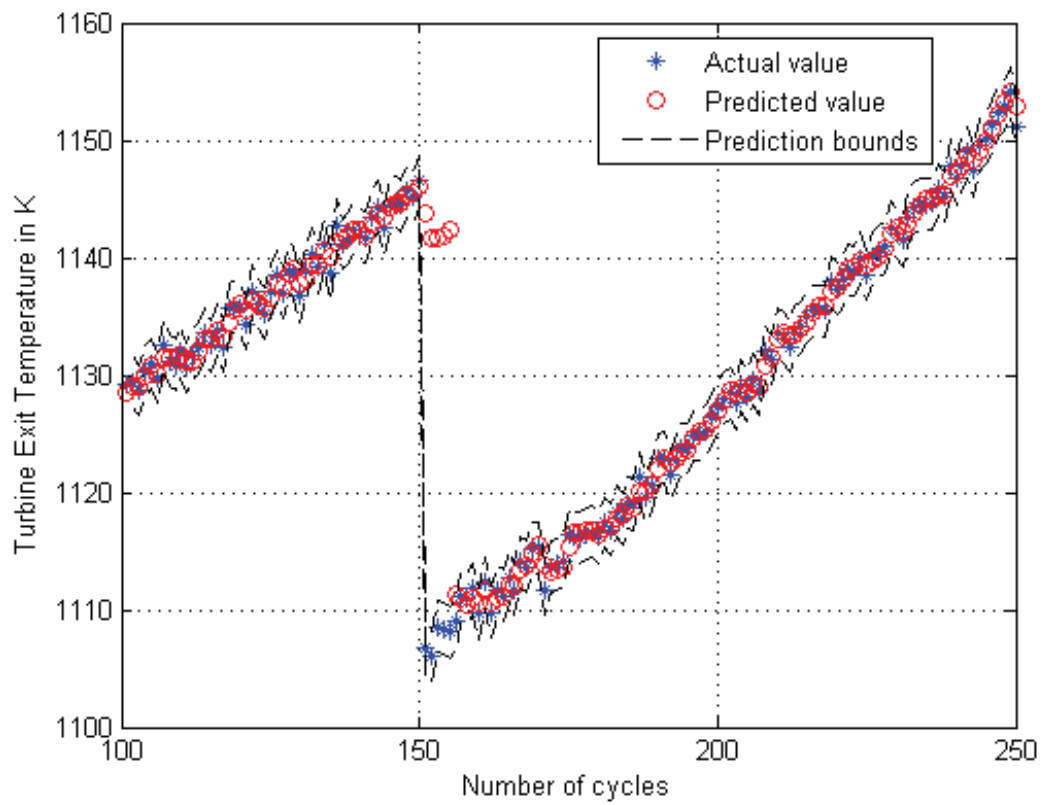


Figure 4.21: Five step ahead prediction results by using the hybrid fuzzy ARIMA(4,5) model for the third scenario in presence of measurement noise with the standard deviation of 1.

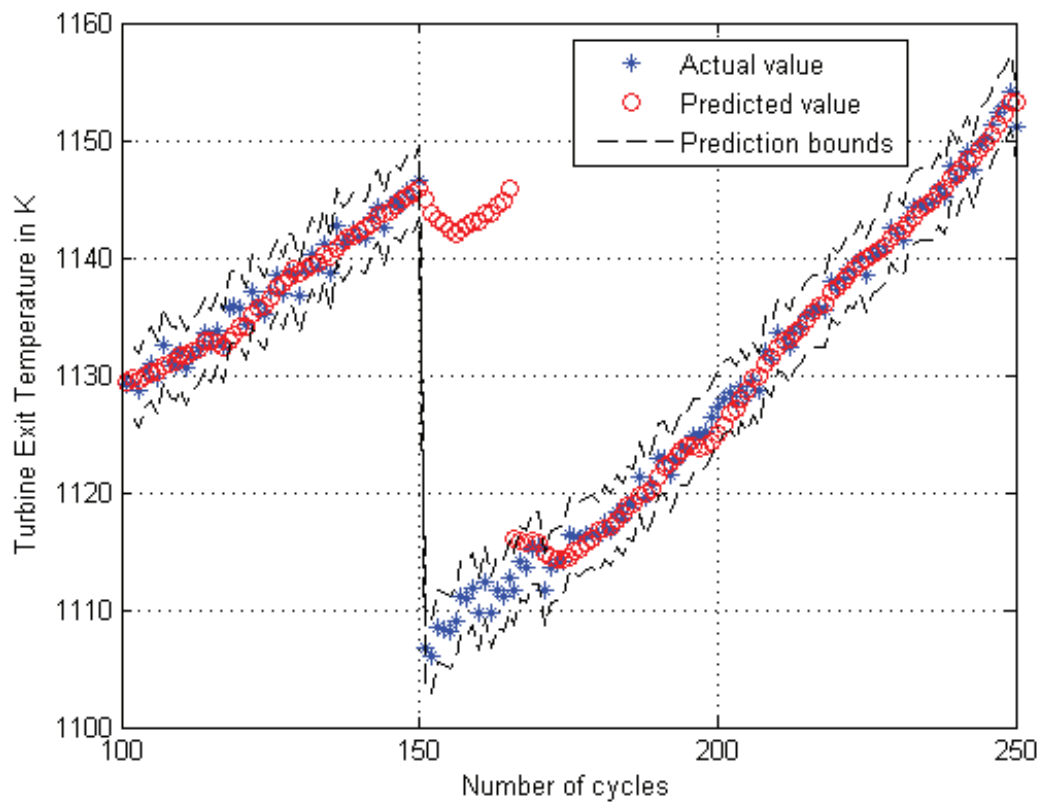


Figure 4.22: Fifteen step ahead prediction results by using the hybrid fuzzy ARIMA(4,5) model for the third scenario in presence of measurement noise with the standard deviation of 1.

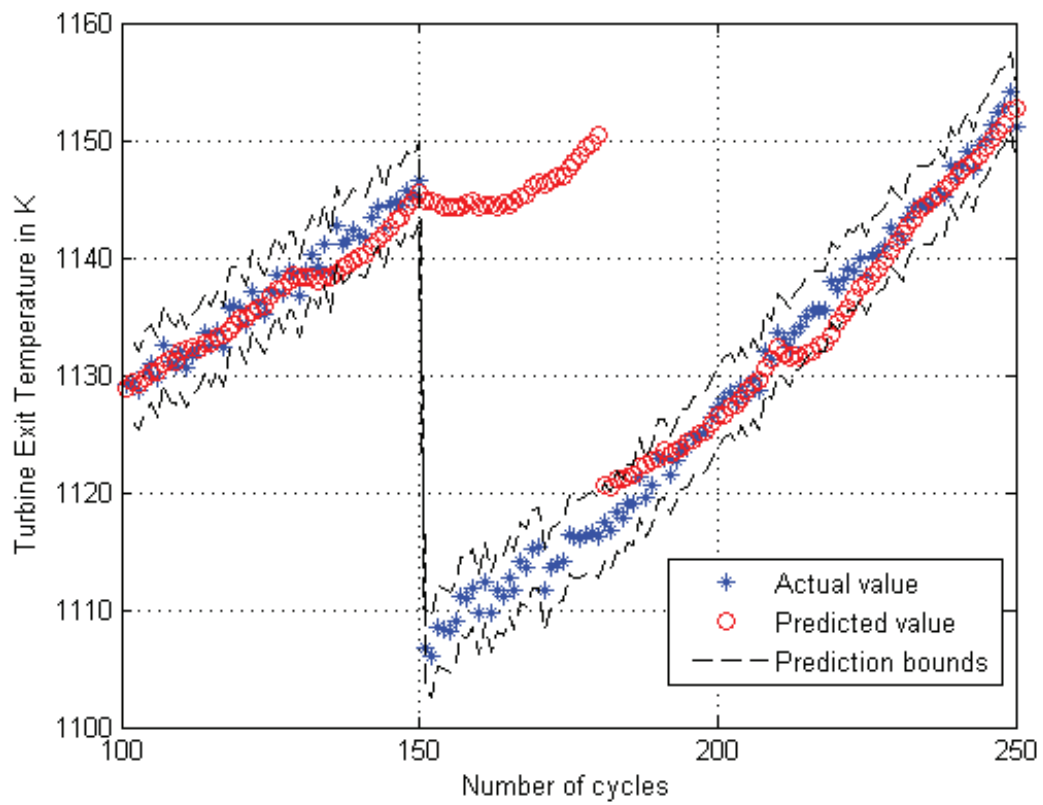


Figure 4.23: Thirty step ahead prediction results by using the hybrid fuzzy ARIMA(4,5) model for the third scenario in presence of measurement noise with the standard deviation of 1.

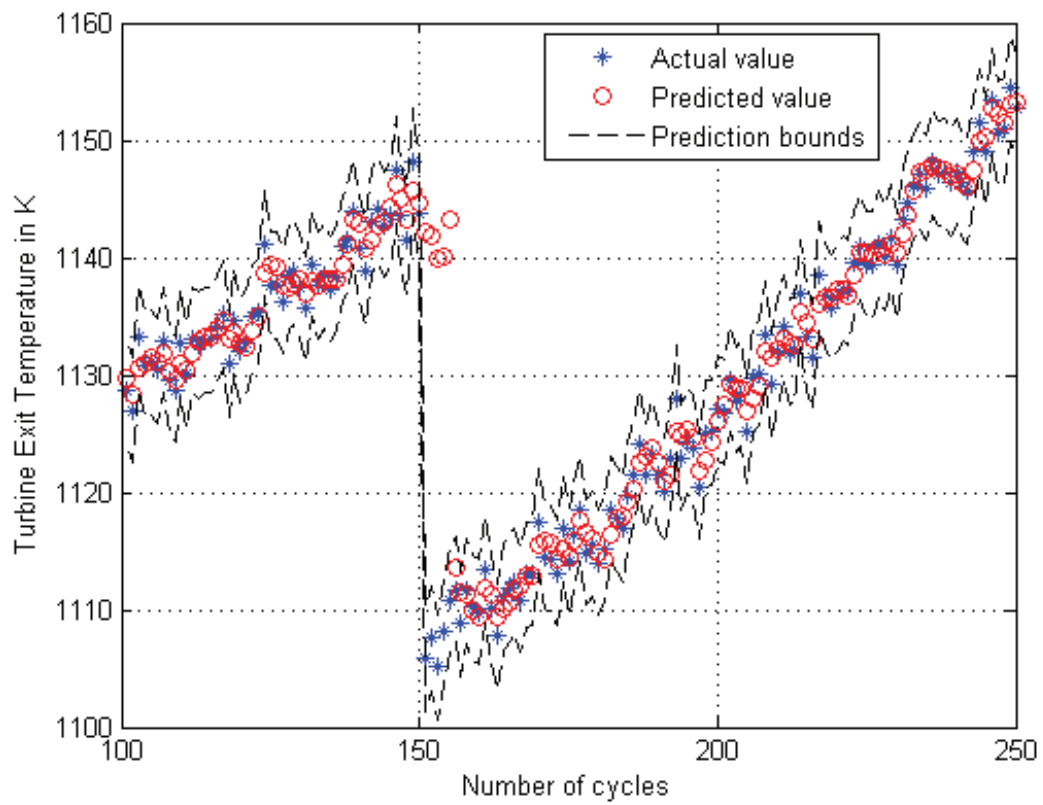


Figure 4.24: Five step ahead prediction results by using the hybrid fuzzy ARIMA(4,5) model for the third scenario in presence of measurement noise with the standard deviation of 2.

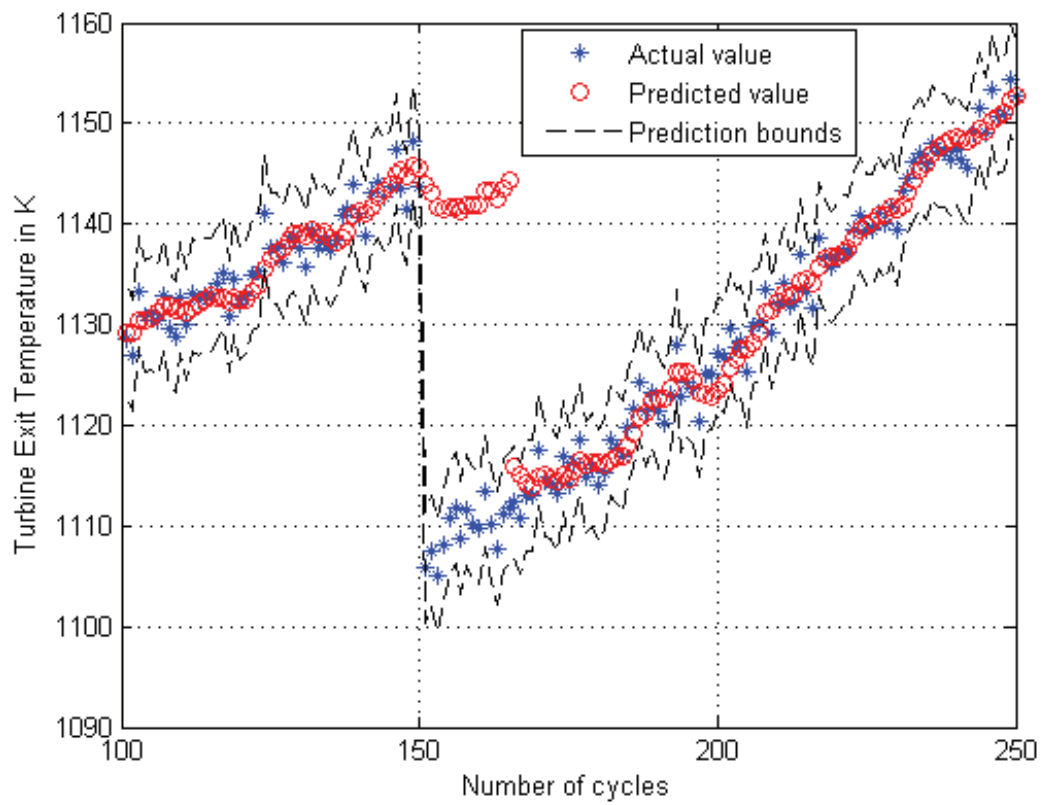


Figure 4.25: Fifteen step ahead prediction results by using the hybrid fuzzy ARIMA(4,5) model for the third scenario in presence of measurement noise with the standard deviation of 2.

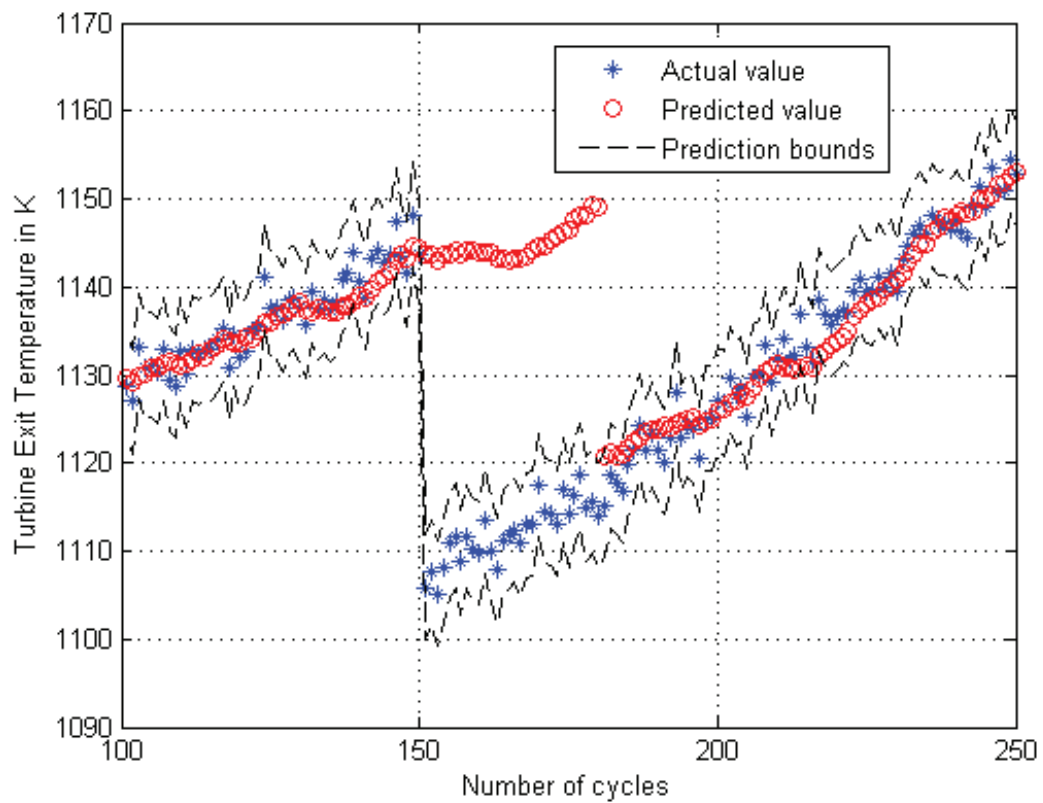


Figure 4.26: Thirty step ahead prediction results by using the hybrid fuzzy ARIMA(4,5) model for the third scenario in presence of measurement noise with the standard deviation of 2.

Table 4.10: Mean and standard deviation of the prediction errors for the hybrid fuzzy ARIMA model for the third scenario in presence of measurement noise with the standard deviation of 1.

Number of steps ahead	Mean	Standard deviation
3	1.2281	5.2677
5	1.6285	6.2951
10	2.8609	8.5008
15	4.0589	10.2555
20	5.2189	11.5711
25	6.5489	12.7982
30	7.7535	13.8067

Table 4.11: Mean and standard deviation of the prediction errors for the hybrid fuzzy ARIMA model for the third scenario in presence of measurement noise with the standard deviation of 2.

Number of steps ahead	Mean	Standard deviation
3	1.7140	5.3362
5	2.1138	6.2380
10	3.3953	8.3608
15	4.5917	10.1159
20	5.7367	11.4094
25	6.7342	12.5442
30	7.9933	13.5580

measurement noise with the standard deviation of 5. Table 4.12 shows the mean and the standard deviation of the prediction errors for different number of steps ahead in presence of measurement noise with the standard deviation of 5.

Figure 4.21 depicts five steps ahead prediction results under the low noise level, where all the predicted values are within the boundaries and the prediction accuracy is completely satisfactory. At 150th flight cycle for 5 flight cycles, the predicted values are outside the boundaries. This happens because of the maintenance that was performed at the cycle 150 in the third scenario and the compressor got washed and the turbine eroded blades were changed. Clearly, the data before the maintenance action is not sufficient to allow for a reliable prediction subsequent to this action. By increasing the number of steps ahead the prediction accuracy is kept even for other noise levels and this can be observed from Figures

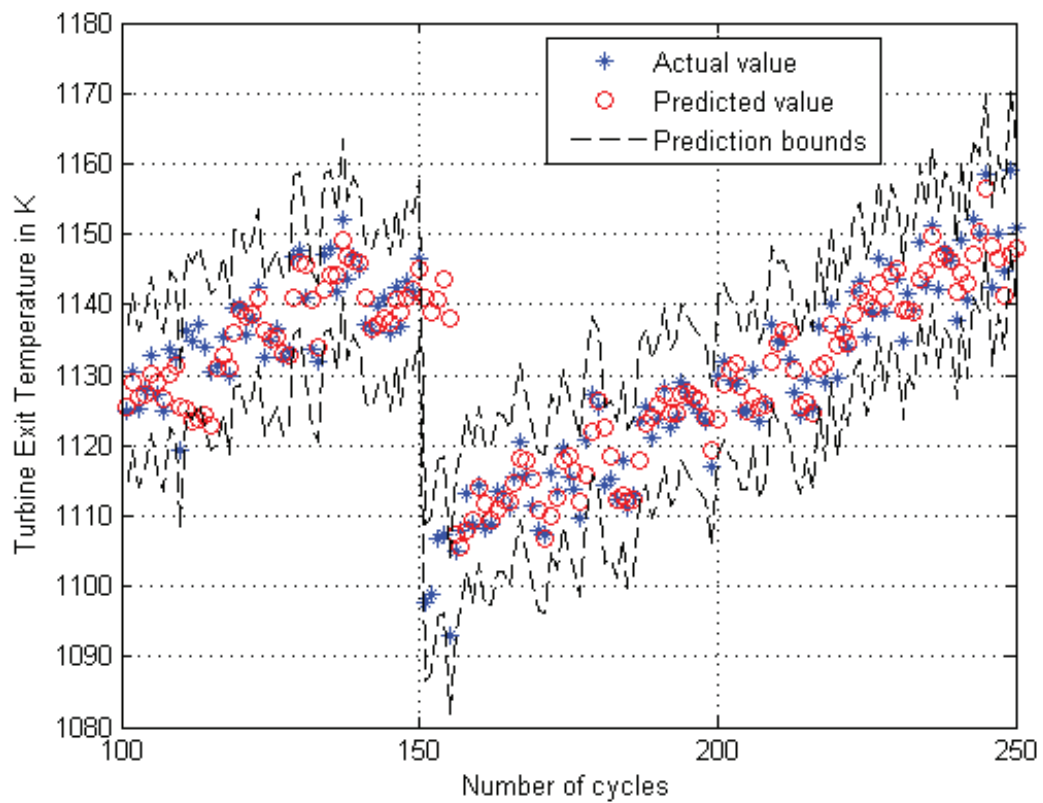


Figure 4.27: Five step ahead prediction results by using the hybrid fuzzy ARIMA(4,5) model for the third scenario in presence of measurement noise with the standard deviation of 5.

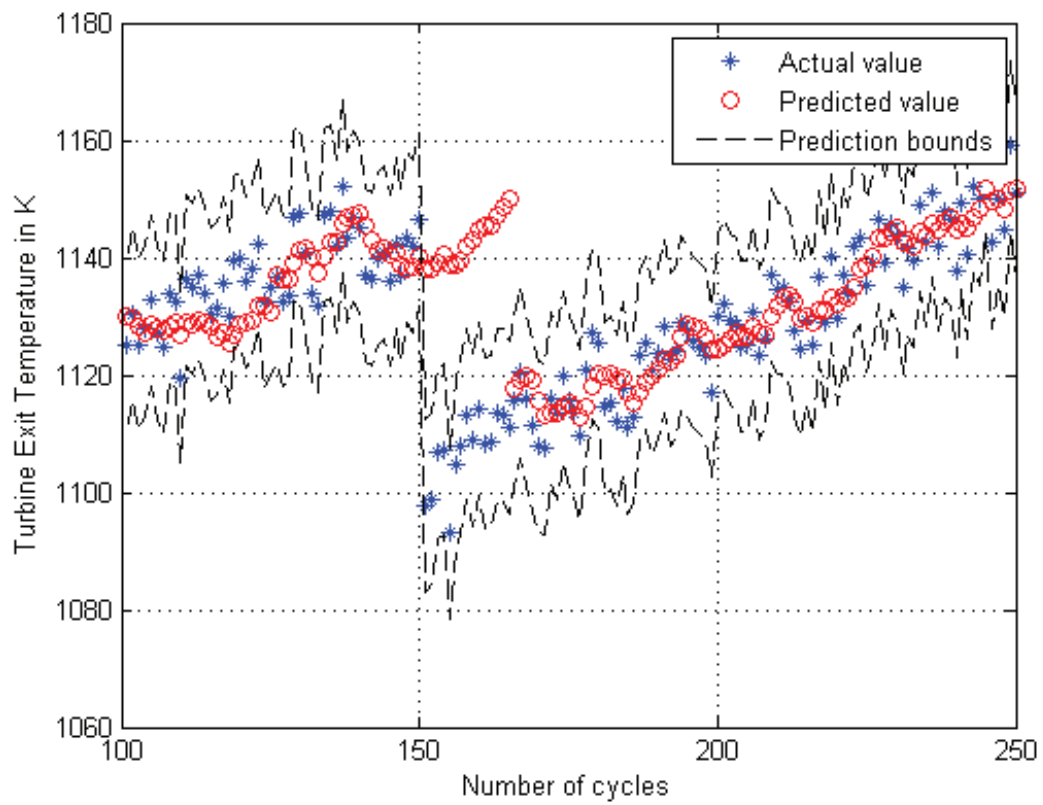


Figure 4.28: Fifteen step ahead prediction results by using the hybrid fuzzy ARIMA(4,5) model for the third scenario in presence of measurement noise with the standard deviation of 5.

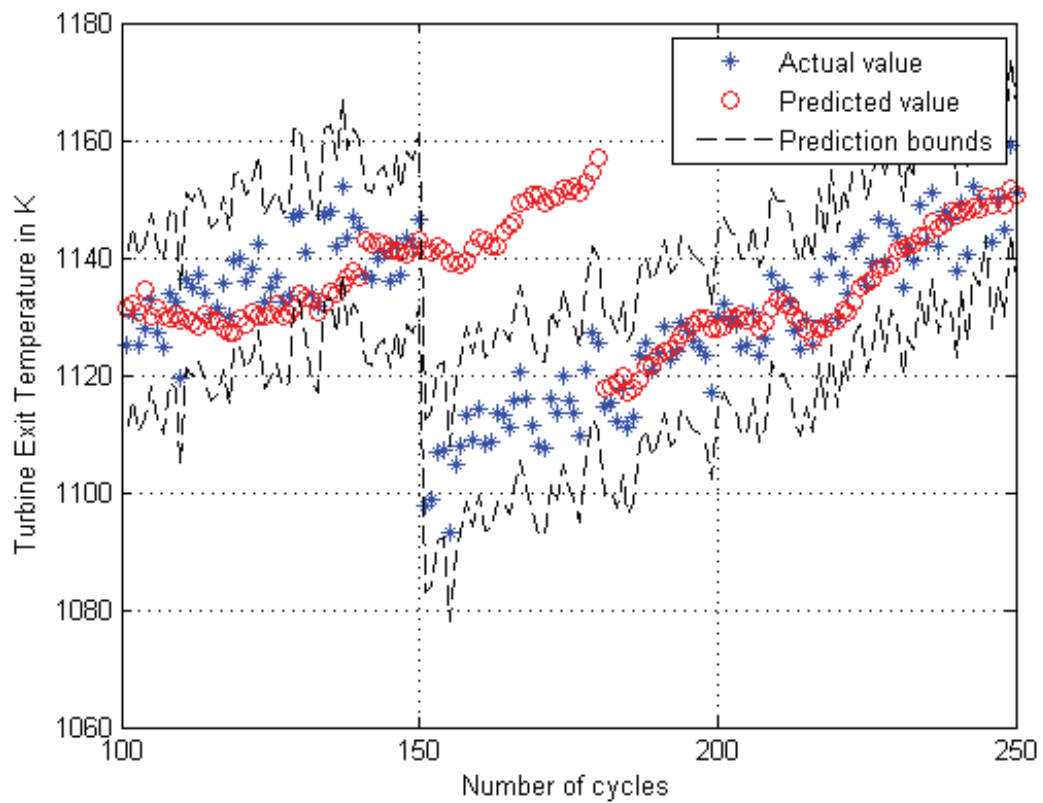


Figure 4.29: Thirty step ahead prediction results by using the hybrid fuzzy ARIMA(4,5) model for the third scenario in presence of measurement noise with the standard deviation of 5.

Table 4.12: Mean and standard deviation of the prediction errors for the hybrid fuzzy ARIMA model for the third scenario in presence of measurement noise with the standard deviation of 5.

Number of steps ahead	Mean	Standard deviation
3	3.4277	6.8423
5	3.9855	8.1131
10	5.8970	10.2022
15	7.1848	11.8886
20	8.4081	13.4111
25	9.7770	14.8535
30	10.7403	15.6441

4.22-4.29.

For the third scenario which is the most complex and realistic scenario, the proposed hybrid fuzzy ARIMA model has good performance in terms of both prediction horizon and accuracy.

4.4 Comparison of Hybrid Fuzzy ARIMA Approach with ARIMA and VAR Models

A hybrid fuzzy ARIMA model was developed in this chapter. The turbine temperature and the spool speed are fused by using a fuzzy inference engine. The time-series generated from the fused data is given to an ARIMA model for prediction purposes. In order to be able to compare the performance of the proposed hybrid fuzzy ARIMA with the presented methods in the previous chapter, the same scenarios under the same noise levels have been considered.

The qualitative results are presented in Figures 4.3-4.29 and the quantitative results are presented in Tables 4.4-4.12. Compared to both the univariate ARIMA model and VAR model, for all the conducted scenarios and under all the noise levels, the hybrid fuzzy ARIMA model performance is better in terms of its accuracy.

It is worth mentioning that the third scenario in which we considered both the fouling and erosion phenomena is a more realistic scenario as in real world the engine is always facing the combination of these two degradation faults. Considering this fact and our results, one can conclude that the hybrid fuzzy ARIMA model performance is more practical and applicable as compared to the other two approaches.

4.5 Summary

In this chapter, a hybrid fuzzy ARIMA approach was proposed for performing engine degradation trend prediction. Towards this end, the procedure in which the turbine exit temperature and the spool speed measurements are fused by using Takagi-Sugeno fuzzy inference engine was presented. The rules and the membership functions associated with the proposed approach were given. Similar scenarios which were used in Chapter 3 were employed to evaluate the proposed method. Finally, the simulation results and comparison

between the three time-based methods were provided.

Chapter 5

Conclusions and Future Work

5.1 Thesis Summary

In this thesis the problem of engine degradation trend prediction has been addressed by using three types of time-series based techniques namely, ARIMA, VAR and hybrid fuzzy ARIMA models. The effects of the compressor fouling, the turbine erosion and their combination as two important reasons of slow degradation in the engine have been investigated and the engine degradation trend due to these phenomena have been predicted. A proper prognostics scheme should be capable of projecting the future state and trend of the identified faults by the FDI scheme on system performance. Moreover, it is required to be able to predict the future condition of the system early enough for the sake of reliability and safety. As mentioned in the first chapter, time-series approaches are delivering promising techniques for short time trend prediction purposes [128, 129, 130].

The required data for performing the engine degradation trend prediction were generated by using a Simulink model [13] that is integrated with models of the aforementioned degradations [18]. First, a controller has been designed to control the EPR level of the engine in the take off phase of the flight. Then, the generated data from the engine under different degradations with different severities are formed as the time-series data which

were fed into the proposed time-series based prognostics approaches. The turbine temperature as the most important parameter of the gas turbine engine was considered as the engine's health indicator.

The proposed VAR model was constructed by using the turbine temperature and the compressor temperature measurement of the engine. The prognostics results showing the prediction values of the turbine temperature trends have been compared with the conventional ARIMA model. In the scenarios dealing with no combination of the fouling and erosion, the ARIMA model has better performance in terms of the number of steps ahead. However, for complex and more realistic scenarios in which there are combinations of both fouling and erosion, the VAR model performance was better in terms of the prediction accuracy.

The third time-series model namely, hybrid fuzzy ARIMA model was constructed by fusing the turbine exhaust temperature and the spool speed via a Takagi Sugeno fuzzy inference engine. Compared to the ARIMA and VAR models, the hybrid fuzzy ARIMA model had better performance in terms of prediction accuracy (mean and standard deviation of the error) for all different scenarios and noise levels. This is due to the flexible nature of the fuzzy method which allows to have more robust prediction results.

One of important challenges in prediction algorithms are how we deal with uncertainties. In this thesis, we have defined confidence bounds based on the normal theory with a given confidence level of 95%. Defining the upper and lower bounds instead of emphasizing on the exact predicted values is more realistic for practical applications.

5.2 Suggestions for Future Work

The ultimate goal and future trend in the gas turbine engine health monitoring area is moving towards developing intelligent engines [98] which are thoroughly automated including self-diagnostics systems along with prognostics capabilities. Towards this end, and based

on the works that have been done in this thesis and the obtained results, some of the potential areas of study and work are suggested as follows:

- In this thesis we have used the gas path measurements for gas turbine engine degradation trend prognostics by using time-series approaches. One of the challenges in time-series modeling and other data-driven methods are employing the most informative data of the system. In VAR approach we employed the turbine exit temperature and the compressor temperature measurements and for hybrid fuzzy ARIMA method, we used the spool speed and turbine exit temperature. Developing effective data mining algorithms to refine the entire raw data without losing the information can boost the effectiveness of this work.
- Available failure prognostics schemes are dealing with determining and evaluating the future state and ultimately the remaining useful life of a component or a subsystem of the system under study. Because proposing a unique scheme covering all the components of the system along with considering their interactions on one another is a challenging area and needs to advance in the software developing area. Developing information/data fusion techniques is a growing field for study.
- Despite the fact that the turbine exhaust temperature is the most important measurement parameter of the engine for inspection and monitoring purposes, employing other measurements can improve the accuracy of the monitoring and prognostics results. In this thesis data fusion by using an fuzzy approach was conducted and the improvements in the prediction results have been achieved. One may use neural networks in order to perform this data fusion and then compare the results.
- In this thesis recursive prediction error method was employed for estimating the ARIMA and VAR model parameters. One can use other techniques such as support vector machines, different neural networks such as radial basis function and dynamic neural

networks for estimating the model parameters. Some of these have already been implemented on the engines but not for the type of degradations we are dealing within this thesis.

- In order to be able to compare the efficiency of our methods in real world, one may apply the proposed methods to some existing practical data available in the prognostics data repository part of the NASA which are available in [171]. Another advantage of using these practical data is in being able to have access to the run-to-failure data which is necessary for determining the remaining useful life time of the system.
- Finally, the proposed prognostics methods in this thesis can be combined with a well-designed fault diagnostics scheme to form a complete and comprehensive health system monitoring for the gas turbine engine. Fault diagnostics schemes will be detecting the slow dynamic degradation in the engine and our prognostics scheme can predict the trend of these degradations which will then be used for condition-based maintenance system.

Bibliography

- [1] L. Fedele, *Methodologies and techniques for advanced maintenance*. Springer, 2011.
- [2] D. Tobon-Mejia, K. Medjaher, N. Zerhouni, and G. Tripot, “A data-driven failure prognostics method based on mixture of gaussians hidden markov models,” *IEEE Transactions on Reliability*, vol. 61, no. 2, pp. 491–503, 2012.
- [3] J. Chen, *Robust residual generation for model-based fault diagnosis of dynamic systems*. PhD thesis, University of York, 1995.
- [4] P. M. Frank, “Fault diagnosis in dynamic systems using analytical and knowledge-based redundancy: A survey and some new results,” *Automatica*, vol. 26, no. 3, pp. 459–474, 1990.
- [5] G. Vachtsevanos, F. Lewis, M. Roemer, A. Hess, and B. Wu, *Intelligent Fault Diagnosis and Prognosis for Engineering Systems Methods and Case Studies*. John Wiley, 2007.
- [6] C. J. Wild and G. A. Seber, “Chance encounters: A first course in data analysis and inference reviewed by flavia jolliffe,” 2000.
- [7] F. L. Toolbox, “for use with matlab users guide,” *Version7, The Math Works Inc*, 2010.
- [8] J. H. Lilly, *Fuzzy control and identification*. Wiley. com, 2010.
- [9] K. M. Passino and S. Yurkovich, *Fuzzy control*, vol. 42. Citeseer, 1998.
- [10] L. S. Langston, G. Opdyke, and E. Dykewood, “Introduction to gas turbines for non-engineers,” *Global Gas Turbine News*, vol. 37, no. 2, 1997.
- [11] R. J. Shaw, “How does a jet engine work?.” <http://www.nasa.gov/centers/glenn/home/index.html>. [Online; accessed 01-Aug-2013].
- [12] R. Royce, *The Jet Engine*. Rolls-Royce, 1966.

- [13] E. Naderi, N. Meskin, and K. Khorasani, "Nonlinear fault diagnosis of jet engines by using a multiple model-based approach," *Journal of Engineering for Gas Turbines and Power*, vol. 134, 2012.
- [14] L. Marinai, *Gas path diagnostics and prognostics for aero-engines using fuzzy logic and time series analysis*. PhD thesis, Cranfield University, 2004.
- [15] S. Genc and S. Lafortune, "Predictability in discrete-event systems under partial observation," in *IFAC Symposium on Fault Detection, Supervision and Safety of Technical Processes, Beijing, China*, Citeseer, 2006.
- [16] "Examples of some severe gas turbine compressor fouling." <http://turbotect.com/product7/index.html>. [Online; accessed 20-Oct-2013].
- [17] "reaction turbine overhaul." <http://mystatesofaggregation.blogspot.ca/search?q=erosion>. [Online; accessed 20-Oct-2013].
- [18] N. Daroogheh, A. Vatani, M. Gholamhossein, and K. Khorasani, "Engine life evaluation based on a probabilistic approach," in *ASME International Mechanical Engineering Congress and Exposition*, pp. 347–358, American Society of Mechanical Engineers, 2012.
- [19] O. Diallo, *A data analytics approach to gas turbine prognostics and health management*. PhD thesis, Georgia Institute of Technology, 2010.
- [20] B. Maggard and D. Rhyne, "Total productive maintenance: A timely integration of production and maintenance," *Journal of Production and Inventory Management*, vol. 33, pp. 6–10, 1992.
- [21] L. Swanson, "Linking maintenance strategies to performance," *International Journal of Production Economics*, vol. 70, no. 3, pp. 237–244, 2001.
- [22] "What is CBM?." <http://cbm.me.sc.edu/>. [Online; accessed 19-Jan-2013].
- [23] A. Jardine, D. Lin, and D. Banjevic, "A review on machinery diagnostics and prognostics implementing condition-based maintenance," *Mechanical Systems and Signal Processing*, vol. 20, no. 7, pp. 1483–1510, 2006.
- [24] B. Rao, *Handbook of condition monitoring*. UK: Elsevier Advanced Technology, 1996.
- [25] I. Loboda, *Gas Turbine Condition Monitoring and Diagnostics*. Gas Turbines, Gurappa Injeti (Ed.), 2010.
- [26] M. Mucino and Y. Li, "A diagnostic system for gas turbines using gpa-index," in *COMADEM Conference*, 2005.

- [27] S. Borguet, *Variations on the Kalman filter for enhanced performance monitoring of gas turbine engines*. PhD thesis, Université de Liege, Liege, Belgique, 2012.
- [28] Y. Li, “Performance-analysis-based gas turbine diagnostics: A review,” *Proceedings of the Institution of Mechanical Engineers, Part A: Journal of Power and Energy*, vol. 216, no. 5, pp. 363–377, 2002.
- [29] M. Koehl, “On-board engine life usage monitoring by real time computation,” in *Proceedings of the 21st Symposium of the International Committee on Aeronautical Fatigue, Toulouse*, 2001.
- [30] L. A. Urban, “Gas path analysis applied to turbine engine condition monitoring,” in *American Institute of Aeronautics and Astronautics and Society of Automotive Engineers, Joint Propulsion Specialist Conference, 8th, New Orleans, La*, 1972.
- [31] M. Khan, “Non-destructive testing applications in commercial aircraft maintenance,” *Journal of Nondestructive Testing*, 1999.
- [32] J. A. Turso and J. S. Litt, “A foreign object damage event detector data fusion system for turbofan engines,” *Journal of Aerospace Computing, Information, and Communication*, vol. 2, no. 7, pp. 291–308, 2005.
- [33] A. Kyriazis, A. Tsalavoutas, K. Mathioudakis, M. Bauer, and O. Johanssen, “Gas turbine fault identification by fusing vibration trending and gas path analysis,” in *ASME Turbo Expo : Power for Land, Sea, and Air*, ASME, 2009.
- [34] P. J. Dempsey and A. A. Afjeh, “Integrating oil debris and vibration gear damage detection technologies using fuzzy logic,” *Journal of the American Helicopter Society*, vol. 49, no. 2, pp. 109–116, 2004.
- [35] A. Volponi, “Data fusion for enhanced aircraft engine prognostics and health management,” *NASA Contractor Report*, vol. 214055, 2005.
- [36] D. Trcka, “General aviation accident analysis.” <http://www.ghafi.org/download/GA-Analysis.1.pdf>, 2000. [Online; accessed 19-Oct-2013].
- [37] O. Dragomir, R. Gouriveau, F. Dragomir, E. Minca, and N. Zerhouni, “Review of prognostic problem in condition-based maintenance.,” in *European Control Conference, ECC’09.*, pp. 1585–1592, 2009.
- [38] B. Zhang, T. Khawaja, R. Patrick, G. Vachtsevanos, M. Orchard, and A. Saxena, “A novel blind deconvolution de-noising scheme in failure prognosis,” *Transactions of the Institute of Measurement and Control*, vol. 32, no. 1, pp. 3–30, 2010.
- [39] S. Simani, *Model-based fault diagnosis in dynamic systems using identification techniques*. PhD thesis, Università degli Studi di Modena e Reggio Emilia, 2003.

- [40] J. Sikorska, M. Hodkiewicz, and L. Ma, “Prognostic modelling options for remaining useful life estimation by industry,” *Mechanical Systems and Signal Processing*, vol. 25, no. 5, pp. 1803–1836, 2011.
- [41] A. Heng, S. Zhang, A. Tan, and J. Mathew, “Rotating machinery prognostics: State of the art, challenges and opportunities,” *Mechanical Systems and Signal Processing*, vol. 23, no. 3, pp. 724–739, 2009.
- [42] S. X. Ding, *Model-Based Fault Diagnosis Techniques: Design Schemes, Algorithms and Tools*. Springer, 2013.
- [43] Z. Sadough, “Fault detection and isolation in gas turbine engines,” Master’s thesis, Concordia University, 2012.
- [44] E. Sobhani-Tehrani and K. Khorasani, *Fault diagnosis of nonlinear systems using a hybrid approach*, vol. 383. Springer, 2009.
- [45] A. Willsky and H. Jones, “A generalized likelihood ratio approach to the detection and estimation of jumps in linear systems,” *IEEE Transactions on Automatic Control*, vol. 21, no. 1, pp. 108–112, 1976.
- [46] H. Sneider and P. M. Frank, “Observer-based supervision and fault detection in robots using nonlinear and fuzzy logic residual evaluation,” *IEEE Transactions on Control Systems Technology*, vol. 4, no. 3, pp. 274–282, 1996.
- [47] F. Gustafsson and F. Gustafsson, *Adaptive filtering and change detection*, vol. 1. Wiley New York, 2000.
- [48] R. Isermann, *Fault-diagnosis applications*. Springer, 2011.
- [49] R. V. Beard, *Failure accomodation in linear systems through self-reorganization*. PhD thesis, Massachusetts Institute of Technology, 1971.
- [50] H. L. Jones, *Failure detection in linear systems*. PhD thesis, Massachusetts Institute of Technology, 1973.
- [51] M. Mrugalski, *Advanced Neural Network-Based Computational Schemes for Robust Fault Diagnosis*. Springer, 2014.
- [52] A. Sallami, N. Zanzouri, and M. Ksouri, “Robust fault diagnosis observer of dynamical systems modelled by bond graph approach,” in *Fault Detection, Supervision and Safety of Technical Processes*, vol. 8, pp. 415–420, 2012.
- [53] D. Luenberger, “An introduction to observers,” *IEEE Transactions on Automatic Control*, vol. 16, no. 6, pp. 596–602, 1971.
- [54] C. Edwards, S. K. Spurgeon, and R. J. Patton, “Sliding mode observers for fault detection and isolation,” *Automatica*, vol. 36, no. 4, pp. 541–553, 2000.

- [55] C. P. Tan, *Sliding mode observers for fault detection and isolation*. PhD thesis, University of Leicester, 2009.
- [56] N. Meskin, *Fault detection and isolation in a networked multi-vehicle unmanned system*. PhD thesis, Concordia University, 2008.
- [57] J. Gertler, “Diagnosing parametric faults: from parameter estimation to parity relations,” in *Proceedings of the American Control Conference*, vol. 3, pp. 1615–1620, IEEE, 1995.
- [58] P. Frank, G. Schrier, and E. A. Garcia, “Nonlinear observers for fault detection and isolation,” in *New Directions in nonlinear observer design*, pp. 399–422, Springer, 1999.
- [59] T. Kobayashi and D. L. Simon, “Application of a bank of kalman filters for aircraft engine fault diagnostics,” tech. rep., DTIC Document, 2003.
- [60] J. Gertler, “Fault detection and isolation using parity relations,” *Control Engineering Practice*, vol. 5, no. 5, pp. 653–661, 1997.
- [61] S. Schneider, N. Weinhold, S. Ding, and A. Rehm, “Parity space based fdi-scheme for vehicle lateral dynamics,” in *Proceedings of IEEE Conference on Control Applications*, pp. 1409–1414, 2005.
- [62] E. M. Cimpoesu, B. D. Ciubotaru, and D. Stefanoiu, “Short investigation on system diagnosis regarding parameter estimation,” in *1st International Conference on Systems and Computer Science (ICSCS)*, pp. 1–6, IEEE, 2012.
- [63] V. Venkatasubramanian, R. Rengaswamy, K. Yin, and S. N. Kavuri, “A review of process fault detection and diagnosis: Part i: Quantitative model-based methods,” *Computers & Chemical Engineering*, vol. 27, no. 3, pp. 293–311, 2003.
- [64] R. Isermann, “Process fault detection based on modeling and estimation methods a survey,” *Automatica*, vol. 20, no. 4, pp. 387–404, 1984.
- [65] E. M. Cimpoesu, B. D. Ciubotaru, and D. Stefanoiu, “Fault detection and diagnosis using parameter estimation with recursive least squares,” in *19th International Conference on Control Systems and Computer Science (CSCS)*, pp. 18–23, 2013.
- [66] E. Sobhani-Tehrani, H. A. Talebi, and K. Khorasani, “Neural parameter estimators for hybrid fault diagnosis and estimation in nonlinear systems,” in *IEEE International Conference on Systems, Man and Cybernetics*, pp. 3171–3176, 2007.
- [67] M. Witczak, *Modelling and Estimation Strategies for Fault Diagnosis of Non-Linear Systems: From Analytical to Soft Computing Approaches*, vol. 354. Springer, 2007.

- [68] R. Patton, F. Uppal, and C. Lopez-Toribio, "Soft computing approaches to fault diagnosis for dynamic systems: a survey," in *4th IFAC Symposium on Fault Detection Supervision and Safety for Technical Processes*, pp. 198–211, 2000.
- [69] M. Mrugalski, "Designing of state-space neural model and its application to robust fault detection," in *ICAISC (1)*, pp. 140–149, 2013.
- [70] J. Korbicz, *Fault Diagnosis.: Models, Artificial Intelligence, Applications*. Springer, 2004.
- [71] R. Mohammadi, E. Naderi, K. Khorasani, and S. Hashtrudi-Zad, "Fault diagnosis of gas turbine engines by using dynamic neural networks," in *IEEE International Conference on Quality and Reliability (ICQR)*, pp. 25–30, 2011.
- [72] S. Mousavi Mirak, *Neural Network-based Fault Diagnosis of Satellites Formation Flight*. PhD thesis, Concordia University, 2013.
- [73] J. W. Hines, R. E. Uhrig, and D. J. Wrest, "Use of autoassociative neural networks for signal validation," *Journal of Intelligent and Robotic Systems*, vol. 21, no. 2, pp. 143–154, 1998.
- [74] A. R. G. Castro, V. Miranda, and S. Lima, "Transformer fault diagnosis based on autoassociative neural networks," in *16th International Conference on Intelligent System Application to Power Systems (ISAP)*, pp. 1–5, 2011.
- [75] S. P. Zhao and K. Khorasani, "A recurrent neural network based fault diagnosis scheme for a satellite," in *33rd Annual Conference of the IEEE Industrial Electronics Society*, pp. 2660–2665, 2007.
- [76] H. A. Talebi, K. Khorasani, and S. Tafazoli, "A recurrent neural-network-based sensor and actuator fault detection and isolation for nonlinear systems with application to the satellite's attitude control subsystem," *IEEE Transactions on Neural Networks*, vol. 20, no. 1, pp. 45–60, 2009.
- [77] M. Sarlak and S. Shahrtash, "High impedance fault detection using combination of multi-layer perceptron neural networks based on multi-resolution morphological gradient features of current waveform," *IET Generation, Transmission & Distribution*, vol. 5, no. 5, pp. 588–595, 2011.
- [78] X. Yangwen, "Study on fault diagnosis of rotating machinery based on wavelet neural network," in *International Conference on Information Technology and Computer Science*, vol. 2, pp. 221–224, 2009.
- [79] R. Mahanty and P. D. Gupta, "Application of rbf neural network to fault classification and location in transmission lines," *IEE Proceedings Generation, Transmission and Distribution*, vol. 151, no. 2, pp. 201–212, 2004.

- [80] L. Xiao-qin, "A method for fault diagnosis in chemical reactor with hybrid neural network and genetic algorithm," in *International Conference on Electronic and Mechanical Engineering and Information Technology (EMEIT)*, vol. 9, pp. 4724–4727, 2011.
- [81] X. Li, Y. Zhang, S. Wang, and G. Zhai, "Analog circuits fault diagnosis by ga-rbf neural network and virtual instruments," in *International Symposium on Instrumentation & Measurement, Sensor Network and Automation (IMSNA)*, vol. 1, pp. 236–239, 2012.
- [82] S. Zhang, T. Asakura, X. Xu, and B. Xu, "Fault diagnosis system for rotary machines based on fuzzy neural networks," in *Proceedings of IEEE/ASME International Conference on Advanced Intelligent Mechatronics*, vol. 1, pp. 199–204, 2003.
- [83] D.-j. Chen and P. Zhao, "Study of the fault diagnosis method based on rbf neural network," in *2nd International Conference on Artificial Intelligence, Management Science and Electronic Commerce (AIMSEC)*, pp. 4350–4353, 2011.
- [84] R. Ganguli, R. Verma, and N. Roy, "Soft computing application for gas path fault isolation," *ASME Turbo Expo., Vienna, Austria*, 2004.
- [85] V. Venkatasubramanian, R. Rengaswamy, S. N. Kavuri, and K. Yin, "A review of process fault detection and diagnosis: Part iii: Process history based methods," *Computers & Chemical Engineering*, vol. 27, no. 3, pp. 327–346, 2003.
- [86] R. Isermann, "On fuzzy logic applications for automatic control, supervision, and fault diagnosis," *IEEE Transactions on Systems, Man and Cybernetics, Part A: Systems and Humans*, vol. 28, no. 2, pp. 221–235, 1998.
- [87] A. Barua and K. Khorasani, "Hierarchical fault diagnosis and fuzzy rule-based reasoning for satellites formation flight," *IEEE Transactions on Aerospace and Electronic Systems*, vol. 47, no. 4, pp. 2435–2456, 2011.
- [88] A. Salar, A. K. Sedigh, S. Hosseini, and H. Khaledi, "A hybrid ekf-fuzzy approach to fault detection and isolation of industrial gas turbines," in *ASME Turbo Expo: Turbine Technical Conference and Exposition*, ASME, 2011.
- [89] T. Back, U. Hammel, and H.-P. Schwefel, "Evolutionary computation: Comments on the history and current state," *IEEE Transactions on Evolutionary Computation*, vol. 1, no. 1, pp. 3–17, 1997.
- [90] G. Dozier, A. Homaifar, E. Tunstel, and D. Battle, "An introduction to evolutionary computation," *Chapter*, vol. 17, pp. 365–380, 2001.
- [91] H. Nayyeri and K. Khorasani, "Modeling aircraft jet engine and system identification by using genetic programming," in *25th IEEE Canadian Conference on Electrical & Computer Engineering (CCECE)*, pp. 1–4, 2012.

- [92] S. Sampath and R. Singh, "An integrated fault diagnostics model using genetic algorithm and neural networks," *Journal of Engineering for Gas Turbines and Power*, vol. 128, no. 1, pp. 49–56, 2006.
- [93] S. Sampath, A. Gulati, and R. Singh, "Fault diagnostics using genetic algorithm for advanced cycle gas turbine," in *ASME Turbo Expo: Power for Land, Sea, and Air*, pp. 19–27, 2002.
- [94] Y.-C. Huang, H.-T. Yang, and C.-L. Huang, "An evolutionary computation based fuzzy fault diagnosis system for a power transformer," in *Proceedings of the 1996 Asian Fuzzy Systems Symposium*, pp. 218–223, 1996.
- [95] G. Liu, *A Study on Remaining Useful Life Prediction for Prognostic Applications*. PhD thesis, University of New Orleans, 2011.
- [96] K. Medjaher, F. Camci, and N. Zerhouni, "Feature extraction and evaluation for health assessment and failure prognostics.," in *First European Conference of the Prognostics and Health Management Society.*, pp. 111–116, 2012.
- [97] C. M. AFNOR, "Diagnostics of machines prognostics part 1: General guidelines," *NF ISO*, pp. 13381–1, 2005.
- [98] A. J. Volponi, "Gas turbine engine health management: Past, present, and future trends," *Journal of Engineering for Gas Turbines and Power*, vol. 136, no. 5, 2014.
- [99] J. Mohammadpour, K. M. Grigoriadis, M. A. Franchek, and B. J. Zwissler, "A survey on failure prognosis research: Theory and applications," in *ASME 2006 International Mechanical Engineering Congress and Exposition*, pp. 235–244, American Society of Mechanical Engineers, 2006.
- [100] Y. Li, S. Billington, C. Zhang, T. Kurfess, S. Danyluk, and S. Liang, "Adaptive prognostics for rolling element bearing condition," *Mechanical Systems and Signal Processing*, vol. 13, no. 1, pp. 103–113, 1999.
- [101] K. Chana, D. Cardwell, L. Gray, and B. Hall, "Disk crack detection and prognosis using non contact time of arrival sensors," in *ASME Turbo Expo: Turbine Technical Conference and Exposition*, ASME, 2011.
- [102] C. J. Li and H. Lee, "Gear fatigue crack prognosis using embedded model, gear dynamic model and fracture mechanics," *Mechanical systems and Signal Processing*, vol. 19, no. 4, pp. 836–846, 2005.
- [103] M. Abbas and G. Vachtsevanos, "A hierarchical framework for fault propagation analysis in complex systems," in *2009 IEEE Autotestcon*, pp. 353–358, 2009.
- [104] C. Sankavaram, A. Kodali, K. Pattipati, B. Wang, M. S. Azam, and S. Singh, "A prognostic framework for health management of coupled systems," in *IEEE Conference on Prognostics and Health Management (PHM)*, pp. 1–10, 2011.

- [105] J. Luo, K. R. Pattipati, L. Qiao, and S. Chigusa, "Model-based prognostic techniques applied to a suspension system," *IEEE Transactions on Systems, Man and Cybernetics, Part A: Systems and Humans*, vol. 38, no. 5, pp. 1156–1168, 2008.
- [106] E. Larsson, J. Aslund, E. Frisk, and L. Eriksson, "Health monitoring in an industrial gas turbine application by using model based diagnosis techniques," in *ASME 2011 Turbo Expo: Turbine Technical Conference and Exposition*, pp. 487–495, American Society of Mechanical Engineers, 2011.
- [107] G. Vachtsevanos and P. Wang, "Fault prognosis using dynamic wavelet neural networks," in *Proceedings of Autotestcon, IEEE Systems Readiness Technology Conference*, pp. 857–870, 2001.
- [108] T. Wensky, L. Winkler, and J. Friedrichs, "Environmental influences on engine performance degradation," in *ASME Turbo Expo: Power for Land, Sea, and Air*, 2010.
- [109] R. Ganguli, "A fuzzy logic system for ground based structural health monitoring of a helicopter rotor using modal data," *Journal of Intelligent Material Systems and Structures*, vol. 12, no. 6, pp. 397–407, 2001.
- [110] M. Naeem, R. Singh, and D. Probert, "Implications of engine deterioration for creep life," *Applied Energy*, vol. 60, no. 4, pp. 183–223, 1998.
- [111] P. Escher, *Pythia: An object-orientated gas path analysis computer program for general applications*. PhD thesis, Cranfield University, 1995.
- [112] M. Naeem, *Implications of aero-engine deterioration for a military aircraft's performance*. PhD thesis, Cranfield University, 1999.
- [113] M. A. Ghafir, Y. Li, R. Singh, K. Huang, and X. Feng, "Impact of operating and health conditions on aero gas turbine: Hot section creep life using a creep factor approach," in *ASME Turbo Expo: Power for Land, Sea, and Air*, pp. 533–545, American Society of Mechanical Engineers, 2010.
- [114] C. Ebmeyer, J. Friedrichs, T. Wensky, and U. Zachau, "Evaluation of total engine performance degradation based on modular efficiencies," in *ASME Turbo Expo: Turbine Technical Conference and Exposition*, pp. 201–210, 2011.
- [115] A. Khoumsi, "Fault prognosis in real-time discrete event systems," in *Proc. Int. Workshop on Principles of Diagnosis, Stockholm, Sweden*, 2009.
- [116] L. Ouédraogo, M. Nourelfath, and A. Khoumsi, "A new method for centralized and modular supervisory control of real-time discrete event systems," in *8th International Workshop on Discrete Event Systems*, pp. 168–175, IEEE, 2006.
- [117] S. Zaidi, *Fault diagnosis and failure prognosis of electrical machines*. PhD thesis, Michigan State University, 2011.

- [118] M. J. Roemer and C. S. Byington, "Prognostics and health management software for gas turbine engine bearings," in *ASME Turbo Expo: Power for Land, Sea, and Air*, pp. 795–802, American Society of Mechanical Engineers, 2007.
- [119] B. Saha, K. Goebel, and J. Christophersen, "Comparison of prognostic algorithms for estimating remaining useful life of batteries," *Transactions of the Institute of Measurement and Control*, vol. 31, no. 3-4, pp. 293–308, 2009.
- [120] D. A. Kumar and S. Murugan, "Performance analysis of indian stock market index using neural network time series model," in *International Conference on Pattern Recognition, Informatics and Medical Engineering (PRIME)*, pp. 72–78, 2013.
- [121] F.-M. Tseng, G.-H. Tzeng, H.-C. Yu, and B. J. Yuan, "Fuzzy arima model for forecasting the foreign exchange market," *Fuzzy Sets and Systems*, vol. 118, no. 1, pp. 9–19, 2001.
- [122] I. Maraziotis, A. Dragomir, and A. Bezerianos, "Gene networks reconstruction and time-series prediction from microarray data using recurrent neural fuzzy networks," *IET Systems Biology*, vol. 1, no. 1, pp. 41–50, 2007.
- [123] W. Wu, J. Hu, and J. Zhang, "Prognostics of machine health condition using an improved arima-based prediction method," in *2nd IEEE Conference on Industrial Electronics and Applications*, pp. 1062–1067, 2007.
- [124] R. Adhikari and R. Agrawal, "An introductory study on time series modeling and forecasting," *arXiv preprint*, 2013.
- [125] G. P. Zhang, "A neural network ensemble method with jittered training data for time series forecasting," *Information Sciences*, vol. 177, no. 23, pp. 5329–5346, 2007.
- [126] A. Guclu, H. Yılboga, O. F. Eker, F. Camci, and I. Jennions, "Prognostics with autoregressive moving average for railway turnouts," in *Annual Conference of the Prognostics and Health Management Society*, Prognostics and Health Management Society, 2010.
- [127] A. Marjanović, G. Kvaščev, P. Tadić, and Ž. Durović, "Applications of predictive maintenance techniques in industrial systems," *Serbian Journal of Electrical Engineering*, vol. 8, no. 3, pp. 263–279, 2011.
- [128] L. Marinai, R. Singh, B. Curnock, and D. Probert, "Detection and prediction of the performance deterioration of a turbofan engine," in *Proceedings of the International Gas Turbine Congress*, 2003.
- [129] H. Wang, J. Lee, T. Ueda, K. H. Adjallah, and M. Ghaffari, "Engine health assessment and prediction using the group method of data handling and the method of match matrix: Autoregressive moving average," in *ASME Turbo Expo: Power for Land, Sea, and Air*, pp. 697–702, American Society of Mechanical Engineers, 2007.

- [130] S. A. Asmai, R. W. Abdullah, M. N. C. Soh, A. S. H. Basari, and B. Hussin, "Application of multi-step time series prediction for industrial equipment prognostic," in *IEEE Conference on Open Systems (ICOS)*, pp. 273–277, 2011.
- [131] W. Visser and M. Broonhead, "Gsp, a generic object-oriented gas turbine simulation environment," *ASME Turbo Expo 2000, Munich, Germany*, 2000.
- [132] A. Pandian and A. Ali, "A review of recent trends in machine diagnosis and prognosis algorithms," in *World Congress on Nature & Biologically Inspired Computing*, pp. 1731–1736, IEEE, 2009.
- [133] G. P. Zhang, "Time series forecasting using a hybrid arima and neural network model," *Neurocomputing*, vol. 50, pp. 159–175, 2003.
- [134] G. Box, G. Jenkins, and G. Reinsel, *Time series analysis*. John Wiley & Sons, 2008.
- [135] A. Senter, "Time series analysis." <http://userwww.sfsu.edu/efc/classes/biol710>. [Online; accessed 06-Aug-2013].
- [136] G. Niu and B. Yang, "Dempster-shafer regression for multi-step-ahead time-series prediction towards data-driven machinery prognosis," *Mechanical Systems and Signal Processing*, vol. 23, no. 3, pp. 740–751, 2009.
- [137] L. Lennart, "System identification: theory for the user," *PTR Prentice Hall, Upper Saddle River, NJ*, 1999.
- [138] L. Ljung and T. Söderström, *Theory and practice of recursive identification*. MIT Press, 1983.
- [139] G. Stephenson, *Mathematical methods for science students*. Longman Scientific & Technical, 1973.
- [140] G. Janacek and L. Swift, *Time series: forecasting, simulation, applications*. Ellis Horwood Chichester, England, 1993.
- [141] G. C. Goodwin and R. L. Payne, *Dynamic system identification: experiment design and data analysis*. Academic press, 1977.
- [142] P. C. Young, "Process parameter estimation and self adaptive control," in *Theory of Self-Adaptive Control Systems*, pp. 118–140, Springer, 1966.
- [143] D. Mayne, "A method for estimating discrete time transfer functions," in *Advances in Computer Control, Second UKAC Control Convention, Bristol, UK*, 1967.
- [144] K. Wong and E. Polak, "Identification of linear discrete time systems using the instrumental variable method," *IEEE Transactions on Automatic Control*, vol. 12, no. 6, pp. 707–718, 1967.

- [145] C. Chatfield, *Time-series forecasting*. CRC Press, 2001.
- [146] M. Priestley, *Spectral analysis and time series*. Academic press, 1981.
- [147] K. P. Burnham and D. R. Anderson, *Model selection and multimodel inference: a practical information-theoretic approach*. Springer, 2002.
- [148] M. Hellmann, *Fuzzy Logic Introduction; a Laboratoire Antennes Radar Telecom*. PhD thesis, Université de Rennes, 2001.
- [149] G. J. Klir and B. Yuan, *Fuzzy sets and fuzzy logic*. Prentice Hall New Jersey, 1995.
- [150] T. J. Ross, *Fuzzy logic with engineering applications*. John Wiley & Sons, 2009.
- [151] L.-X. Wang, *A Course in Fuzzy Systems*. Prentice-Hall press, USA, 1999.
- [152] L.-X. Wang, *Adaptive fuzzy systems and control: design and stability analysis*. Prentice-Hall Inc., 1994.
- [153] H. Ying, *Fuzzy control and modeling: analytical foundations and applications*. Wiley-IEEE Press, 2000.
- [154] R. Ganguli, "Application of fuzzy logic for fault isolation of jet engines," *Journal of Engineering for Gas Turbines and Power*, vol. 125, no. 3, pp. 617–623, 2003.
- [155] M. G. Simoes, "Introduction to fuzzy control," *Colorado School of Mines, Engineering Division, Golden, Colorado*, 2010.
- [156] T. Takagi and M. Sugeno, "Fuzzy identification of systems and its applications to modeling and control," *IEEE Transactions on Systems, Man and Cybernetics*, no. 1, pp. 116–132, 1985.
- [157] A. Kaur and A. Kaur, "Comparison of mamdani-type and sugeno-type fuzzy inference systems for air conditioning system," *International Journal of Soft Computing and Engineering (IJSCE)*, 2012.
- [158] "Gas turbines summary." <http://www.aerostudents.com/thirdyear/gasTurbines.php>. [Online; accessed 01-Aug-2013].
- [159] L. Smith, H. Karim, S. Etemad, W. C. Pfefferle, *et al.*, *The Gas Turbine Handbook*. National Energy Technology Laboratory, DOE, Morgantown, 2006.
- [160] R. Mohammadi, *Fault diagnosis of hybrid systems with applications to gas turbine engines*. PhD thesis, Concordia University, 2009.
- [161] J. Kamaraj, *Modeling and simulation of single spool jet engine*. PhD thesis, University of Cincinnati, 2004.

- [162] M. Gholamhossein, A. Vatani, N. Daroogheh, and K. Khorasani, "Prediction of the jet engine performance deterioration," in *ASME International Mechanical Engineering Congress and Exposition*, pp. 359–366, 2012.
- [163] R. Kurz, K. Brun, and M. Wollie, "Degradation effects on industrial gas turbines," *Journal of Engineering for Gas Turbines and Power*, vol. 131, no. 6, 2009.
- [164] R. Kurz and K. Brun, "Degradation in gas turbine systems," *Journal of Engineering for Gas Turbines and Power*, vol. 123, no. 1, pp. 70–77, 2001.
- [165] A. V. Zaita, G. Buley, and G. Karlsons, "Performance deterioration modeling in aircraft gas turbine engines," *Journal of Engineering for Gas Turbines and Power*, vol. 120, no. 2, pp. 344–349, 1998.
- [166] R. Kurz and K. Brun, "Degradation of gas turbine performance in natural gas service," *Journal of Natural Gas Science and Engineering*, vol. 1, no. 3, pp. 95–102, 2009.
- [167] I. S. Diakunchak, "Performance deterioration in industrial gas turbines," *Journal of Engineering for Gas Turbines and Power*, vol. 114, no. 2, 1992.
- [168] S. Ogaji, S. Sampath, R. Singh, and S. Probert, "Parameter selection for diagnosing a gas-turbine's performance-deterioration," *Applied Energy*, vol. 73, no. 1, pp. 25–46, 2002.
- [169] C. Patricia, "Phases of a flight." <http://www.fp7-restarts.eu/index.php/home/root/state-of-the-art/objectives/2012-02-15-11-58-37/71-book-video/parti-principles-of-flight/126-4-phases-of-a-flight>, 2014. [Online; accessed 17-March-2014].
- [170] A. Babbar, V. Syrmos, E. Ortiz, and M. Arita, "Advanced diagnostics and prognostics for engine health monitoring," in *Aerospace Conference*, pp. 1–10, IEEE, 2009.
- [171] D. Koga, "Prognostics center of excellence." <http://ti.arc.nasa.gov/tech/dash/pcoe/prognostic-data-repository/>, 2007. [Online; accessed 17-March-2014].